Thesis presented for a Doctorate of Philosophy at the University of Oxford, Michaelmas term, 1989.

THE NORTH HELVETIC FLYSCH OF EASTERN SWITZERLAND: FORELAND BASIN ARCHITECTURE AND MODELLING

Hugh D. Sinclair

Wolfson College, Oxford

CONTENTS

ABSTRACT

Hugh D. Sinclair
Wolfson College

D.Phil
Michaelmas, 1989

The North Helvetic Flysch of Eastern Switzerland: Foreland Basin Architecture and Modelling

The North Alpine Foreland Basin (NAFB) comprises sediments of late Eocene to middle Miocene age. The earliest deposits are the North Helvetic Flysch which are exposed in the regions of Glarus and Graubunden, eastern Switzerland. The Taveyannaz sandstones are the first thrust wedge (southerly) derived sediments of the North Helvetic Flysch. The Taveyannaz basin was divided into two sub-basins by a thrust ramp palaeohigh running ENE/WSW (parallel to the thrust front). Palaeocurrent directions were trench parallel towards the ENE. Sedimentation in the Inner basin (140m thick) is characterised by very thick bedded turbidite sands generated by thrust induced seismic events confined within the thrust-top basin. The Outer basin (240m min. thickness) comprises 10-15 sand packages (5-100m thick) formed by turbidite sands which are commonly amalgamated. Sedimentation in the Outer basin is considered to have been controlled by thrust-induced relative sea-level variations. The Inner basin underwent intense deformation at the sediment/water interface prior to the emplacement of a mud sheet over the basin whilst the sediments were partially lithified. Later tectonic deformation involved fold and thrust structures detaching in the underlying Globigerina marls.

The stratigraphy of the NAFB can be considered as two shallowing upward megasequences separated by the base Burdigalian unconformity. This stratigraphy can be simulated by computer by simplifying the foreland basin/thrust wedge system into 4 parameters: 1) the effective elastic thickness of the foreland plate, 2) a transport coefficient to describe the erosion, transport and deposition of sediment, 3) the surface slope angle of the thrust wedge, 4) the thrust wedge advance rate. The Alpine thrust wedge underwent thickening during the underplating of the External Massifs at about 24-18Ma. This event is simulated numerically by slowing the thrust wedge advance rate, and increasing the slope angle and keeping all other parameters constant. This event causes rejuvenation of the forebulge, and erosion of the underlying stratigraphy, so simulating the base Burdigalian unconformity without recourse to eustasy or anelastic rheologies to the foreland plate.

ABSTRACT

The North Alpine Foreland Basin (NAFB) of Switzerland and France comprises an early (late Eocene/base Oligocene) underfilled stage, characterised by deep-marine sediments, and an overfilled stage with shallow marine and continental deposits during the early Oligocene to middle Miocene. The sediments of the underfilled stage are collectively termed the North Helvetic Flysch. This work focusses on the formation and sedimentology of the North Helvetic Flysch of Glarus and Graubunden, in eastern Switzerland, where there is a tectonic window through the Helvetic nappes into the parautochthonous cover to the Aar Massif. The entire stratigraphy of the NAFB of eastern Switzerland is then studied using computer modelling techniques to evaluate geomorphological and tectonic controls on the stratigraphy of the NAFB.

The North Helvetic Flysch of eastern Switzerland can be divided into four sequences, in ascending stratigraphic order, these are: 1) the Nummulitic limestones which unconformably overlie the Jurassic-Cretaceous, 2) the Globigerina marls, 3) the Taveyannaz sandstones and 4) the overlying mud sheet which was emplaced over the basin. This dissertation examines the development of the Taveyannaz sandstone basin, and its subsequent deformation. The Taveyannaz sandstones are a sequence of turbidites which were deposited in two sub-basins, separated by a topographic high running ENE/WSW, parallel to the encroaching Alpine thrust front. Palaeocurrents were trench parallel towards the ENE. The topographic high on the sea-floor is considered to have formed by the growth of a leading edge anticline underlain by a blind thrust. The Inner (more southerly) basin comprises 140m of very thick bedded (1-10m) turbidite sands and muds interpreted as being generated by low frequency thrust induced seismic events. Intercalated with the very thick bedded turbidites are medium to thin bedded (3-30cm) turbidite sands which occasionally contain wave ripples, and are interpreted to represent relatively high frequency storm-induced turbidite events. The Outer

basin comprises at least 240m of turbidite sands and muds, characterised by approximately 10-15 packages of thick to medium bedded (30-100cm) sands commonly exhibiting marked amalgamation. Sand packages range from 5-100m thick, and are intercalated with finely bedded to laminated muds and silts. The development of sand packages is thought to have occurred during relative sea-level falls caused by thrust-related uplift, the intercalated silts and muds representing the intervening relative high stands of sea level. The sedimentology of the mud sheet overlying the Taveyannaz basin is similar to the intercalated muds and silts of the Outer basin, deposited by dilute turbidity currents.

During deposition of the Taveyannaz sandstones, a 2km wide zone of the Inner basin underwent intense deformation. This involved the breakup and imbrication of beds whilst the sediment was partially lithified. The resultant structural style is extremely chaotic, with blocks and slabs of remnant beds detached and floating in muds. The sheared contacts between blocks demonstrate partial lithification of the sediments. Prior to the emplacement of the mud sheet, sedimentary reworking of the deformed upper surface of this part of the basin formed intra-formational sand breccias at the upper contact. During the emplacement of the mud sheet, large blocks of the underlying sandstones were plucked from topographic highs and incorporated into the mud sheet. Blocks of Mesozoic limestones within the mud sheet indicate synchronous exposure of the underlying sequences in thrust scarps.

An analogy of the sedimentology and early deformation of the Taveyannaz sandstones can be made with similar processes occurring at present in the Middle America Trench off the west coast of Mexico. The Inner basin was a thrust-top basin developed behind the leading edge anticline on the slope. It is likely that the Outer basin represents the outer trench to the sub-marine thrust wedge, fed by a point source such as a canyon along strike in the basin. This would explain the simultaneous deposition of muds higher on the slope due to sediment bypassing to the trench; this is necessary to produce the mud sheet. These muds were then transported to the front of the thrust wedge and emplaced over the

Taveyannaz basin.

Superimposed on the early deformation described above is the typical fold and thrust deformation of the region associated with development of the Helvetic nappes during the Oligocene and Miocene. During this tectonic deformation, the thrust-ramp palaeohigh which separated the Inner and Outer basins continued to develop into the Jetzalp anticline. The area to the south (the Southern Domain) is characterised by harmonic folding through the Taveyannaz sandstones, detaching in the upper Globigerina marls. The Outer basin became intensely deformed into an antiformal stack of three thrust sheets (the Central Domain). Each of these thrust sheets detached within the upper Globigerina marls.

Foreland basin stratigraphy can be considered as the result of three interacting processes; thrust loading, flexural downwarping, and sedimentary dynamics. The resultant stratigraphy of foreland basins is commonly composed of a small number of shallowing and coarsening upward megasequences bounded by regional unconformities. I present a simple model of an evolving thrust wedge on a linear elastic plate with erosion and sedimentation governed by the law of diffusion. This demonstrates the development of regional unconformities without recourse to either eustasy, or complex visco-elastic models for the continental lithosphere.

The model describes the thrust wedge/foreland basin system in terms of four parameters: 1) The effective elastic thickness of the foreland plate (Te); 2) the sediment transport coefficient (K); 3) the thrust wedge advance rate; 4) the surface slope of the thrust wedge. The model is applied to the case study of the North Alpine Foreland Basin (NAFB) of eastern Switzerland; geological information is taken from the NAFB to estimate suitable values for the parameters listed above. The value for Te is estimated at 10+-5km from decompacted sediment profiles and the plate is assumed to have a linear elastic rheology. Data to constrain the sequential development of the thrust wedge come from structural geology (Pfiffner, 1986). The early stages (40-22Ma) of compression involved a relatively

low angle thrust wedge with an advance rate of approximately 4mm/yr. At about 22Ma, the wedge slowed down, and increased its critical angle of taper by underplating crystalline basement of the foreland plate. The value for the transport coefficient is currently the least understood of the parameters and has been estimated from previous studies.

Prior to attempting to simulate the broad-scale geometry of the NAFB, the role of each parameter was assessed individually. The values for Te and K are held constant throughout the simulation of the NAFB at 7.5km and 800m^2/yr respectively. The geometry of the base Burdigalian unconformity is reproduced by variations in the parameters describing the thrust wedge. The slope angle is increased from 1.5° to 4° over 1.5Myr; thrust advance is halted during this thickening event. The rejuvenation of the internal parts of the thrust load causes backtilting of the foreland basin sediments, and erosion of the underlying stratigraphy over the forebulge.

CHAPTER 1

INTRODUCTION

1.1 Aims.

This work attempts to provide a fuller understanding of the formation and sedimentation of the North Alpine foredeep. This has been carried out by (a) stratigraphic, sedimentological and structural studies of the North Helvetic Flysch, which allows a basin reconstruction to be made of the early underfilled stage of the foreland basin, and (b) computer modelling to investigate the tectonic and geomorphological controls on basin stratigraphy.

Sedimentation in the North Alpine Foreland Basin (NAFB) started in the middle Eocene and continued until the middle/late Miocene. The stratigraphy of the NAFB suggests that the late Eocene was a time of rapid subsidence in the Helvetic realm (Funk, 1985), the European foreland being drowned by a shallow marine transgression: this is reflected by Nummulitic limestones passing up into deeper water pelagic marls and turbidites. Subsidence curves from Homewood et al (1986) show a convex-up geometry to the post-Eocene subsidence, a signature that is characteristic of flexural subsidence associated with orogenic loading. Siegenthaler (1974) and Pfiffner (1986) suggest that the depositional basin of the North Helvetic Flysch in eastern Switzerland was controlled by a major extensional fault. In western Switzerland and south-east France, the presence of structural highs sub-dividing the equivalent basins, plus the presence of extensive olistostromes led Lateltin (1988) to speculate that these basins were underlain by front-runner thrusts forming thrust-top basins (piggy-back basins, sensu Ori and Friend, 1984). The intentions of this research

is to carry out a more detailed study of the North Helvetic Flysch of eastern Switzerland in order to evaluate the mechanics of basin formation, ie. to establish whether the North Helvetic Flysch represents the deposits of a flexural, extensional or thrust-top basin or some combination of these. This must first involve an understanding of the structural complexities of these sediments, combined with an understanding of the processes and environments of deposition of the sediments.

Fieldwork involved analysis of fold and thrust structures, with the aim of producing a series of structural cross-sections. In certain regions, detailed mapping was required to clarify problematic structures. With this information, sedimentary logs of the North Helvetic Flysch were measured and were related in terms of their original positions during deposition.

1.2 Structural Setting

Figure 1.1 is a tectonic map showing the main structural elements of the Helvetic Alps. In simple terms the Helvetic Alps can be divided into three main units: 1) The External Massifs - upthrust blocks of Hercynian European basement; 2) The Helvetic nappes - detached thrust sheets of the sedimentary cover to the basement (allochthon); 3) The Parautochthon - the deformed sedimentary cover between the overlying nappes and the underlying basement. For a regional cross-section, see figure 6.6b. The North Helvetic Flysch of eastern Switzerland is exposed in a structural window through the Helvetic nappes within the parautochthon of the cantons of Glarus and Graubunden (fig.1.2). The fieldwork for this research was carried out at the head of the valleys of Sernftal and Linthal, overshadowed by the ridges extending away from the main peak of the area, the Hausstock (3157m).

Milnes and Pfiffner (1977) describe the rocks within the structural window of this region as the Infra-Helvetic complex. This represents everything underlying the Glarus Overthrust, which is the basal thrust to the overlying Helvetic nappes. The Infra-Helvetic complex comprises five units; in ascending structural order these are:

1) Basement of the Aar Massif.

2) Mesozoic cover to the basement.

3) Tertiary cover to the basement.

4) Exotic strip sheets.

5) Sub-Helvetic blocks of Mesozoic limestone.

Chapter 2 focusses on the structural development of the Tertiary cover. Chapter 3 deals with the turbiditic deposits of the North Helvetic flysch, and chapter 4 explores the method of emplacement of the exotic strip sheets, and their relevance to the development of the Tertiary stratigraphy.

1.3 Historical Perspective

The Glarus Alps of eastern Switzerland have been a classic field area of the Alps, with research dating back nearly 200yrs. It was in this area that many of the early geologists first recognised some of the basic mountain building processes. It is therefore considered important to recognise and respect the historical perspective within which this relatively minor addition to our understanding of the area is set.

Hans-Conrad Escher (1809) and Leopold von Büch (1817) recognised that in relation to the underlying limestones, the Permo-Carboniferous Verrucano rocks overlying the Glarus thrust were not in their correct stratigraphical order. This led onto the era of Arnold Escher from Zürich, who was the first to consider that basement rocks had been deformed

simultaneously to cover. He made detailed studies of the Nummulites and Ammonites of the Helvetic limestones, and the fish of the North Helvetic Flysch, which led him to consider the role of the Glarus thrust contact (Escher 1841,1846). The only previous British contribution to the area was that of Sir Roderick Murchison (1849), who whilst working in the field with Escher, began to realise the great mechanical problems of producing such a vast inverted sequence, as observed by the Tertiary flysch overlain by Mesozoic limestones. Murchison also suggested that there had been phases of deformation, with the flysch "lying in troughs or depressions due to some grand early plication, were covered by the lateral extrusion over them of older more crystalline masses".

In 1872 Albert Heim became the successor to Escher at Zürich and was to dominate Swiss geology during his lifetime. He made detailed studies of fold geometries and of much smaller scale structures. Heim published his hypothesis of the Glarus double fold in 1878 based on his observations of ductility contrasts in rocks during folding and the presence of the highly deformed Lochseiten calc-mylonite below the Verrucano. As this contact dips both north and south he considered it as two huge converging overfolds. Heim's data on the Glarus overthrust was also being studied by the french geologist Marcel Bertrand, who in 1884 re-interpreted the structure, postulating a single overthrust, and so introduced the concept of nappe tectonics into Alpine literature. Maurice Lugeon became a fluent advocate of nappe structures in the Glarus region, describing the Santis thrust separating the "nappe superièure glarronaise" (Santis nappe), from the "nappe inferièure glarronaise" (Axen, Murtschen, and Glarus nappes), (Lugeon 1902).

Following the excitement of the research in the 19th century culminating in the acceptance of nappe theory, the first half of the 20th century was somewhat more subdued. The research focussed more on the details of stratigraphy and petrographic analysis. Arnold Heim (1908) worked on the Eocene stratigraphy and Lugeon (1923) dated the Taveyannaz

sandstone as Priabonian. Attention was then geared towards the tectonic and stratigraphic relationships between the North Helvetic Flysch and the overlying Blattengrat unit by Arnold Heim and J.Oberholzer (1933); Leupold (1937) went on to describe the Blattengrat as "Einwicklung" meaning an exotic thrust sheet. He also recognised the basal Lutetian unconformity with a transgressive middle Eocene sequence overlying Upper Cretaceous limestones, later to be described as the "Paleocene Restoration" (Trümpy 1973).

It had long been known that the North Helvetic Flysch was very rich in volcanic detritus of a dominantly andesitic composition. The first detailed petrographic study of the volcanic component was by De Quervain (1928), working from Rheintal in the east to Dauphine in the west. He separated the Taveyannaz sandstones containing 95% volcanics, from the Val d'Illiez sandstones with less volcanics of more varied and acidic compositions. This was followed up by Vuagnat (1952) who used the clasts found within microbreccia units to subdivide the North Helvetic Flysch into the "Grès de Taveyannaz","Grès du Val d'Illiez", and the "Grès du Matt-Gruontal" being the youngest. The Taveyannaz sandstone was then subdivided into:-

Type 1- Clasts of true andesite. (only found in French Alps).

Type 2- Clasts containing albite + augite + or - hornblende.

Type 3- " " altered plagioclase + secondary Ca silicates + altered augite + or - hornblende.

Type 4- " " albite + chlorite.

The Val d'Illiez sandstones contain albitic and chloritic fragments with varying textures, non volcanic acidic clasts, plus a few sedimentary fragments of limestones, dolomites, sandstones, shales, and cherts. The Matt-Gruontal sandstone contain no volcanics at all. The origin of the volcanic material is not fully understood, but subduction-related volcanism to the south would seem the most promising candidate.

Styger (1961) has provided some of the best stratigraphical detail on the Tertiary of the north Helvetic province. He has attempted a certain degree of lateral correlation from the basal Lutetian unconformity. This work is complemented by Wegmann (1961) on the exotic strip sheets of the Blattengrat and Sardona, studying their stratigraphy and evolution. In terms of their palaeogeography, he suggests a south Helvetic origin for the former, and an Ultrahelvetic or north Penninic origin for the latter. Siegenthaler (1974) focussed on the North Helvetic Flysch of the Sernftal, canton Glarus, studying the facies variations from the flysch of late Eocene age, to the molasse transition at the Eocene/Oligocene boundary. This transition is marked by a sharp sedimentological and petrographical break, from deep water trench parallel sedimentation (WSW to ENE), rich in volcanic detritus, to shallow water deposits with a radial flow pattern and less to no volcanics.

The style of structural analysis amongst researchers such as Styger, Wegmann, and Siegenthaler was to divide the area into tectonic units (schuppen), which can be hard to interpret in terms of modern structural analysis. Attempts were made at palinspastic restoration (i.e. Siegenthaler, 1974; figs. 13 and 14). Trümpy (1969) produced a palaeogeographical restoration throughout the entire Helvetics of eastern Switzerland, which still remains to be improved upon.

More recently in the 1970's and 80's research has been strongly influenced by the growing knowledge of structural geology. K. Hsu (1969) described the mechanics of movement along the Glarus overthrust, considering its arched topology as being due to later uplift on the Aar massif. This is contended by S.Schmid (1975) who considers this arching as an original feature, with an estimated 35km displacement occurring mainly during the Miocene.

Attempts have been made at subdividing the deformation within the Infrahelvetic complex into a number of phases (Trümpy 1969, Schmid 1975), the most recent of these was by

Milnes and Pfiffner (1977) and is used as the basis for the structural work within this research.

Adrian Pfiffner has followed this up with a bulk of excellent work studying fold and thrust geometries and determining thrust motion directions using strain analysis and fold axis data (Pfiffner, 1977;1978;1980;1981). He has also analysed the strain partitioning within the Helvetics (Groshong, Pfiffner and Pringle, 1984) and described the obliquity and lateral discontinuity of certain structures, thought to be related to inherent transverse faults. Milnes and Pfiffner (1980) describe the evidence for gravity tectonics in the Helvetics and conclude that gravity gliding is a possible mechanism for the emplacement of the Blattengrat and Sardona units (the exotic strip sheets), and that compression aided by gravity spreading would explain the deformation and transportation of the Helvetic nappes. Laubscher (1983) incorporates the nappes into a large model of mid crustal detachment during subduction and collision, with the nappes comprising a huge shear zone at the base of an orogenic lid of Penninic and Austroalpine thrust sheets.

In the recent I.A.S. special publication on Foreland basins (1986), two papers describe the North Alpine Foreland Basin which runs parallel to the Alpine front, from French Savoy to Linz in Austria. The North Helvetic Flysch are recognised as the earliest deposits of the NAFB. The shallow marine and continental deposits (molasse) of the NAFB demonstrate a northwardly migrating depocentre, with associated stratigraphic onlap onto the European foreland (Homewood et al 1986). Pfiffner (1986) produced a series of cross-sections illustrating the evolution of the foreland basin in eastern Switzerland. His interpretation is dominated by flexurally controlled subsidence, although there is an indication of normal faulting influencing sedimentation, particularly during deposition of the North Helvetic Flysch.

1.4 Stratigraphy

The basic lithostratigraphy of the Tertiary sequence in this region can be divided into four sequences (fig.1.3); in ascending order these are:

1) Nummulite-rich limestones intercalated with greensands and quartz sands. This sequence ranges from 20-50m thick and is referred to as the Nummulitic limestones.

2) Light grey, occasionally phosphatic Globigerina marls, up to 400m thick.

3) Alternating turbidite sands and muds of the Taveyannaz sandstones, 140-350m thick.

4) Parallel laminated muds and silts of the uppermost mud-sheet (exotic strip sheet).

The Nummulitic limestones are Eocene in age, and sit unconformably on Cretaceous limestones. This basal unconformity underlies the entire foreland basin fill and is a part of the "Palaeocene Restoration" as described by Trümpy (1973). The stratigraphic significance of this basal unconformity, overlain by four distinct sequences is discussed in chapter 5. The focus of this study is the Taveyannaz sandstones, which unfortunately cannot be directly dated due to the complete lack of preserved fauna (Styger, 1961; Siegenthaler, 1974). Consequently, determination of the age of these rocks is inferred from the underlying Nummulitic limestones and Globigerina marls. In the area of study, the micro-fossil zonation of the sequence is documented by Styger (1961). The pervasive cleavage has obliterated the planktonic foraminifera, and so the biostratigraphy is based on Nummulites and Assilinids. The bulk of the work on Nummulite zonation was done by W.Leupold in the 1930's and 40's which was collated in 1964 in the Lexique Stratigraphique International.

Based on this zonation scheme, Styger (1961) examined sections through the Kistenpass and Muttsee areas. The initial transgression over the exposed Upper Cretaceous limestones occurred during the lower to middle Lutetian (45-44Ma), this deposited a thin layer (<1m)

of greensands containing vast accumulations of Assilina exponens. These are overlain by limestones containing numerous nummulites including Nummulites Sismondia, d'Arch which is a zonal fossil for the middle Lutetian (Styger, 1961). Herb (1988) uses palinspastic reconstructions of the Helvetic nappes of Switzerland to demonstrate the diachroneity of the unconformity. The Eocene deposits of the transgression young progressively towards the NNW from basal Lutetian to Priabonian (late Eocene). This results in a northward stratigraphic onlap of the initial Tertiary deposits of the NAFB which continues into the Oligo/Miocene deposits of the more external, undeformed part of the basin (fig.6.2).

The most relevant data for dating the Taveyannaz sandstones of this area comes from a micro-conglomerate found at the Globigerina marl/Taveyannaz sandstone transition, at Kistenstöckli (fig.2.8). This contains fragments of Cretaceous limestones, plus many reworked nummulites, the youngest of which is Heterostegina helvetica Kaufman which marks the onset of the Priabonian. This gives an oldest age to the Taveyannaz sandstones.

Siegenthaler (1974) divides the North Helvetic Flysch into three formations which are exposed progressively northwards along the Sernftal valley. The lowermost is the Taveyannaz sandstones, overlain by the Elm and Matt formations, which also comprise turbidite sands and muds separated mainly on their petrography. The relationship between the Elm formation (Siegenthaler, 1974) and the Grès du Val D'Illiez (Vuagnat, 1952) is not fully understood. Within the Elm formation are reworked nummulites with a youngest age of upper Eocene. Whilst recognising the limitations of reworked material, this must be taken as an uppermost age limit. Consequently the deposition of the Taveyannaz sandstones of this region occurred within the late Eocene. Comparisons between this and the dominantly early Oligocene dates from the western Alps will be discussed in chapter 5.

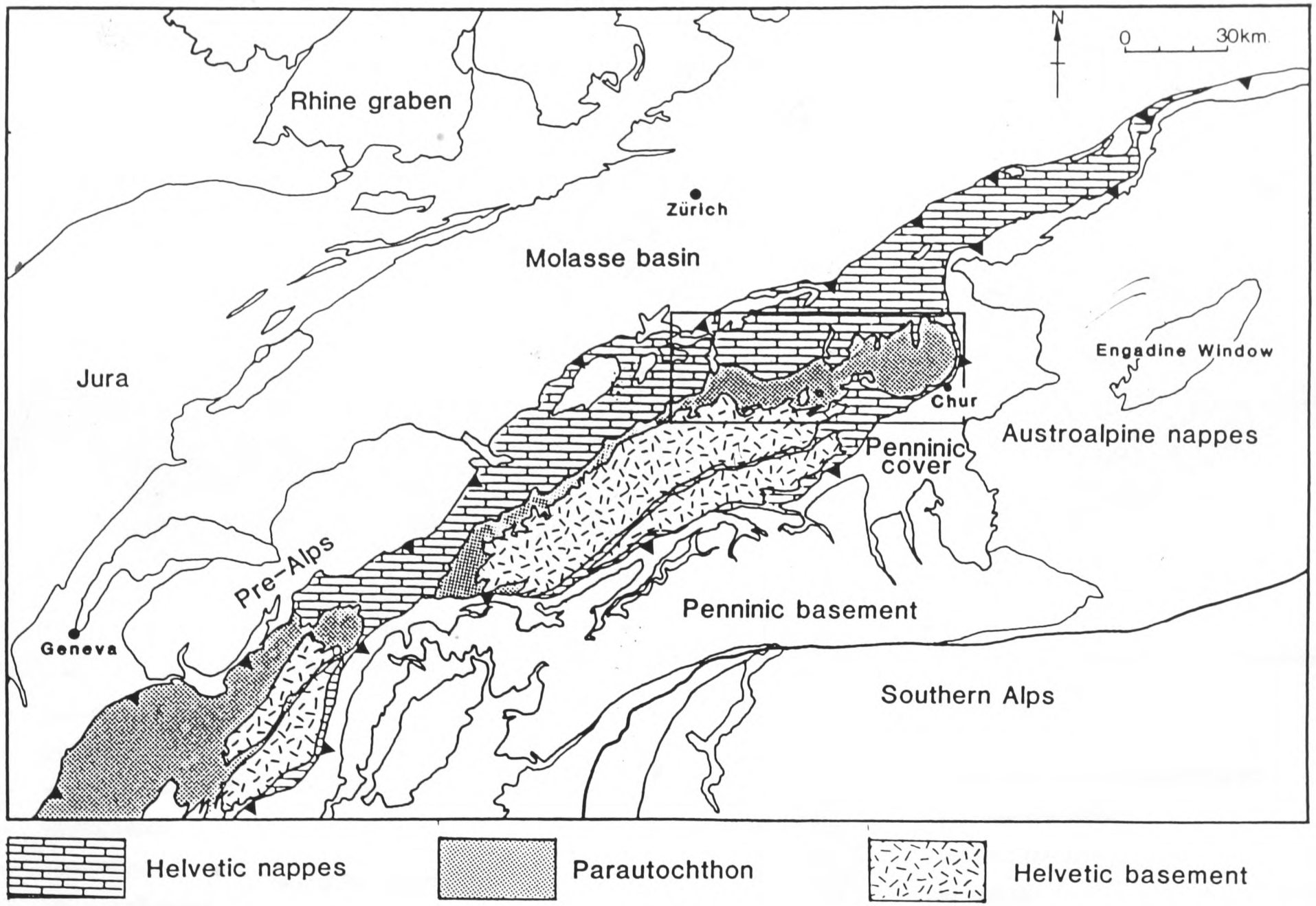

Fig.1.1. Tectonic map of the Helvetic Alps. Boxed area is illustrated in Fig.1.2.

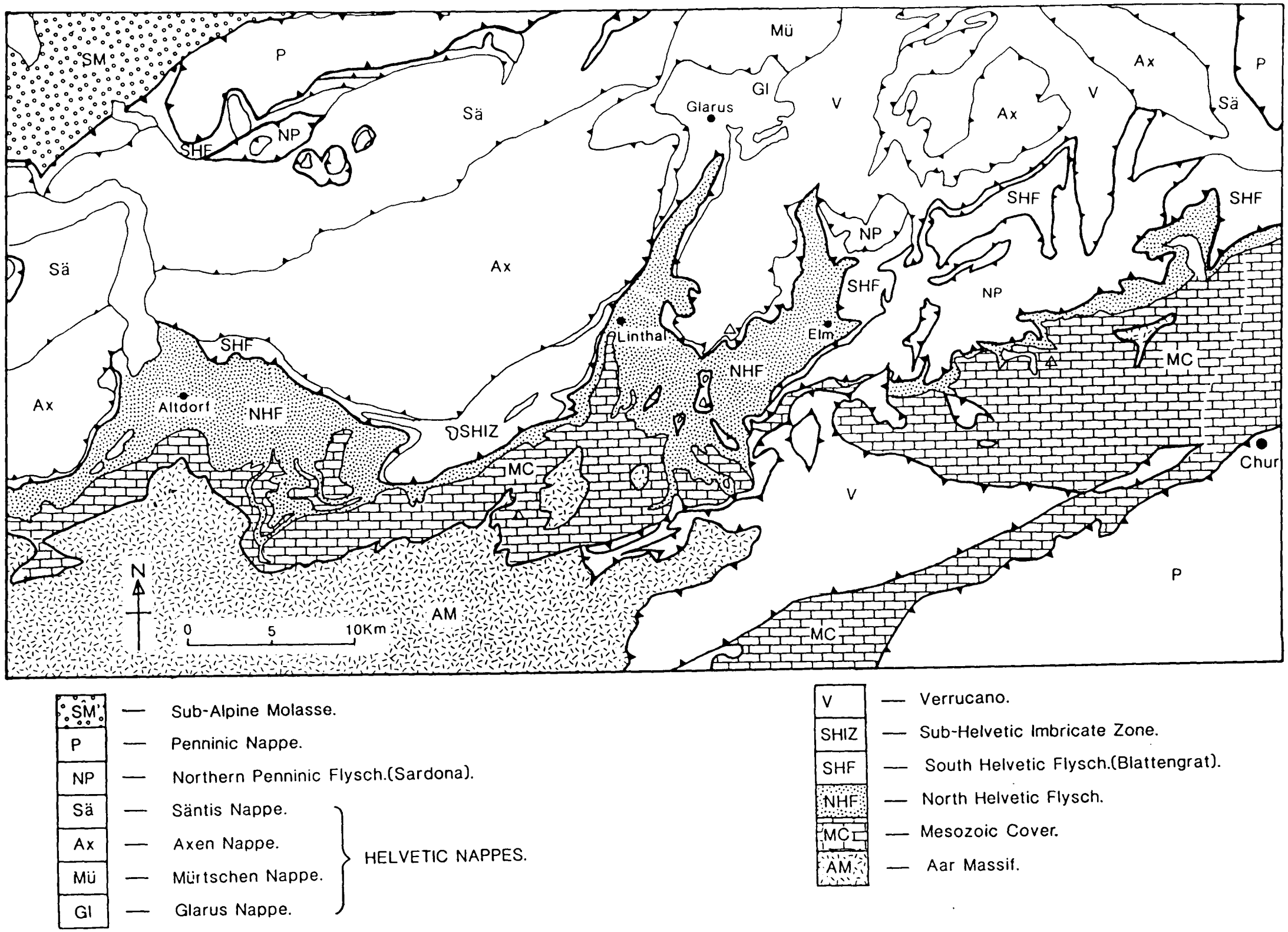

Fig.1.2. Close-up of Fig.1.1 showing the structure of Glarus and Graubunden area of eastern Switzerland. Ornamented units represent rocks exposed in the tectonic window through the Helvetic nappes (unornamented). The area of study is within the North Helvetic Flysch between Elm and Linthal.

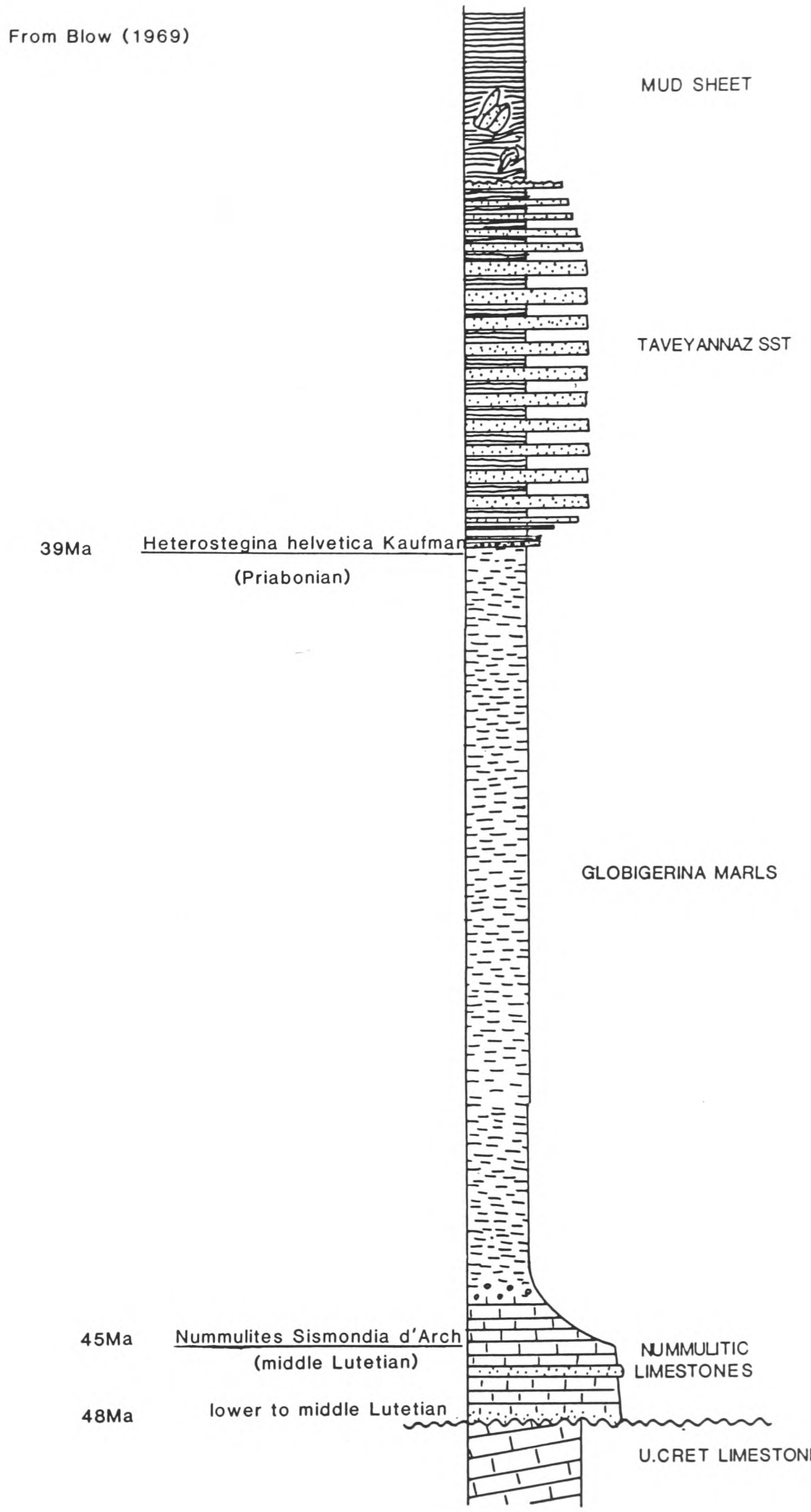

Fig.1.3. Simplified stratigraphy of the North Helvetic Flysch of eastern Switzerland.

CHAPTER 2

STRUCTURE OF THE TERTIARY ROCKS OF THE INFRAHELVETIC COMPLEX, GLARUS ALPS

2.1 Introduction

The tectonic window through the Helvetic nappes of E.Switzerland exposes the Infrahelvetic complex which comprises the Aar Massif with its Mesozoic and lower Tertiary sedimentary cover. The structural development of this complex is described in detail in Milnes and Pfiffner (1977). They recognise four phases of deformation, which they give locality names rather than numbers so as not to imply discrete structural phases, but instead a continuous development. The phases can be summarised as follows:

1) Pizol phase - initial emplacement of exotic strip sheets over the North Helvetic Flysch basin. The sheets include material of South and Ultra-Helvetic origin (Sardona and Blattengrat flysch units; Wegmann 1961).

2) Cavistrau phase - overthrusting of large overfolds of Mesozoic rocks of the Helvetics, now partially preserved under the Glarus Overthrust, described as Sub-Helvetic.

3) Calanda phase - regional folding and thrusting with penetrative cleavage. This dominates the Infrahelvetic complex.

4) Ruchi phase - localised upright kink bands associated with the last stages of movement on the Glarus Overthrust.

Milnes and Pfiffner (1977) suggest a middle Oligocene date for the onset of Pizol phase deformation. This research indicates that deformation of the Infrahelvetic complex commenced earlier, during deposition of the Taveyannaz sandstones in the Priabonian

(chapters 3+4). Deformation continued until the middle Miocene with minor movements within the overlying Helvetic nappes (Schmid 1975). The regional orientation of the maximum compressive stress was from the SSE, towards the NNW (figs.2.1 and 2.2).

The bulk of previous research into the Infrahelvetic complex of the Glarus Alps has focussed on regional structural work, leading to a large database of bedding, cleavage and fold readings (Siegenthaler, 1974; Schmid, 1975; Pfiffner, 1977;1978;1980). This enables a clear understanding of the general structural trends. The regional Calanda phase cleavage dips between 25-50 degrees to the SSE, with stretching lineations running down dip. Fold axes generally run WSW-ENE, although these can become strongly rotated in areas of high strain.

The aims of this research are to study the Eocene/Oligocene sedimentological and structural development of the Taveyannaz sandstones of Eastern Switzerland. It is therefore necessary to understand the tectonic deformation to discern the original positions of sedimentary sequences during deposition. To achieve this, we need to be confident in our knowledge of the orientation of the plane of maximum movement during deformation by the use of kinematic indicators.

2.2 Kinematic indicators and shear criteria

In order to evaluate the principal stress axis of deformation in this area it is necessary to describe the kinematic data obtained from this research, and previous literature (figs.2.1 and 2.2). Figure 2.1 illustrates the orientation of quartz and calcite fibre alignment, taken within the NHF from shear veins and pressure shadows. Shear veins are commonly found along thrust surfaces, or parallel to bedding; within the Globigerina marls, veins and pressure shadows run parallel to cleavage planes. The slight scatter of the data is considered to be

due to several stages of progressive mineral growth associated with stages of fold and thrust development, resulting in rotation of early formed fibres. The visual mean for mineral fibre orientations is 38°-153°.

Figure 2.2 illustrates stretching lineation data taken from deformed oolites of the Liassic Blegi Oolites of the overlying Helvetic nappes (Pfiffner, 1977). Each point represents the orientation of the long axis of a strained oolite, which have a regional axial ratio of 2:1:0.5. The visual estimate of the mean is 32°-165°.

Micro-structural shear criteria comprise fibre steps in shear veins, extensional shear zones in the multi-layered veins (fig.2.3), pressure shadows, tension gashes and micro-fold vergence. Figure 2.3 illustrates a multilayered vein with extensional shear zones indicating movement towards the NNW, this deformation post-dates an earlier cleavage formation causing fracture along the cleavage planes and thin calcite veins to form in a similar manner to tension gashes. The data from within the Taveyannaz sandstones consistently indicates northward movement, but within the Globigerina marls, localised evidence indicate an early phase of southward relative movement; this is discussed further in sections 2.3.2 and 2.3.3. All major fold and thrust structures indicate movement towards the north-north-west.

2.3 Regional cross-sections and structural development of the Tertiary.

The cross-sections illustrated in figures 2.4 to 2.7 show the present structure of the Tertiary rocks of the area. Figure 2.8 locates each of these sections with respect to the main structures of the region. Section 2.4 runs through the only exposure of the Aar Massif seen at the margins of the Limerensee reservoir, Kistenpass. The updomed massif plunges eastwards at about 5°. The sedimentary cover to the Aar Massif comprises a thick (800m)

Mesozoic sequence dominated by carbonates. There are two important detachment horizons within the Cretaceous, the lowermost being the lower Barremian Drusberg beds, and above that, the contact between the Gault and the Seewerkalk which represents the Albian/Cenomanian boundary. These surfaces enable detachment of the entire Tertiary sequence. Within the Tertiary, the upper 20m of the Globigerina Marls is an extremely weak horizon which accommodates the bulk of the folding and thrusting that occurs in the Taveyannaz Sandstones.

The late stage uplift of the Aar Massif not only resulted in an eastwardly plunge to the area, but also uplift in the south by about 1500m relative to the north. It can be seen from the cross-sections that the deformation within the Taveyannaz sandstones becomes more complex from south to north, until one reaches the Richetlipass Frontal Thrust (RFT). Within the area bounded to the south by the root zone of the Glarus Overthrust, and to the north by the RFT there are two main structural domains; the Southern and the Central domains. The dividing line between these two domains is the Jetzalp anticline (sections 2.6,2.7), and its westerly, along strike equivalent, the Muttsee Imbricate Zone (MIZ), (fig.2.8).

2.3.1 The Southern domain

The Southern domain is characterised by fold and thrust geometries that ramp up from the Upper Cretaceous and through the Nummulitic limestones then flatten out into the upper Globigerina marls. At Crap Ner in section 2.5 there is approximately 1Km of thrust duplication of the Nummulitic limestones and Seewerkalk. This deformation translates upward into arching of the Taveyannaz sandstones with various scales of folding detaching in the upper Globigerina marls. The change from discrete thrusts in the limestones to

distributed folding in the sandstones is a function of the extreme incompetence of the marls. Figure 2.9 illustrates a possible consequence of decoupling in the marls, allowing the limestones to act as an advancing chisel, with a passive roof backthrust for the upper detachment, indicating relative southward movement. Evidence of southward movement is seen in the Globigerina marls from the upper limb of the Jetzalp anticline (figs2.10a+b,2.11a+b). This demonstrates the superimposition of two cleavages, S_1 and S_2, the latter being the regional Calanda phase cleavage. S_1 is an earlier cleavage which has been strongly overprinted, and is preserved only in localised pockets. The intersection lineation of S_1 and S_2 (α25-242°) runs approximately parallel to the strike of S_2, indicating that S_1 had a similar WSW-ENE strike. Calcite fibre growth in pressure shadows around pyrite nodules are commonly found in S_1 planes, and indicate movement towards the south. S1 cleavage planes commonly develop calcite growth along them during the thrusting towards the north (figs.2.10a and b). It can be seen therefore, that in the hanging wall to major thrust ramps in the Nummulitic limestones, there is good evidence for early backthrusting, associated with calcite mineralisation.

Associated with the Calanda phase is the predominant asymmetric, northward folding of the Taveyannaz sandstones. Folds are harmonic through the sandstones on a decimetric scale, with axial planes moderately inclined towards the SSE, and varying interlimb angles from 30°-170°. Thinner bedded (<1m thick) units can produce chevron geometries, although rounded hinges are more common. Occasional thinning of the limbs in tighter folds can produce 1c type geometries. The contrasting sedimentology of the Taveyannaz sandstones between the Southern and the Central domains is reflected in the fold styles. The more massive beds of the Southern domain results in a more even distribution of stress, resulting in mainly cylindrical folding, whereas the thinner bedded units of the Central domain lead to a focussing of the stress, resulting in rotated fold hinges and non-cylindrical geometries

(see section 2.3.3 for data).

The only evidence for a major lateral structure running parallel to the transport direction is seen west of Panixerpass. The Panixerpass transverse line (Krüsi 1977; Pfiffner 1978) is located between the Chalchorn and Crena Martin (Figs.2.8+2.12), running NNW-SSE. A cross-section of the transverse line is exposed in the cliffs by Haxenseeli, 1Km east on the footpath from Panixerpass, and is illustrated in figure 2.13 from Krüsi (1977). This demonstrates the complexity of the Sub-Helvetic structures, with the Glarus overthrust which cuts through large scale, Cavistrau phase folding, verging into the transverse line from both the north-east and south-west. As seen in figure 2.12 there is a rapid reduction in the thickness of the Sub-Helvetic Malm limestones from north-east to south-west across this line. The Panixerpass transverse line is considered to have acted as a lateral ramp during Cavistrau phase folding and thrusting. The presence of Nummulitic limestones in this zone, and their lateral outcrop termination from the north-east, suggests that this was also an important structure during the deformation of the Tertiary.

2.3.2 The Central domain

The Central domain is defined as the area between the Jetzalp anticline and the RFT (fig.2.8). In the east, the lower limb to the Jetzalp anticline is highly imbricated, as seen in the lower part of Jetzalp (section 2.7). It is thought likely that this imbrication continues into the underlying limestones, as in the MIZ to the west. Immediately north of this is the Leiterberg Antiformal Stack (LAS) (sections 2.4,2.5,2.6), comprising three thrust sheets, each of about 500m stratigraphic thickness, culminating in an antiformal stack. These thrust sheets have a basal detachment in the upper Globigerina marls. The best exposures of structures within the LAS are seen on the footpath up to Wicklenmatt from the Wicklen

tank range, west of the Hausstock. At the base of the cliffs, where the path intersects the Leiterbergbach stream, there is an outcrop of the Globigerina marls (grid ref. 72618,19450). This is interpreted as being located on the overturned limb of the footwall syncline to the lower thrust sheet of the LAS (section 2.6). The marls are intercalated with silt laminae between 1-15mm thick, which are strongly folded on a 10cm scale, with a slaty axial planar cleavage. Bedding around this folding is plotted in figure 2.14, a best fit π-girdle indicates an average fold axial plunge of 35°-215°; the cleavage/bedding intersection lineations are parallel to the fold axis. Calcite veining occurs parallel and oblique to bedding. Figure 2.15 shows folded marl and silt laminae with a thin, bedding parallel veinlet with small scale folds and thrusts which indicate a southward relative motion. Associated with the veinlets are small tension gashes which also indicate a sense of shear to the south. This is similar to shear criteria associated with the S_1 cleavage in the upper limb of the Jetzalp anticline (section 2.3.2).

Continuing up the Wicklenmatt footpath for another 200m, on the left are the Leger cliffs. At this locality, bedding dips steeply to the south and is overturned; this is the upper limb of the footwall syncline to the lower thrust sheet (figs.2.5,2.6). Bedding and slickenside data taken from this outcrop are illustrated in figure 2.16; the fold axis plunges approximately 12°-257°, with 90% of the readings falling within 10° of the great circle for the π-girdle, indicating that within the area of the outcrop, the fold is cylindrical. The difference in the fold axis of this large scale fold compared to that illustrated in figure 2.14, suggests that there has been rotation of the fold axes towards the transport direction, associated with higher strain in the less competent marls.

As one reaches the edge of Wicklenmatt on the footpath, and crosses the Mattbach stream, one can view the south-west face of Erbserstock (fig.2.17). This exposes an oblique section through the foreland dipping thrust contact between the middle and upper thrust

sheet. The contact between the lower and middle thrust sheets can be seen approximately 50m up the Mattbach stream (grid ref.72575,19532), where there is a tight overfold in the Globigerina marls which have been smeared out along the base of the thrust (fig.2.6).

If one then climbs to the top of Erbserstock, and looks towards the southwest at Leiterberg, complex fold geometries can be seen, suggestive of refolding. Increasing complexity in the upper thrust sheets of an antiformal stack is to be expected as a result of overprinting during the growth of underlying sheets. Overprinting of structures of this kind is best illustrated in the western outcrops of the LAS in Hintersulz, north-west of the Hausstock (fig.2.4). The cross-section in figure 2.4 demonstrates an along strike variation in the structure of the LAS, where the basal thrust to the lower sheet cuts up through the middle sheet, causing major deformation of the upper sheets. This results in the overprinting of cleavages formed during the growth of each sheet (Fig.2.18).

The basal thrust to the LAS ramps up to form the Richetlipass Frontal thrust. This is exposed in the eastern part of the region, on the north-east face of Tierbodenhorn (Fig.2.19). Meso-scale (20m) folds exposed next to the thrust in the hanging wall have non-cylindrical geometries, indicating high strain near the thrust. The RFT can then be traced towards the WSW to the northern edge of Erbserstock, and then across Wicklenmatt to Richetlipass. Further to the west, the eastern face of Hintersulz reveals a thrust contact with a highly deformed hanging wall and a relatively undeformed footwall, intersecting the Barlisplanngenrus stream. It is considered that this is still the RFT, although it isn't directly along strike from the Richetlipass exposure; this could be due to an oblique frontal ramp to the RFT. At the present erosion surface, the general dip of the RFT is about 60° to the SSE, separating highly deformed rocks of the upper thrust sheet in the hanging wall to relatively undeformed beds in the footwall, this being the boundary between the Central and Northern domains.

2.3.3 The Northern Domain

The Northern domain is relatively poorly exposed, making stratigraphic correlation extremely difficult, reducing its significance to this research. In most localities of the RFT, the footwall is relatively undeformed, with a low angle northerly dip. A cross-section of the Northern domain up the Sernf valley between Engi and Elm is shown in Siegenthalers' thesis (1974, fig.2,pg.17). This illustrates intense northward vergent folding, without any thrusting; this is inevitably highly interpretive. It is possible that major thrust duplication of the stratigraphy occurs without any visible evidence, making stratigraphic work unsatisfactory.

The northern domain is extremely important, as it represents the link between the North Helvetic Flysch of the Infrahelvetic complex and the Lower Marine Molasse of the Sub-Alpine zone. Unfortunately, this contact becomes smothered by the Helvetic nappes as the Glarus Overthrust dives down to the north in the area of Schwanden.

2.4 Summary and Discussion

Deformation of the Tertiary rocks of the Infrahelvetic complex started during the Priabonian with the initiation of the Jetzalp anticline overlying a blind thrust (chapter 3). This thrust ramped up from the Upper Cretaceous to form a palaeohigh on the sea floor. The thrusting was constrained to the south-west by a lateral structure (Panixerpass transverse line) that continued to play a major role in the development of the Sub-Helvetic thrust sheets, until it was truncated by the Glarus Overthrust (fig.2.13). The Jetzalp anticline forms a dividing line between the Southern and Central domains which are characterised by

differing sedimentological and structural evolution.

As thrusting continued after the deposition of the Taveyannaz sandstones, so the upper Globigerina marls became a major detachment horizon. Localised backthrusting along this horizon suggests that the limestone thrust sheet chiselled into the soft marls which were overlayn by a rigid sandstone sequence, resulting in the formation of a passive roof backthrust.

Approximately contemporaneous to the thrusting of the Tertiary sequence was the emplacement of exotic thrust sheets over the entire Taveyannaz sandstone basin (Pizol phase); these include the Blattengrat and Sardona sheets. The stratigraphy of the Sardona sheet implies an Ultra-Helvetic palaeogeography (Wegmann,1961; Rüefli,1959). This leads to the conclusion that the Helvetic nappes are out-of-sequence with respect to a simple piggy-back succession. The Pizol phase is discussed in detail in chapter 4.

Pervasive deformation of the Infrahelvetic complex occurred during the emplacement of the overlying Helvetic nappes. This was the Calanda phase which resulted in intense folding and thrusting with a penetrative axial planar cleavage. Major thrust duplication of the Taveyannaz sandstones occurred in the Northern domain resulting in the formation of the Leiterberg Antiformal Stack. This comprises three thrust sheets which detach in the upper Globigerina marls. The upper sheet was transported a minimum of 3km northwards and was subsequently updomed and deformed during incorporation of its footwall. The presence of the extremely deformed basal thrust contact to the upper sheet has been interpreted as a major thrust detachment carrying what now forms the Northern domain from south of the present Southern domain (the Vorstegstock Thrust - Siegenthaler, 1974). The increasing thickness of the Taveyannaz sandstones from south to north towards this thrust was interpreted as due to active normal faulting during deposition of the Taveyannaz sandstones (Pfiffner, 1986). It is considered here that thickening in the footwall of the

upper thrust sheet is mainly the result of thrust duplication and does not represent true stratigraphic thickening.

The depth to detachment of thrusts can be observed in the field in the Southern domain. Thrusting in the Northern domain has resulted in at least 6km shortening, based on a simple area balance, but the extent to which thrusts involve the underlying limestones is unknown, and is not inferred on the cross-sections presented. It is possible that the RFT runs under the entire Northern domain at the level of the Globigerina marls until it is cut by the core thrust to the Jetzalp anticline. This would necessitate at least 6km of shortening in the limestones across the Jetzalp anticline. We do not observe 6km of shortening in the Taveyannaz sandstones across the Jetzalp anticline, but this may be the result of relative backthrusting of the sandstone sequence which acts as a rigid block overlying the incompetent Globigerina marls, for which there is evidence. It is considered likely that there is some deformation of the limestones under the Northern domain, as in the west of the area where imbrication of the limestones occurs in the footwall of the Jetzalp anticline (Muttsee Imbricate Zone).

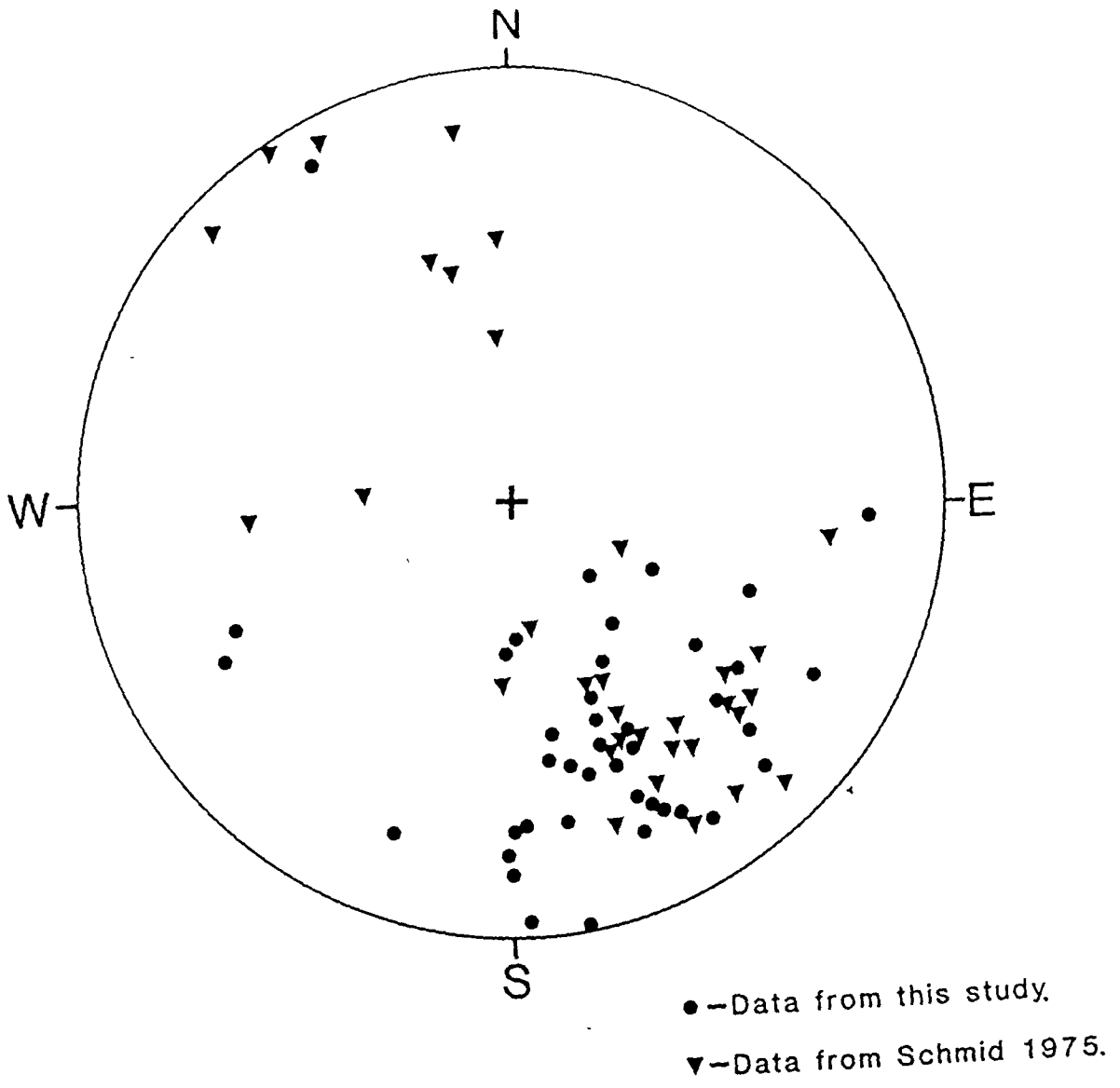

Fig.2.1. Mineral fibre lineations from within the Taveyannaz sandstones. Data from this study is based on calcite slickensides and extensional shear zones, this is combined with data from Schmid (1975). These have a dominant NNW-SSE trend.

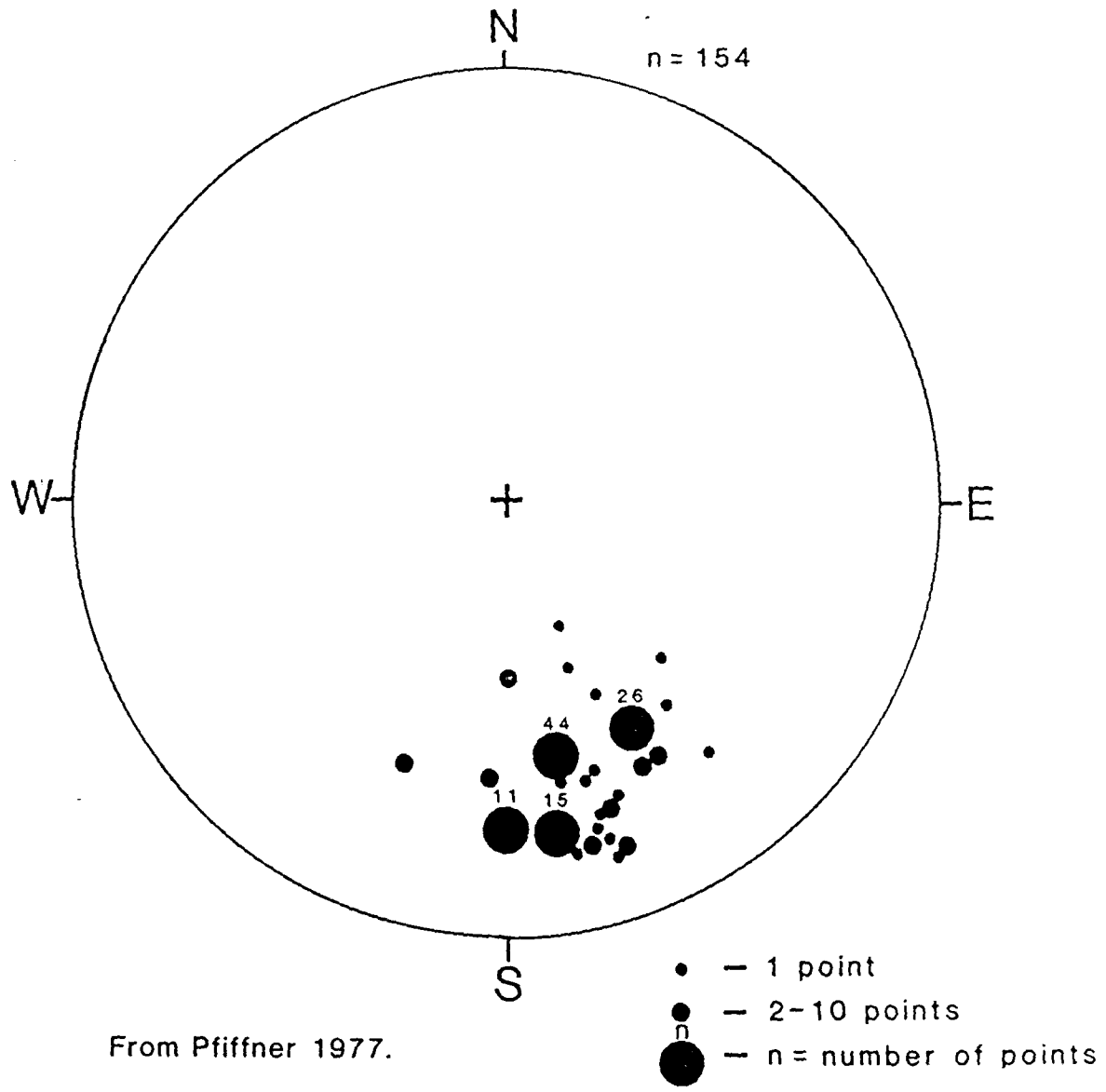

Fig.2.2. Stretching lineations from the long axes of strained oolites from the Liassic Blegi Oolite. These are taken from the Helvetic nappes, and show the same alignment as kinematic data from the Infrahelvetic complex (fig.2.1). Shear criteria indicate movement towards the NNW.

Fig.2.3. Extensional shear zones in multi-layered calcite vein showing downthrow to the right giving a dextral motion. This represents northward directed thrusting. This is overprinting the S1 cleavage, which results in using the cleavage planes as tension gashes, leading to veining parallel to the cleavage. This is a common feature of S1.

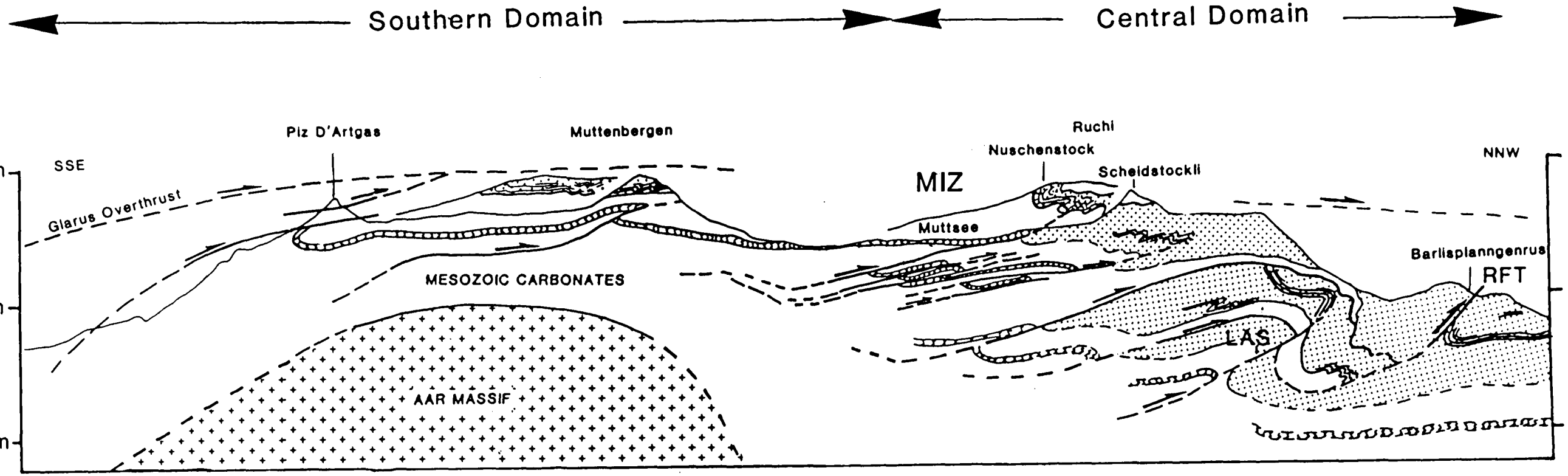

Fig.2.4

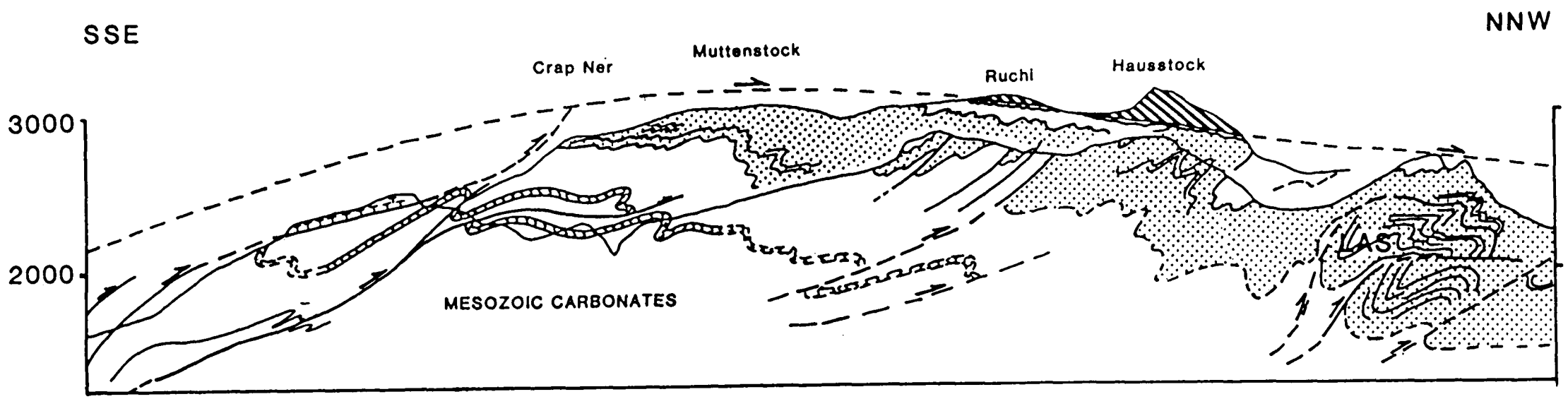

Fig.2.5

Fig.2.4. Structural cross-section from Piz D'Artgas to Barlisplanngenrus.

Fig.2.5. Structural section through Crap Ner and Ruchi.

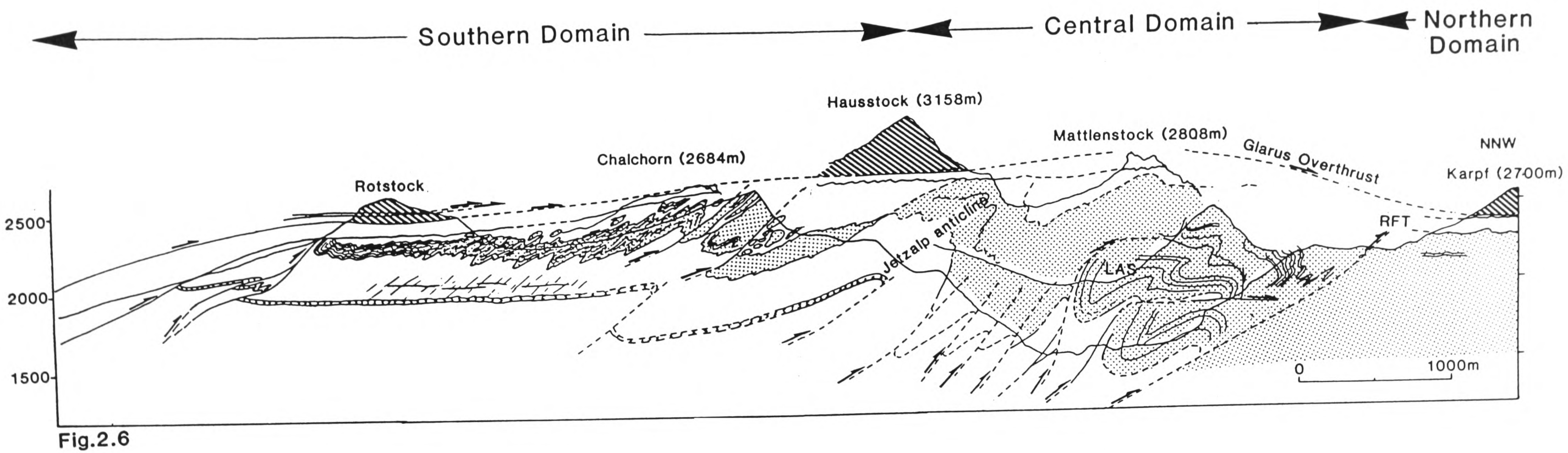

Fig.2.6

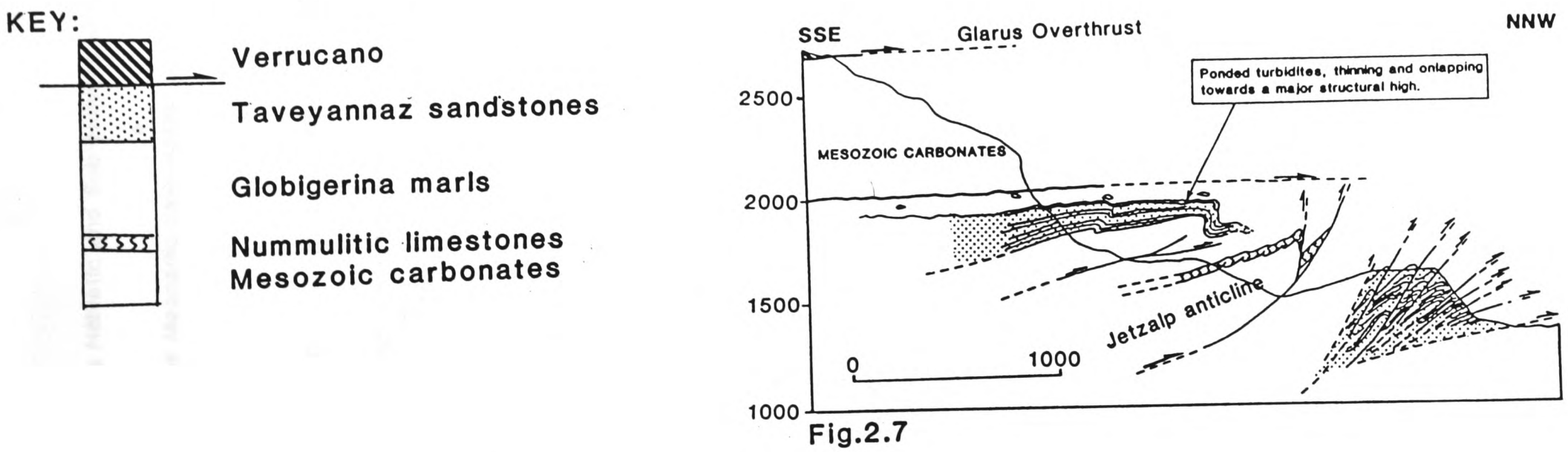

Fig.2.7

Fig.2.6. Structural section through Rotstock and the Hausstock.

Fig.2.7. Structural section through the type locality of the Jetzalp anticline. A detail of the Taveyannaz sandstones in the hanging wall is illustrated in fig.3.17.

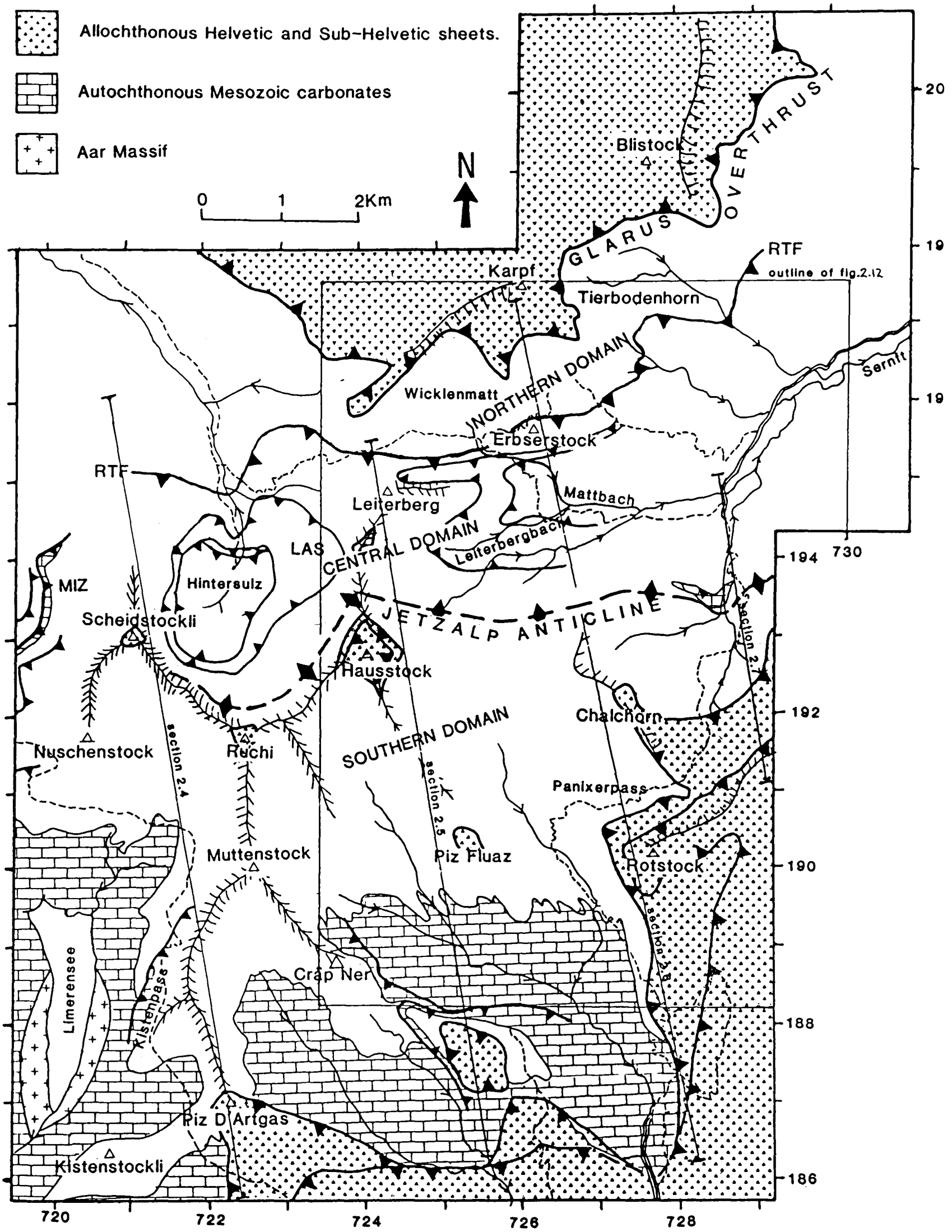

Fig.2.8. Structural map of the field area shownig main structural features discussed in text and locating structural sections.

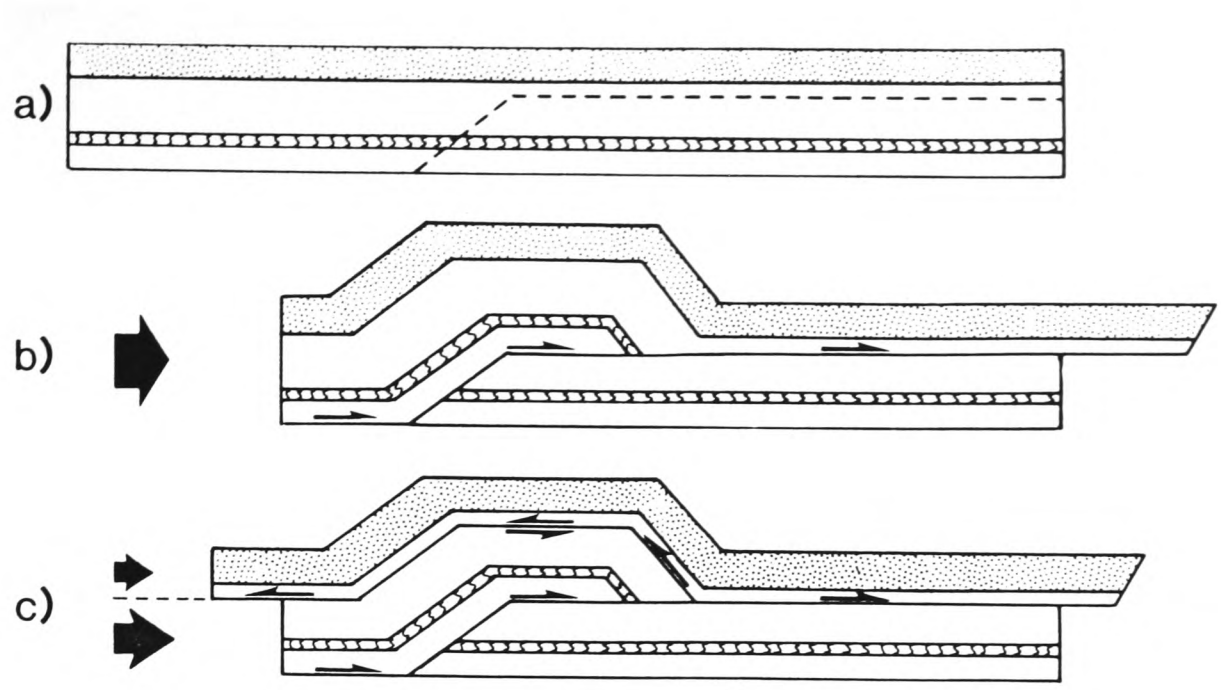

Fig.2.9. Suggested interpretation of the mechanism by which southward directed thrusting occurs in the globigerina marls. b) illustrates a thrust ramp from the mesozoic limestones into the marls, with the hanging wall strata behaving as an homogenous block. c) represents the proposed alternative to b), with a detachment surface in the Globigerina marls, resulting in the formation of a passive roof backthrust with a southward relative motion. This results from the sandstones acting as a rigid lid over the weak marls, this is probably enhanced by high pore-fluid pressures in the marls as indicated by the calcite mineralisation (figs.2.10 and 2.15).

a.

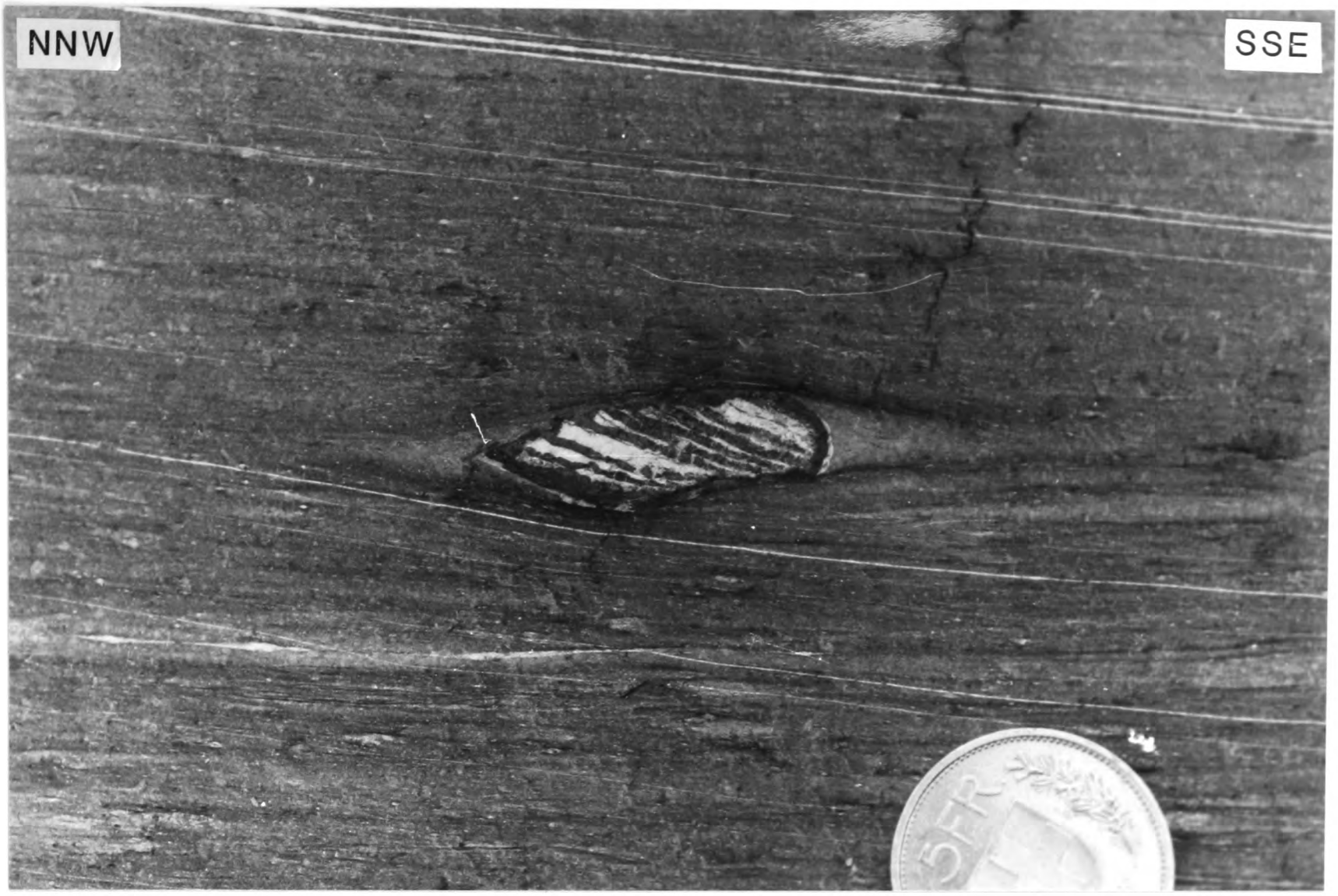

b.

Fig.2.10a+b. Calcite pressure shadows around fractured pyrite in Globigerina marls. These are good shear criteria, showing dextral motion by the fracturing of the pyrite in the nature of tension gashes. This represents motion towards the SSE and is associated with the S1 cleavage, which has later undergone extension perpendicular to the cleavage planes during the formation of S2 as shown by calcite growth along the cleavage.

a.

b.

Fig.2.11a+b. S2 overprint of S1 cleavage. a) shows folding of S1, with S2 developing axial planar to the fold. b) shows a close-up from a) with folded calcite pressure shadow around fractured pyrite following S1.

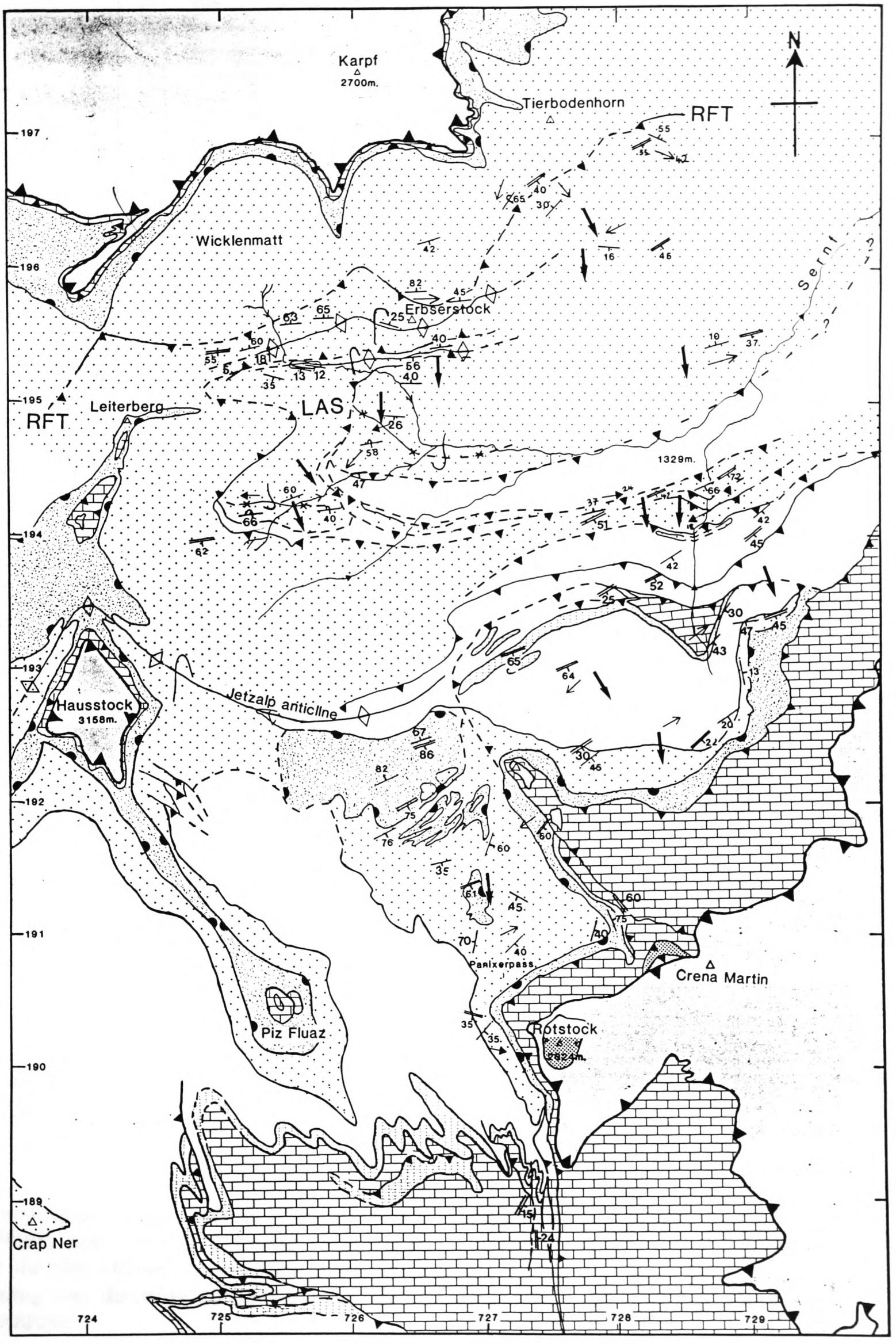
Karpf
2700m.
Tierbodenhorn
RFT
N
Wicklenmatt
Erbserstock
Sernf ?
Leiterberg
RFT
LAS
1329m.
Hausstock
3158m.
Jetzalp anticline
Piz Fluaz
Panixerpass
Crena Martin
Rotstock
2912 m.
Crap Ner
197
196
195
194
193
192
191
190
189
724
725
726
727
728
729

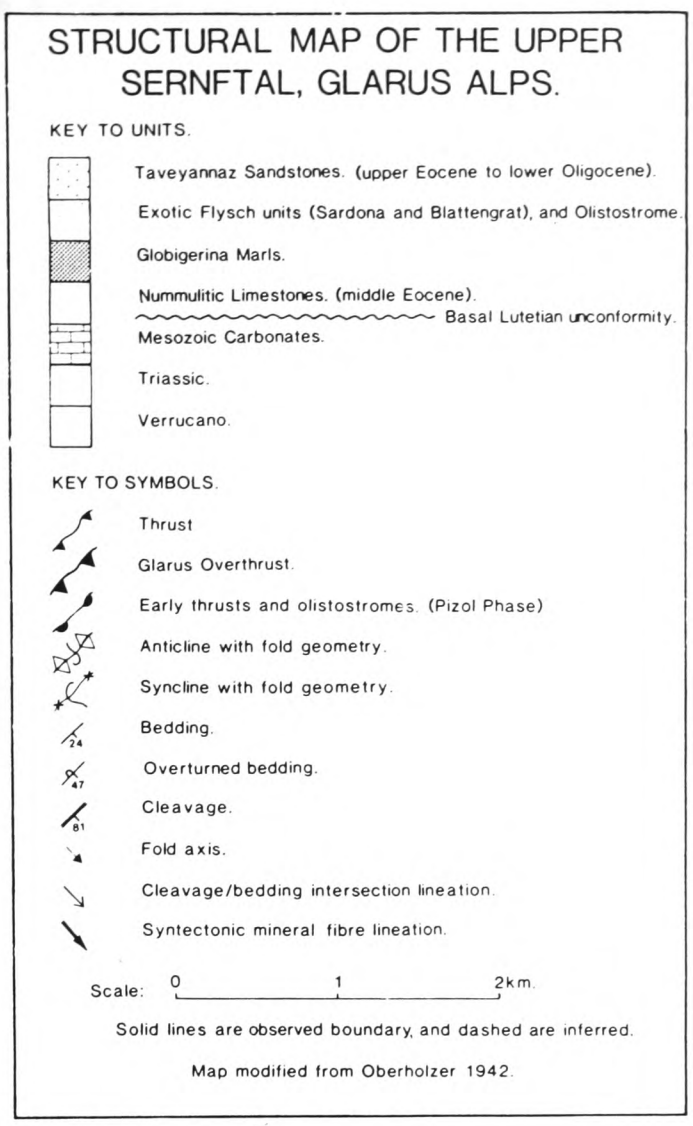

Fig.2.12. Previous page - Structural map of upper Sernftal and Panixerpass region. Located on fig.2.8. Key is above.

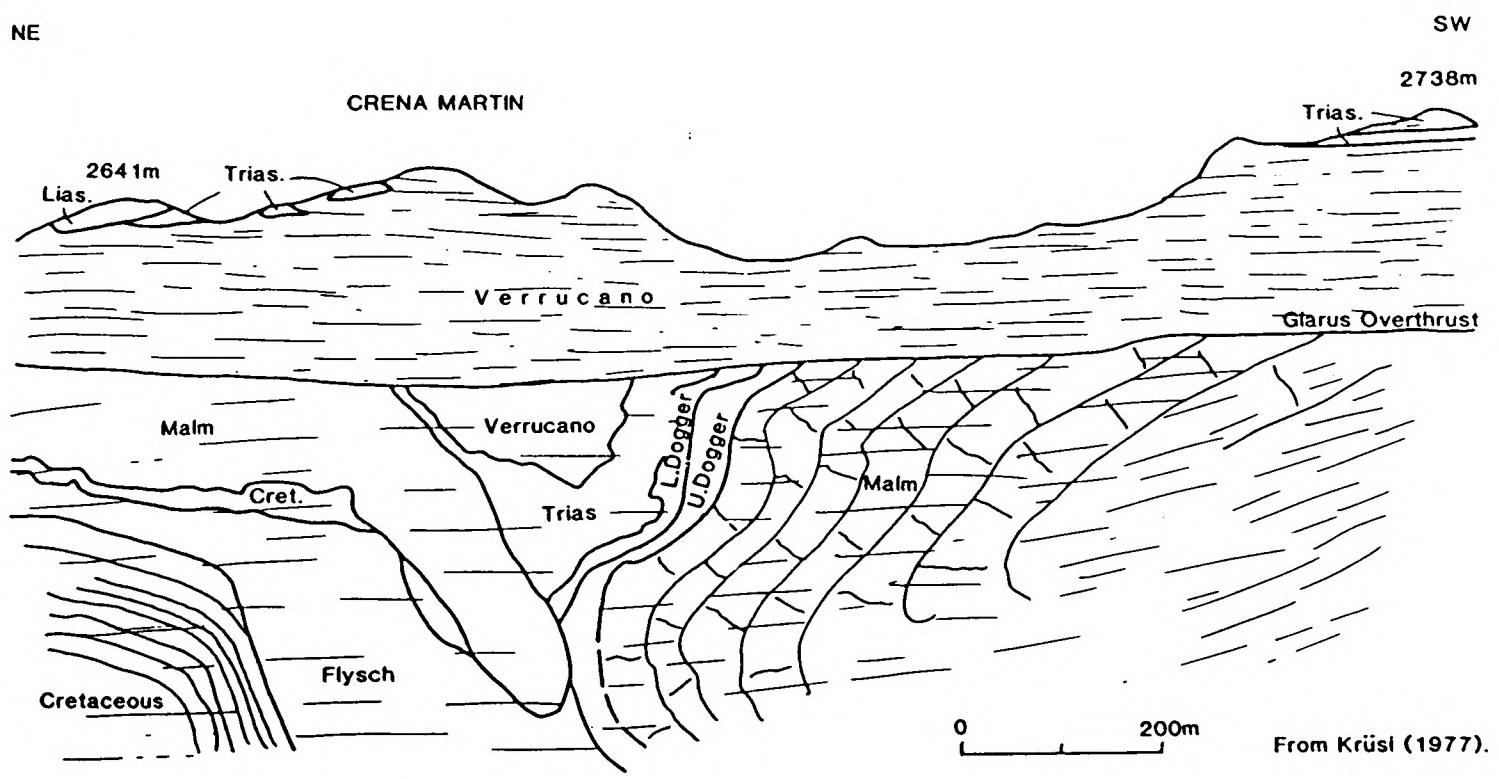

Fig.2.13. Panixerpass lateral zone as exposed on the south side of Haxenseeli (grid ref.72810,19095) from Krüsi (1977).This shows convergent folding from southwest and northeast in the Sub-Helvetic limestones; demonstrating the use of this structure as a lateral ramp to folding and thrusting during Cavistrau deformation. This is then truncated by the Glarus Overthrust.

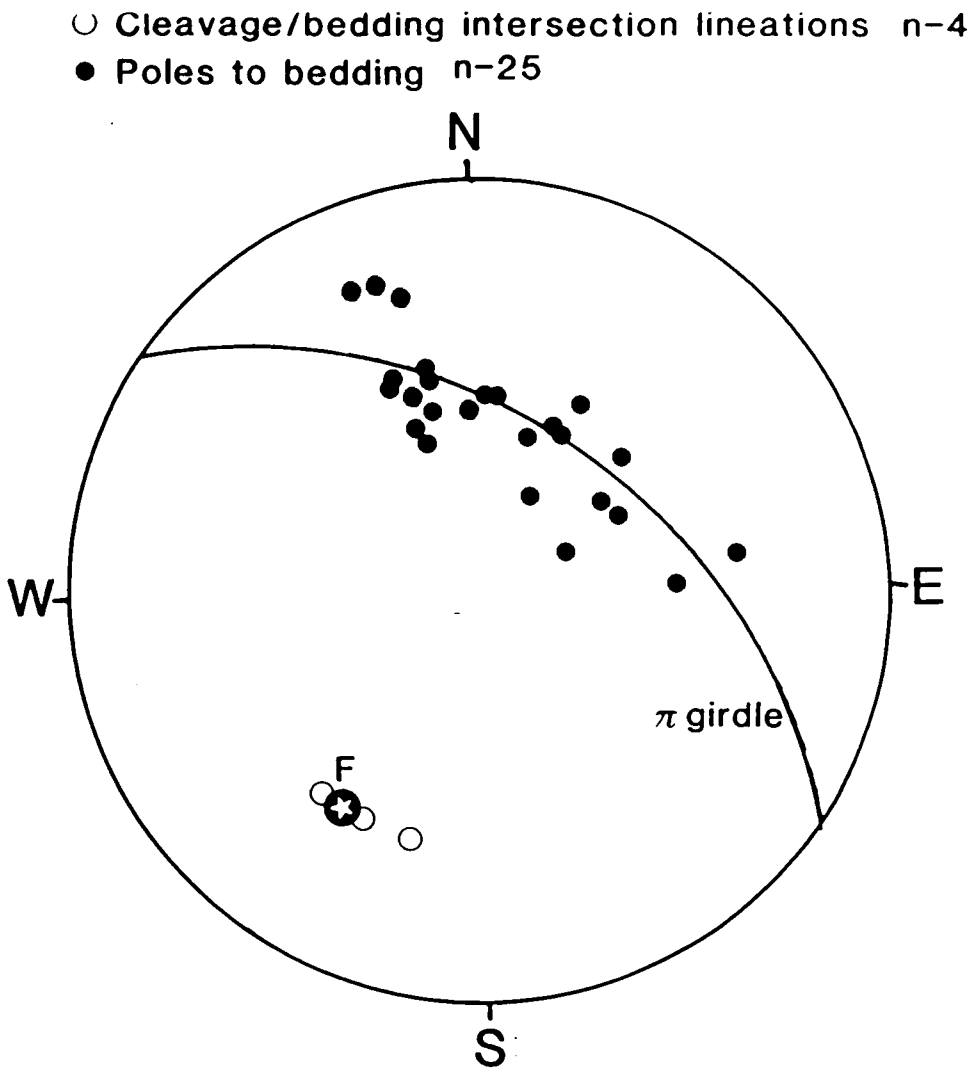

Fig.2.14. Poles to bedding in minor folds within the Globigerina marls of the Central Domain (grid ref.72618,19450). The fold axes have been rotated towards the thrust transport direction, and the spread of points around the pi girdle indicate a sub-cylindrical geometry. Compare this to fig.2.16.

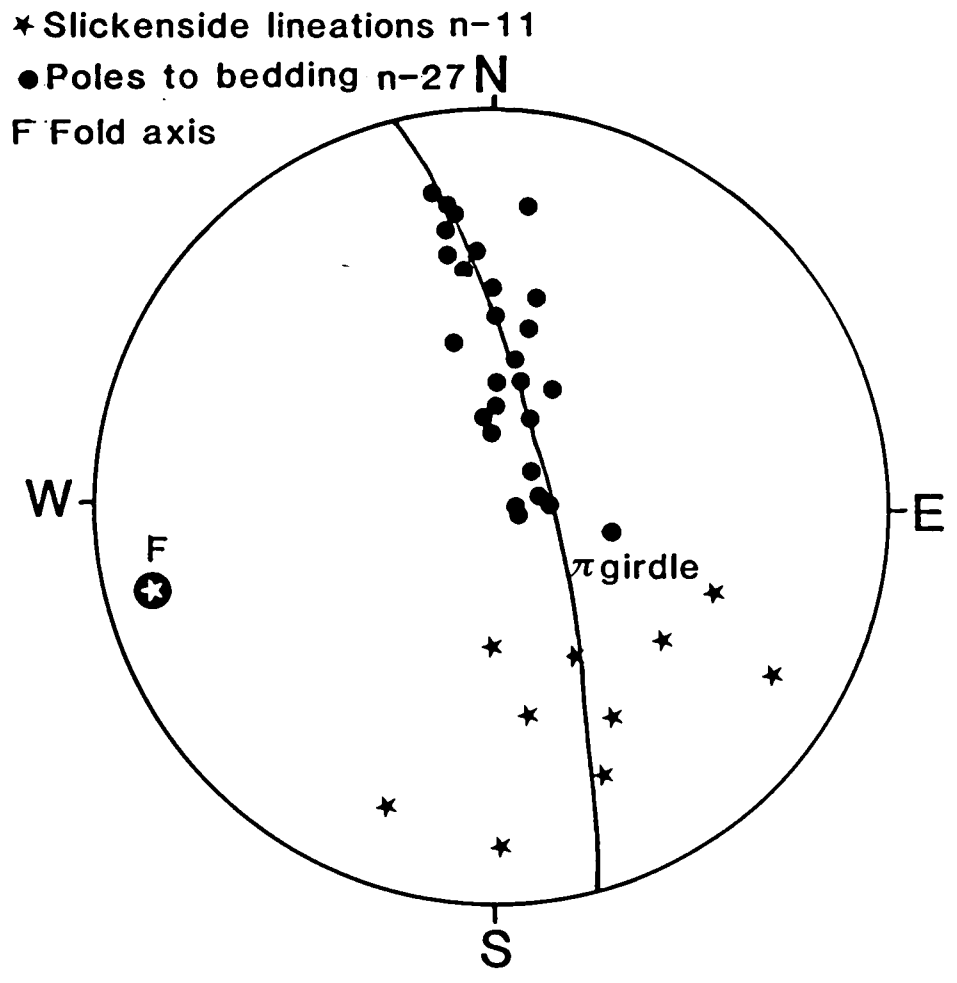

Fig.2.16. Poles to bedding in large scale footwall syncline in lower thrust sheet of LAS, Central domain. The fold axis is perpendicular to the thrust transport direction, and data are closely distributed around the pi girdle indicating a cylindrical nature to the fold. This is in contrast to the folding in the less competent marls illustrated in figure 2.14.

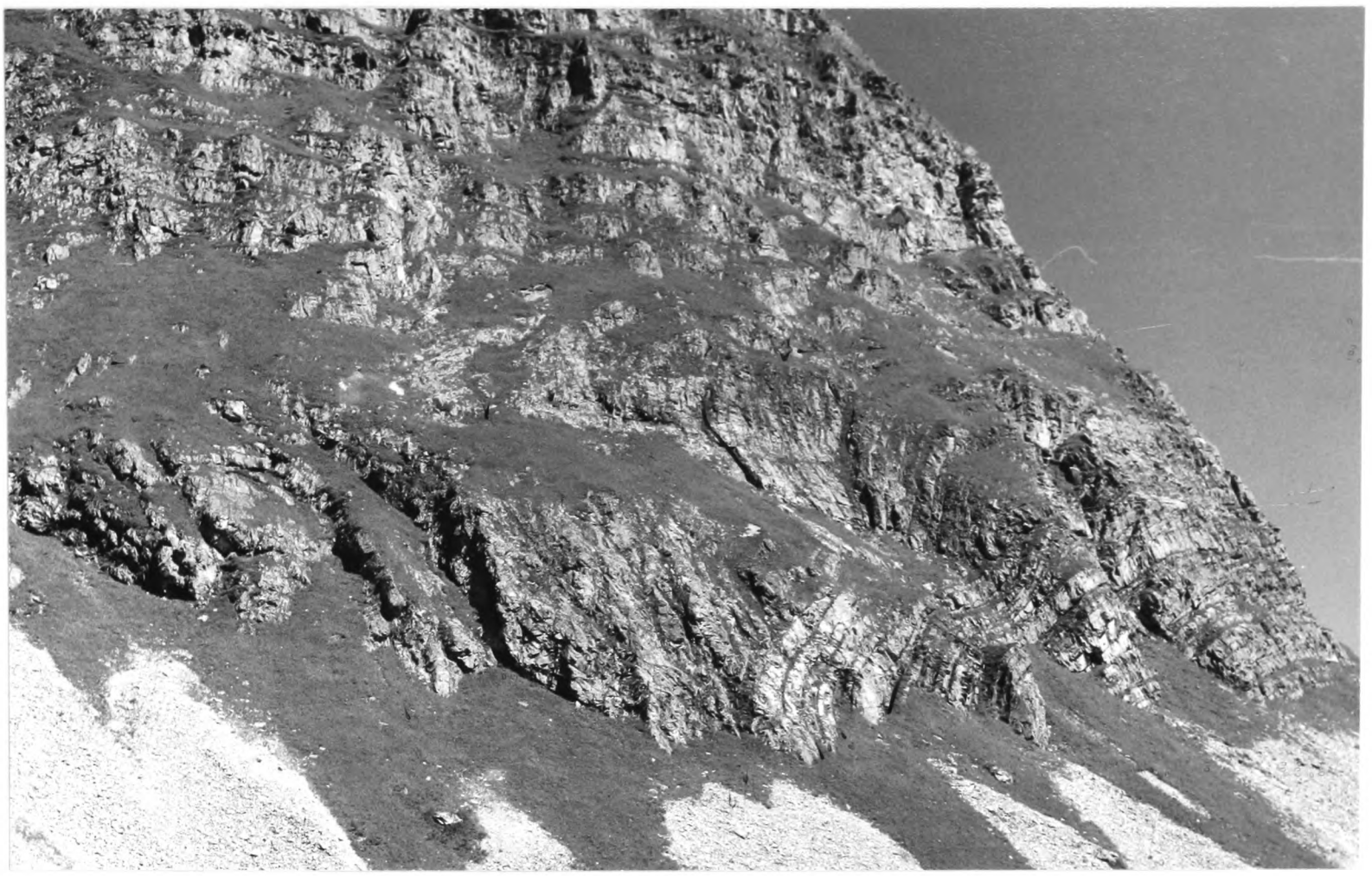

Fig.2.17. View of southwest face of Erbserstock, showing foreland dipping thrust at the front of the LAS separating the lower sheet from the middle sheet.

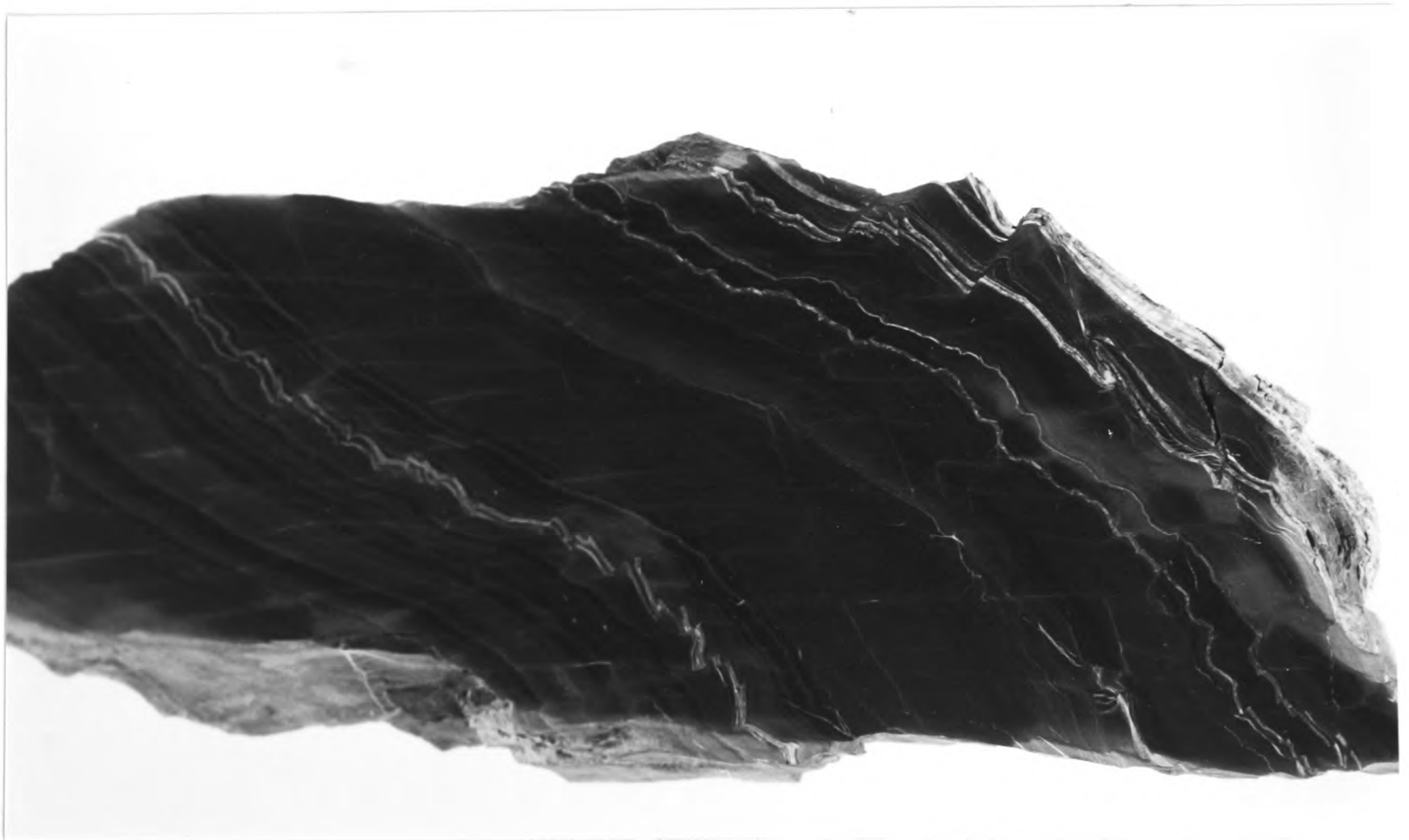

Fig.2.15. Hand specimen of marls from locality in fig.2.14. Thin calcite veins occur parallel to silt laminae. Close inspection of the geometry of minor folds and faults in these veins indicate that they are not related to the cleavage. These minor structures show a vergence towards the SSE, and are considered to represent the S1 associated southward relative movement in the marls (figs.2.10 and 2.11).

a.

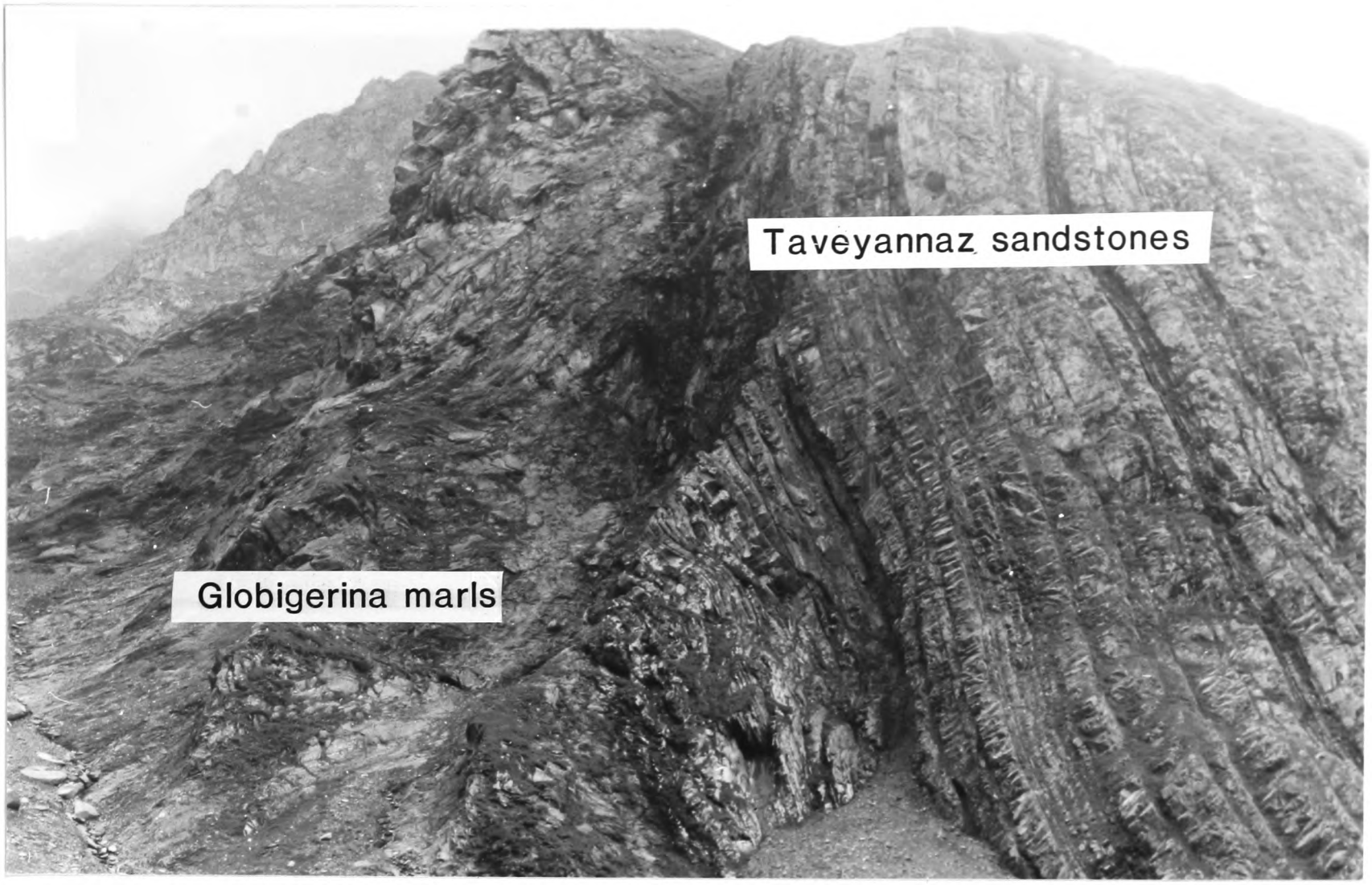

b.

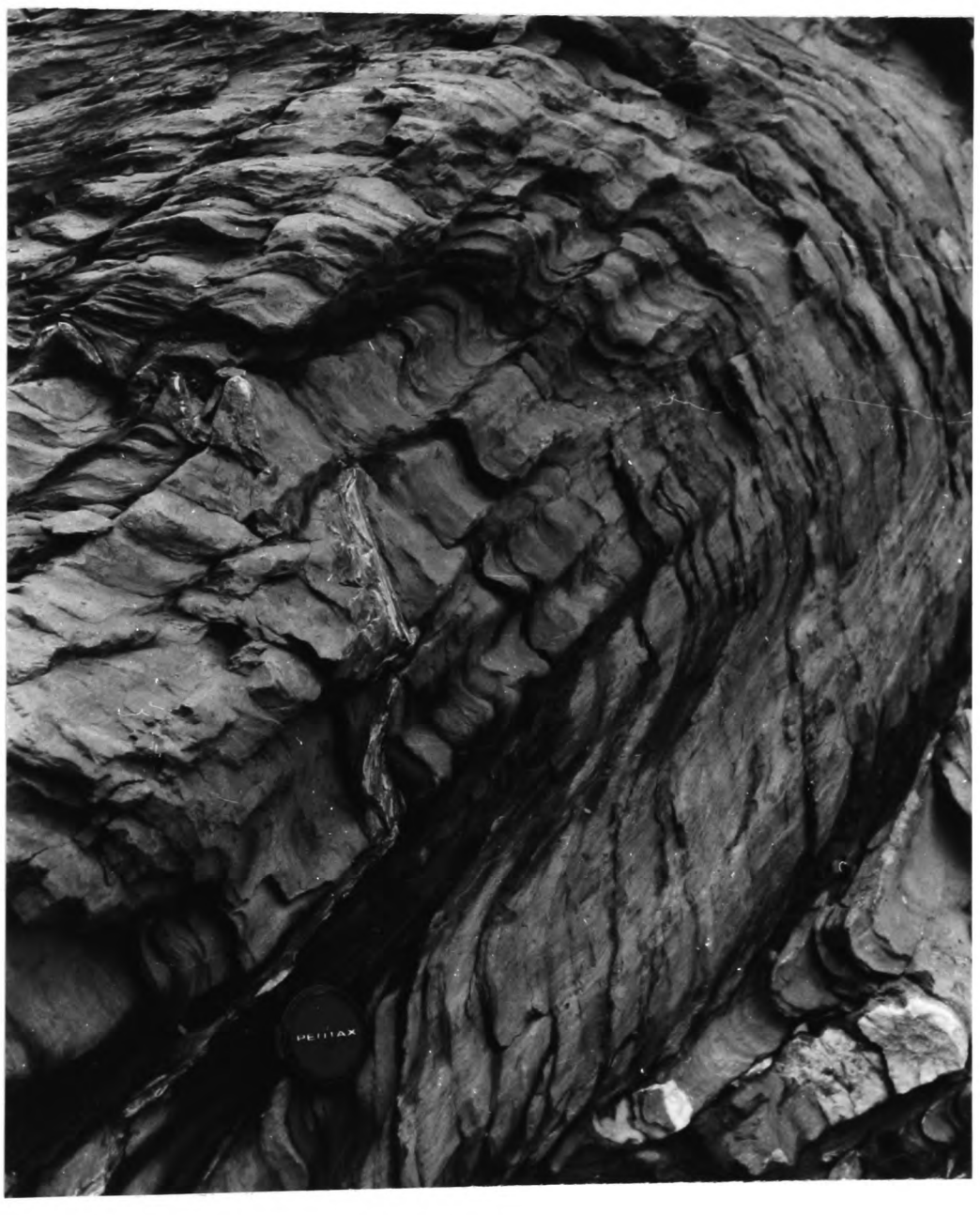

Fig.2.18a+b. a) Globigerina marl/Taveyannaz sandstone contact in the hanging wall of the middle thrust sheet of the LAS in Hintersulz, Central domain (grid ref.72220,19415). Note steeply dipping thrust towards the foreland. b) Close-up of structure in marls. This demonstrates an early cleavage formed during the initial thrusting of the middle sheet. This is then truncated by a spaced crenulation cleavage formed during the formation of the underlying lower thrust sheet. Note the rotation of the multi-layered vein with slickensides formed parallel to the first cleavage. These two cleavages are not called S1 and S2, as are formed under different circumstances to those of the Southern domain.

CHAPTER 3

SEDIMENTOLOGY OF THE TAVEYANNAZ SANDSTONES

3.1 Introduction

The Taveyannaz sandstones of the Glarus region have been studied by looking at their overall sediment-body geometry, their relation to the underlying Globigerina marls and by detailed measurement of sedimentary sections. If these sections are to be interpreted correctly, it is essential that they are related in terms of their palaeogeography during deposition. Their present geograhical locations are shown on figure 3.1. This is totally reliant on the understanding of the cross-sections described in the previous chapter. Figure 3.2 attempts to illustrate the relative structural positions of the sedimentary sections on a simplified cross-section through the area. Precise relative palaeogeographic locations can be achieved with confidence in the Southern domain, but within the Central and Northern domains the structural sections have more uncertainties, resulting in merely qualitative positioning of the sedimentary sections. Figure 3.3 attempts to relate the sections in terms of the overall stratigraphy. Unfortunately, the only reference point for this is the Globigerina marl contact.

The area is divided into two depositional environments which are closely linked to the three structural domains (Southern, Central and Northern). The Jetzalp anticline, separating the Southern and Central domains is considered to be a fundamental boundary during the deposition of the Taveyannaz sandstones. Consequently, the term Inner basin will be synonymous with Southern domain when referring to sedimentation; the Central and Northern domains are likewise synonymous with Outer basin.

The classification of turbidite systems into distinct sedimentary facies has evolved from the early scheme of Bouma (1962) to the more complex systems of Mutti and Ricci-Lucchi (1972,1975). The most recent attempt by Pickering et al (1986) is more complex still, forming an extremely useful reference source, but an impractical facies classification for every-day use. Without discussing the numerous other schemes that have been proposed for varying types of turbidite systems (Piper, 1978; Stow and Shanmugan, 1980; Lowe, 1982), I will clarify the approach taken in this research. The purpose of facies analysis is to facilitate the description and communication of information on sedimentary sequences. Therefore, any proposed facies scheme must be kept simple, easily definable, and purely descriptive. More complex schemes commonly infer knowledge of the process of deposition and occasionally the environment of deposition. Application of these schemes encourages the description and understanding of new sequences by the use of subjective pigeon-holing rather than objective scientific observation.

A simpler and more broad-based scheme cannot on its own infer either process or environment, and requires a more detailed literary description to enable any sort of interpretation. The Inner basin sequence is described in terms of four basic facies: 1) very thick bedded sands, 2) homogenous muds, 3) thick to medium bedded sand/mud couplets, and 4) thin to finely bedded silt/mud couplets. The Outer basin is then described in terms of three facies: 1) amalgamated sands, 2) sand/mud couplets, and 3) thin to finely bedded silt/mud couplets. Abbreviations of these classes is avoided. These classes do not have distinct characteristics other than that suggested in their names, and will inevitably have many features in common between them.

The column to the left of each of the sedimentary sections is a three point moving average bed thickness curve with a 1m spacing. Thickening upward trends have been used to identify cyclic sedimentation in turbidite lobe systems (Mutti and Ghibaudo, 1972;Ricci-

Lucchi and Valmori, 1980), with particular attention paid to the work of Ghibaudo (1980) in the Macigno Formation, Apennines. Ghibaudo produced bed thickness curves by plotting the thickness of each sand layer opposite the top of the layer; Hiscott (1981) demonstrated that this procedure results in an upward skew of the peaks, causing a bias in favour of thickening-upward cycles. For this research, it is considered that a moving average curve with a fixed spacing would provide the most objective statistical method.

The sedimentary sections from the region will be described in detail using this simple facies scheme plus the bed thickness curves, with interpretation of the processes involved in deposition of the sediments. Bed thicknesses are defined according to Ingram (1954): laminae, less than 1cm; very thin beds 1-3cm; thin beds, 3-10cm; medium beds, 10-30cm; thick beds, 30-100cm; and very thick beds, greater than 100cm. Section 3.4 discusses the interpretation of the environment and of the controlling parameters on the deposition of this turbidite system.

3.2 The Inner Basin

Six sedimentary sections were measured from south of the Jetzalp Anticline, and are considered to have similar characteristics representing the Inner basin. These sections are discussed firstly in terms of the contact between the Taveyannaz sandstones and the underlying Globigerina marls. Then, a description of the sedimentology is given, followed by an interpretation of the environment.

3.2.1 The Globigerina Marl/Taveyannaz Sandstone contact.

The Globigerina marls comprise up to 400m of highly cleaved, homogeneous calcareous

mudstones. They have a flecked, light grey appearance with a buff coloured weathering. These marls contain many foraminifera, with plankton/benthos ratio of between 50 and 80%. The spectrum of benthonic types indicate water depths of several hundred metres (Eckert, 1963; Herb, 1988). When cleavage and bedding surfaces are parallel, many tubular foraminifera can be seen lying on the bedding planes, weathering to a deep rusty brown. These are 1-2mm in diameter and up to 3cm long, with occasional dichotomous branching. The many fragments of these foraminifera show a strong alignment running approximately NNW/SSE (fig.3.4). This alignment is slightly oblique to the maximum extension direction associated with the structural deformation of the area (figs.2.1,2.2). Figure 3.3 is the traced surface of a representative slab of the Globigerina marls. This demonstrates that the foraminifera alignment is not tectonic, but an earlier feature. The alignment is interpreted as due to current activity on the sea-floor rotating the tubular foraminifera into parallelism to the current flow. The maximum tectonic extension direction can be accurately measured on the slab using calcite fibre orientation in pressure shadows, and this shows a 25° divergence with the alignment of the foraminifera. There is also a lack of any significant internal structural linear fabric in the marls that would be expected with such a strong alignment.

The transition between the marls and the overlying sandstones is extremely variable. The sedimentary sections from Piz Fluaz and W. Ober Stafel show a sharp contact into the sandstones, with the marls being directly overlain by a massive sandstone (figs.3.9,3.6). In the other sections from the Inner basin, the contact is more gradual. At N. Ober Stafel and Rotstock the marls are replaced over 5m by dark grey, finely laminated micaceous muds with occasional iron pyrite-rich layers, followed by a medium to thick sandstone bed (figs.3.5,3.6).

The section at Muttenbergen displays a quite different sequence of lithologies. Within

the top 5m of the marls are three distinct beds (fig.3.11), the lower bed is 15cm thick and coarsens upwards from marls to a med./coarse sandstone. The lower 5cm of the bed is rich in clasts of the marls, and a light grey limestone. The bed is capped by 1cm of horizontally laminated fine sands. The inverse grading of the matrix of this bed indicates that deposition invloved grain support by dispersive grain pressure, although the bed is too thick to have been transported far as a grain-flow (Lowe, 1982). The most reasonable interpretation is that the transport mechanism was a turbidity current, and that after the deposition of the medium and coarse sands, downslope movement caused shear in the bed, resulting in inverse grading. During this, the fine sand component was deposited as horizontal laminae from the tail end of the turbidity current.

Immediately overlying this bed is a 10cm thick normally graded sand deposited as a turbidite, containing similar clasts to the underlying bed, and capped by horizontal laminated fine sands. These two beds exhibit slumping and syn-sedimentary normal faulting reflecting slope instability. Above these beds are more marls, containing a 10cm limestone band, which are then followed by sands and muds of the Taveyannaz sandstones.

Styger (1961) describes a micro-conglomerate located at the Globigerina marl/Taveyannaz sandstone transition from the top of Kistenstöckli, approximately 2km south of Muttenbergen. This contains clasts of Lower Cretaceous limestones. It would seem likely that the lowermost bed described above, correlates with the Kistenstöckli micro-conglomerate.

In summary, the Globigerina marl/Taveyannaz sandstone transition of the Inner basin is extremely variable. In the eastern part of the basin, large turbidite sands were deposited directly on the marls in part, but within 1km, a much more gradual transition is to be found. It is possible that the former contact represents a slightly irregular scour surface, and that in pockets, the laminated muds and silts have been removed by erosion; although no

signs of truncation were observed, this would be hard to see due to the intense cleavage overprint.

The Kistenstöckli micro-conglomerate (Styger, 1961) and the clast-rich inverse graded bed at Muttenbergen indicate erosion of the Cretaceous limestones prior to deposition of the Taveyannaz sandstones (see section 3.2.3).

3.2.2 Sedimentology

The sedimentology of the Inner basin is characterised by the intercalation of very thick bedded sands with thick muds and finely bedded sands, silts and muds. These facies are described with reference to the relevant sedimentary sections:

1) Very thick bedded Sands

The very thick bedded sands range from 1m up to 10m in thickness, comprising fine sands (Log Piz Fluaz) to very coarse sands (Log Chamerstock). Bedding is laterally traceable for up to 1.5km, with little signs of variation, except when approaching the Jetzalp anticline where thinning of the beds is prominent (fig.3.17).

The internal grain-size distribution varies between beds. A constant upward decrease in grain-size is most common, occasionally with a coarse tail at the base of beds. Approximately 20% of the beds have a practically uniform grain-size distribution, consisting of coarse sands with a sharp upper contact into fine sands and silts (Log Chamerstock between 20-30m, and at 70m). The medium and fine sand component is mixed in with the coarse sands as a result of rapid dumping of sediment out of suspension from the turbidity current.

Commonly, rather than a gradual grain-size reduction up through a bed, there are sharp grain-size changes dominating the upper section of individual massive sands (see log Chamerstock between 0-10m and 40-50m), 90% of the breaks involve an upward decrease in grain-size. The extent to which the grain-size varies across a break is extremely variable, commonly involving very minor changes in grain-size. Each of the breaks are considered to represent an amalgamation surface between two turbidite sands deposited in rapid succession. The extent to which amalgamation surfaces are preserved as distinct surfaces varies rapidly along the bed; surfaces occasionally become enhanced by the occurrence of small mud-clasts, but may also disappear due to intense mixing of the sands. Amalgamation surfaces in very thick bedded sands have been described by Pickering (1979) in terms of thinning and fining upward packages within massive sand units from the Kongsfjord formation, Norway. These are interpreted to result from the steady reactivation and backstepping of a slump scar causing repeated turbidity currents in rapid succession. Similar grain-size changes are described from the Cloridorme formation, Quebec, by Pickering and Hiscott (1985). This has been suggested to result from reflection of turbidity currents within a confined basin. This mechanism is not thought applicable in the present case, as it is considered unlikely that repeated flow reversals would maintain sufficient flow velocities to carry coarse sands in suspension.

The base of the very thick bedded sands is commonly planar. Less than 50% have grooves or flutes on the base; these indicate a range of flow directions from 010° to 103°, with an average value of 060°. All flutes indicate flow towards the east. Occasional large scours can be seen as illustrated at 21m on Log Chamerstock, where a gulley cuts approximately 1m deep into the underlying muds.

Sedimentary structures are rare, the most common feature being a pronounced horizontal layering, often comprising over 70% of the bed (Log Piz Fluaz; fig.3.12). The layers

consist of 0.5-1.0 cm thick mica-rich zones, with the mica flakes flattened along the layers, intercalated with 2-5 cm thick medium and coarse sands which show no signs of grading. These are not thought to represent either upper or lower flow regime horizontal lamination due to the thickness, and the lack of grading. Similar scale layering is described by Lowe (1982) from the Precambrian Thunderhead sandstones, S. Appalachians, and by Hiscott and Middleton (1979) from the Tourelle formation, Quebec. The Thunderhead sandstones contain 5-15cm thick units which have a basal micaceous shear lamina, overlain by inversely graded sands. These are interpreted to result from the successive "freezing" of traction carpets; the term traction carpet is a misnomer as they actually represent modified grain flows (Lowe, 1976). The formation of these stacked traction carpet units is summarised in figure 3.10.

Within the Taveyannaz sandstones, the lack of inverse grading puts doubt on this horizontal layering representing traction carpets. Inverse grading results from the shear sorting of grains supported by dispersive grain pressure. In this case, the mica content, and the poor sorting in the sands reduces the internal shear and the dispersive grain pressure respectively. The high levels of mica in the sand aids the formation of an extremely efficient basal shear lamina allowing the sand-rich upper part of the traction carpet to effectively float with little internal shear. It is likely that this process is aided by high pore fluid pressures in the basal shear lamina. The sands contain a large amount of suspended fines, which reduces the effective weight of the larger grains and hence the influence of dispersive pressure. In this example, the traction carpet is a density modified grain flow (Lowe 1976) underlain by an extremely efficient mica-rich basal lamina. Figure 3.14 demonstrates the difference between this, and the previous examples from Lowe (1982) and Hiscott and Middleton (1979).

Other internal structures include horizontal lamination in the fine sands, sometimes

becoming convolute leading to the development of pseudonodules in layers which are rarely greater than 10cm thick. Within the upper third of a very thick bedded sand are occasional sand injections from the coarse sand into the overlying medium and fine sands (between 50-70m, Log Muttenbergen). The injections are up to 50cm thick, dominantly forming irregular sills with thinner interconnecting dykes. Above 70m on Log Muttenbergen, the upper two thirds of two massive sandstones consist entirely of irregularly injected sands. These are dominantly bedding parallel and are considered to have acted as zones of decollement, allowing downslope movement of the overlying beds prior to lithification. This is discussed in the context of regional soft-sediment deformation in chapter 4.

2) Homogeneous muds - including injected sands

The homogeneous muds are found on top of the very thick bedded sands described above. They range from a few centimetres up to 5m of highly cleaved, dark grey structureless muds. These muds are considered similar to the thick mud-caps described by Pickering and Hiscott (1985), deposited from a concentrated mud-cloud in a confined basin. In their example, the size of the mud-cap is related to the thickness of the underlying sand bed. In this case there seems to be no such correlation; for example compare Log Muttenbergen between 30 and 60m to Log Piz Fluaz, these show similar thicknesses of muds, but associated with much thicker sand beds in the latter.

Log N.Ober Stafel and Log Rotstock between them, contain three zones of intense sandstone injection into the homogenous muds. On Log N.Ober Stafel this occurs at approximately 30m from the base, and comprises a 5m zone of ungraded medium and fine sands with injections sub-parallel to bedding. These sandstone sills show bifurcation with occasional interconnecting thinner dykes perpendicular to bedding. The thickest of the

injections is 60cm, all display irregular upper and lower surfaces. Both of these surfaces may show prominent grooves, which indicate the flow direction of the liquefied sand. If the liquefaction was associated with downslope instability then the grooves may also indicate the displacement vector between the walls of the injection. The two measurements recorded for the alignment of the grooves are 100° and 120°. This is coincident with the syn-depositional extension direction as demonstrated by the alignment of sandstone dykes in the Panixerpass area. The relevance of this is discussed in the following chapter.

It is noticeable that the zones of intense sand injections occur within the homogenous muds, and in these sections show no signs of being linked to a massive sand. It is probable that they are linked out of the observed section by means of a feeder dyke. Alternatively, they may represent the liquefied remnants of thinner sand beds which have become over-pressured during the emplacement of overlying massive sands.

3) Sand/mud couplets

Medium to thin-bedded sand/mud couplets are found overlying the homogeneous muds. The majority of the beds display fining upwards grading of varying styles, and only 4% of the sands show no grading. Coarse sand bases are commmon, with the bulk of the beds comprising medium to fine sands. Approximately 12% of the beds display step-wise grading, noticeably on Log Rotstock between 80 and 90m. The sharp steps usually grade from medium-fine sands at the base, with a step into silts, followed by a step into the overlying muds. Each step is marked by a laterally continuous planar surface across which occurs a rapid grain-size reduction. This differs to amalgamation surfaces which appear more irregular and laterally discontinuous, commonly exhibiting loading and occasional mudstone clasts scattered along the boundary. Step-wise grading is also found in the Outer

basin; its interpretation is given in section 3.3.2.

Internal sedimentary structures are rare. Horizontal and wavy lamination is common in the fine sand and silt components, with occasional mud clasts floating in the medium sands. One bed at 85m on Log Rotstock displays clear dish structures demonstrating the escape of trapped fluids during deposition. Some of the silt horizons appear mottled, with occasional small burrows representing bioturbation.

Thin-bedded medium sands show low undulations to the upper surface with a 10-20cm wavelength. Figure 3.15 illustrates a vertical section through these structures, showing symmetrical trochoidal ripples with a 15cm wavelength. Laminations within the ripples thin away from the crests into the troughs. These are aggrading supercritically climbing wave-induced ripples with a slight translatory component. These ripples are transitional upwards into lower amplitude undulations. The presence of wave ripples amongst turbidite sands indicates post-depositional reworking of the upper surface by wave action prior to the deposition of the silts and muds. The overlying undulatory laminations show no evidence of erosion, and most probably represent draping of the ripples at the cessation of the wave activity. The sequence described is illustrated in figure 3.16.

These beds are interpreted as the result of storm activity leading to small volume turbidity currents transporting material to the deeper waters. Continued storm wave action reworked the upper portion of the sand producing wave ripples which were then draped as the storm ceased. The presence of medium sands forming the drape suggests a waning of the turbulent flow associated with declining storm activity. The presence of storm waves sheds some light on the water-depth during deposition; at present, the deepest observed wave ripples occur at 204m, from the Oregon continental shelf (Komar et al, 1972).

4) Silt/mud laminations

Thin horizontal silt/mud laminations are commonly found associated with the sand/mud couplets. The laminations range from 1mm to 2cm in thickness, grading from fine sands and silts to muds, lacking internal structure. They are laterally continuous over 0.5-10m.

3.2.3 Vertical and lateral variations in bedding.

Vertical trends in bed thickness using a three point moving average curve, and grain-size are illustrated on the sedimentary sections. The bed-thickness curves for the Inner basin display a distinctive pattern. For 40-50m above the contact with the Globigerina marls, the curves are dominated by large isolated peaks having a fairly regular vertical spacing, ranging from 4-20m, averaging 12m. These spaced peaks reflect the repeat interval of the massive sand/homogenous mud couplets. Log N. Ober Stafel displays a regular 10m spacing between three large peaks in the curve; similar regularity can be observed on the other sections.

Towards the upper portions of the sedimentary sections, the peaks in the bed-thickness curve become less pronounced. This is best illustrated on the longer sections, Log Chamerstock and Log Rotstock, where more medium to fine bedded sands replace the homogenous muds towards the top. Associated with the decrease in bed thickness is a grain-size reduction from dominantly coarse to medium sands. This trend is seen from 70-115m on Log Chamerstock, and from 60-105m on Log Rotstock.

The most westerly of the sedimentary sections (Log Muttenbergen) is significantly different, demonstrating along strike variations in the basin. This section is dominated throughout by regular isolated peaks, becoming more pronounced towards the top. This is associated with an overall upward coarsening from fine to medium to coarse sands. This

section displays a much more gradual arrival of the massive sands, which are generally thinner (<2m) than in the more easterly sections.

Figure 3.17 illustrates the geometry of the beds, perpendicular to strike, from Jetzalp (Log N.Ober Stafel). This outcrop demonstrates the upward decrease in bed thickness, and represents the upper limb of the Jetzalp anticline as illustrated in the cross-section in figure 2.7, with the core of the structure approximately 100m to the north. The stratigraphy of the Inner basin in this cliff section exhibits a rapid thinning from 130m total thickness in the south, to 75m in the north; this change occurs over a horizontal distance of 150m. It is noticeable that this thinning is not represented in all of the very thick bedded sands, for example, the lowermost bed pinches out completely, whereas the third bed up, shows no thickness variation. Figure 4.. is a drawing of the Inner basin, as seen in the cliff section from Piz Fluaz to Hausstock. This also demonstrates a rapid thinning, and complete pinch-out of the stratigraphy towards the north.

3.2.4 Summary and Interpretation

The Inner basin comprises 150m of turbiditic sandstones overlying Globigerina marls. The upward transition from the marls into the sandstones is variable; very thick bedded sands directly overlie marls in some areas, but have a more gradual transition in others. In the west of the basin, the contact is marked by sand layers containing clasts of Cretaceous origin. The marls reflect water depths of several hundred metres, with NNW/SSE orientated current. The sands indicate deposition above storm wave base, with current flow parallel to the thrust front, running WSW to ENE. This rapid change in the sedimentation of the area is interpreted as being the result of thrust tips propagating from the south into the basin, leading to a relative drop in sea-level, with erosion of the upthrusted hanging walls

resulting in the presence of Cretaceous clasts occuring at the boundary. The stratigraphic significance of this boundary is discussed in chapter 5.

Trench-parallel turbidite deposits thin laterally towards the north onto a palaeohigh formed by the ramping-up and emergence of a thrust plane onto the sea-floor. Within this laterally confined basin, very thick bedded sands and thick homogeneous mud couplets were deposited by high density turbidity currents, with a repeat interval of approximately 12m. Higher in the sequence, thin to medium bedded sands become more prominent. Thin-bedded medium sands occur between the very thick bedded sands with a repeat interval of approximately 40cm. These contain wave ripples and are interpreted as being the result of storm activity. The lack of wave ripples associated with the very thick bedded sands suggests that they are the result of a different generating mechanism for the turbidity currents. It is suggested that the low frequency, but high volume very thick bedded sands are the result of fault movement on foreland-propogating thrusts (Fig.3.40). The very thick bedded sands are intercalated with high frequency, low volume storm-induced turbidites. The large volume of sand and mud deposited by the very thick bedded sands are interpreted not only as due to seismically induced generation of the turbidites, but also the confinement and ponding of the flows within the Inner basin.

3.3 The Outer Basin

The sedimentology of the Outer basin is represented by nine sedimentary sections (figs. 3.18-3.26) from the Central and Northern structural domains.

3.3.1 The Globigerina marl/Taveyannaz sandstone contact.

The contact between the marls and the sandstones is measured in three of the sections from the Outer basin; logs Leiterberg, Hintersulz and Nuschenstock. These are all structurally located within the Leiterberg Antiformal Stack, with logs Leiterberg and Hintersulz in the middle thrust sheet; log Nuschenstock is part of the upper thrust sheet, and therefore the most southerly derived. The Globigerina marls are lithologically identical to those of the Inner basin.

The contact in log Leiterberg is marked by a 1m thick, amalgamated fine sand. Overlying this, the marls are replaced by a 15m thick sequence of alternating massive sands and muds, then up into amalgamated sands. Log Hintersulz has a similar pattern, but with only 8m of massive sands and muds. In contrast, log Nuschenstock has 4m of medium bedded sands and muds, overlain by amalgamated coarse sands.

In summary, the initial clastic input into the Outer basin is characterised in the south by a rapid transition from medium bedded sands and muds to thick amalgamated sands. Further north, the transition is marked by a thicker sequence of massively bedded sands and muds prior to the amalgamation of the sands. If the first arrival of turbidite sands into this part of the basin is synchronous, then the sections measured demonstrate a thinning of the lowermost beds of the Taveyannaz sandstone towards the south. This is interpreted as the result of the outer northern slope of the thrust-ramp palaeohigh separating the Inner from the Outer basins.

3.3.2 Sedimentology

The sedimentology of the Outer basin differs significantly from that of the Inner basin. The vertical sequences illustrated in figures 3.17-3.26 are characterised by sand-rich

packages separated by laminated muds. The term sand package is defined as a sequence of sand beds which are commonly amalgamated with few or no mud intercalations. Sand packages range from 5-100m thick, separating each package is a sequence of laminated silts and muds representing periods of relative depositional quiescence. These are laterally continuous in outcrop (300m max.), although structural deformation makes basin-wide correlation of packages difficult. Individual beds show no signs of channelling, but commonly display scours over 10s of metres which are near parallel to bedding. These sand packages are considered to represent some form of depositional lobe environment (Mutti and Ricci-Lucchi, 1972).

The aims of the following descriptions of the sequences from the Outer basin is to understand the controls on lobe deposition in this turbidite system. Early research in the 1970's explained the origin of depositional lobes as analogous to the progradation of deltaic lobes resulting in thickening-upward sand packages (Mutti and Ricci-Lucchi, 1975). Hiscott (1981) contended the wide occurrence of thickening-upward packages and the validity of the progradational model. Instead, he believed that the vertical stacking of turbidite sands in the lobe environment was predominantly random, resulting from depositional aggradation and variations in volumes of turbidity currents due to external controls. The role of external (allocyclic) controls has increased in emphasis with the recognition of the importance of relative sea-level fluctuations on depositional systems. This is demonstrated by Coleman et al, (1983) for the Pleistocene Mississippi fan system. Prior to the Holocene rise in sea-level, a huge volume of sediment was removed from the shelf-edge of the Mississippi delta in less than 5000yrs, due to slope instability during lowering Pleistocene sea-levels. These sands were redeposited as turbidites on the slope. It is now considered that the basic factor controlling large volume tuurbidite systems is relative sea-level fluctuations produced either tectonically or eustatically (Mutti, 1985).

Without the correlatable shelf sediments, and significant lateral correlations, the differentiation between autocyclic and allocyclic controls on the depositional lobe system of the Outer basin is difficult. This will be discussed further in the light of the following descriptions in section 3.4.

1) Amalgamated sands

Amalgamated sands usually occur in the middle of sand packages, although in the few thickening-upward packages they occur at the top (70-120m, log Tierbodenhorn). Bed thicknesses vary from 0.1-10m, and can form upto 70m of virtually uninterrupted coarse sands (60-170m, log Erbserstock). Log Erbserstock is the most sand-rich section, and comprises three complete packages. The upper package is the most extensive and contains many amalgamation surfaces. These occur as abrupt changes in grain-size across a commonly loaded boundary (fig.3.27); this can be within coarse sands, or from the fine sands and silts at the top of a bed into the base of another coarse sand. These surfaces are extremely variable along strike, and may be impossible to identify 10m along the bed (fig.3.28). Whether each bed within an amalgamated sequence was originally overlain by a mud-cap is not known. Certainly, mud-clasts are commonly found immediately underlying amalgamation surfaces, indicating that the turbidity current had passed over a mud-rich surface upstream.

Amalgamated sand beds are similar in thickness (0.1-1m) to sand/mud couplets with no amalgamation seen within the same sedimentary section. Why then, should certain beds amalgamate and others not? Firstly, we must consider whether the amalgamation surfaces represent increased erosional power, or increased sedimentation rates. Increased erosional power to turbidity currents is a function of flow density and slope, whereby, above critical

values, all the grains are in suspension and erosion is dominant over deposition on the base of the turbidite flow; this is described as autosuspension (Bagnold, 1962). But, according to Allen (1982) and Pantin (1979) autosuspension is only predicted for sediment finer than fine sand suspended in thick turbibity currents on steep slopes. Therefore, these coarse sand turbidite flows will be dominantly depositional. With no reason to infer excessive amounts of erosion, the interpretation of the cause for amalgamation must lie in the rate at which turbidite events occur. Therefore, zones of intense amalgamation as seen in the centre of the sand packages must represent a significant increase in not only sedimentation rates, but more importantly, the repeat rate of turbidite events.

2) Sand/mud couplets

With larger packages, sand/mud couplets occur at the upper and lower margins of the package, between the amalgamated sands and the laminated muds. Bed thickness varies from 0.1-1m and beds have a constant thickness along strike in outcrop (300m max. extent), although a few beds can be seen to wedge out over this distance. Some sand packages comprise dominantly sand/mud couplets with only minor development of amalgamated sands, for example: 50-80m - log Chuetal, 0-10m - log Wolfisbach, 70-90m - log Chueboden.

Maximum grain-size is usually medium to coarse sand, grading up into silts and muds. Step-wise grading is more common than in the Inner basin, often showing three steps within one bed, from medium sand to fine sand, fine sand to silt and then silt into the mud cap. Figures 3.29a and b illustrate typical step-wise grading within thin bedded sand/mud couplets from log Tritt. The lower 5cm of the bed is lightly coloured with irregular, muddier dark areas and a few mud-clasts. This is a poorly sorted unit comprising a mixture

of sand and mud, with occasional 1mm quartz grains showing a near random distribution through the unit, although a coarse basal lag is evident. The 3cm dark band overlying the lighter unit also contains 1mm grains, and is more dominated by a muddy matrix. The boundary between these two units is sharp, but becomes more diffuse to the left of the photograph. The uppermost step into the muds is now strongly contorted by the formation of pseudonodules, but is as sharp as the previous boundary. This bed, involving three units, is not the product of simple suspension fall-out from a waning turbulent flow. The observations that need to be accounted for are: 1) the extremely poor sorting, 2) the distribution of 1mm grains throughout the lower units, 3) the sharp boundaries between units, and 4) pseudonodule formation in the muds.

Explanation of step-wise grading:

The depositional mechanism for these stepped beds must involve rapid dumping of sediment, and rapid changes in the hydrodynamic state of the flow. Pantin and Leeder (1987) experimentally demonstrate the formation of low amplitude, large wavelength internal waves caused by the interaction between the forward and reverse turbidite flows resulting from the reflection off an opposing slope; these internal waves are called solitons. Figure 3.30 illustrates the development of four solitons formed in a flume tank. Initially, the reflected flow interacts with the forward flow to form a bulge at the base of the slope, from which the solitons develop; this bulge may well play an important role in sedimentation as it resides for a longer period of time over a point than do the solitons. Solitons are waves of translation (water particles move only in the direction of wave advance), and provided that the residual velocity in the tail of the turbidity current is not too great, will cause reverse flow at a given point as the crests pass by.

Pantin and Leeder (1987) propose solitons to explain the flow reversals seen within the

turbidites of the Cloridorme formation, Quebec (Pickering and Hiscott, 1985). The flow reversals are represented in the Cloridorme formation by ripple cross-laminated sands separated by a muddy parting, with no evidence of erosion between each reversal. Each reversal is interpreted to represent the passage of a soliton crest. Consider deposition at a given point along the length of a reflected turbidite with a series of solitons. After the initial passage of the forward flow, subsequent reverse and forward flows have to have passed through a point of zero velocity where the original turbidity current and the reflected soliton cancel each other out. At these points of zero velocity, it is assumed that the bulk of the suspended material will be rapidly deposited, infact in the case of the Cloridorme formation, muddy partings occur between reversals, suggesting that all of the sand component would have fallen out of suspension. This necessitates that subsequent reflected flows would require extensive erosion and resuspension of material to initiate bedforms in sand with an opposing sense of flow. The lack of any erosion seen between flow reversals in the examples from the Cloridorme formation questions the validity of this mechanism to explain the features described by Pickering and Hiscott (1985).

However, solitons would seem a highly suitable mechanism in the formation of step-wise grading in the Taveyannaz sandstones as illustrated in figure 3.29b. Consider again, a point underlying an initially forward flowing turbidity current, with the bulk of material in suspension, and a coarse lag travelling as bed-load. The current is then met by the reflected flow which interacts with the forward flow to form the initial bulge at the base of the slope (Fig.3.30) causing rapid deceleration and dumping of suspended material, so forming a poorly sorted unit with no tractional reworking. Reverse flow then becomes dominant as the crest of the bulge passes over and starts to break down into a series of solitons; the reflected bulge contains mainly fine sands and silt in suspension plus a certain amount of reworked medium to coarse sand. Prior to the return of forward directed flow, there is

again a period of stagnant water with associated dumping of material out of suspension. This forms another unit of poorly sorted finer material separated from the underlying unit by a sharp erosive break. The residual flow is then deposited as laminated muds. The formation of pseudonodules is considered to result from the final sloshing of the turbidity current in the confined basin. M^{c}Manus and Duck (1987) describe storm-induced internal waves forming at the thermocline of Loch Earn, Scotland. These internal waves lead to slumping of material at the margins of the loch. It is considered that the final sloshing of a confined turbidity current would produce similar internal waves resulting in intense liquefaction of the deposited silts and muds, and so form the upper pseudonodule layer illustrated in figure 3.29b.

Returning to the description of the sand/mud couplets of the Outer basin. The occurrence of mud-clasts is common, often comprising >90% of an individual sand bed (Fig. 3.31). These clasts are extremely variable in both size and shape, often appearing as large rafts of mud up to 3m long floating within a sand bed. The margins of clasts can be wispy and diffuse, or angular and sharp depending on the degree of lithification of the muds upon incorporation. Figure 3.32 illustrates small wispy mud fragments concentrated towards the top of a bed, which are strongly elongate and aligned. This demonstrates post-depositional shearing of the bed due to downslope moveqment at or near the sediment/water interface.

The lower surface of mud-clast-rich beds are often grooved and occasionally illustrate the process of incorporation of the mud fragments. Figure 3.33 shows the detachment of a small mud fragment into the overlying sand. Figure 3.34 illustrates the mechanism of incorporation of a large mud raft into a sand unit by means of peeling a 10cm mud layer away from its lower surface, and rotating it to form an isoclinal fold. These observations demonstrate that the erosion and incorporation of mud into the turbidite sands occurs within

the sand lobe environment, and that the mud has not travelled in from a more proximal source such as a channel margin.

The distribution of mud-clast-rich sand beds in relation to sand packages shows a weak trend. The presence of mud clasts is not surprisingly more commonly associated with muddier sequences, and they are therefore found nearer the margins of packages. The lowermost package of log Chuetal shows an abundance of mud-clasts associated with an overall muddier than average package.

Mutti and Nilsen (1981) suggest that the distribution and character of mud-clasts within beds can be used as a distinguishing criterion for channelised and non-channelised sequences. They consider that non-channelised beds contain more uniformly organised and better sorted mud-clasts, with a maximum size of about 1m. The chaotic distribution, and great variety of mud-clasts within these lobe sequences contradicts this usage of mud-clasts as environmental indicators. The presence of mud clasts is an indicator of the interaction between the erosive power of the turbidite, and the instability of the muds. An attempt at incorporating these observations into a broader context is made in section 3.3.4.

Muddier layers intercalated with sand/mud couplets occasionally exhibit slumping and faulting. This occurs between 80 and 85m on log Nuschenstock in two successive mud bands. Figure 3.35 illustrates these examples, demonstrating contrasting mechanical responses to downslope instability. 3.35b shows syn-depositional brittle, listric normal faulting within a 15cm mud layer, the deformation occurring prior to the deposition of the overlying sand turbidite. Figure 3.35c shows a 1m thick slump zone with irregular ductile folding, in the same lithology as the underlying brittle faulting. Whether the ductile slumping represents deformation at the sediment/water interface or at shallow levels of burial cannot be directly deduced. But it is thought likely that a certain amount of overburden leading to higher pore-fluid pressures is likely to be the cause of the more

ductile deformation.

Ripple cross-lamination is common within the fine sands and silts of the sand/mud couplets, and always indicates current flow towards the ENE. Undulatory and ripple lamination can be highly convoluted. Figure 3.36 illustrates the typical features associated with the the silt and mud component of the sand/mud couplets. Extensive convolute lamination, loading and ripple cross lamination occurs within silt layers separated by minor erosion surfaces. These silt lamina represent rapid successive deposition by dilute turbidity currents.

3) Thin bedded silts and muds.

Figure 3.37 illustrates the typical appearance of this facies in outcrop from log Chueboden. Thick sequences (upto 20m) of silt and mud are most abundant in the north of the area, for example in logs Chuetal, Chueboden and Tierbodenhorn.

Commonly intercalated within this facies are thin bedded fine sand turbidites, frequently rich in mud-clasts. The silt beds range from 0.1-3cm thick, fining up into muds, and are extremely uniform along strike. Common sedimentary features within the silts are thin (1mm) horizontal lamination, current ripples, convolute lamination and small scale loading. This facies represents slow uniform deposition from low concentration turbidity currents. Horizontal lamination results from the sorting of silt grains and clay flocs in the viscous sub-layer of the flow (Stow and Bowen, 1978).

Figure 3.38 illustrates silt and mud laminae from an outcrop on the northern edge of Jetzbach (Grid ref.72870,19450). Palaeogeographically this occurs just north of the Jetzalp palaeohigh, and is thought to represent the northern slope of the palaeohigh. Throughout the outcrop there is clear evidence of slope instability towards the north. This can result in

disaggregated shear zones (fig.3.39) or on a smaller scale as northward vergent load structures (fig.3.38).

The thin bedded silts and muds described here differ from the silt/mud laminations from the Inner basin due mainly to their lateral continuity, and higher occurrence of ripple and horizontal laminations. It is thought that the fine deposits of the Outer basin represent more gradual fall-out from the turbidity current than within the Inner basin where sedimentation occurred more rapidly.

3.3.3 Summary and Interpretation

In the Outer basin, the contact with the Globigerina marls demonstrates a thickening of the initial sand/mud couplets towards the north away from the Jetzalp anticline. This is considered to be due to the northward dipping outer slope of the thrust-ramp palaeohigh.

The Taveyannaz sandstones can be divided into three main facies, 1)amalgamated sands, 2)sand/mud couplets, 3) finely bedded silts and muds. Vertical sedimentary sections illustrate the presence of sand packages comprising varying proportions of these facies. The bed thickness curves demonstrate that 85% of the packages are symmetrical, the other 15% show a thickening upward trend. Packages contain a central portion of amalgamated sands; between these and the silts and muds are a sequence of sand/mud couplets which are often rich in mud-clasts. The presence of amalgamated sands in the centre of packages suggests an increase in the recurrence rate of successive turbidite events compared to the sand/mud couplets. This is based on the assumption that turbidity currents containing dominantly coarse sand will not be in a state of autosuspension, consequently deposition will be dominant over erosion. Therefore the fact that sand beds are amalgamated suggests that the medium sand to silt components were not deposited, indicating a rapid repeat interval

between turbidite events. This would indicate that the controlling mechanism in the development of these sand packages is allocyclic, related to an increased instability in the source region for the sediment, associated with a relative drop in sea-level. The increase in mud clasts in the transitional sand/mud couplets may represent the onset of slope instability.

Mutti and Sonnini (1981) suggest that bed thicknesses in depositional lobe environments are dominantly controlled by the depositional topography of the lobes. This leads to small-scale (<5m) thickening upward 'compensation cycles' caused by the lateral shifting and infilling of topographic depressions. There is no evidence of compensation cycles occurring within this basin, suggesting that either, 1) the lobes did not develop a significant topography and were more sheet-like in geometry, and/or 2) varying bed thickness is a function of varying sediment supply. A more sheet-like geometry would be expected if the Outer basin, like the Inner basin, was topographically confined. Confinement is suggested by the presence of step-wise grading, which is interpreted here as being the result of the reflection of turbidity currents off an opposing slope, forming internal solitons (Pantin and Leeder, 1987) and leading to rapid hydrodynamic changes in the flow. Varying sediment supply is also to be expected if there is a change in the recurrence rates of the turbidites as suggested by the amalgamation. Consequently, bed thicknesses in the sand packages are considered to be a function of varying sediment supply.

In contrast to the rapid sedimentation rates of the sand packages, the intervening silts and muds indicate relatively slow rates of deposition. If the sand packages represent lobe deposits, then an autocyclic approach would interpret the silts and muds as basin plain and lobe fringe deposits shifting laterally over the lobes. But, as the basin is interpreted to be confined, containing sheet sands and reflected turbidites, then true lobes would not develop and lateral shifting would be restricted. The silts and muds must therefore represent either

1) a progradation of more proximal channel overbank deposits, or 2) a retrogradation of more distal basin plain deposits. Without any evidence of channel development, the former hypothesis is abandoned. The thin bedded silts and muds are therefore interpreted as representing periods of relative sea-level rise.

Variation between sedimentary sections is obvious, notably the significant increase in the mud content of the sections from the Northern structural domain, particularly logs Chueboden and Chuetal. This is considered to be mainly a function of the variation in sampling through the stratigraphy. The sections of the Northern domain are taken from high topograhic levels in areas of relatively minor deformation, and certainly there is no evidence of major stratigraphic duplication as seen in the Central domain. Consequently, the stratigraphy of the Outer basin as a whole also shows a longer term fining-up which may indicate progressive sea-level rise.

In summary, the Outer basin comprises a series of sand packages intercalated with silt/mud sequences, which are considered to represent periods of relative sea-level fall and rise respectively. Overall, there is an fining-up suggesting a steady background relative rise in sea-level throughout the deposition of this sequence.

3.4 Discussion and Conclusions

The transition from the Globigerina marls into the Taveyannaz sandstones represents a major stratigraphic boundary from hemipelagic deposits with a NNW current flow, to clastic deposition with trench parallel flow (ENE). This also records a relative fall in sea-level interpreted as due to the propagation of thrust tips into the basin.

Tectonic uplift in the hinterland to the south led to erosion of large amounts of sand

from the shelf which is then reworked and redeposited as a low stand turbidite wedge (sensu Vail et al, 1977). Reworking of shelf sediments to develop a low stand turbidite wedge requires that an equal volume of sands and muds are deposited on the shelf at sufficient rates to prevent lithification as are redeposited in the turbidite system. This condition is more than adequately met in the case of deposition in advance of a thrust front. Steep slopes with large drainage basins provide abundant shelfal accumulation of sediment, which, during thrust activity and concomitant relative lowering of sea-levels is reworked into deeper water.

The turbidites were deposited in two distinct sub-basins, separated by a thrust-ramp palaeohigh running ENE-WSW. The exposed Inner basin has a lateral extent of about 10km and 7km perpendicular to strike. The maximum stratigraphic thickness is about 140m which pinches out onto the frontal palaeohigh. Sedimentation in the Inner basin comprises tectonically induced very thick bedded turbidite sands and muds intercalated with thin-bedded storm induced turbidite sands. The vertical succession in the Inner basin shows a decrease in bed thickness towards the top of the stratigraphy representing a return to relatively higher sea-level deposits.

The Outer basin has a greater stratigraphic thickness of at least 240m. Sedimentation is dominated by relative sea-level fluctuations leading to the deposition of low stand sand packages and intervening high stand silts and muds. The lower deposits of the Outer basin are more sand-rich with mud becoming dominant higher in the stratigraphy, marking a longer wavelength relative sea level rise imposed upon the higher frequency fluctuations.

Unfortunately, there is no biostratigraphic correlation between the Inner and Outer basins. If we are to attempt to link the processes involved in the two basins we must make two stratigraphic assumptions: 1) The Globigerina marl/Taveyannaz sandstone contact is synchronous between the two basins; 2) The emplacement of the overlying mud sheets is

synchronous (chap.4). If these assumptions are correct, then we have a lower and upper boundary to the timing of deposition. Even if these boundaries are slightly diachronous, it would be hard to believe that the bulk of the sedimentation between the basins did not occur at the same time.

Both basins show an overall upward transition from lowstand sand deposition to relatively higher stand thin bedded sands or mud deposition in the Inner and Outer basin respectively. Is it possible that the Inner basin represents a condensed equivalent to the Outer basin? Figure 3.17 illustrates approximately 10 major turbidite event beds within the Inner basin. This is within the region of the number of sand packages in the Outer basin, although this is never seen in one section. It is proposed that for each very thick bedded sand turbidite event in the Inner basin, there is a stratigraphically equivalent sand package in the Outer basin. What is the controlling mechanism for these two separate but synchronous events? Low stand fan deposits result from the by-passing of sediment from the eroded shelf via point sources into the base of slope region. If the Outer basin was fed laterally by point sources, it would receive the bulk of the sediment generated by the steady erosion of the shelf. The Inner basin would be by-passed by the bulk of the shelf sediments. The only sediments to reach this relatively starved basin would be those resulting from generating mechanisms that were not dependent on point sources to transport the sediment, for example storm and thrust induced seismic events. The events leading to the formation of a very thick bedded sand/sand package couple would be triggered by a thrust induced seismic event. This would form a large seismo-turbidite emanating from the shelf/slope break, the sediments of which would be trapped in the confined perched basin higher up the slope than the outer trench. The resultant relative fall in sea-level associated with the thrust activity leads to rapid slumping and erosion of shelf sediment which is transported to the low-stand wedge of the Outer basin to form a sand package. Steady

background flexural subsidence continues, and the sand package is blanketed by high-stand muds until the next episode of thrusting repeats the process. Thrust-tip advance rates can be estimated from the restored cross-sections of Pfiffner (1986), time averaged rates approximate to 4mm/yr for Eocene/Oligocene times. With this value for the advance rate, uplift in the hanging wall of a thrust dipping at 40 degrees would be in the range of 3-4mm/yr. When this figure is compared to <0.3mm/yr for flexural subsidence for the NAFB in western Switzerland (Homewood et al, 1986), it becomes clear that pulses of thrust movement must play a controlling role in the development of the stratigraphy overlying these blocks.

Obviously, this scenario is highly speculative, but serves as a useful working hypotheses from which to base future research (chapter 5).

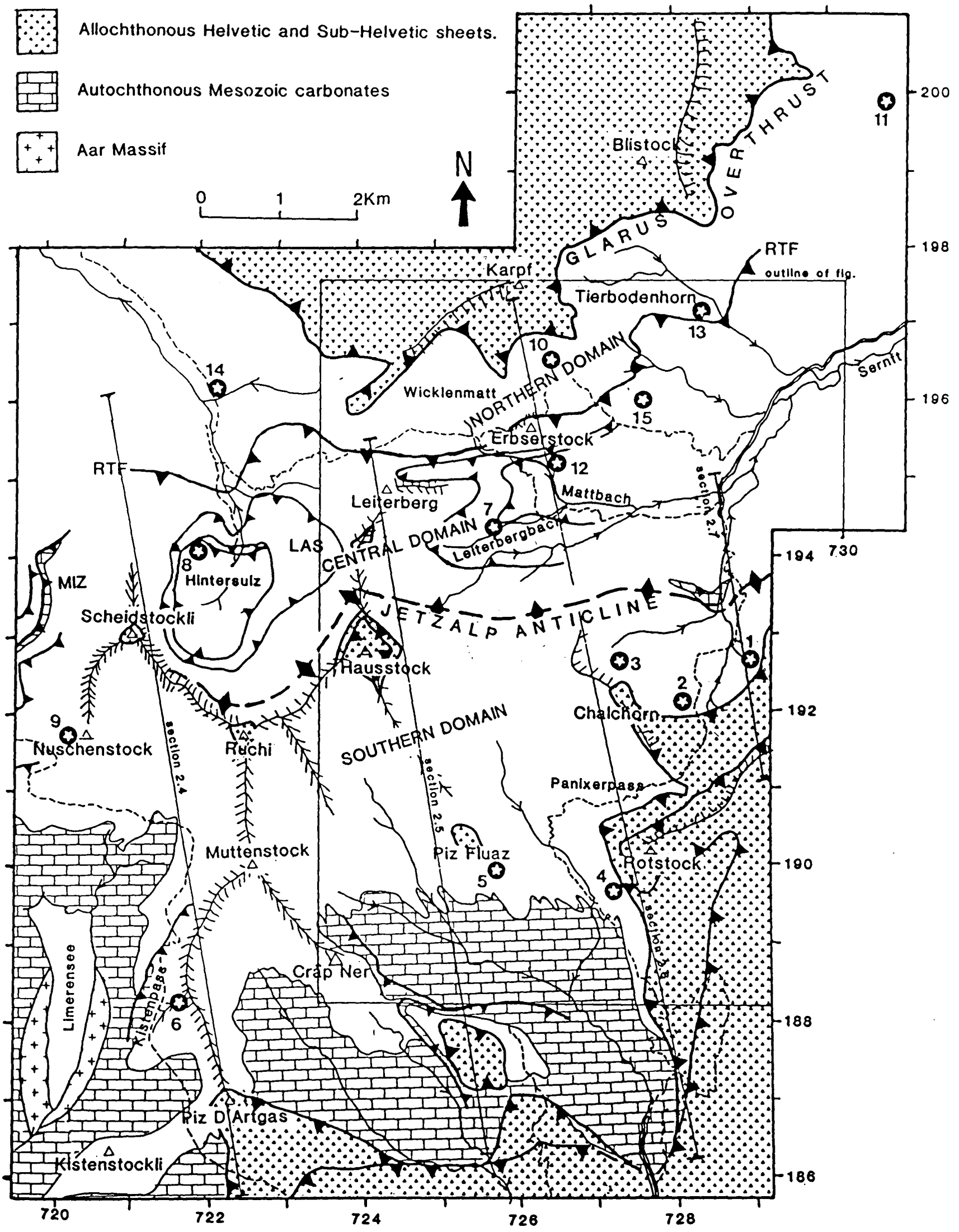

Fig.3.1. Structural map of area with sedimentary sections located.

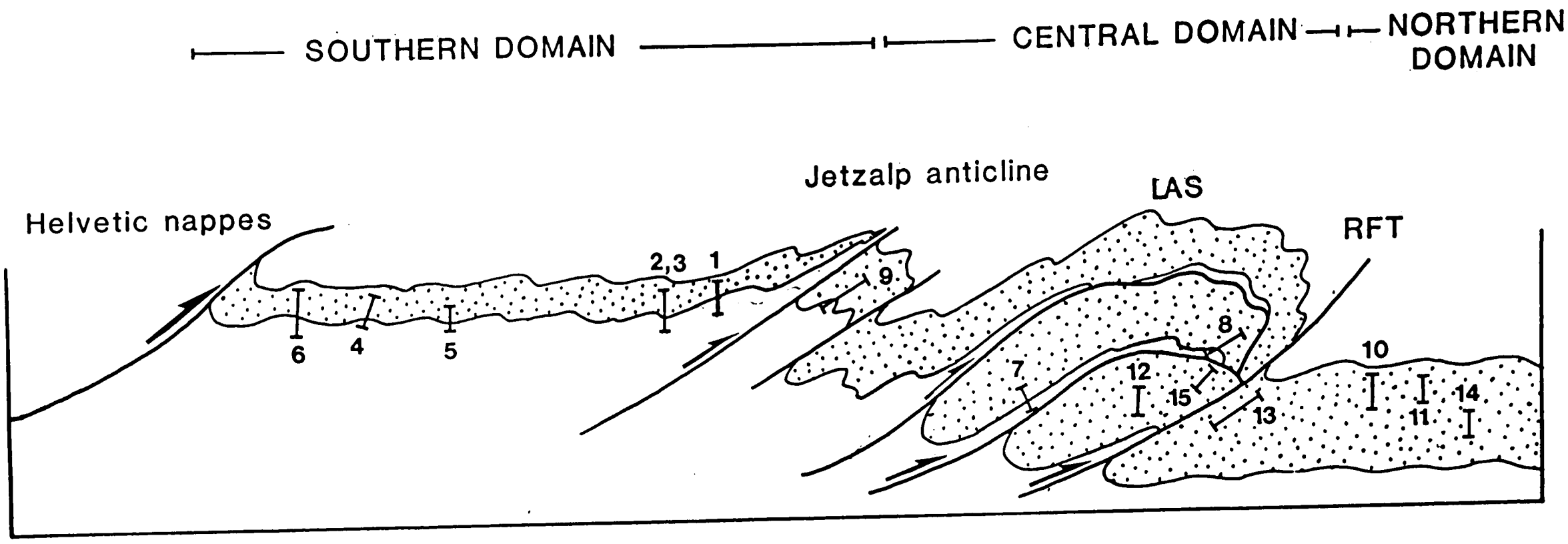

SEDIMENTARY LOGS: 1-N.Ober Stafel, 2-W.Ober Stafel, 3-Chamerstock, 4-Rotstock, 5-Piz Fluaz, 6-Muttenbergen, 7-Leiterberg, 8-Hintersulz, 9-Nuschenstock, 10-Chuetal, 11-Chueboden, 12-Erbserstock, 13-Tierbodenhorn, 14-Wolfisbach, 15-Tritt.

LAS - Leiterberg Antiformal Stack, RTF - Richetlipass Frontal thrust.

Fig.3.2. Simplified structural cross-section through area with locations of sedimentary sections.

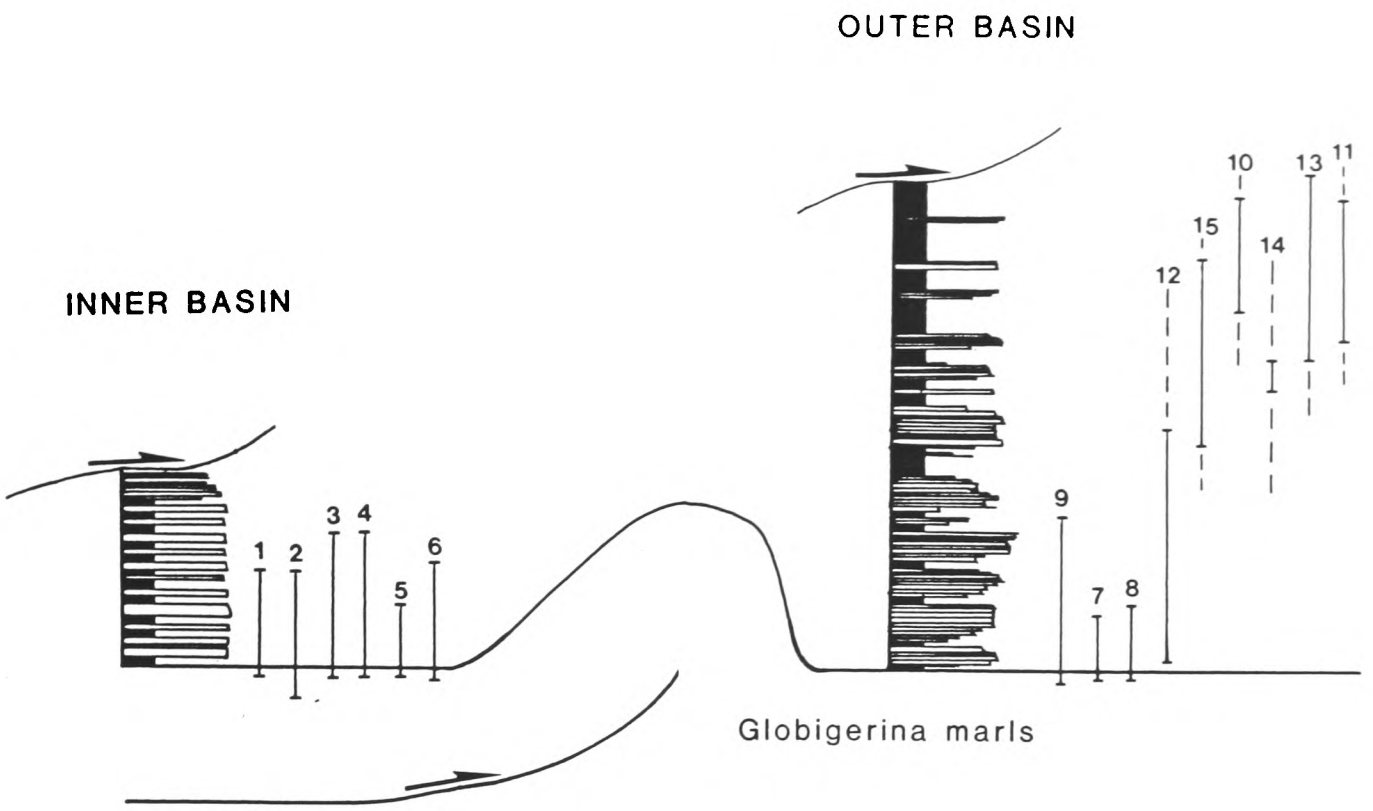

Fig.3.3. Schematic stratigraphy of the Inner and Outer basins separated by a topographic high, with approximate positions of sedimentaary sections. Dashed lines indicate likely error bars.

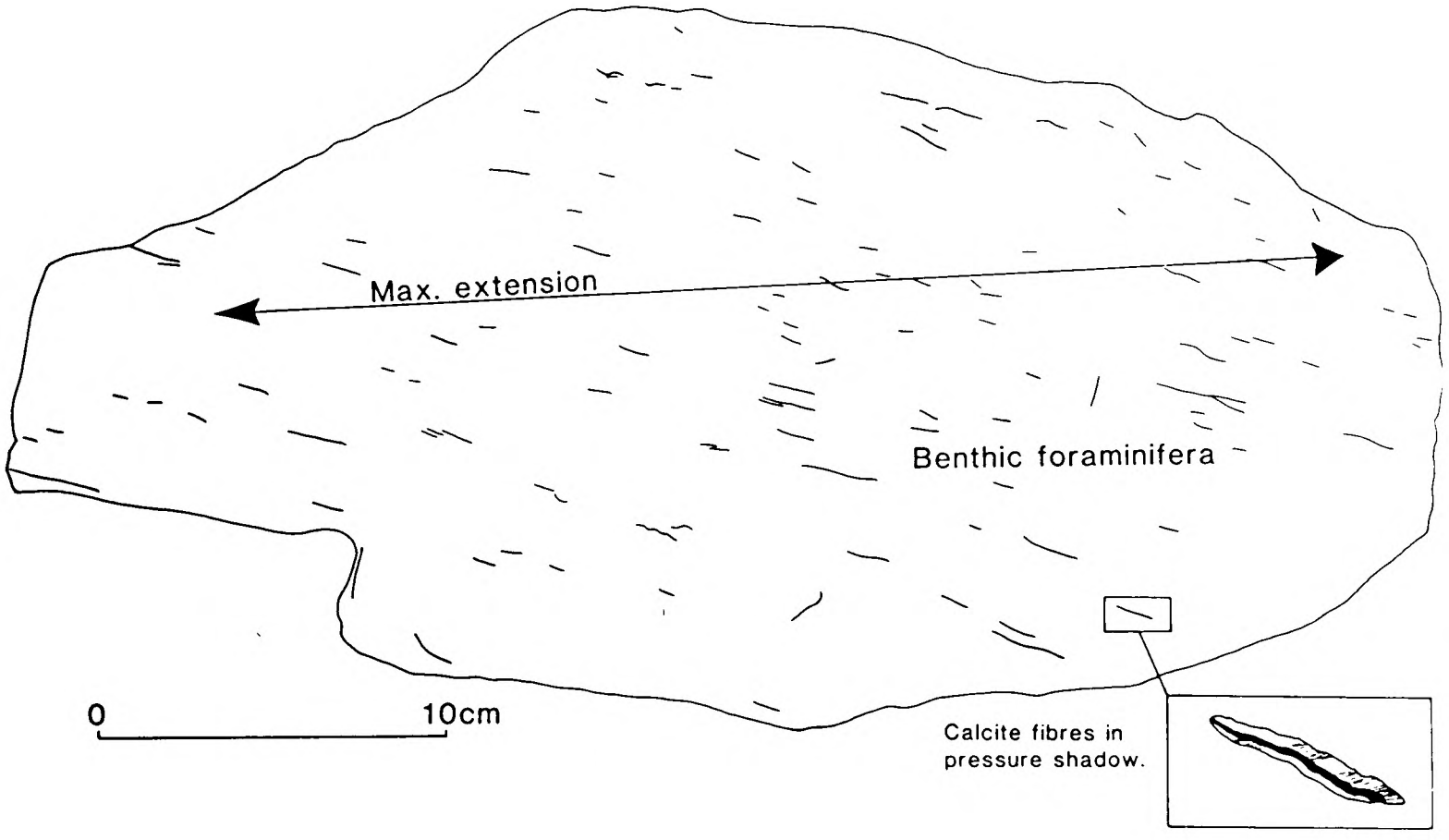

Fig.3.4. Drawing of a bedding surface in the Globigerina marls illustrating the discrepancy between the structural maximum extension direction as measured from calcite fibres (inset) and the alignment of benthonic foraminifera. This alignment is interpreted as representing current flow direction.

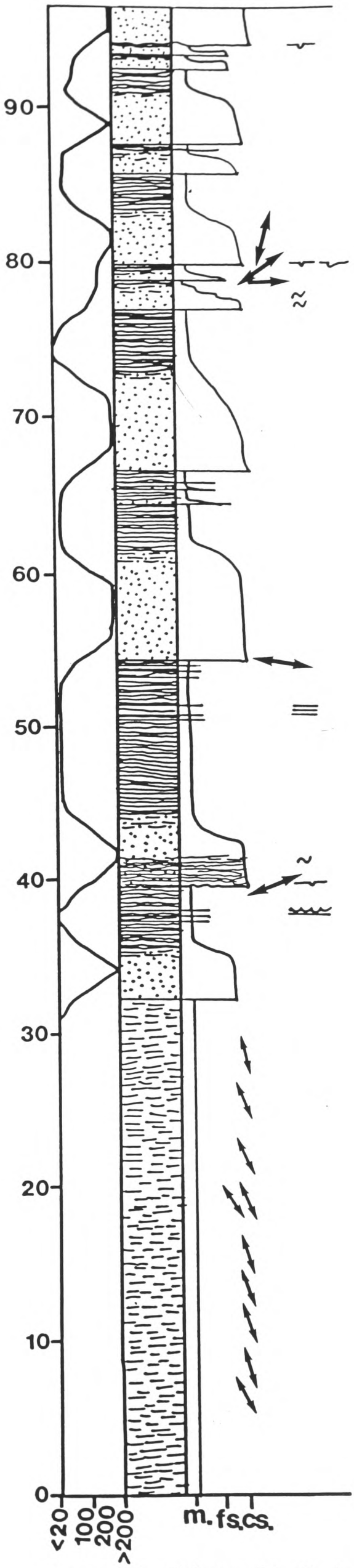

Log W. Ober Stafel

(grid ref. 72832,19245).

Fig.3.6. Log W.Ober Stafel.

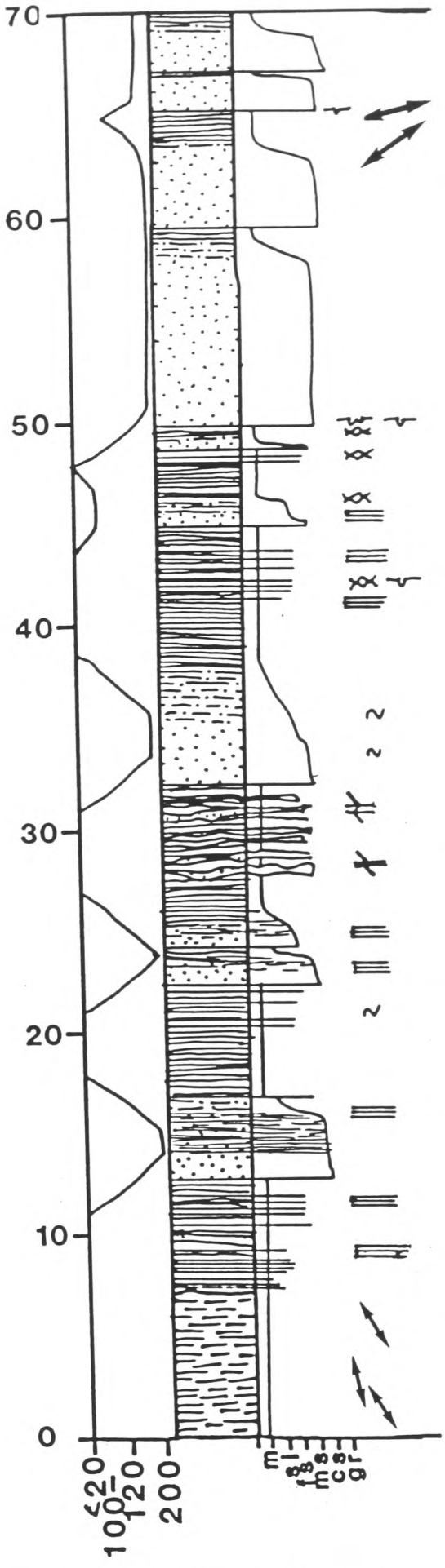

Log N.Ober Stafel

(Grid ref. 72892,19260).

Fig.3.5. Log N.Ober Stafel.

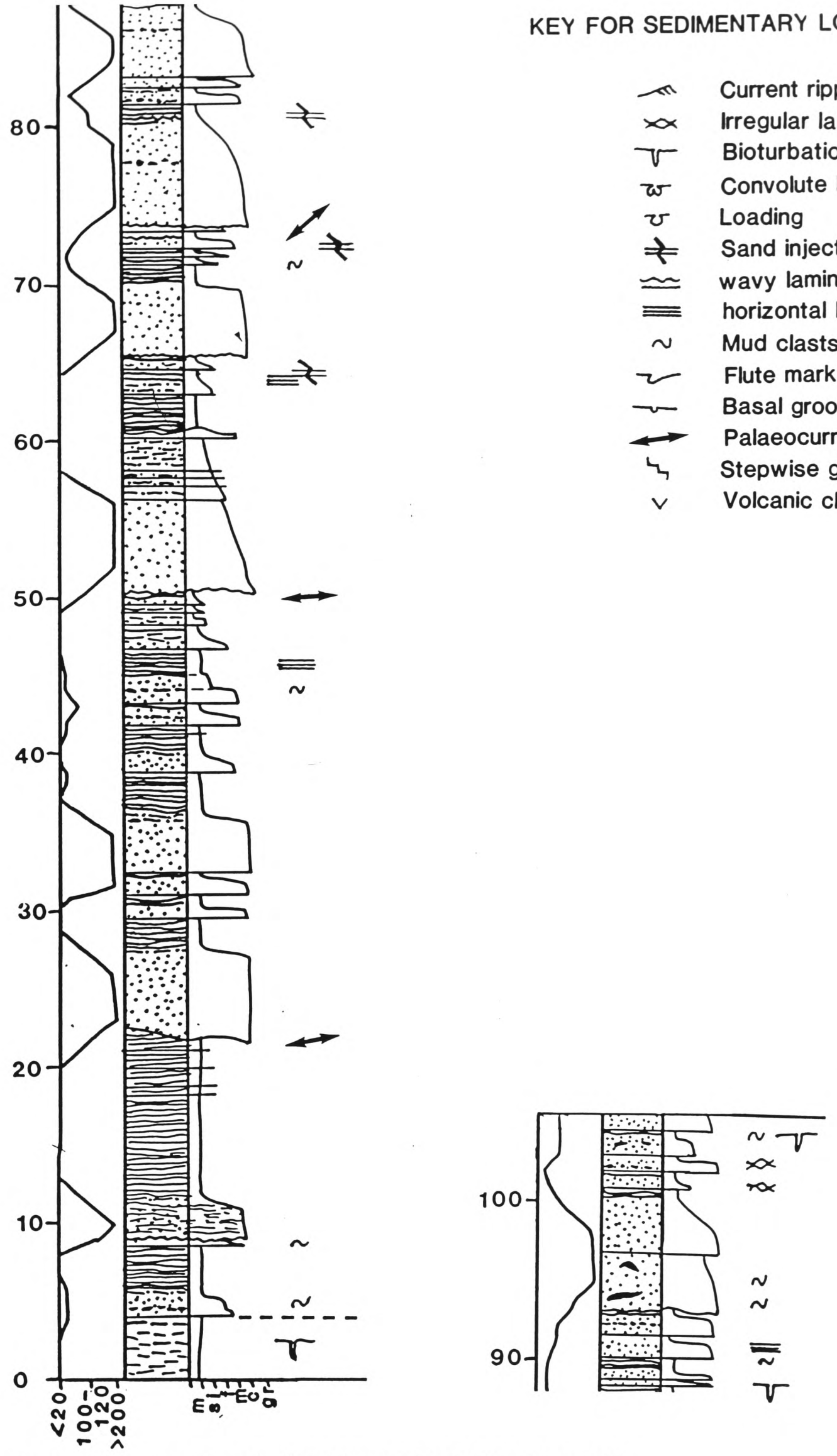

Fig.3.7. Log Chamerstock.

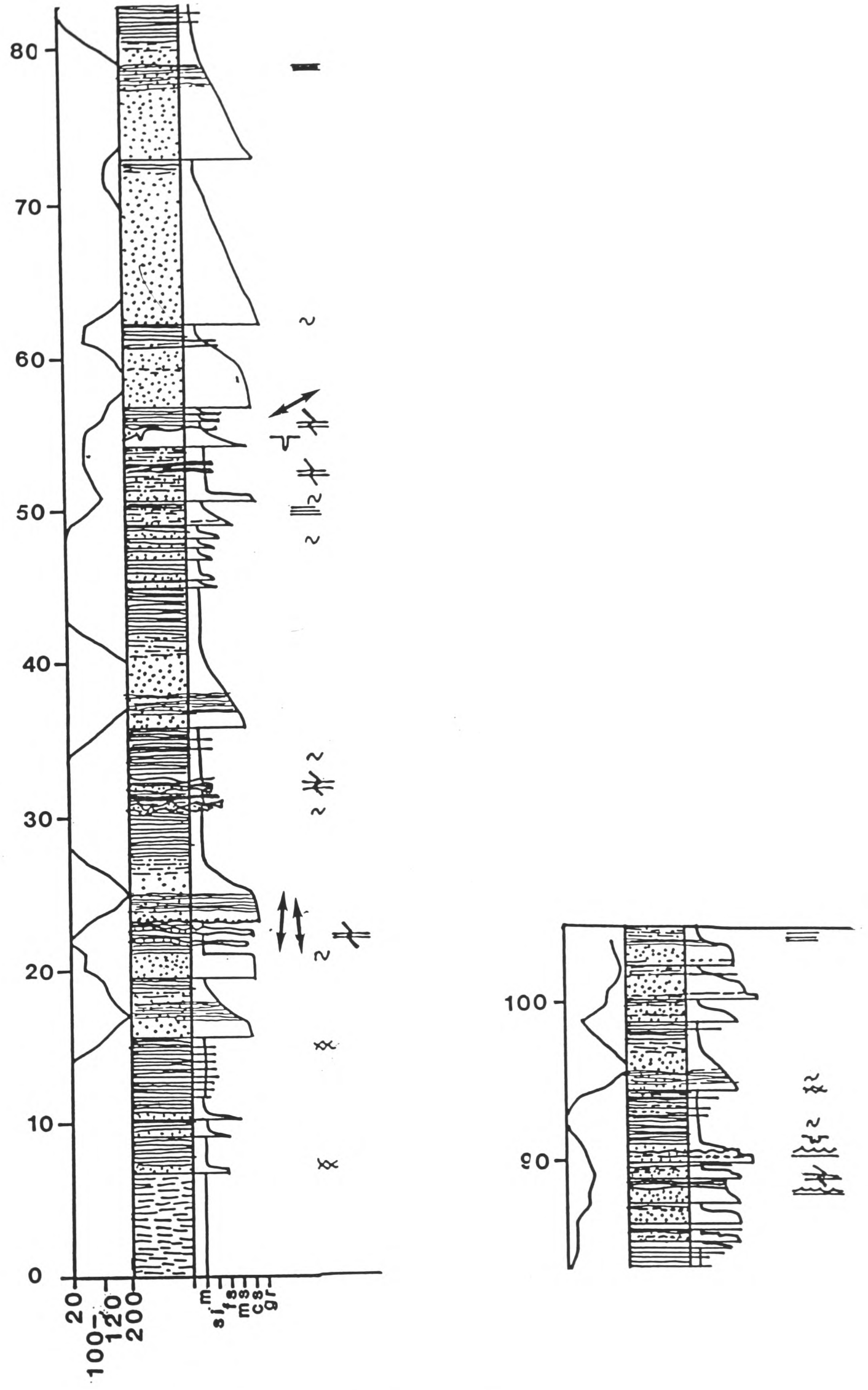

Log Rotstock, Grid ref. (72690,19025)

Fig.3.8. Log Rotstock.

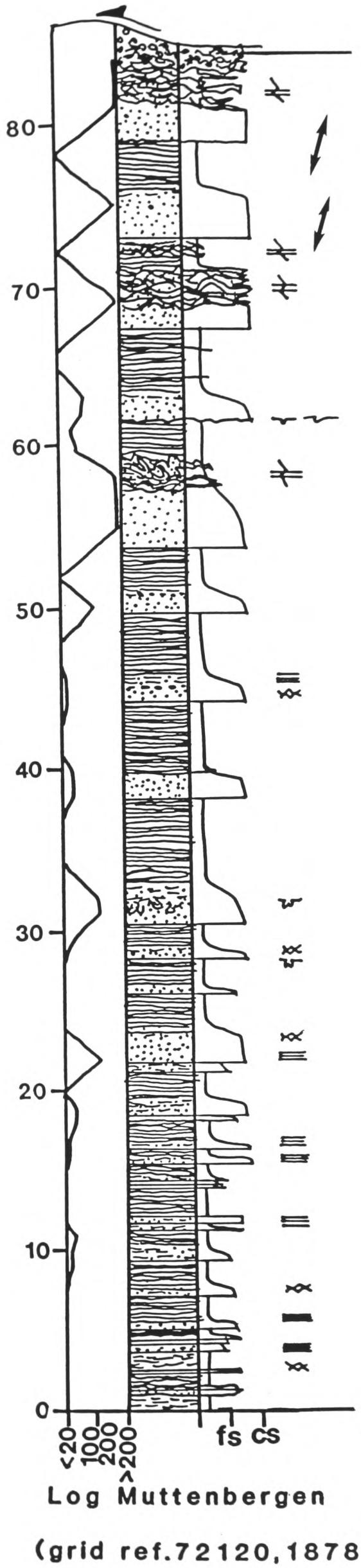

Log Muttenbergen

(grid ref.72120,18785).

Fig.3.10. Log Muttenbergen.

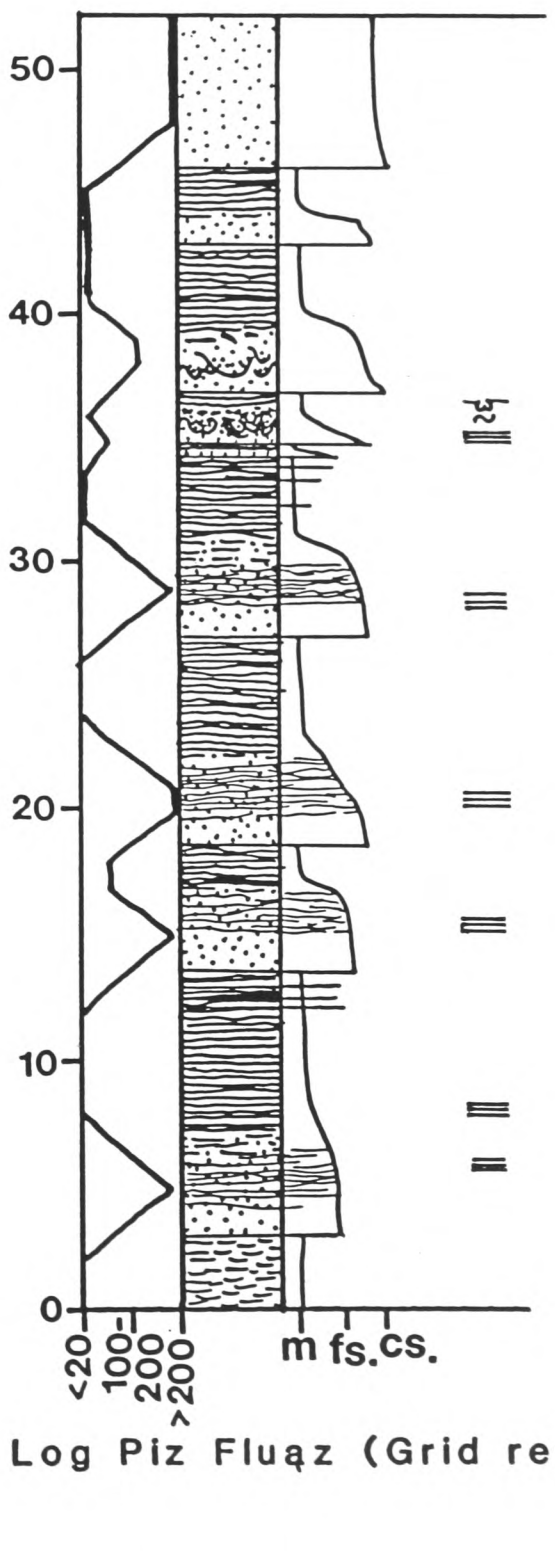

Log Piz Fluąz (Grid ref.72575,18984).

Fig.3.9. Log Piz Fluaz.

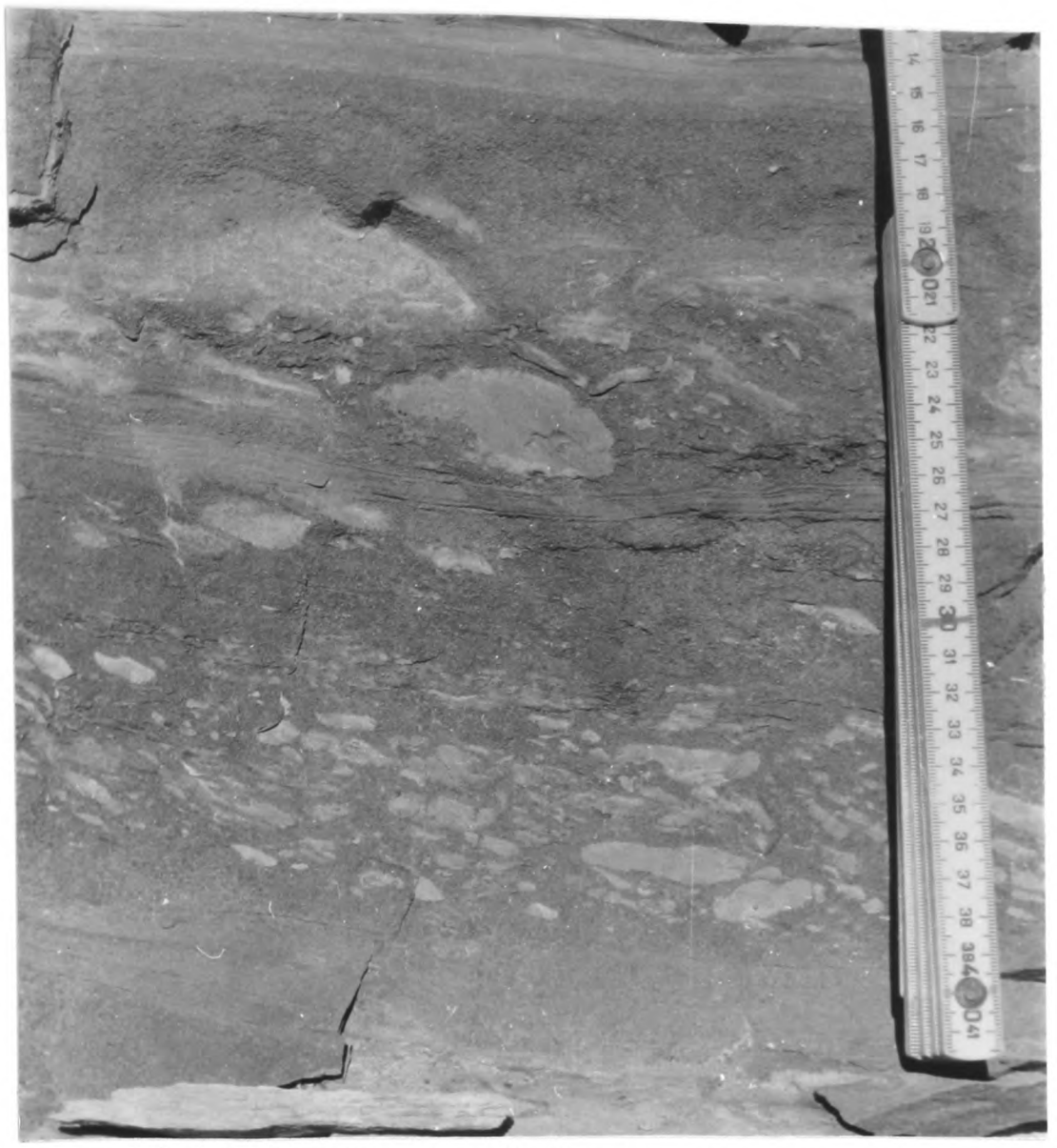

Fig.3.11. Inverse graded bed within the Globigerina marls at the base of log Muttenbergen. This is overlain by horizontal laminated fine sands, then by a normally graded turbidite sand. The clasts include fragments of Cretaceous limestone suggesting that these beds correlate with the Kistenstöckli micro-conglomerate (Styger, 1961). The exposure of cretaceous rocks at the Globigerina marl/Tayeyannaz sandstone contact is interpreted as resulting from thrust-tip propogation which then leads to the relative drop in sea-level and the formation of the Taveyannaz sandstones as a low stand wedge/fan.

Fig.3.12. Spaced horizontal layering in the massive sands of log Rotstock. The interpreted mechanism of formation is as density modified grain flows forming during successive freezing of a traction carpet during deposition from a high density turbidite. Figs.13 and 14 summarise this process.

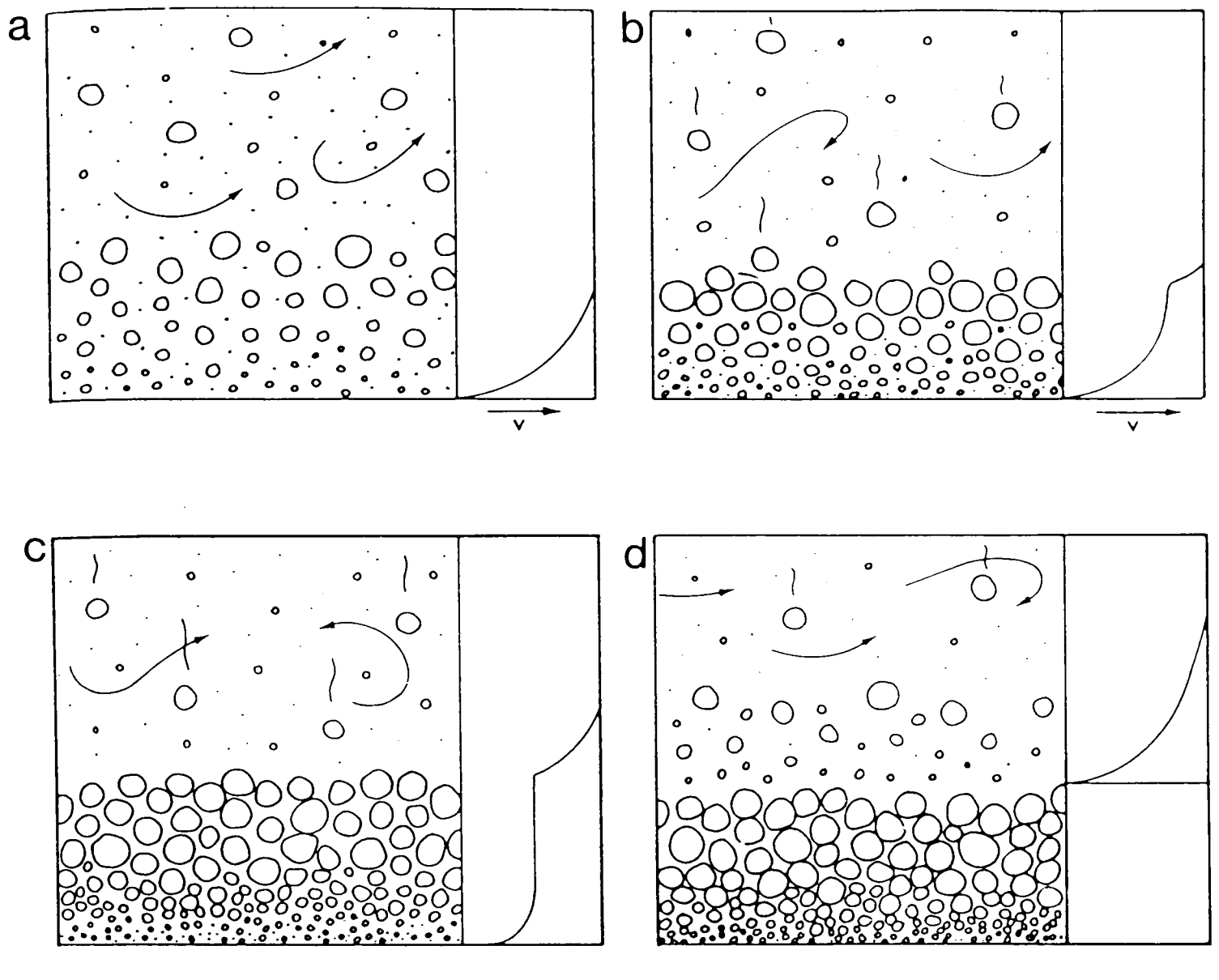

Fig.3.13. Origin of traction carpet layers from Lowe (1982). A) Basal part of high density flow develops inverse grading due to intergranuler dispersive pressure. Note generalised velocity profile on right. B) Fallout from suspension increases clast concentration in basal layer and results in formation of traction carpet. C) Continued fallout loads traction carpet and causes freezing. D) Final freezing of traction carpet results in formation of new inversely graded basal flow layer above deposit. Process is then repeated.

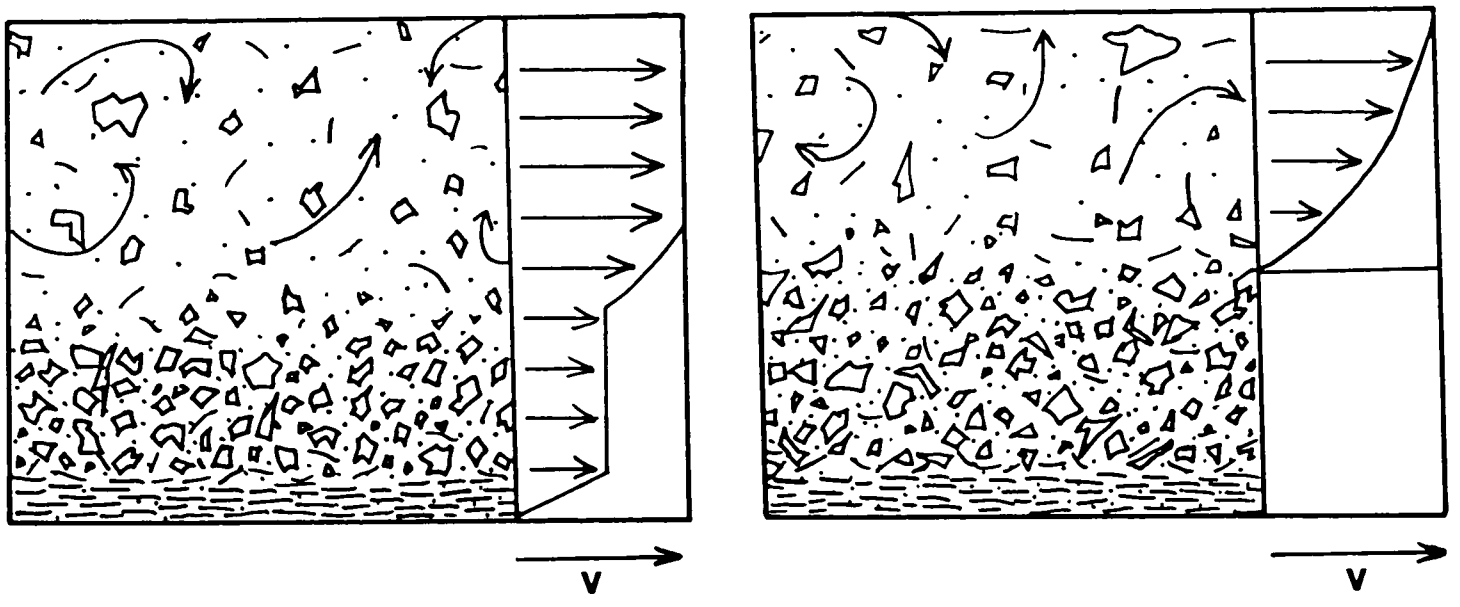

Fig.3.14. Origin of traction carpet layers formed in poorly sorted, mica-rich sands. Modified versions of figures 3.13c and d. This produces an ungraded traction carpet for two reasons: 1) The mica forms an extremely efficient basal shear layer, reducing shear within the sands. 2) The fine component in the sands reduces the influence of intergranular dispersive pressure.

Fig.3.15. Trochoidal wave ripples from log Rotstock within turbidite sand generated by storm activity.

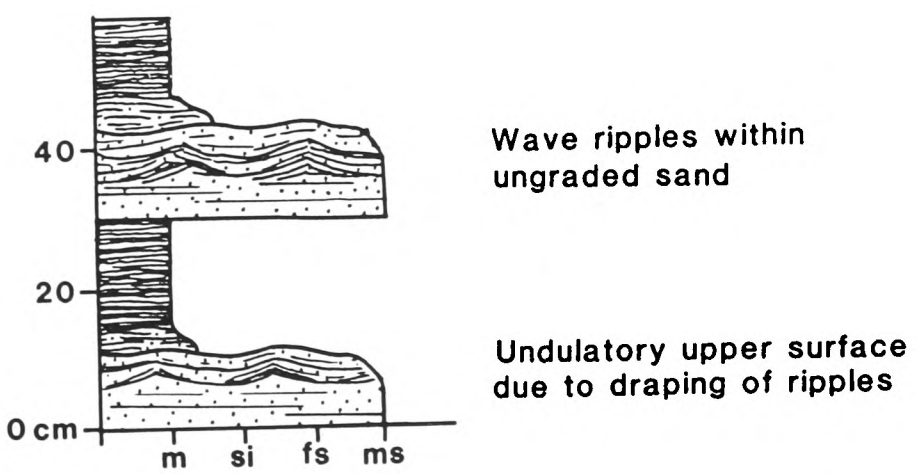

Fig.3.16. Log of storm generated turbidite sands as illustrated in fig.3.15.

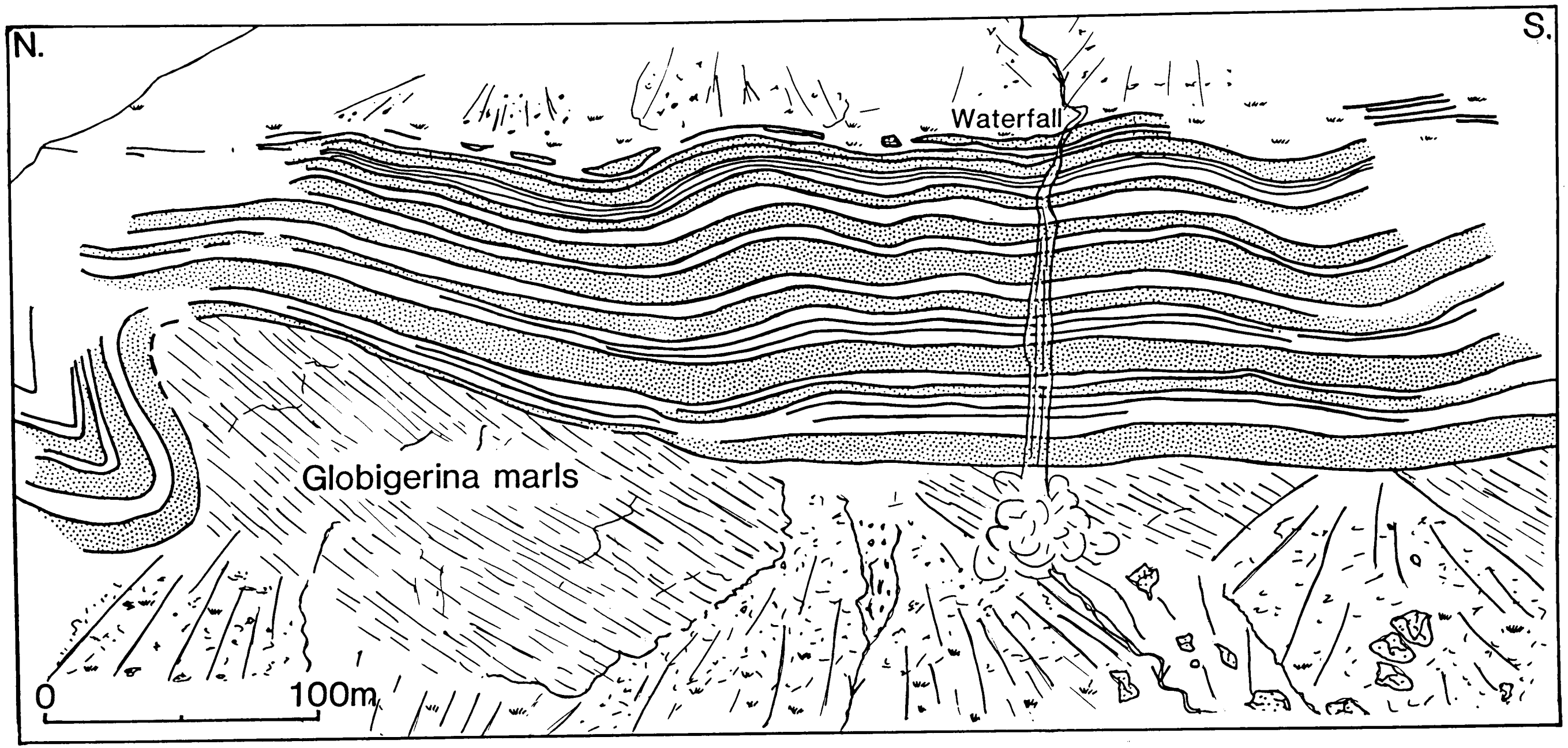

Fig.3.17. Drawing of outcrop to the east of Ober Stafel, Jetzalp. This demonstrates thinning and pinching-out of massive sand beds of the Inner basin towards the Jetzalp thrust-ramp palaeohigh.

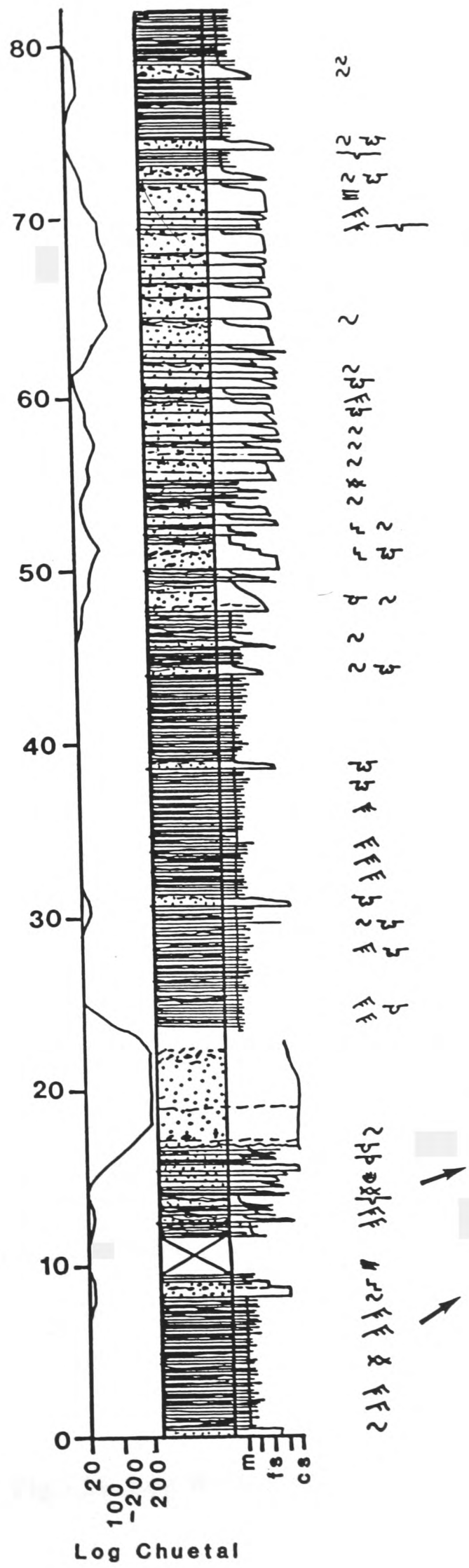

Log Chuetal

Fig.3.19. Log Chuetal.

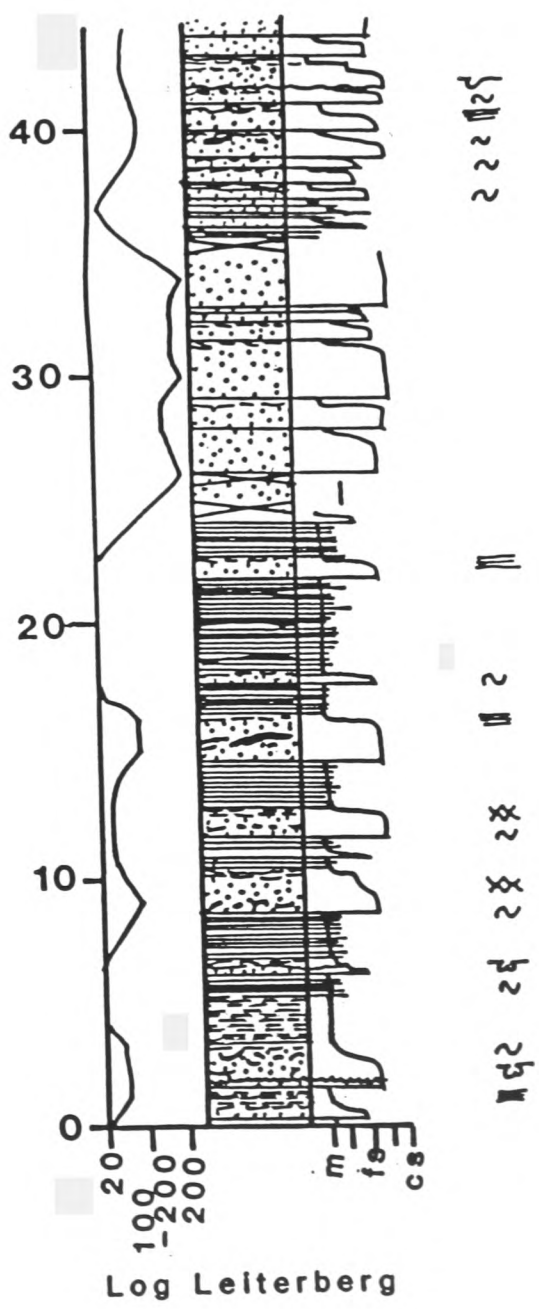

Log Leiterberg

Fig.3.18. Log Leiterberg.

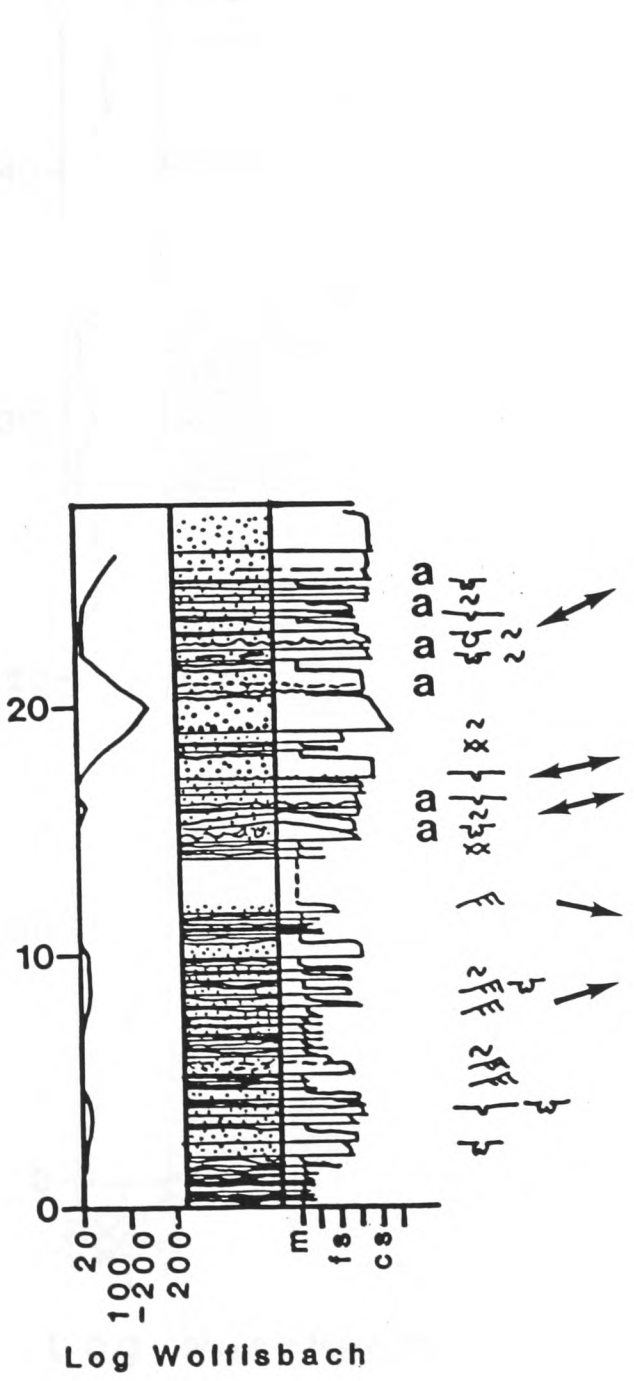

Fig.3.20. Log Hintersulz.

Fig.3.21. Log Wolfisbach.

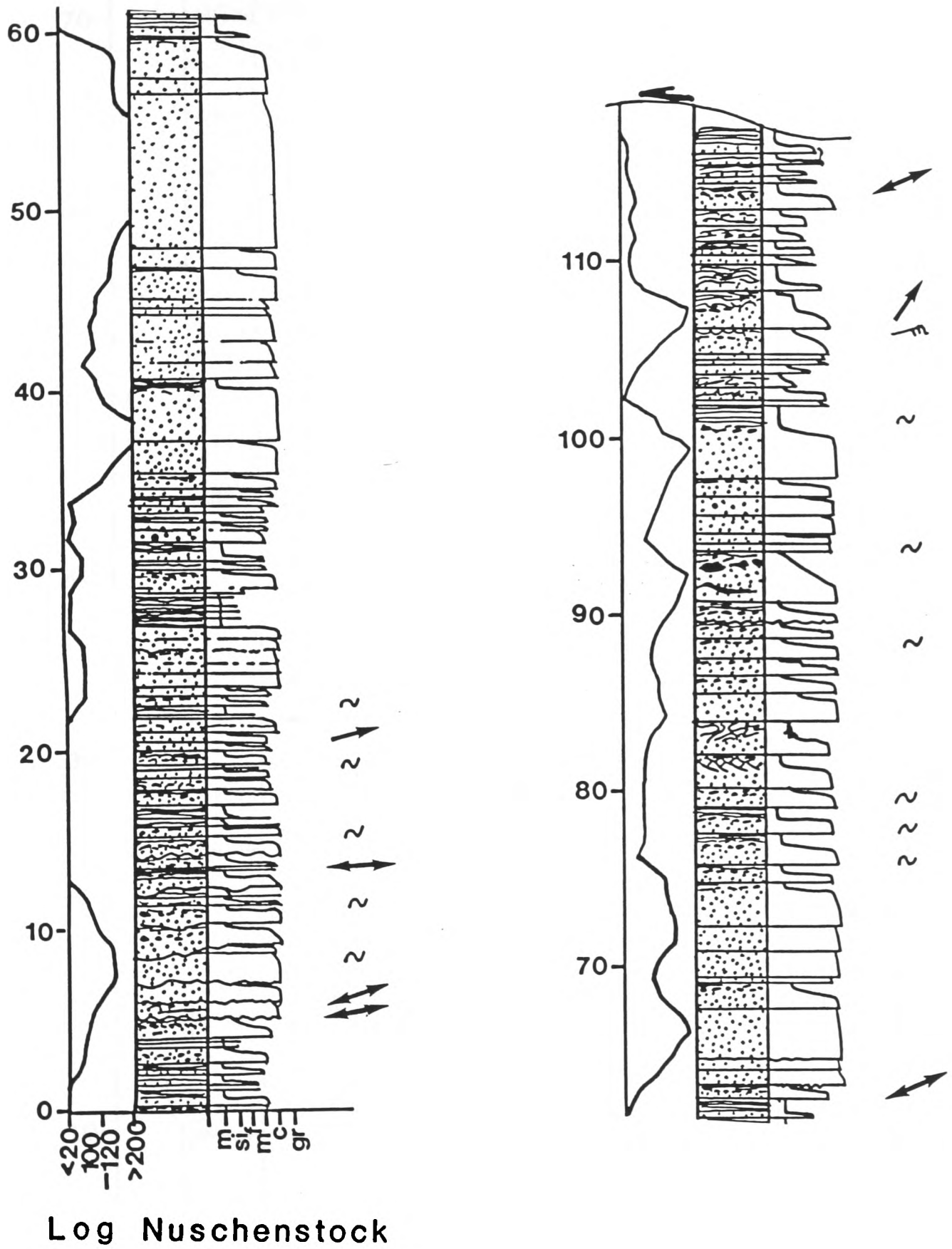

Fig.3.22. Log Nuschenstock.

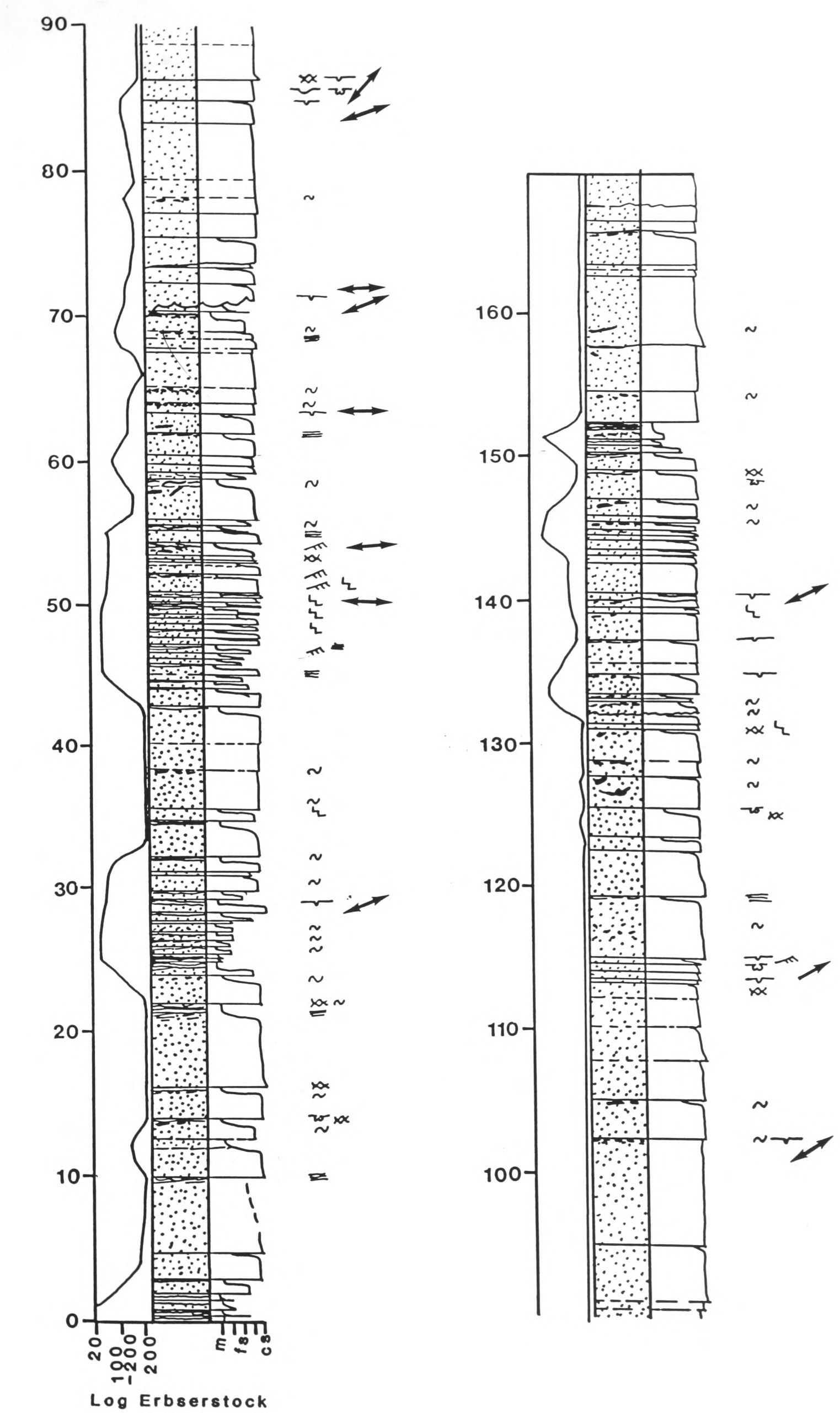

Fig.3.23. Log Erbserstock.

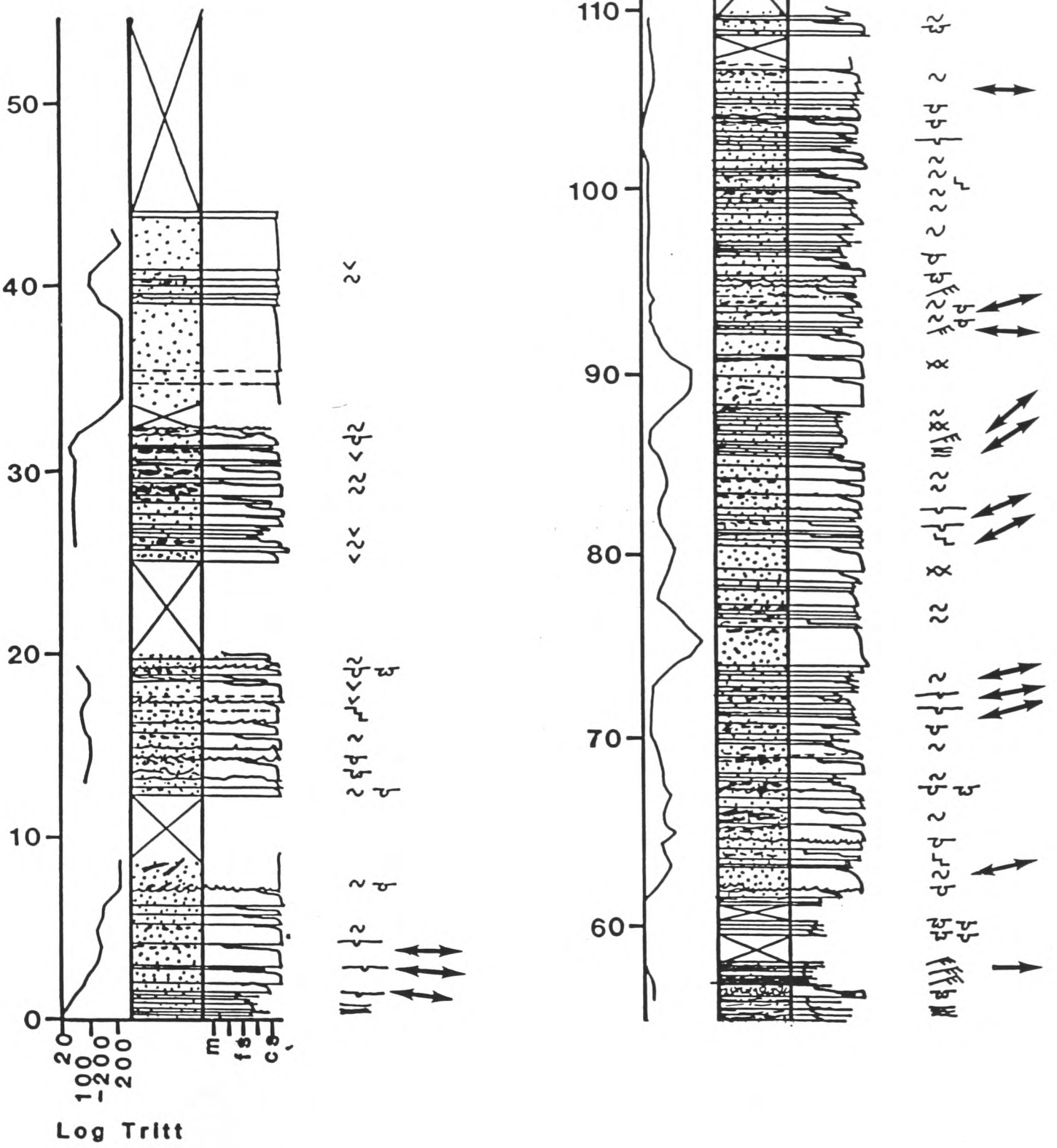

Fig.3.24. Log Tritt.

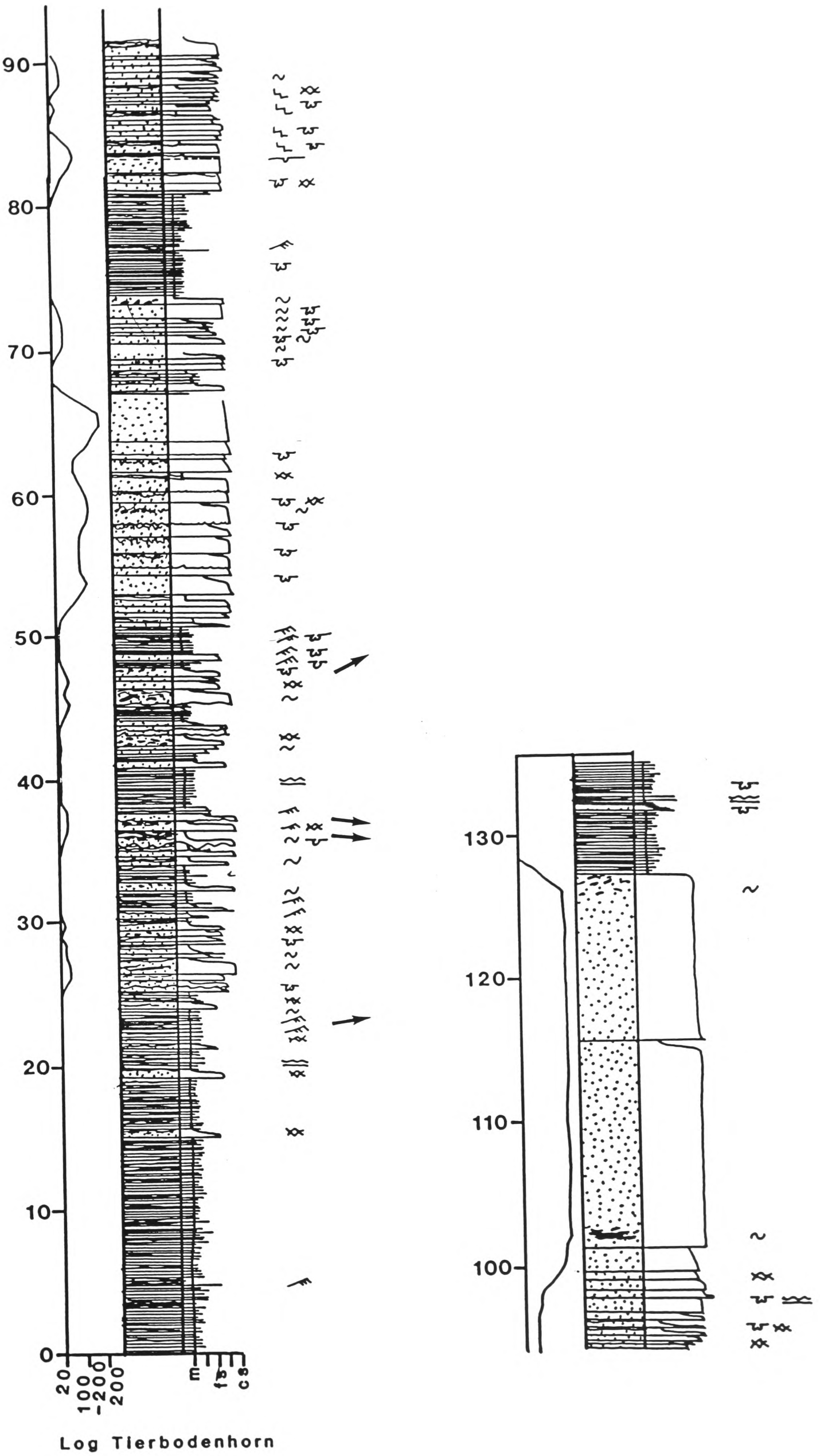

Fig.3.25. Log Tierbodenhorn.

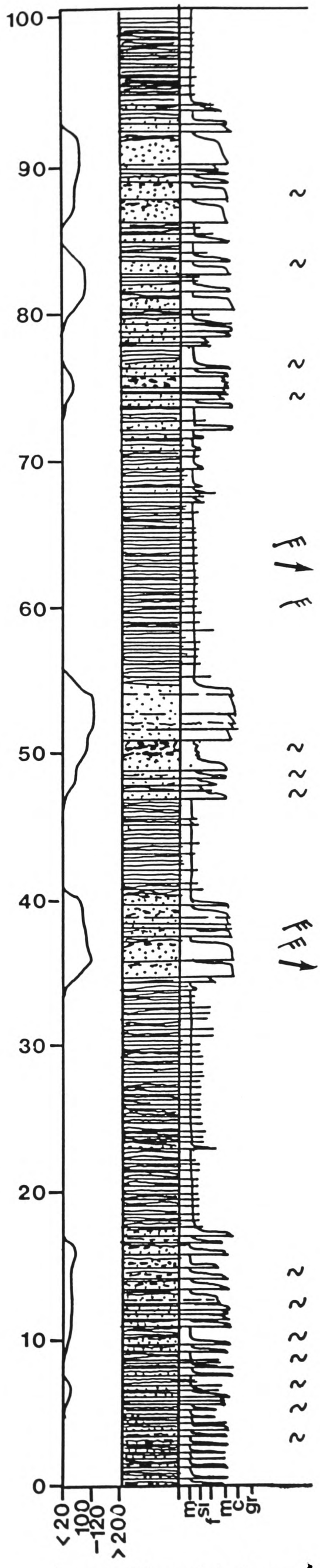

Log Chueboden (Grid ref. 73080, 19980)

Fig.3.26. Log Chueboden.

Fig.3.27. Two loaded amalgamation surfaces from log Tritt. The central bed is separated into two units by a sharp planar grain-size break, this is step-wise grading as illustrated in fig.3.29.

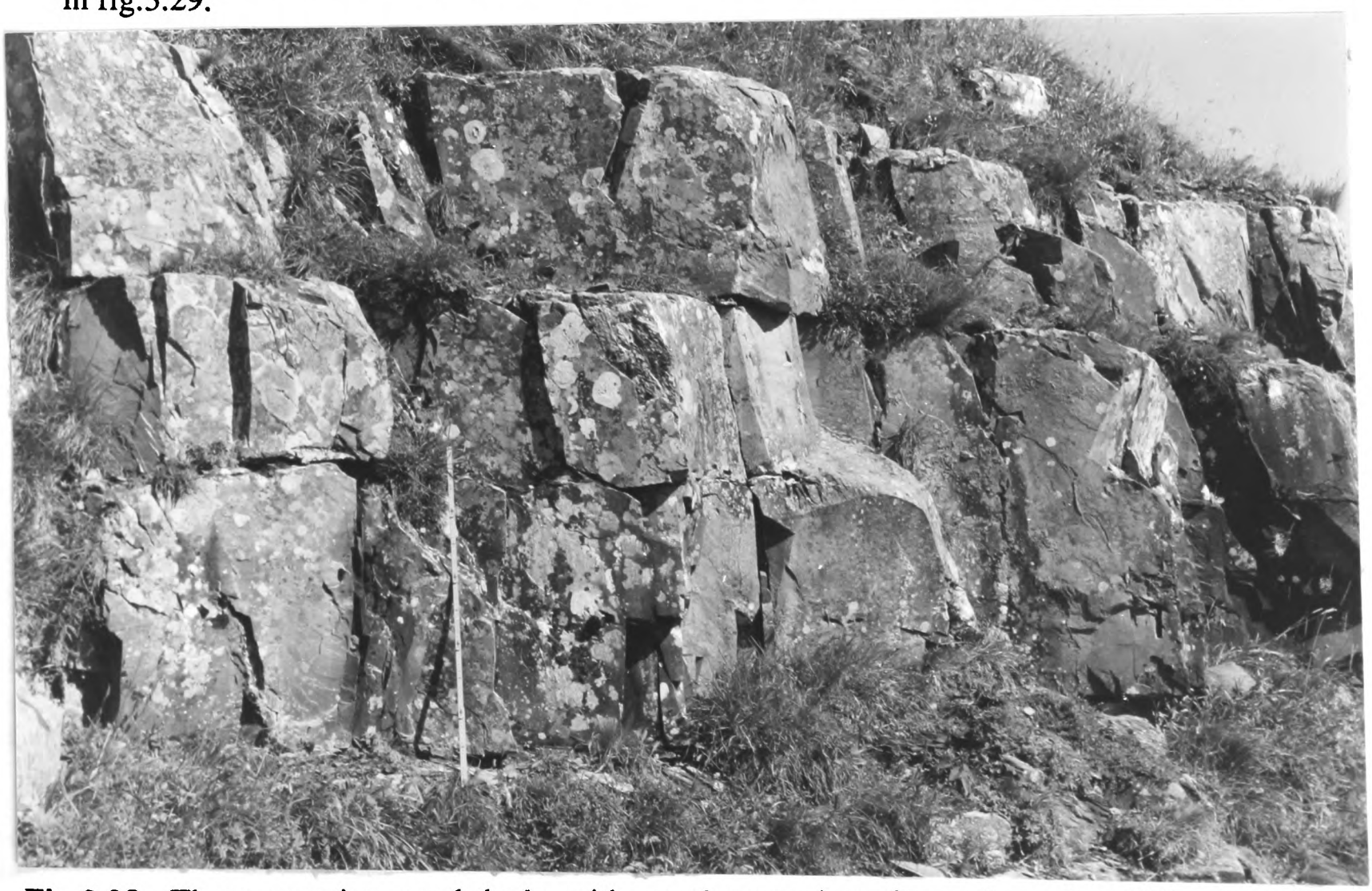

Fig.3.28. Three massive sand beds with amalgamated surfaces from log Tritt. The lower amalgamation surface which occurs at the level of the top of the ruler, becomes much less obvious to the right of this outcrop.

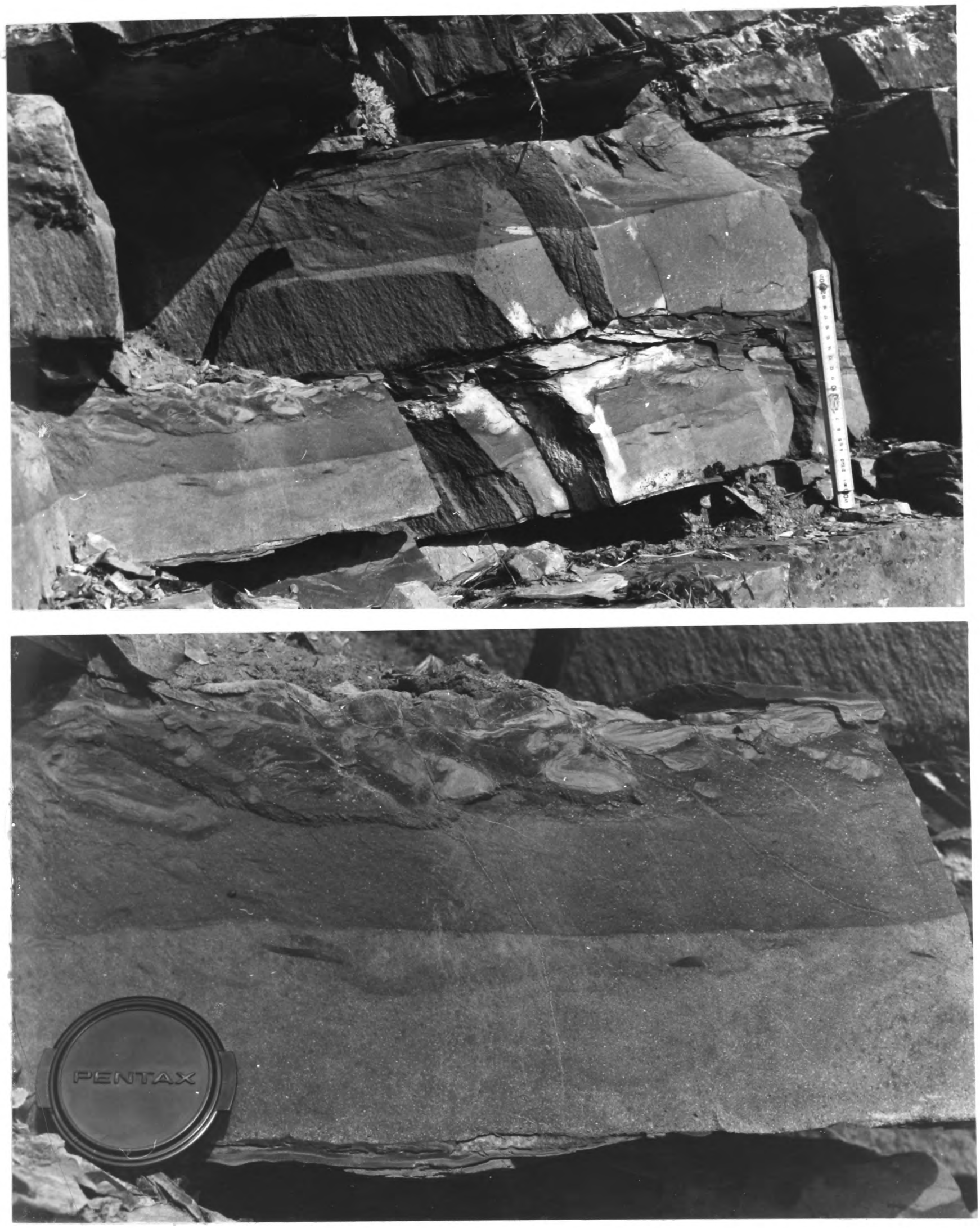

Fig.3.29a). Step-wise grading in two successive medium bedded sands from log Tritt. b) Close-up of left section of lower bed. showing the clear grain-size step within this bed between the lower medium coarse sand with a slight basal lag, and an upper muddier unit. The upper unit is then separated from the overlying muds by an equally sharp break in grain-size, but this is masked by intense pseudonodule formation. Note the presence of large (0.5-1mm) white sand grains throughout bed. Step-wise grading is interpreted as resulting from the rapid flow velocity fluctuations associated with a reflected turbidity current which forms internal solitons as described by Pantin and Leeder (1987). Deposition of each of the poorly sorted units occurs when the summed flow velocities of the foreward flow and the reflected reverse flow of the soliton equals zero. Erosion, forming the sharp break, occurs during the resumption of foreward or reverse flow.

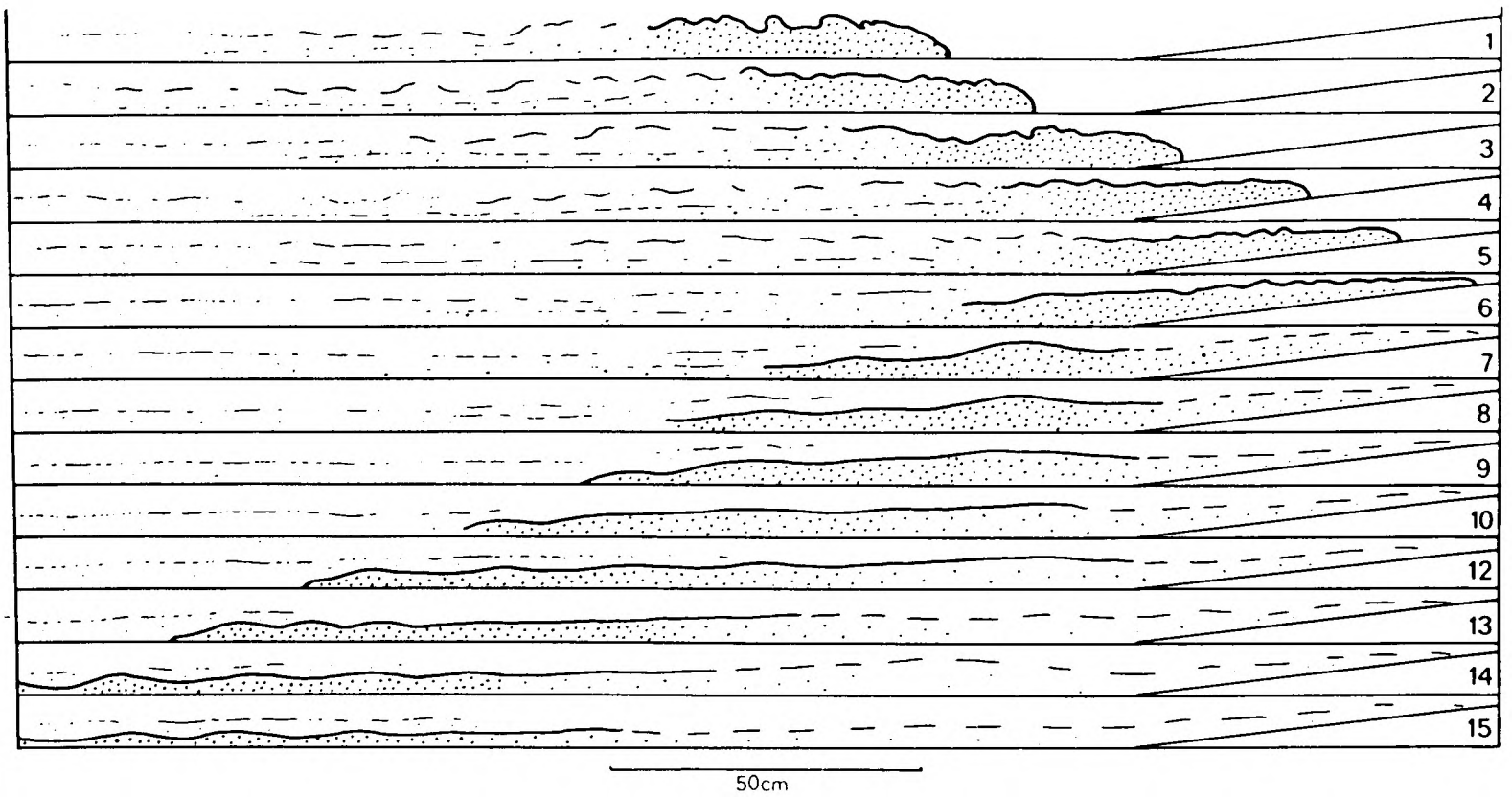

Fig.3.30. Formation of internal solitons during the reflection of a turbidity current off an opposing slope taken from Pantin and Leeder (1987). These are tracings of sequential time lapse photographs of flume tank experiments. Note that at stages 7 and 8 there is a large bulge formed at the change of slope. This represents the initiation of the solitons which form from the reverse surge of the bulge. It would seem likely that it would be in these early stages that maximum flow velocity fluctuations would occur. This is backed up by the observation that no more than two grain-size steps ever occur in one bed. Therefore the steps in fig.29 are likely to have formed by this initial bulge at the base of the slope and not by the later formed train of four solitons.

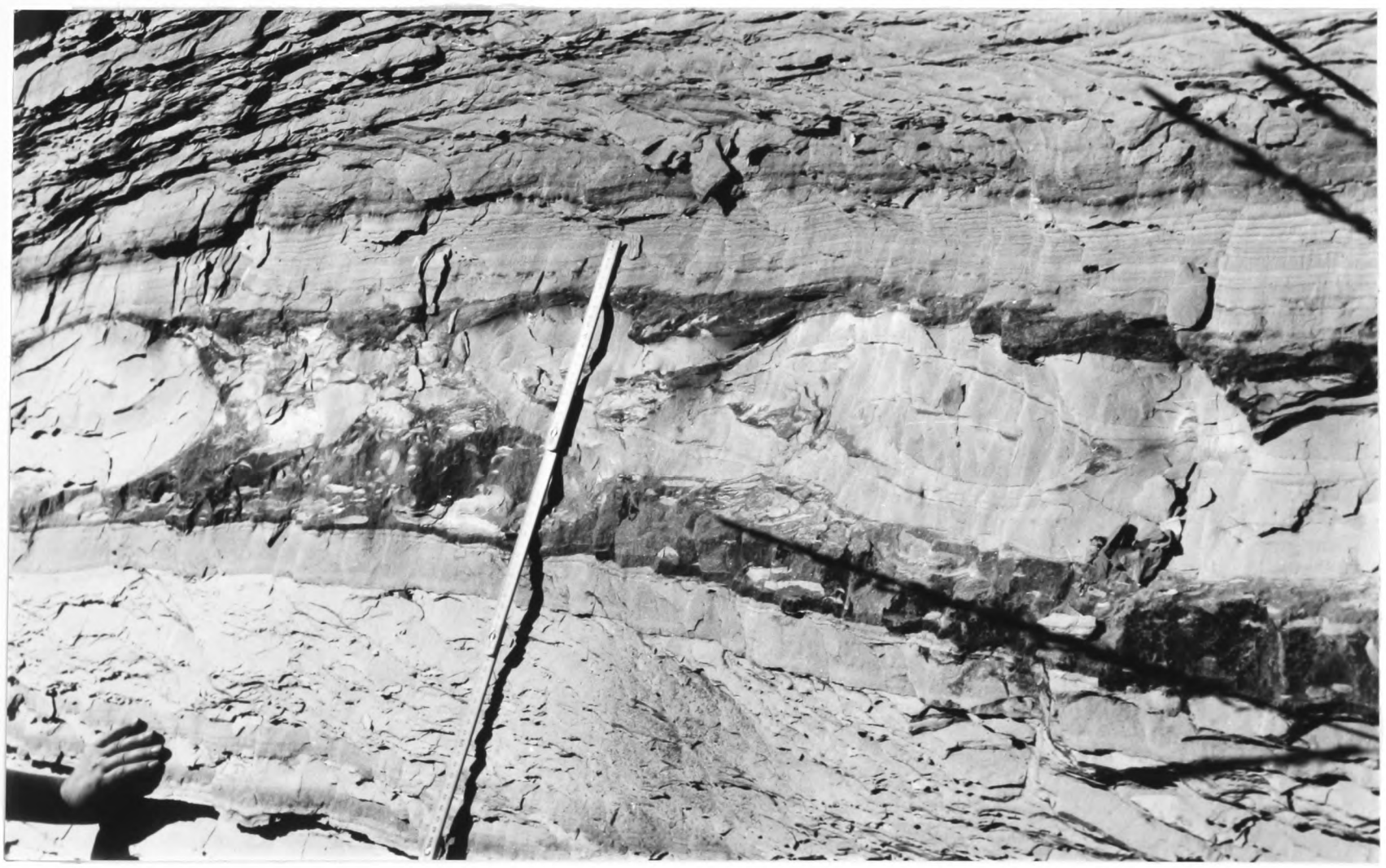

Fig.3.31. Mud clasts comprising approximately 70% of a fine sand turbidite from log Chueboden.

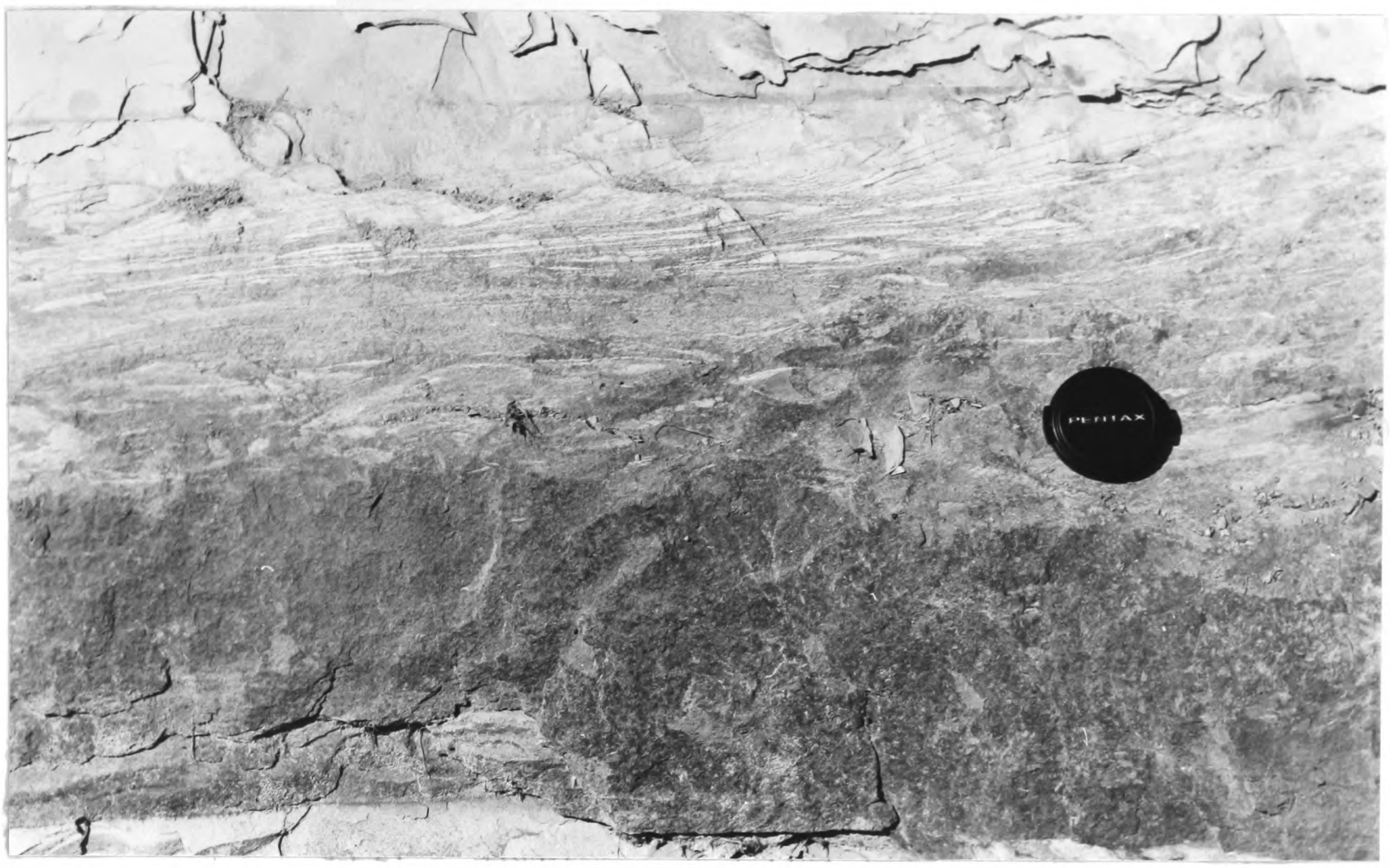

Fig.3.32. Graded turbidite containing highly sheared mud-clasts at top of bed. These have a dextral shear sense indicating down slope movement direction.

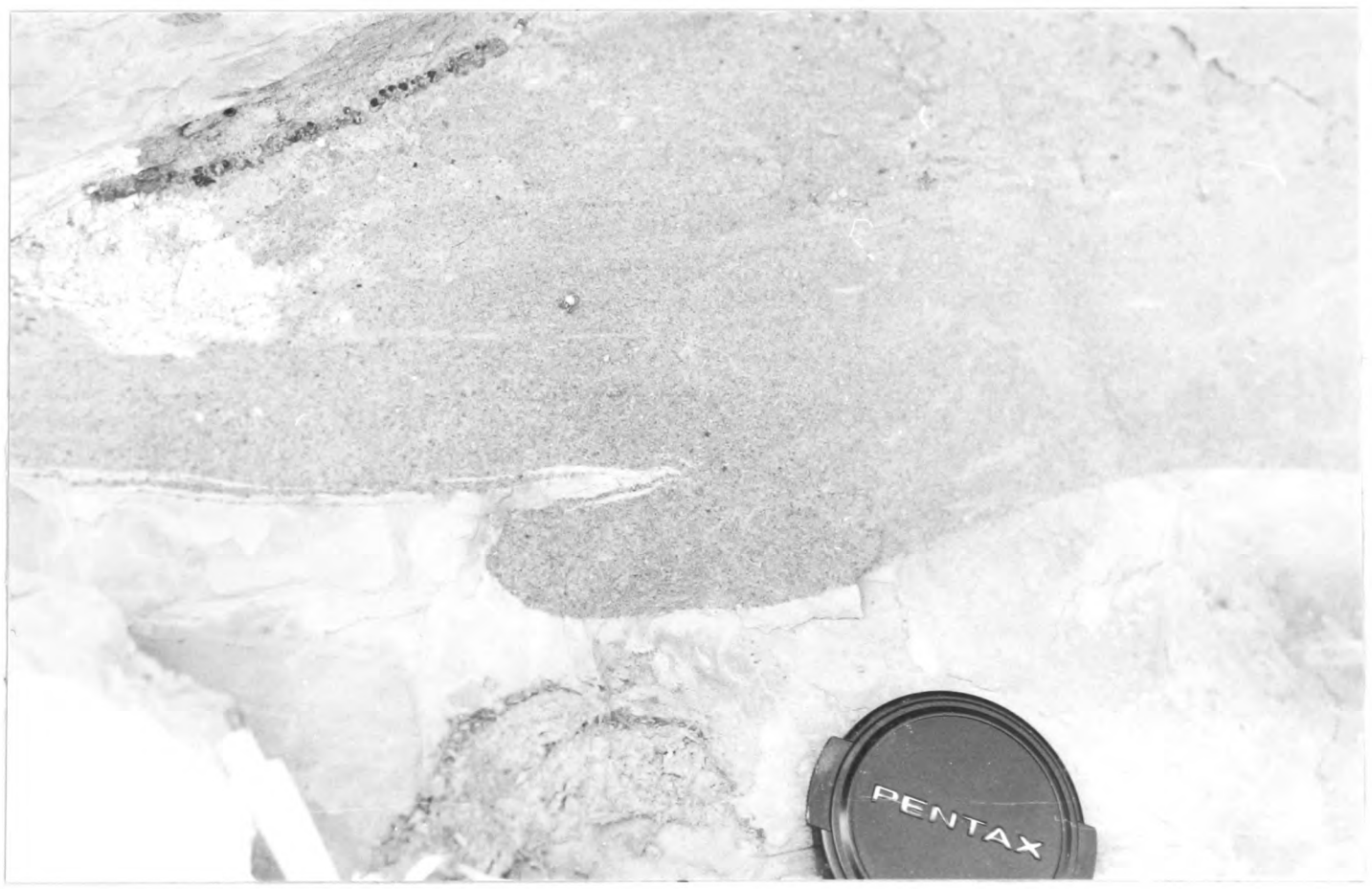

Fig.3.33. The plucking of soft mud clasts from the base of a turbidite sand. This indicates down slope movement to the right.

Fig.3.34. Isoclinal slump fold formed during the deposition of the turbidite sand to the right of the picture. The forces associated with the surge of the flow caused the peeling off of the mud layer from its lower bedding surface. This would then be incorporated into the sand as a mud raft.

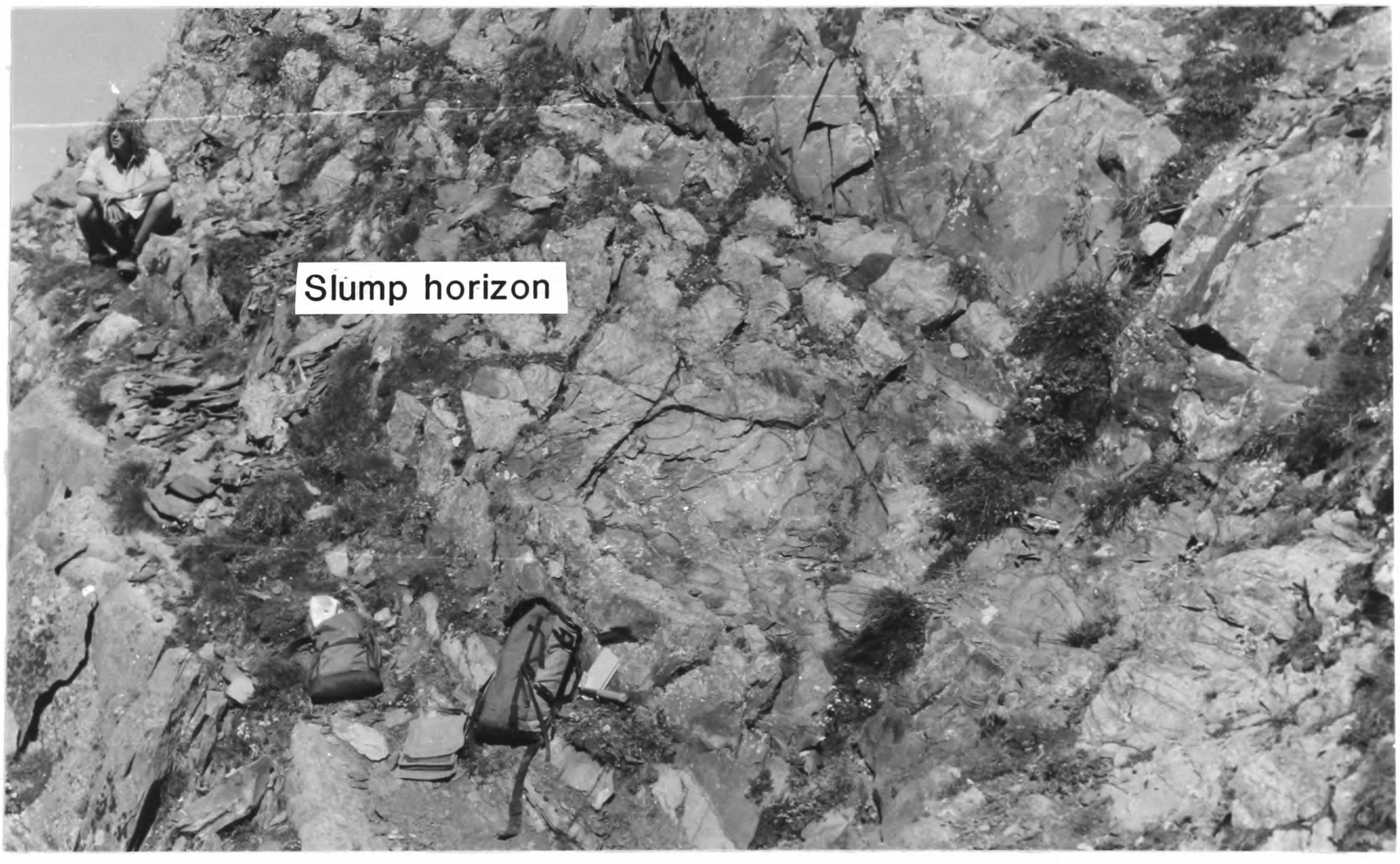

Fig.3.35a) Slump horizon from log Nuschenstock, forming the 1.5m band above the rucsac. Fig.b) is a close-up of a 20cm mud band at the level of the base of the rucsac. This shows syn-depositional brittle listric normal faults displacing laminae within the mud band. This is then eroded by the overlying sand. Fig.c) is a close-up of examples of slump folds in the overlying mud. Note the contrasting mechanical behaviour of the muds in these examples. It is thought that the slump horizon was formed with a slight overburden causing higher pore-fluid pressures resulting in the more ductile deformation. Both fold vergence and fault displacements indicate downslope movement to the ENE (parallel to curent flow).

b.

c.

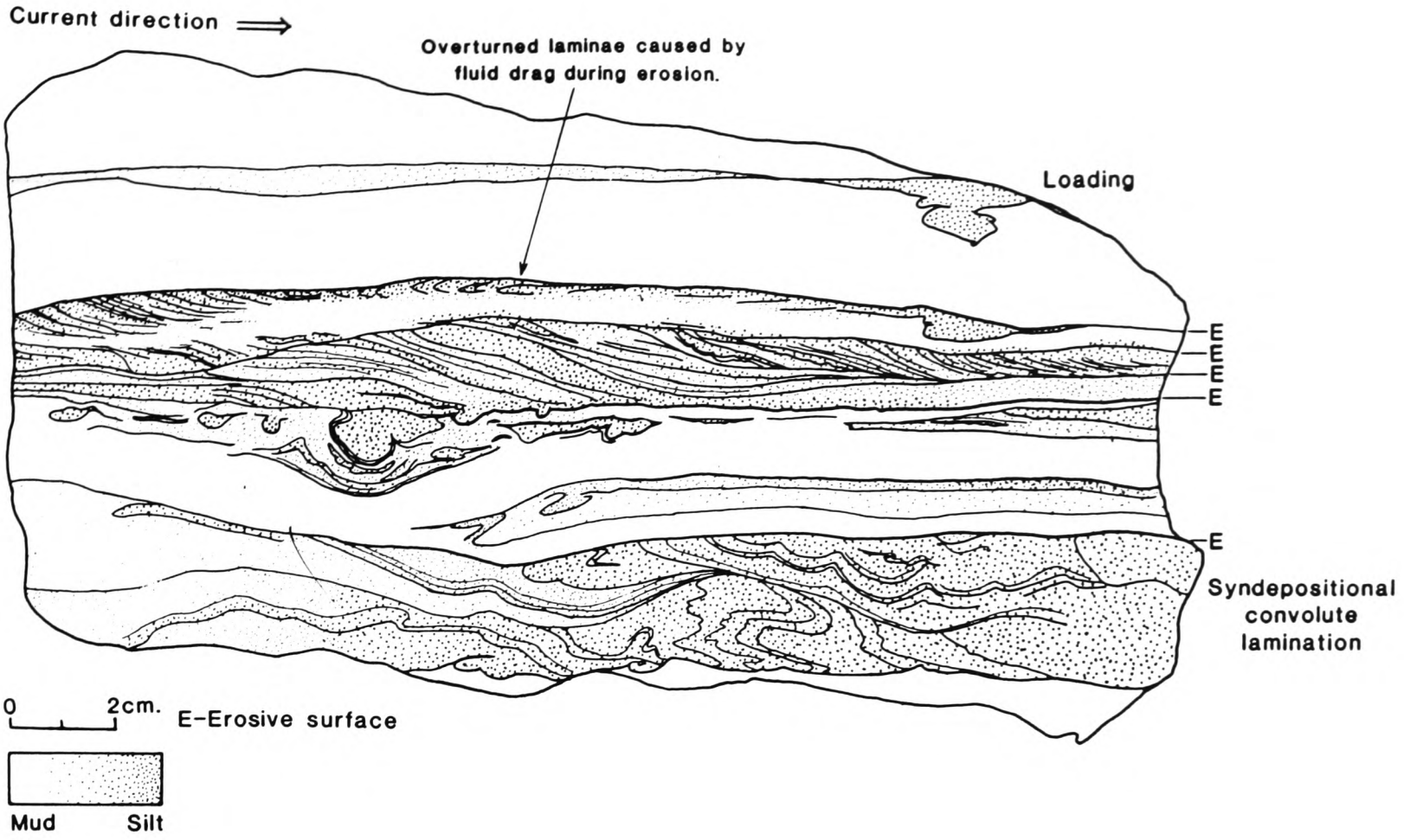

Fig.3.36. Sedimentary characteristics of the silt/mud laminations from log Chuetal.

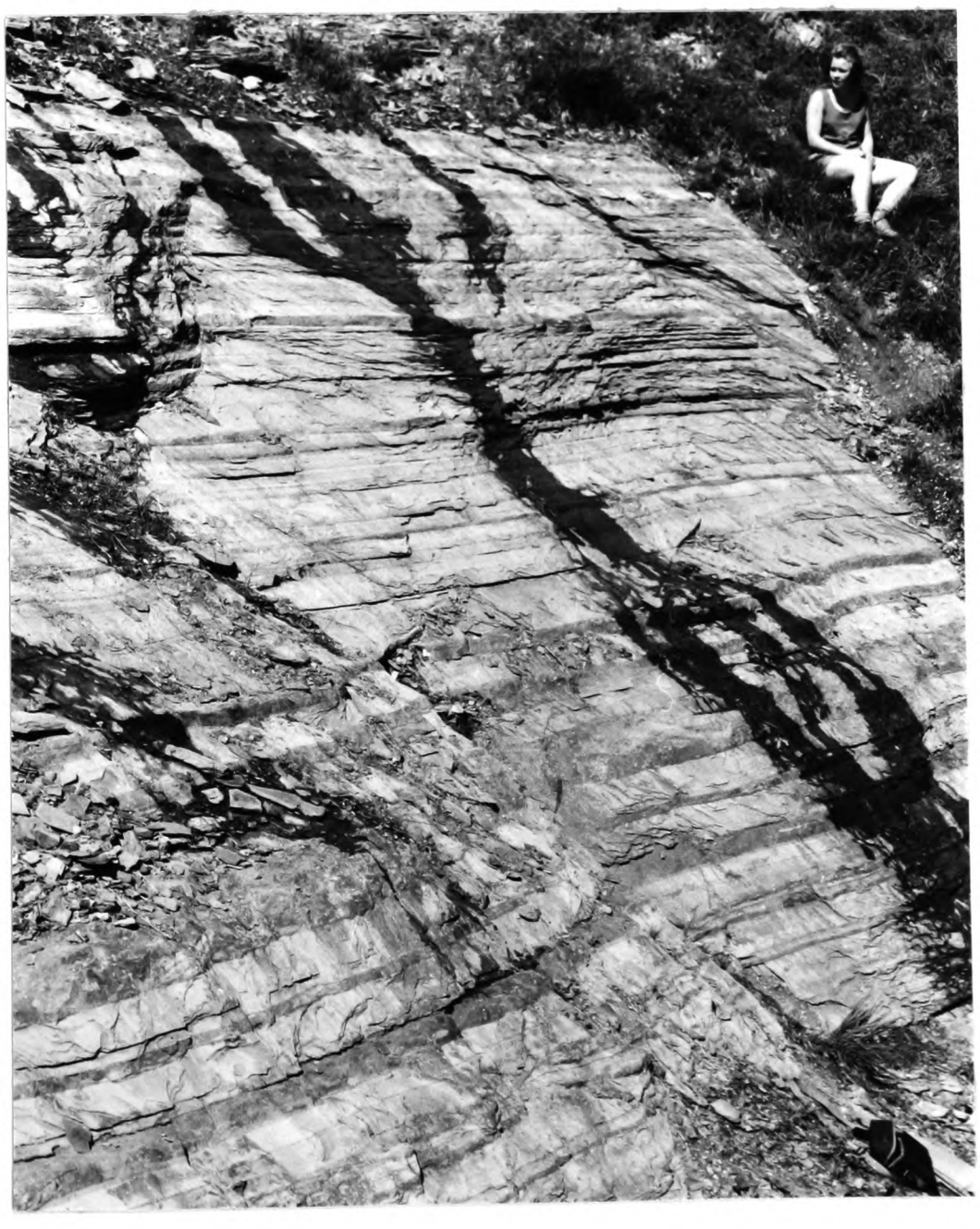

Fig.3.37. Thin bedded silt/mud couplets from log Chueboden. This facies is considered to represent high stand deposits of the Outer basin. The continuous nature of the bedding and the current and horizontal lamination suggest steady fall-out from a low density turbidite. This is compared to the laterally discontinuous thin bedded silt units of the Inner basin, which have no sedimentary structures and are considered to have been deposited relatively rapidly to the this equivalent facies of the Outer basin.

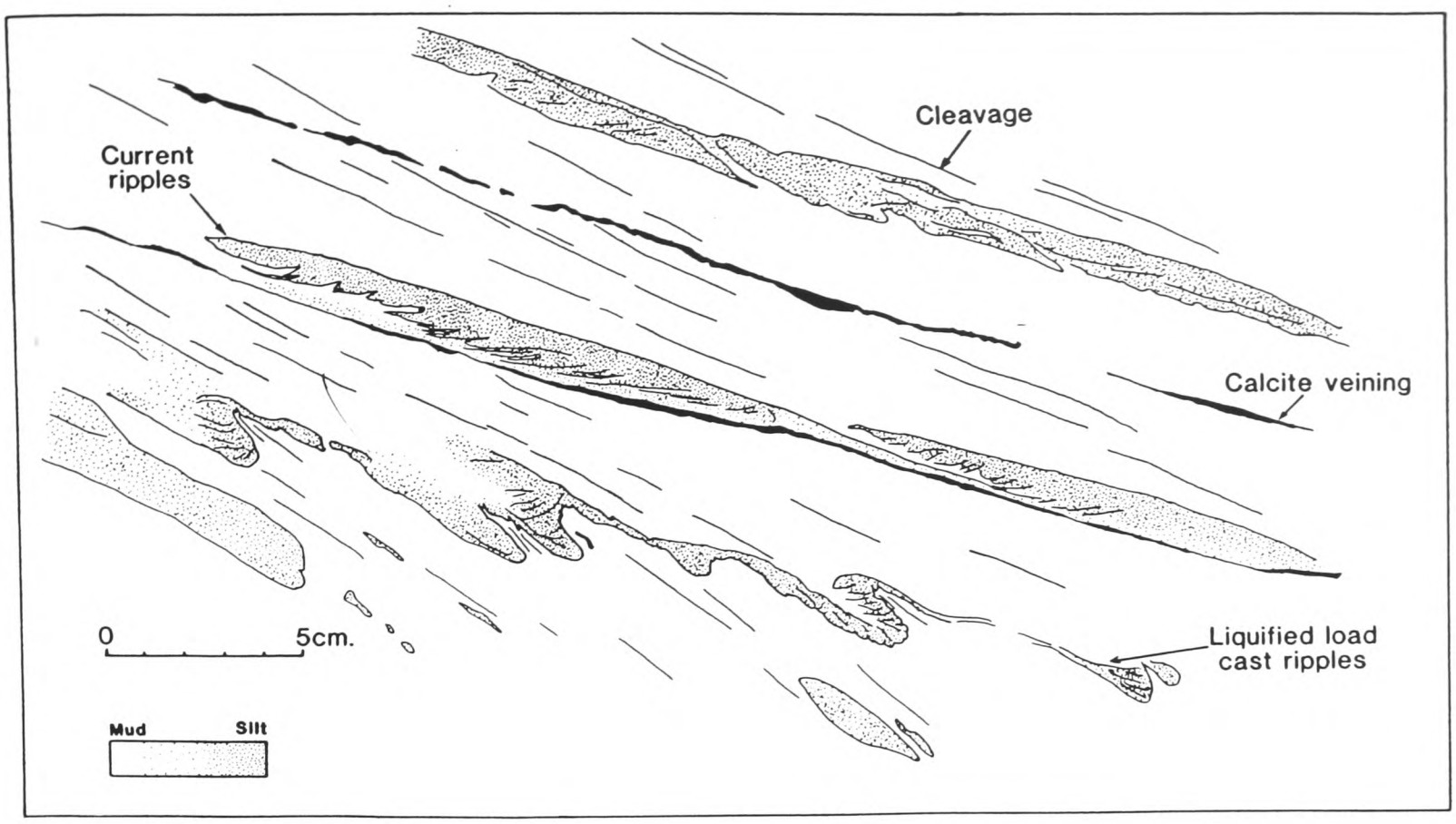

Fig.3.38. Drawing of silt/mud laminations from outcrop on northern edge of Jetzalp (Grid ref.72870,19450). The liquefied load cast ripples indicate down slope movement towards the NNW. These are palaeogeograhically located just north of the Jetzalp palaeohigh and indicate an outer northward dipping slope. This slope is also suggested by the thinning of stratigraphy from the Outer basin.

Fig.3.39. Soft-sediment shearing of muds and sands from the same locality as fig.38. This also indicates downslope movement to the NNW.

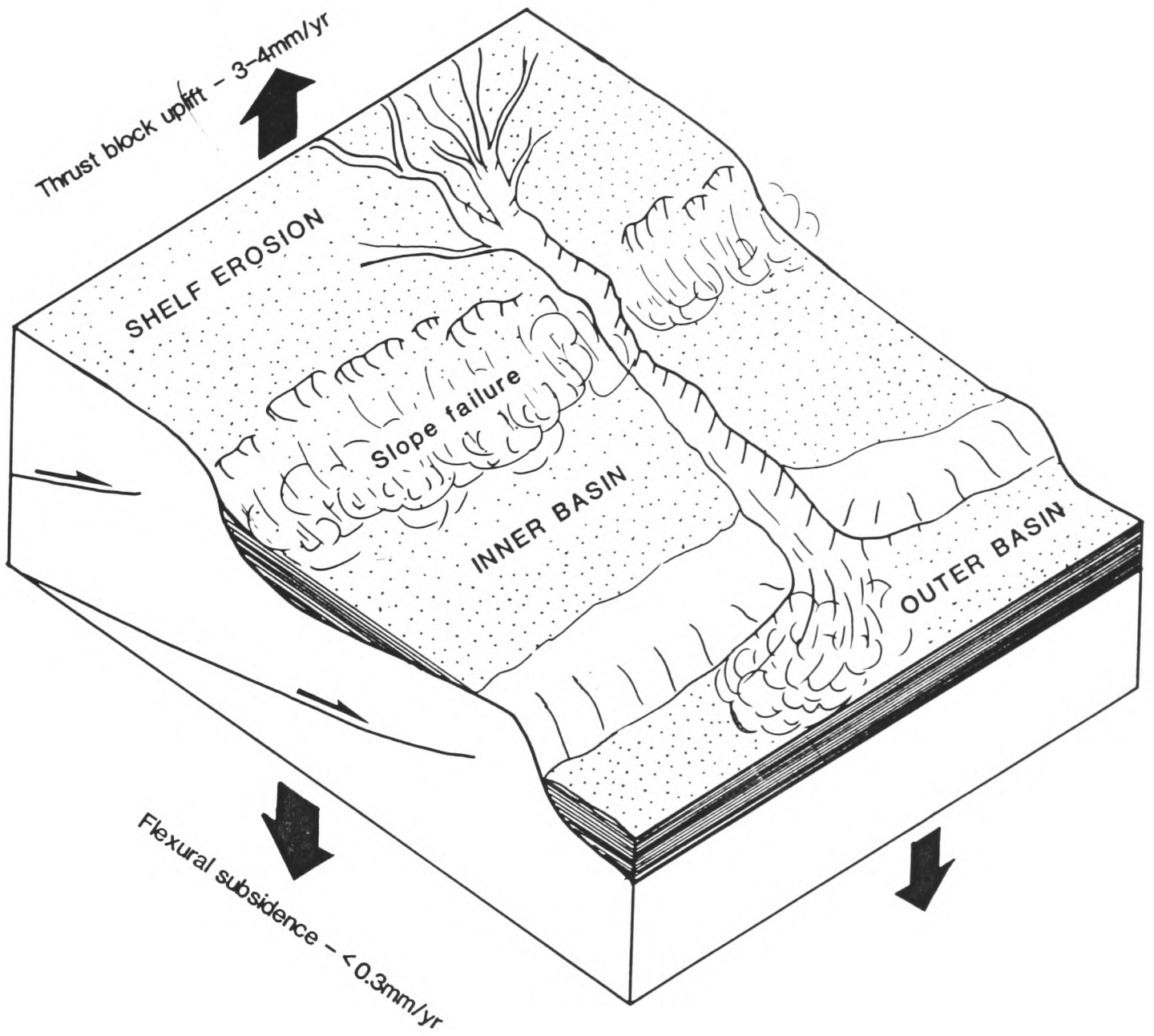

Fig.3.40. Schematic reconstruction of the Taveyannaz sandstone basins. The Inner and Outer basins are separated by a thrust-ramp palaeohigh causing pinchout of the stratigraphy of the Inner basin. The Inner basin is fed by catastrophic slope failure associated with movement on the innermost thrust. The resultant massive sands and muds are topographically confined. Intercalated with the massive sands are storm induced turbidite sands removed from the shelf. The Outer basin is fed by a point source which bypasses the Inner basin, so forming a thicker sequence. The thrust activity that causes slope failure feeding the Inner basin, also results in a relative lowering of sea level causing erosion of the shelf, and the formation of thick sand packages in the Outer basin. The high frequency low stand events are counteracted by the steady background flexural subsidence. Calculated relative uplift on a thrust sheet with an advance rate of 4mm/yr and a slope angle of 40° is 3-4mm/yr. Rates of flexural subsidence are <0.3mm/yr (Homewood et al, 1986).

CHAPTER 4

SHALLOW LEVEL DEFORMATION AND EMPLACEMENT OF MUD SHEETS INTO THE TAVEYANNAZ BASIN

4.1 Introduction

The first detailed description of the thrust sheets immediately overlying the Taveyannaz sandstones of the Glarus Alps was by Leupold (1942), who separated what was known as the Glarner Wildlysch into the Blattengrat and Sardona Flysch units. These form the mountains to the south-east of the Sernftal valley in the region of the village of Elm. Wegmann (1961) described the sedimentology and stratigraphy of these units in the area south of Elm. The structurally lower Blattengrat unit comprises dominantly limestones overlain by marls, and ranges in age from late Campanian to Lutetian. The structurally higher Sardona flysch comprises marls, quartzites, and turbiditic sands and muds, ranging in age from Cenomanian to basal Lutetian.

In terms of the palaeogeography, Ruefli (1959) considered the Sardona flysch to be Ultra-Helvetic, and Wegmann (1961) considered that the Blattengrat unit was separated from the Sardona flysch by a structural high and was therefore South Helvetic in origin. The interpretation of these units as being derived from south of the Helvetic realm is based on their differing stratigraphy to the Helvetic and North Helvetic units of the nappes and the parautochthon respectively.

Milnes and Pfiffner (1977) identify the emplacement of the Sardona and Blattengrat units as the first evidence of compressional deformation in the area; this was named the "Pizol phase" of deformation. The South Helvetic and Ultra-Helvetic origin to these

structural units, and their structural position (underlain by North Helvetic flysch and overlain by Helvetic nappes) necessitates that they were transported over the Helvetic province and emplaced upon the Taveyannaz sandstone basin. Trümpy (1969) suggests that some form of gravity glide mechanism is likely for the emplacement of these units.

The regional geometry of the Blattengrat and Sardona units exhibits a marked thinning from the east into the region of this study. Wegmann (1961) considers that the relatively thin (50-100m) mud sheet that overlies the Taveyannaz sandstone in this region is laterally connected to the Sardona Flysch.

The aims of this study are to elucidate the timing and the approximate depth of emplacement of the mud sheet. Metamorphic data indicate that these rocks have been buried to depths of up to 10km (Frey, 1978), and have been intensely deformed during this burial, forming fold and thrust structures with a penetrative cleavage (chapter 2). The results of my work indicate that the initial transport and emplacement of the mud sheet onto the Taveyannaz sandstone occurred at, or near the sediment/water interface, terminating sedimentation within the basin.

The term "tectonic deformation" is often used with reference to deformation of lithified sediments, as opposed to "soft-sediment deformation" involving partially or unlithified sediments near the depositional surface; this observance is followed in this study. The recognition of the degree of lithification of sediments during deformation is not simple, as few unequivocal criteria exist to distinguish between soft sediment and tectonic structures (Maltman, 1984). It is therefore necessary to assess as many criteria as possible; listed below are those used in this research:

1) The sedimentological nature of the rocks; evidence of rapid deposition, dewatering, liquefaction and slope instability in the sediments (chapter 3).

2) The style of folding compared to the regional deformation. ie. disharmonic and irregular

fold geometries transected by later fabrics.

3) The muddy nature of detachment zones, compared to the later brittle, mineralised fault zones.

4) The unlithified nature of the sand during deformation (this being the most important criterion).

5) Sedimentary reworking of the upper surface of the Taveyannaz sandstones prior to the emplacement of the mud sheet.

The interpreted deformational development of the basin in the Panixerpass region is illustrated in figure 4.25. This will be discussed at the end of the chapter, but is worth referring to during the following descriptions.

4.2 Sedimentology of the mud sheet (Sardona Flysch - Wegmann, 1961)

The mud sheet appears light grey in colour, with a distinct buff to rusty coloured weathering. It comprises predominantly thin bedded muds and silts; these are sometimes calcareous forming marls. Silt beds range in thickness from 0.1-5cm, with sharp bases fining up into homogeneous or occasionally horizontally-laminated silts (Fig.4.1), then up into muds; starved current ripple lamination and convolute lamination are sometimes present. Silt beds vary in thickness laterally by up to 50% over 0.5m. Disruption of laminae and mottling of the silt horizons indicate bioturbation, although this is not evident in the thinner laminated muds. Laterally continuous, undisturbed laminated muds are illustrated in Fig.4.2. Occasionally, tubular foraminifera similar to those seen in the Globigerina marls are present.

These sediments are interpreted as having been deposited by dilute turbidity currents. The confinement of bioturbation to the silt horizons suggests that organisms were carried

out of their usual habitat in the shallower waters, into deeper water by the initiation and flow of the turbidite currents. An environmental interpretation of this sequence is difficult, the possibilities include more proximal overbank deposits, or pro-delta muds. This will be discussed further in section 4.5.

4.3 The large scale structural relationship between the Taveyannaz sandstone and the mud sheet.

The gross structural relationship between the Taveyannaz sandstone and the overlying Mud sheet will be described with reference to three sections from the Inner basin taken perpendicular to the strike of the basin. Figure 4.3 illustrates a simple reconstruction of the Taveyannaz basin at about 40Ma, based on the structural and sedimentological data described in chapters 2 and 3. Located on this reconstruction are the three cross-sections described, which from east to west are named Jetzalp, Panixerpass and Piz Fluaz. These are illustrated in the form of a box diagram in figure 4.4, showing an approximate representation of the styles of deformation seen within each section.

4.3.1 The Jetzalp section

This section is illustrated in figure 3.17 and exhibits a relatively undeformed sequence of very thick bedded Taveyannaz sands of the Inner basin. The only deformation involves 50-100m scale northward vergent folds with a pervasive axial planar cleavage, typical of the regional structural style. The contact with the overlying mud sheet is conformable with bedding in the sandstones, showing no signs of brecciation or mineralisation. Within the overlying mud sheet are a few blocks of the underlying sands, ranging from 1-2m across.

The exact nature of the blocks is not known due to the inaccessibility of the outcrop.

4.3.2 The Panixerpass section

Figures 4.5 and 4.6 illustrate the style of deformation within the Taveyannaz sandstones to the north of Panixerpass. This demonstrates the extreme intensity of the structural deformation of the very thick bedded sands of the Inner basin. Individual, 10m thick sand beds are detached into 30-100m long slabs which are imbricated and tightly folded. Rapid thinning and pinching out of the beds results in irregular geometries; structures are completely disharmonic; a structure developed within one bed bears no relation to structures in the neighbouring bed. Scattered between the relict sandstone beds are chaotic blocks of sandstone of varying shape and size (0.01-10m).

The contact with the mud sheet is intensely deformed as illustrated on the geological map of the area north of Panixerpass (fig.4.7). Within the mud sheet are large blocks of sandstone up to 130m across containing some relict bedding, but which are predominantly chaotic in nature. Figure 4.8 illustrates a large block with bedding preserved, which demonstrates imbrication and folding of the beds similar to that illustrated in figures 4.6 and 4.7. It is often difficult to establish if blocks are truly detached from the underlying sandstones, as the intensity and chaotic nature of the imbrication in the sands results in complicated interfingering of the sandstone and mud sheet. Approximately 100m south of the Panixerpass hut, there is a large (80m) block of Jurassic Malm limestone totally isolated within the mud sheet.

The region to the north of Panixerpass has been studied in detail, and will be used to describe the medium and small scale structures associated with the large scale gross

geometry of these sequences.

4.3.4 The Piz Fluaz section

The cliff-section exposed on the north-east side of the ridge running between Piz Fluaz and the Hausstock (fig.2.12) represents a complete exposure of the Inner basin and its relation to the overlying mud sheet; this is illustrated in figure 4.9. In terms of the intensity of the deformation, this section is considered to be intermediate between the relatively undeformed Jetzalp section and the intensely deformed Panixerpass section.

The Inner basin sediments clearly show a rapid thinning and pinching out of the stratigraphy towards the north-west. The deformation comprises a gentle tilting of the bedding towards the south-south-east, with thrusts running sub-parallel to bedding. Gentle to open folding on a 100m scale can be seen, which is usually harmonic through the sandstone stratigraphy. This folding is considered to be relatively late-stage in origin, in view of its similarity to the regional style of deformation.

The upper contact of the sandstones with the mud sheet in this section is particularly important to the interpretation of the deformational history of this sequence. A great deal of the contact is conformable to bedding in the sandstones, as seen in the Jetzalp section. Interrupting this are major disconformable steps in the contact, where the sandstone becomes truncated perpendicular to bedding. These steps are nearly vertical and have a topographic relief of up to 50m. Figure 4.10 and 4.11 illustrate the geometry of these steps. From this, it is clear that they are generally formed in the hanging wall to thrusts.

Within the mud sheet are blocks of sandstone similar to those in the Jetzalp and Panixerpass sections. Figure 4.9 shows a large block of bedded sandstone (100m across)

floating in the mud sheet, located above the northerly pinchout of the underlying stratigraphy. Figure 4.10 illustrates various irregular blocks comprising detached fragments of individual beds, showing thickening and thinning resulting from boudinage. Below these blocks, a vague layering sub-parallel to the contact with the sandstones can be seen; this is thought to represent bedding in the mud sheet. However, the exposure is vertical and inaccessible and this cannot be proven.

4.3.4 Summary

Within a distance of 5km along strike, there are three major outcrops yielding sections through the northern edge of the Inner basin. The most easterly of these is the Jetzalp section, which shows very little deformation, and has a conformable contact into the overlying mud sheet which contains occasional (<1% in outcrop section) small sandstone blocks. The most westerly of the sections (Piz Fluaz) demonstrates an increase in deformation, with major truncations of the bedding at the contact with the mud sheet. Within the mud sheet are several (5-10% of outcrop) large sandstone blocks. Between these two sections is the Panixerpass section, where there is intense chaotic deformation of the sandstone, with a highly irregular contact into the mud sheet. The mud sheet includes 40-50% sandstone blocks, each up to 130m across.

These three sections display rapid along-strike variations in style and intensity of deformation. They also demonstrate a correlation between the degree of deformation and the percentage of blocks in the overlying mud sheet. Based on the above observations, the mud sheet can be considered as a type of melange. Cowan (1985) discusses the various locations and mechanisms of melange formation associated with accretionary wedges along the active margins of the Western Cordillera, North America. There are a number of

locations in the thrust wedge environment in which this deformation may have occurred:

1) A relatively deep-level, broad shear zone, which would be dominated by brittle and ductile behaviour. The ductile deformation would be associated with a penetrative fabric.

2) A relatively shallow level broad shear zone near the frontal toe of the thrust wedge. This would be characterised by a mixture of brittle behaviour, and soft sediment deformation caused by the superimposition of lithified sediments in the hanging-wall, scraping the upper levels of unlithified sediment off the footwall.

3) Gravity driven downslope mass transport on the surface of the thrust wedge. This would involve some sort of glide sheet, and would be dominated by the deformation of partially lithified sediments near the sediment/water interface. The only unambiguous distinguishing criterion for a gravity glide from a shallow level shear zone is evidence of similar amounts of extension to the rear of the sheet compared to compression at the front of the sheet. Cowan (1982) suggests that the type of strain can also be used to distinguish gravity glide sheets from shallow shear zones. Coaxial strain reflects laterally unconfined stresses, characteristic of surface deformation, whereas non-coaxial strain is considered to represent relatively confined deformation in a shear zone.

4.4 Medium and small scale structures in the Panixerpass region

The purpose of this section is to describe the smaller scale structural features associated with the intense deformation in the Panixerpass section. A portion of this area was mapped as a strip perpendicular to strike, running north-north-west from the Panixerpass mountain hut. The following descriptions are located
on this map which is illustrated in figure 4.7.

4.4.1 Initial slope instability in the Inner basin

The first evidence of slope instability is represented by vertical sandstone injections caused by bedding parallel extension. These injections are exposed on upper bedding surfaces of massive sandstones, appearing as coarser sand dykes from 1-10cm thick injected into fine sands and silts (fig.4.12). The intersection of the dykes with the upper bedding surface can be measured to give the strike of the injection. The trend of these dykes is illustrated in figure 4.13, demonstrating a dominantly NNE-SSW direction. Associated with the dykes are sand mounds on the top of beds, measuring approximately 15cm in diameter and 1-2cm height. The mounds are often linked to the dykes illustrating their synchroneity in formation, but unfortunately no cross-sections of these structures are exposed, making their interpretation difficult. The sand injections represent shallow level extension parallel to bedding in a ESE-WNW direction. Overall extensional values for individual beds are less than 2%.

At location 2 (fig.4.7) there is a 6m thick, massive sand bed with a loaded base onto muds of the underlying turbidite unit. The muds are 10-20cm thick, with a mottled appearance due to the presence of small fragments of silt which are either rolled into small (1-4mm) ellipses or form wispy lenses (<1mm thick) (fig.4.14). The boundaries to these fragments vary from sharp to diffuse. The irregular texture of the silts and muds is interpreted to have formed during liquefaction of the sediments under simple shear, causing flattening and rolling of the silts to form pseudonodules. The underlying silts and fine sands contain many sand injections confirming the influence of liquefaction and/or fluidization.

4.4.2 Early compressional structures in the sandstone

The sandstone dykes and the mottled mudstones described above are considered to be the first evidence of slope instability after the deposition of the thick sands and muds of the Inner basin in the Panixerpass area. The intense compressional deformation illustrated in figures 4.5 and 4.6 may or may not be associated with this early instability.

In order to assess the approximate depth of burial of this sequence during the break-up and imbrication of the sandstone beds, it is necessary to examine the zones of detachment between the deformed blocks and slabs of sandstone. Figure 4.15 illustrates the upper surface of a sandstone slab which is overlain by an imbricated block transported on a muddy shear zone. Looking down on the upper bedding surface of the underlying slab, there is an irregular intercalation of small (<1cm) mud and sand fragments, cut by cleavage perpendicular to bedding, forming an intersection lineation. A thin section cut through the upper surface of the sandstone up into the mud shear zone (fig.4.16) illustrates a thin (0.1mm) mud injection into the sands. Within the muds are chaotic fragments of sand with sharp and diffuse boundaries into the muds, with individual sand grains floating in the mud matrix. This clearly demonstrates that the sand was partially lithified during the imbrication of these slabs of relict sand beds.

Elsewhere there are more prominent thrust zones ramping up through several massive sandstone beds. Figure 4.17 is a photograph of one of these thrust zones at location 3 (fig.4.7). The zone of deformed fault rock is about 6m thick, parallel to bedding in the hanging wall, but oblique to bedding in the footwall. The fault rocks comprise irregularly intercalated muds and sands (fig.4.18); the sands form pods and ribbons in a mud matrix, and are occasionally linked by sand injections. There is no evidence of zones of intense shear, and deformation seems to be distributed throughout the thrust zone. This therefore represents a broad zone of ductile deformation in soft, partially lithified sediment. In

contrast, at the base of the thrust zone is a 0.5-1m thick mineralised fault breccia (fig.4.19), containing angular sand and mud clasts set in a matrix dominated by calcite mineralisation. Some clasts comprise fragments of the overlying ductile shear zone. In summary, this demonstrates a broad zone of thrust movement which was initiated at shallow levels of burial prior to the complete lithification of the sediments, and later re-used to form a brittle fault breccia. The controls on the deformational behaviour of these sediments will be discussed in section 4.5.

4.4.3 Sedimentary reworking of the thrust blocks

On the top of upthrust blocks of the sandstone, there is evidence which suggests sedimentary reworking of the sandstones prior to the emplacement of the mud sheet. Figure 4.20 illustrates a bedding surface of a steeply dipping sandstone bed at the contact with the overlying mud sheet (location 4, fig.4.7). The sandstone has been reworked to form an intraformational breccia comprising angular coarse sandstone clasts (0.1-4cm) with a chaotic distribution, set in a coarse sandstone matrix; importantly, there is no mud present in the matrix. The basal contact of the breccia with the bed is oblique and highly erosive. The obliquity of the bedding and the erosion surface, plus the mixture of angular lithified clasts with an unlithified matrix suggests that this was formed by exposure of buried sandstones at the sediment surface. The sandstone was broken up to form clasts during erosion and subsequent sand deposition. This is interpreted as representing the upthrusting of sandstone beds on the sea floor during shallow level deformation. If this interpretation is correct, it indicates that the intense deformation of the Panixerpass section occurred prior to the emplacement of the mud sheet.

4.4.4 Deformation within the Mud sheet

I now consider the deformation within the mud sheet, focussing firstly on the sandstone blocks therein. The margins of the blocks, and their contact with the mud sheet should yield information on the deformational behaviour of the blocks during their incorporation. Figure 4.21 illustrates the margin of one of the large sandstone blocks, with a 3m wide zone at the margin of the block comprising muds with pervasive sand injections forming interconnecting pods and sheets which are sub-parallel to relict bedding at the margin of the block. Within this zone are occasional remnants of strongly boudinaged bedding showing grading. This suggests that the margin of the block represents a zone of shear, with liquefaction and boudinage destroying bedding.

Immediately south of the Panixerpass hut, towards the southern margin of the basin, smaller slabs of sandstone (10m long) occur within the Mud sheet. These demonstrate similar zones of sand and mud injections upto 1.5m thick, but in this case these zones only occur on the base of the slabs. This indicates that these slabs slipped into the Mud sheet along a basal glide zone. Evidence of this geometry is not seen in the larger blocks described previously from further north in the basin. Associated with these sandstone blocks is the larger block of Malm Limestone described in section 4.3.2.

The Mud sheet itself is strongly folded on a 0.1-20m scale. The folds are very irregular with curved fold axes and refolding. Figure 4.22 shows two small ductile folds with oblique fold axes, transected by the regional slaty cleavage.

4.5 Summary and Conclusions

The Taveyannaz sandstones are overlain by a thin (50-150m) mud sheet comprising

laminated silts and muds deposited by dilute turbidity currents. The gross structural relationship between the Taveyannaz sandstones and the mud sheet can be studied in three cliff sections (Jetzalp, Piz Fluaz and Panixerpass). The sections demonstrate rapid along-strike variations in style and degree of deformation. The Jetzalp section is relatively undeformed, with the contact into the mud sheet being conformable to bedding in the sandstones. In the Piz Fluaz section, the contact is disrupted by major topographic steps which truncate bedding in the sandstones. At the extreme, the Panixerpass section exhibits intense imbrication and disharmonic folding at the contact with the mud sheet. These sections also demonstrate that regions of most intense deformation in the Taveyannaz sandstones correlate with a greater amount of sandstone blocks in the mud sheet; this is an important observation for the following interpretation.

A more detailed study of the medium and small scale structures of the Panixerpass section reveals a number of features characteristic of shallow level deformation. Aligned sedimentary dykes evince small amounts (<2%) of early bedding-parallel extension within the basin, which is considered as being due to downslope gravitational instability. The interbed slip horizons that accommodated this extension occurred in the mud portion of the massive turbidites forming shear-induced pseudonodules of silt. The break-up and imbrication of the very thick bedded sands is facilitated by shear zones in the intervening muds. These shear zones comprise liquefied sands and muds, representing near surface deformation of partially lithified sediments. The upthrusted hanging wall blocks involved in this early deformation were erosively truncated to form sandy intraformational breccias prior to the emplacement of the mud sheet. The contact between the mud sheet and the sandstones is characterised by sand injections and muddy shear zones. Blocks of sandstone within the mud sheet vary in size up to 130m across and show marginal boundaries with the mud sheet similar to the basal contact with the sandstones. Towards the south of the

basin, blocks are underlain by similar soft sediment shear zones suggesting that they slipped into the basin on basal glide zones. These glided blocks are associated with a large block of Malm limestone.

The interpreted sequence of events that led to the features and structural configuration described above are as follows:

1) Rapid deposition of very thick bedded sands in confined Inner basin, leading to overpressuring and liquefaction represented by injected sandstone sills (chapter 3).

2) Downslope instability causing bedding-parallel extension and the formation of aligned sandstone dykes.

3) Intense break-up and imbrication of sandstone blocks and slabs on the sea-floor due to thrust propagation into the inner margins of the basin. The blocks and slabs moved by the liquefaction of partially lithified sands and muds, allowing ductile deformation on a meso and micro-scale by intergranular flow.

4) Minor reworking of the resultant hummocky sea floor topography occurred, developing intraformational sandstone breccias.

5) Emplacement of initial pulse of mud sheet over the irregular topography of the deformed Taveyannaz Inner basin. The emplacement resulted in the "plucking" of huge blocks of sandstone from impeding topographic highs on the sea-floor. This resulted in large steps in the sandstone/mud sheet contact, truncating bedding in the underlying sandstones as seen in the section at Piz Fluaz. This plucking of blocks is analogous to the development of "roche moutonee" in glacial terranes caused by the flow of ice over topographic highs. This process explains the correlation between the extent of deformation in the sands and the number of blocks in the overlying mud sheet, ie. the more hummocky the sea-floor topography after imbrication, the more blocks will be plucked into the overlying mud sheet.

6) Continued movement on the southern thrust to the basin exposed Jurassic limestones.

This led to blocks of sandstone and limestone slipping off the hanging wall ramp down into the southern edge of the basin, now exposed between Rotstock and Panixerpass. This was followed by continued emplacement of muds into the basin.

7) The southerly thrust continued to propagate over the basin carrying Mesozoic limestones as part of the initial development of the Helvetic nappes (chapter 2).

The processes described above that occurred during the deformation of the Taveyannaz turbidite basin are closely analogous to those associated with the formation of melanges at zones of subduction. Cowan (1985) discusses the various mechanisms by which melanges form from the western Cordillera of North America. Some of these were discussed at the end of section 4.3 as possible explanatory mechanisms for the Taveyannaz basin. We are now able to identify the environment of deformation as being at or near the sediment/water interface, at the frontal toe of the thrust wedge. Sedimentological data from chapter 3 indicate that the Taveyannaz basin was already underlain by a thrust plane which ramped up to form the northern frontal topographic high to the basin. Continued underthrusting detached the Taveyannaz sandstones along a decollement in the upper part of the Globigerina marls. As the sandstones were accreted onto the front of the thrust wedge, so the unlithified sandstone beds were broken up and imbricated. At approximately the same time the mud sheet was emplaced over the basin. The muds must have been transported from a more internal origin, then emplaced over the frontal margin of the wedge. Moore and Shipley (1988) describe seismic sections from the modern accretionary wedge from the Middle America Trench off Mexico (Fig.5.1). These illustrate thrust sheets reactivated from more internal parts of the wedge transporting material which then becomes gravitationally unstable, and slumps into perched basins at the thrust front. It is thought that this would be a suitable mechanism for the emplacement of the mud sheet (Fig.5.2), although clear differentiation between thrust propagation mechanisms, and downslope gravity transport mechanisms is not considered feasible in this case.

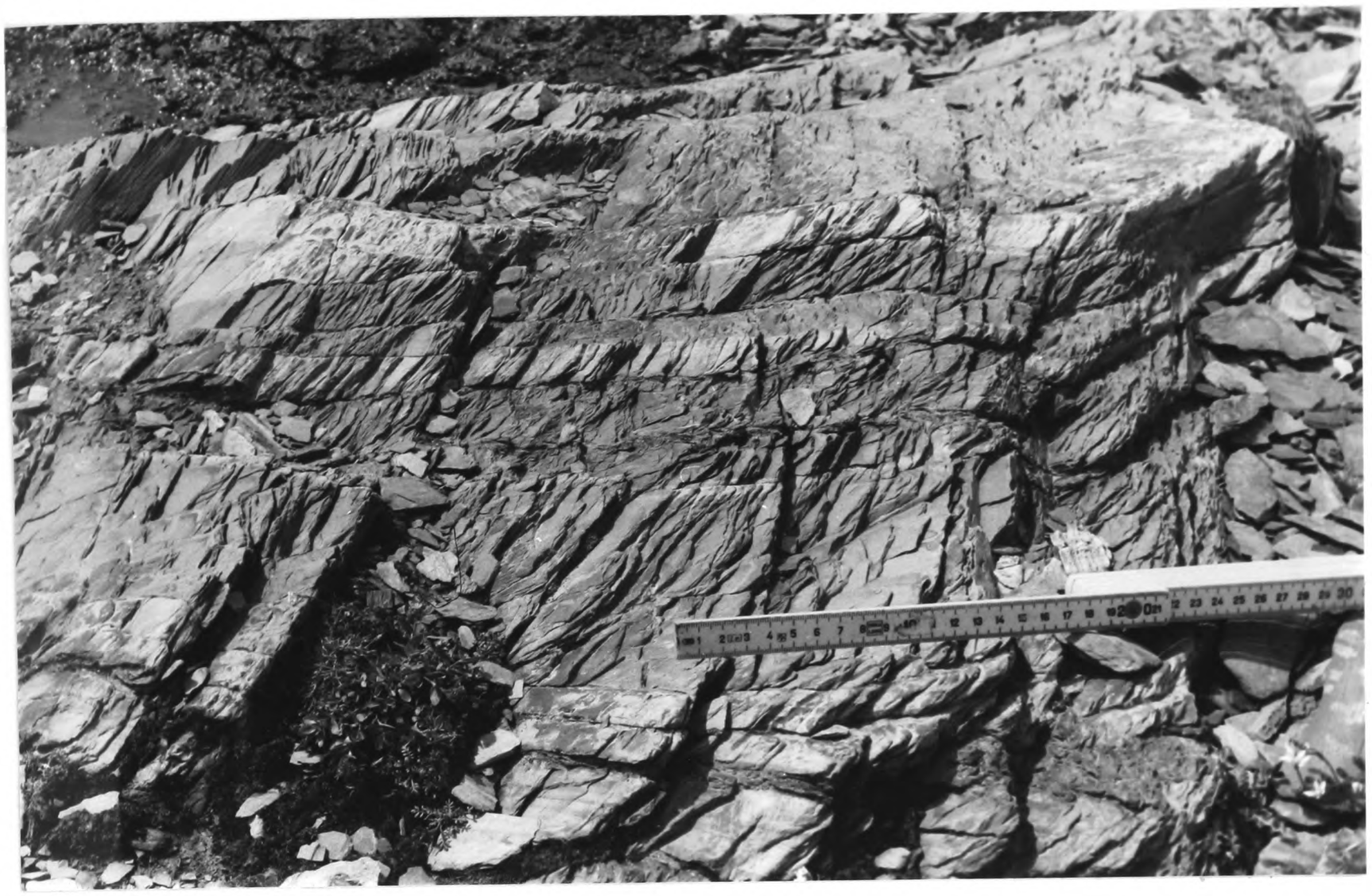

Fig.4.1. Finely bedded silts and muds of the Mud sheet, with high angle slaty cleavage.

Fig.4.2. Laminated muds of the Mud sheet.

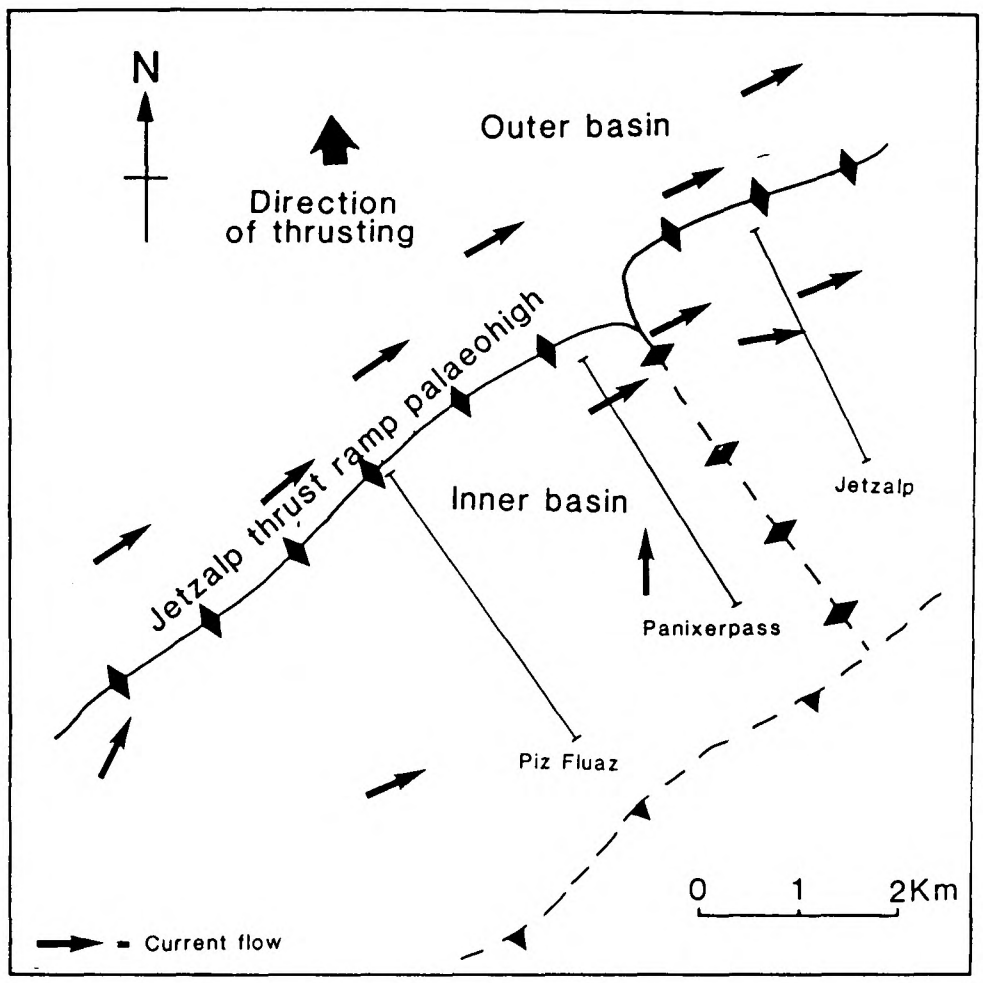

Fig.4.3. Simple palaeogeographic reconstruction of the Taveyannaz basin, with the Jetzalp, Panixerpass and Piz Fluaz sections located.

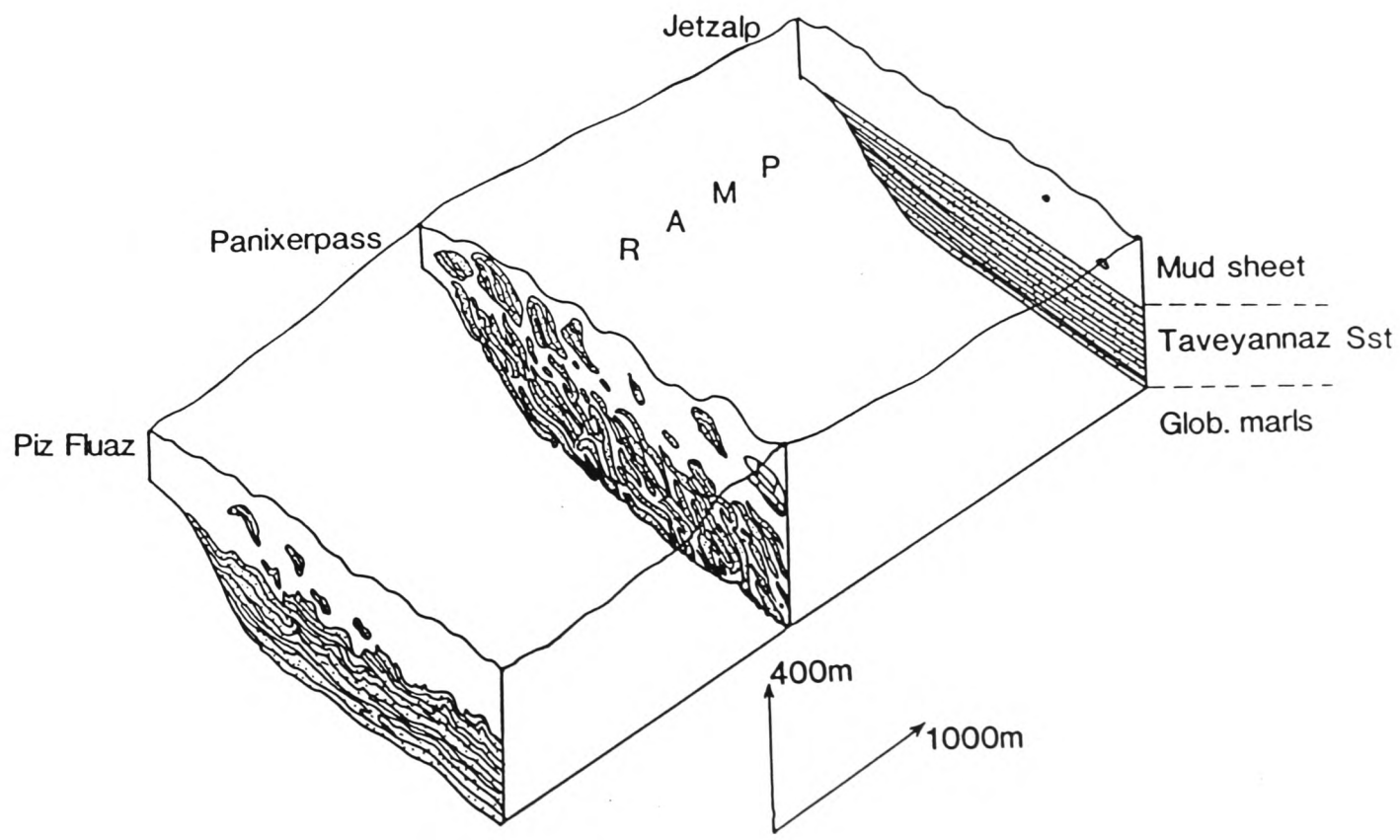

Fig.4.4. Three-dimensional reconstruction of the three sections of study , illustrating the gross structural relationship between the Taveyannaz sandstones and the Mud sheet. Note the rapid along-strike variations in style and intensity of deformation.

Fig.4.5. Photograph of Panixerpass section. This demonstrates the chaotic nature of the deformation which is characterised by imbricated slabs of sandstone, and disharmonic folds. The pervasive cleavage verges in the same direction as these chaotic structures, but is believed to have formed at a later date. This deformation is interpreted as being formed at shallow levels in partially lithified sediments, dominated by intergranular flow. (Grid ref.7270,1920 - 7272,1913).

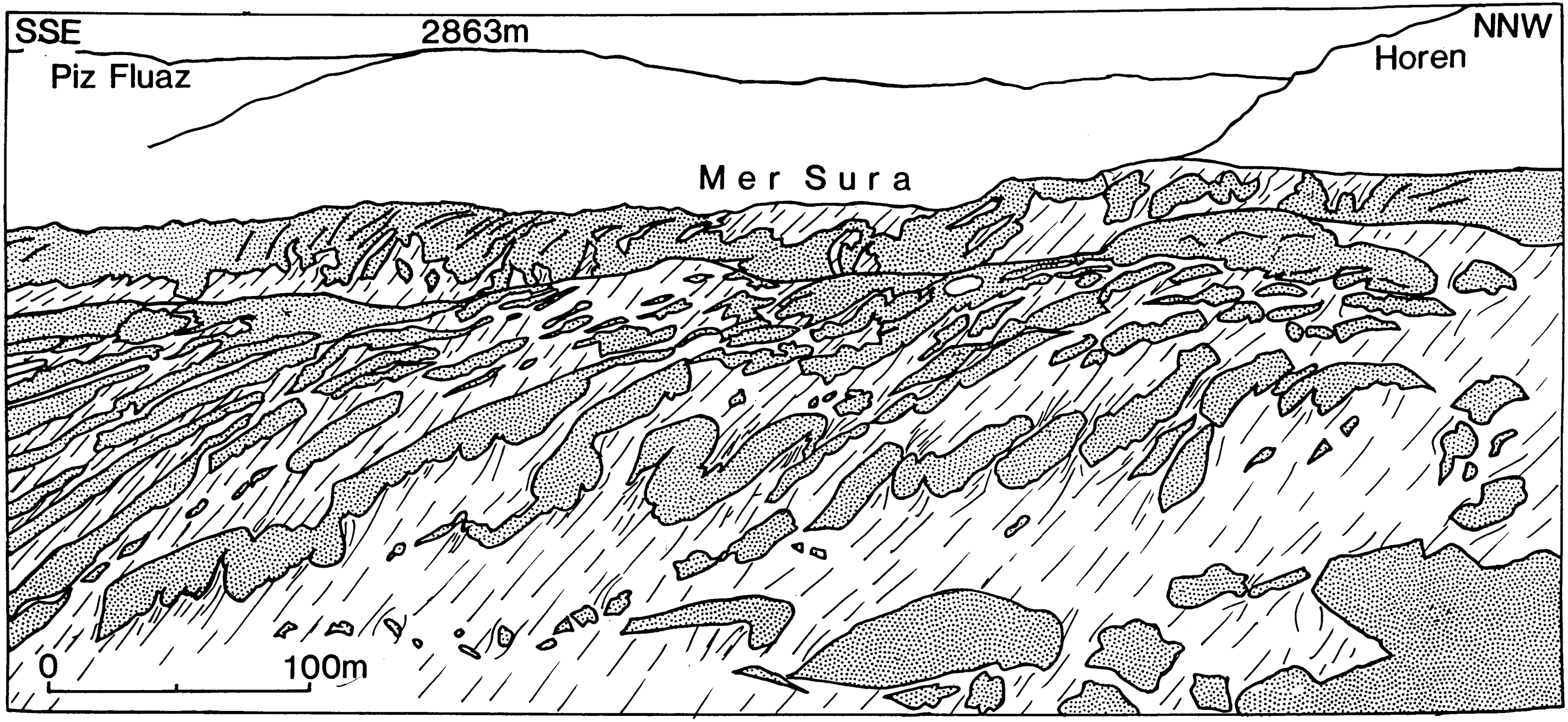

Fig.4.6. Line drawing of Panixerpass section.

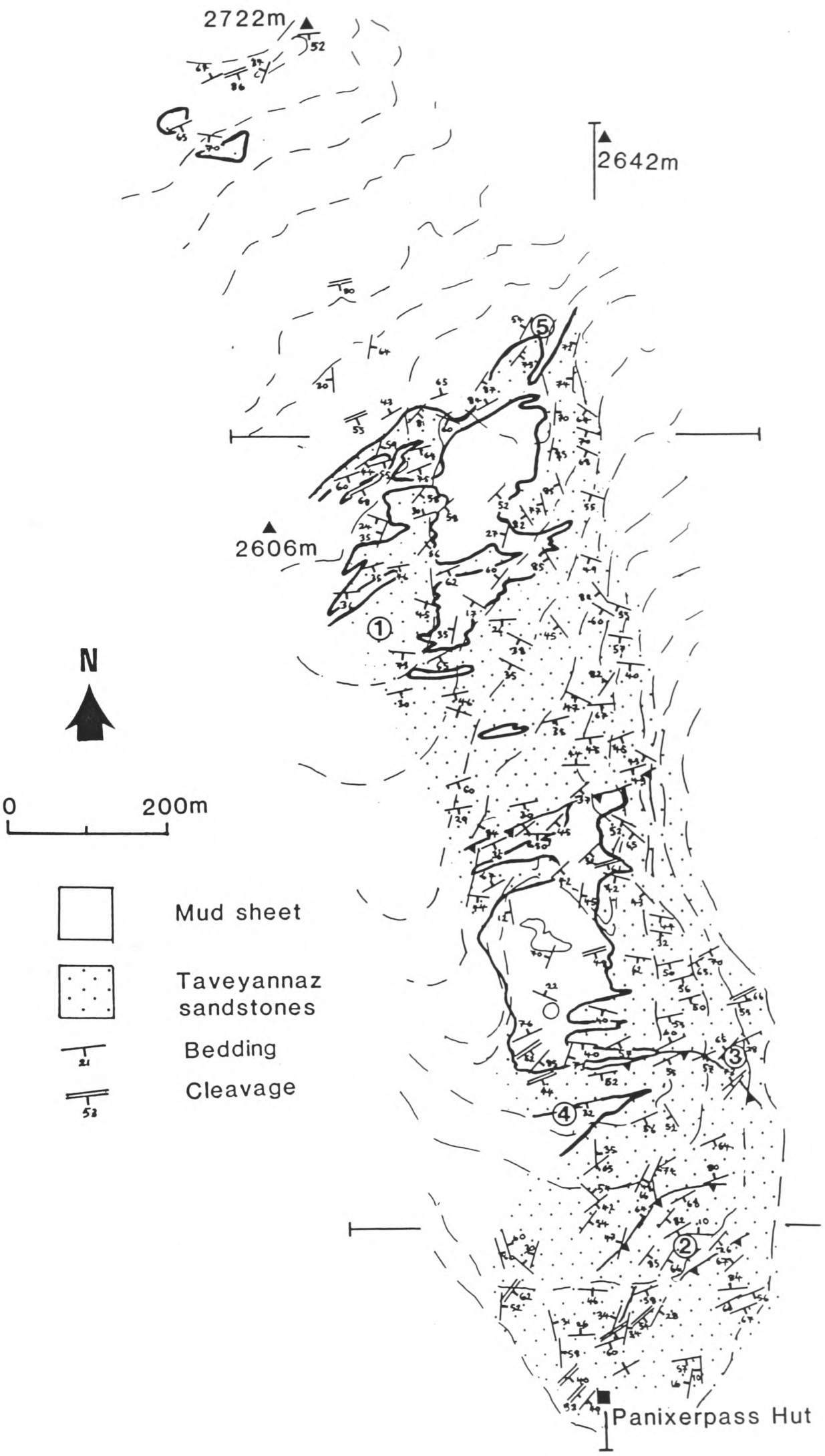

Fig.4.7. Geological map of area to the north of Panixerpass hut. This demonstrates the chaotic nature of the bedding, and of the contact between the Taveyannaz sandstone and the Mud sheet. Locations are given to outcrops which typify certain features discussed in the text.

Fig.4.8. Large block of sandstone located 100m north-west of the Chli-Chalchorn, Panixerpass. This block contains relict bedding, exhibiting internal thrusting.

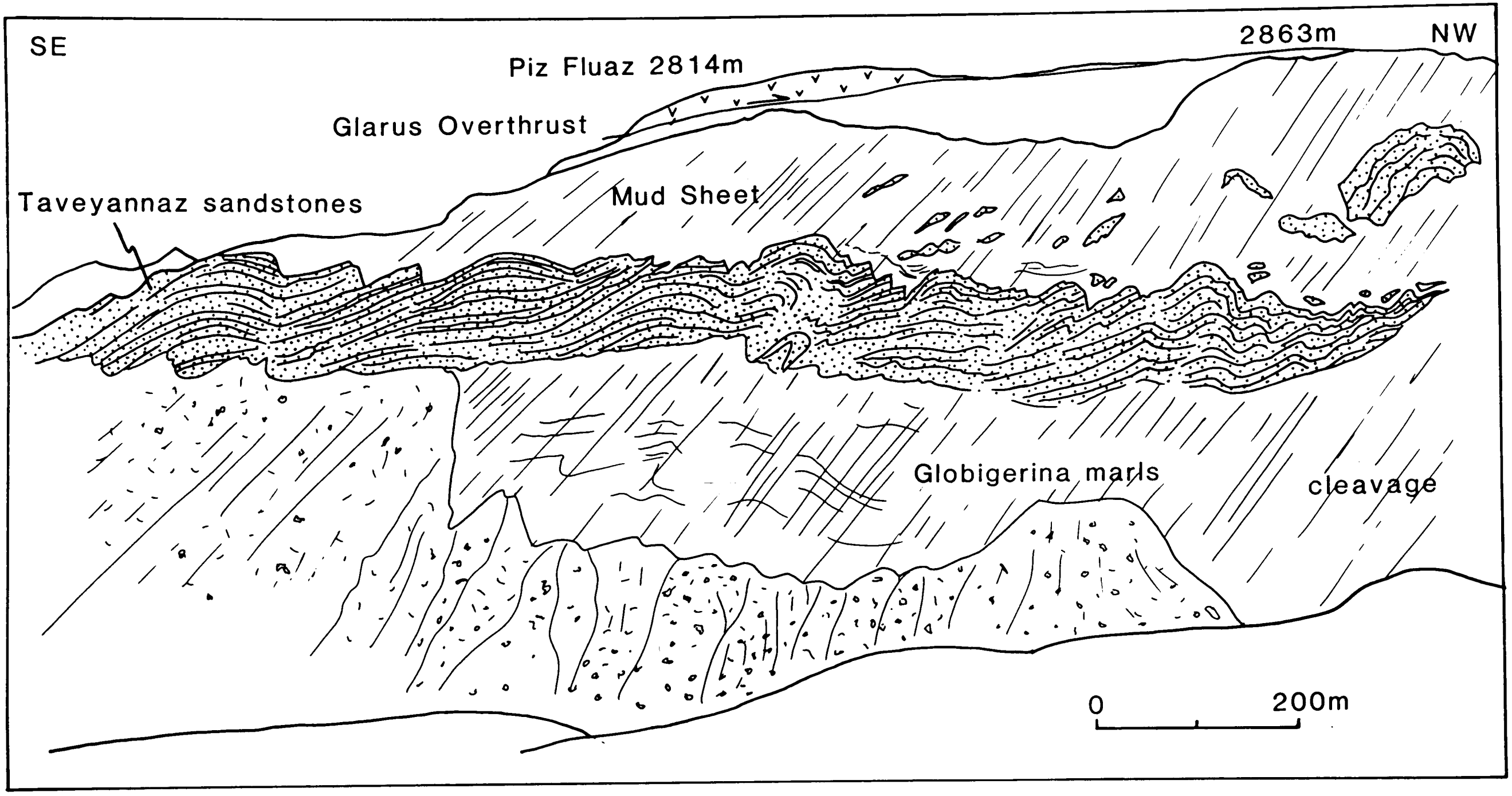

Fig.4.9. Line drawing of Piz Fluaz section (grid ref. 7250,1910 - 7245,1914). This illustrates the northerly termination of the Taveyannaz Inner basin onto the Jetzalp thrust ramp palaeohigh. Internal deformation within the basin comprises thrusting sub-parallel to bedding, this results in the formation of thrust-ramp topographic highs at the contact with the overlying Mud sheet. These now form major steps in the contact, with bedding being truncated. A large sandstone block is present in the Mud sheet, it is interpreted that this was plucked from the surface of the sandstones during emplacement of the Mud sheet.

a.

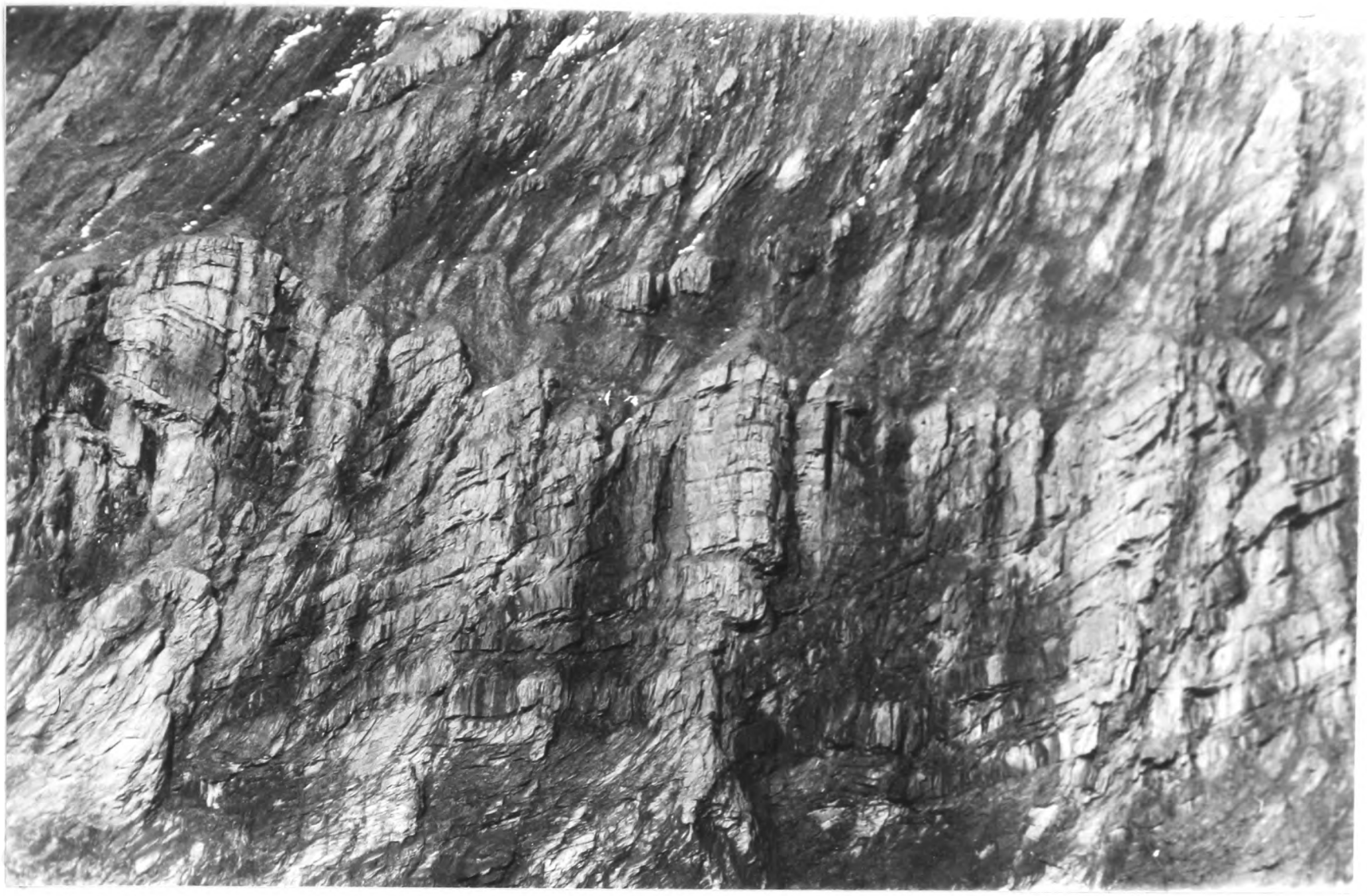

b.

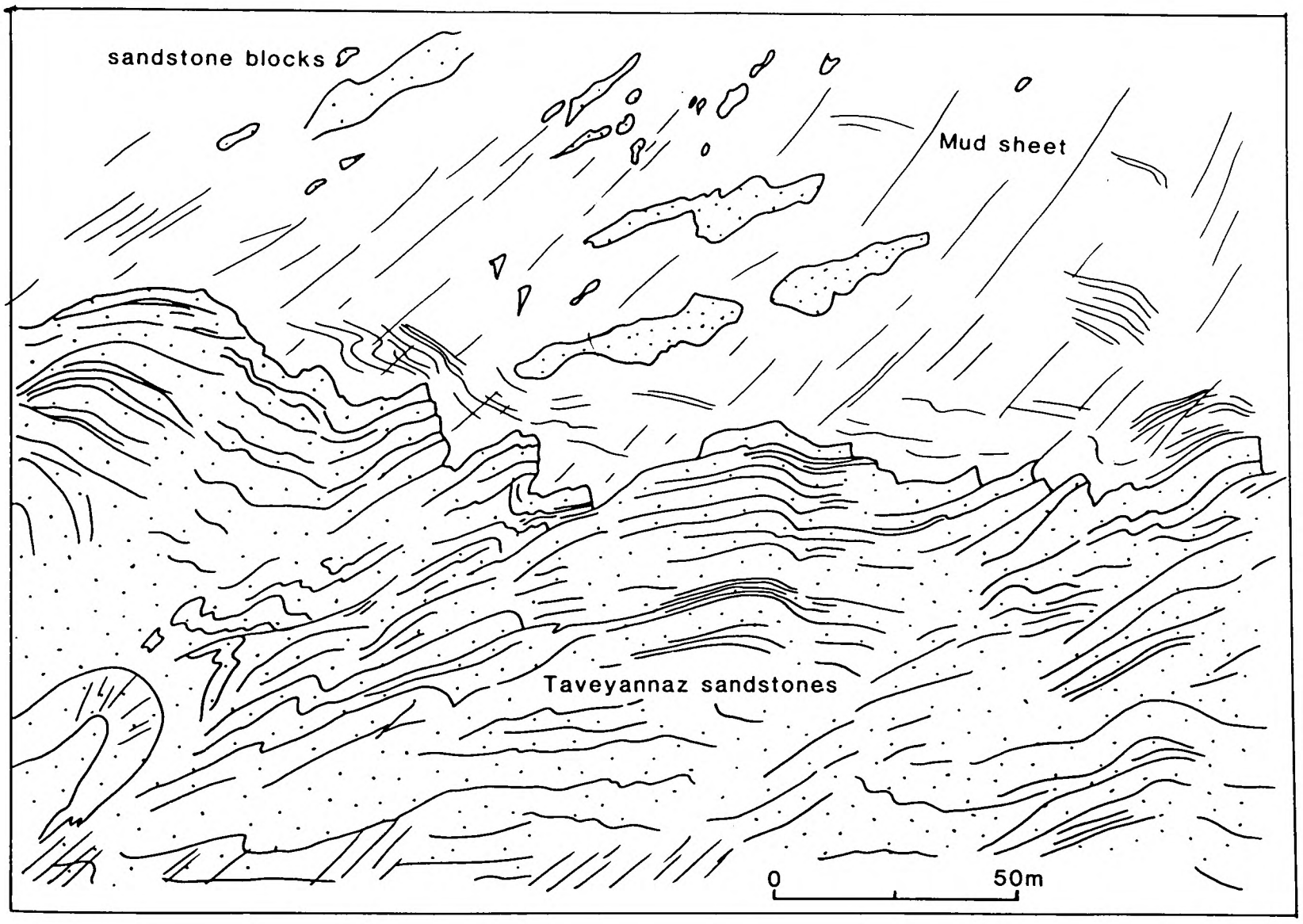

Fig.4.10a+b. Photograph and line drawing of major step in the contact between the Taveyannaz sandstones and the Mud sheet from the Piz Fluaz section (fig.4.9). This shows the truncation of bedding in a thrust hanging wall within the sandstones.

Fig.4.11. Close-up of the Piz Fluaz section illustrated in figure 4.9 showing thrust hanging walls in the Taveyannaz sandstones forming large steps in the contact with the mud sheet.

Fig.4.12. Looking down on the upper bedding surface of a massive sandstone in the Panixerpass section illustrating a sandstone dyke. The alignment of these dykes was measured and plotted in figure 4.13.

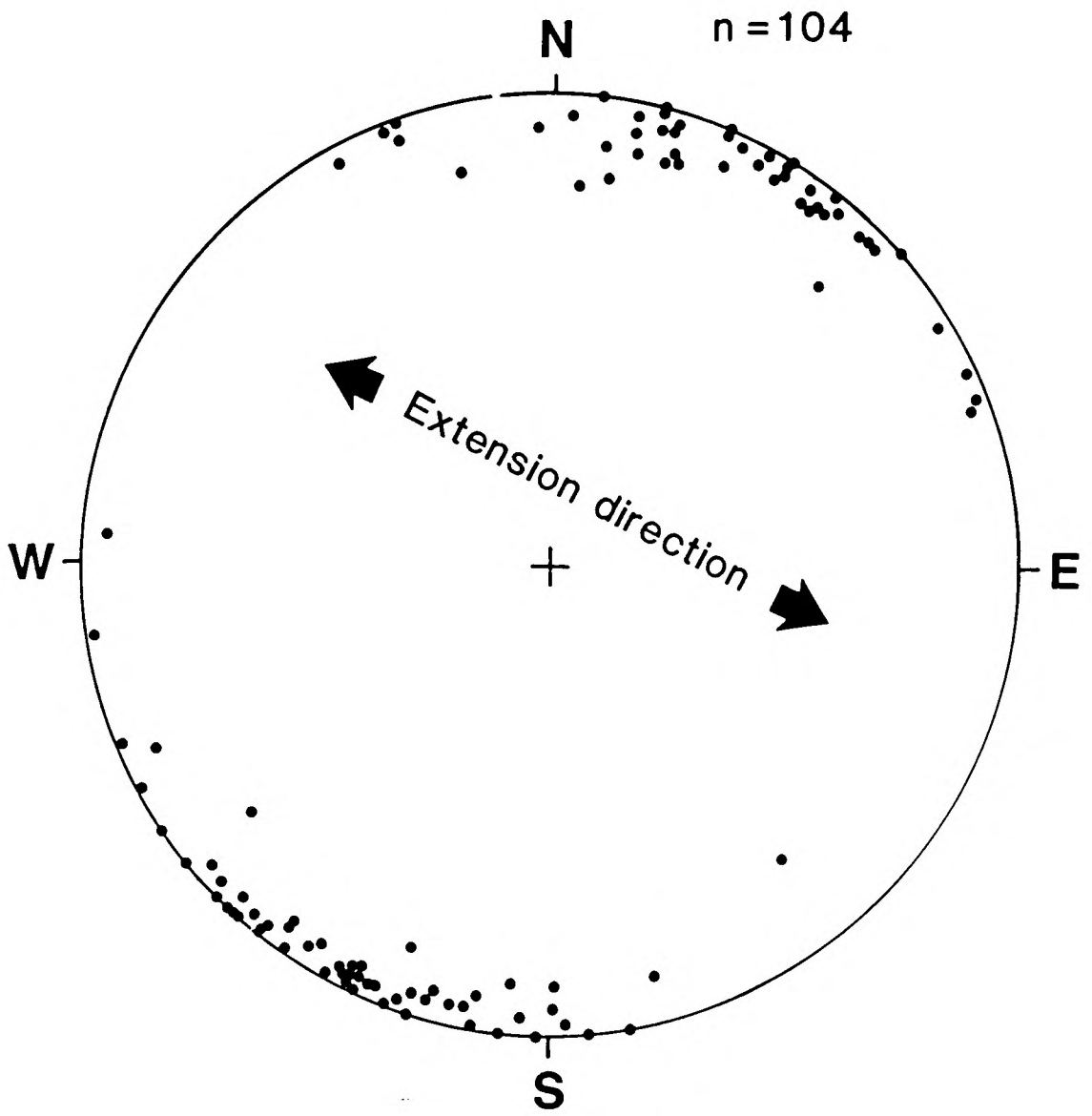

Fig.4.13. Stereogram of the aligned sandstone dykes from the Inner basin as shown in figure 4.14. This alignment indicates an early WSW-ESE orientated extension in the basin.

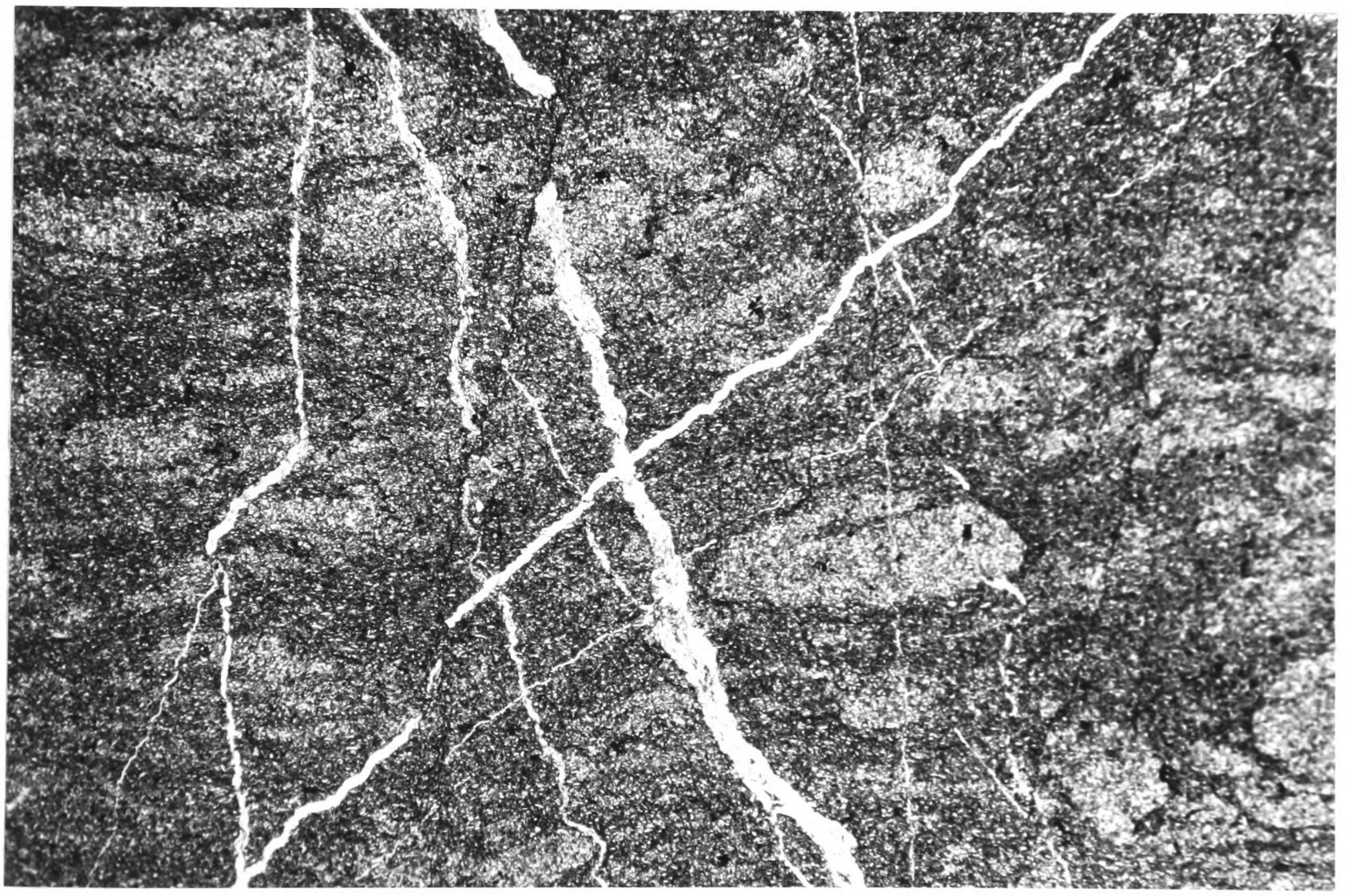

Fig.4.14. Thin section of shear induced pseudonodules in the mud units of the Panixerpass area. Field of view is 3mm. The silt fragments in the muds show sharp and diffuse boundaries.

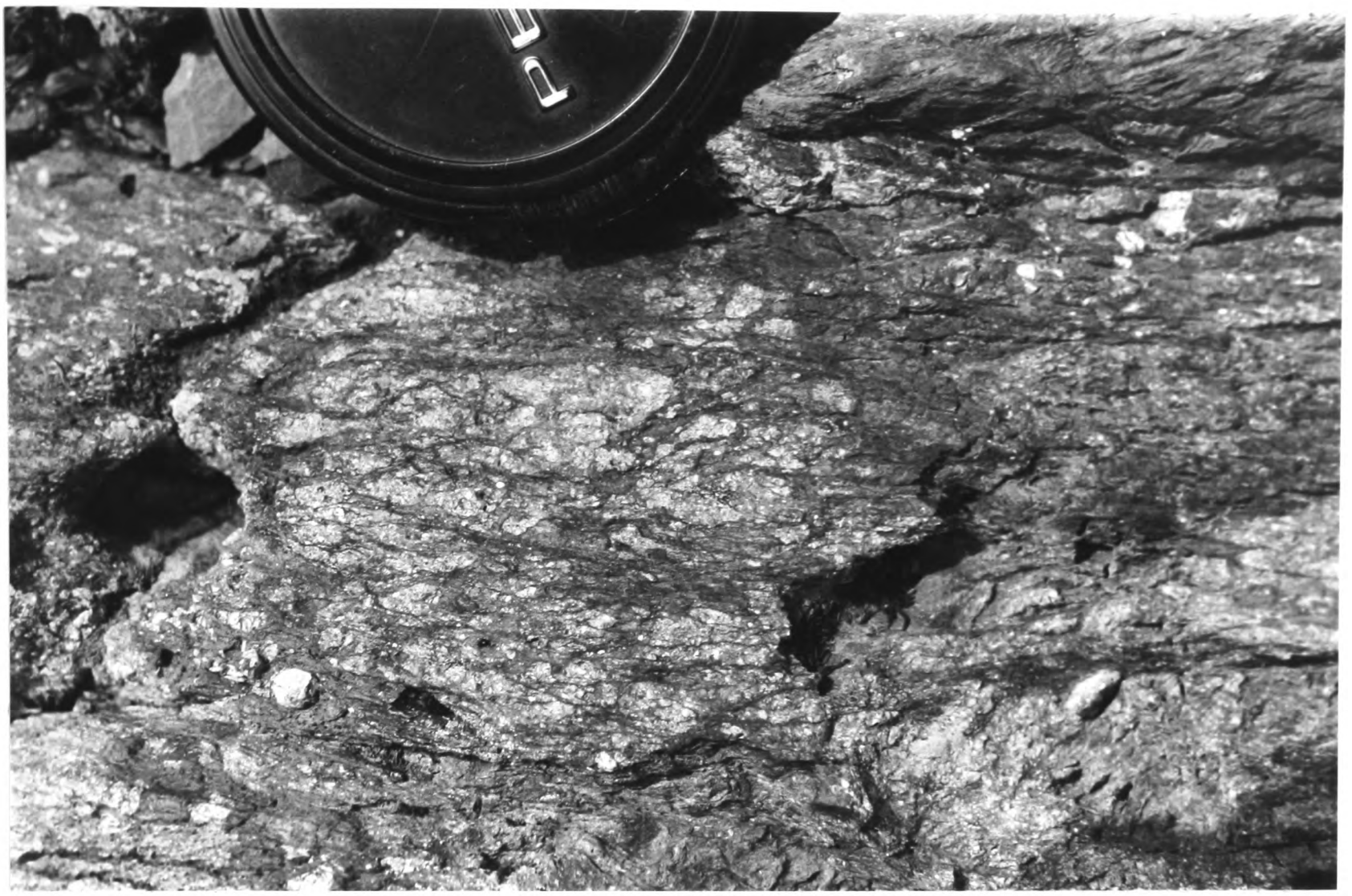

Fig.4.15. Looking down on the upper bedding surface of a sheared sandstone in the Panixerpass area. This shows fragments of silt in a mud matrix. The horizontal fabric is a cleavage/bedding intersection lineation. Fig. 4.18 shows a thin section perpendicular to this surface demonstrating the unlithified nature of the sands during this deformation.

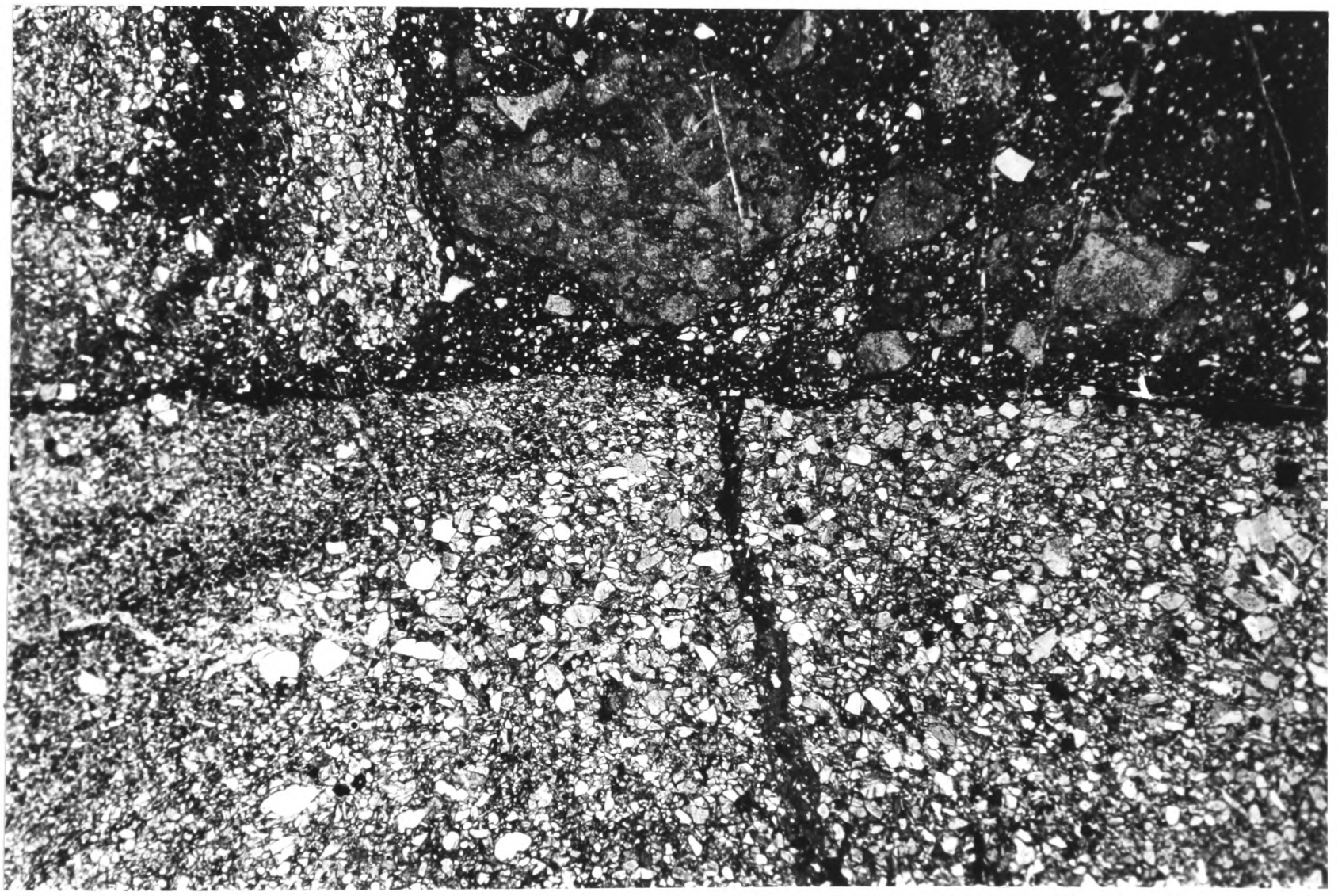

Fig.4.16. Thin section of upper surface of sandstone bed illustrated in fig.4.15. The sandstone has been injected by a thin mud intrusion. The muds contain fragments of partially lithified sand, this is particularly well demonstrated by the right hand fragment which shows a diffuse boundary with individual grains floating off into the muds.

Fig.4.17. Photograph of location 3, fig.4.7. This shows bedding in the background, underlain by a 6m thick thrust zone dominated by liquefied sands in a mud matrix as illustrated in fig.4.18. The bedding in the footwall is oblique to that in the hanging wall, and is truncated by the thrust zone immediately above the hammer. This zone was later reactivated to form a brittle mineralised fault breccia (fig.4.19).

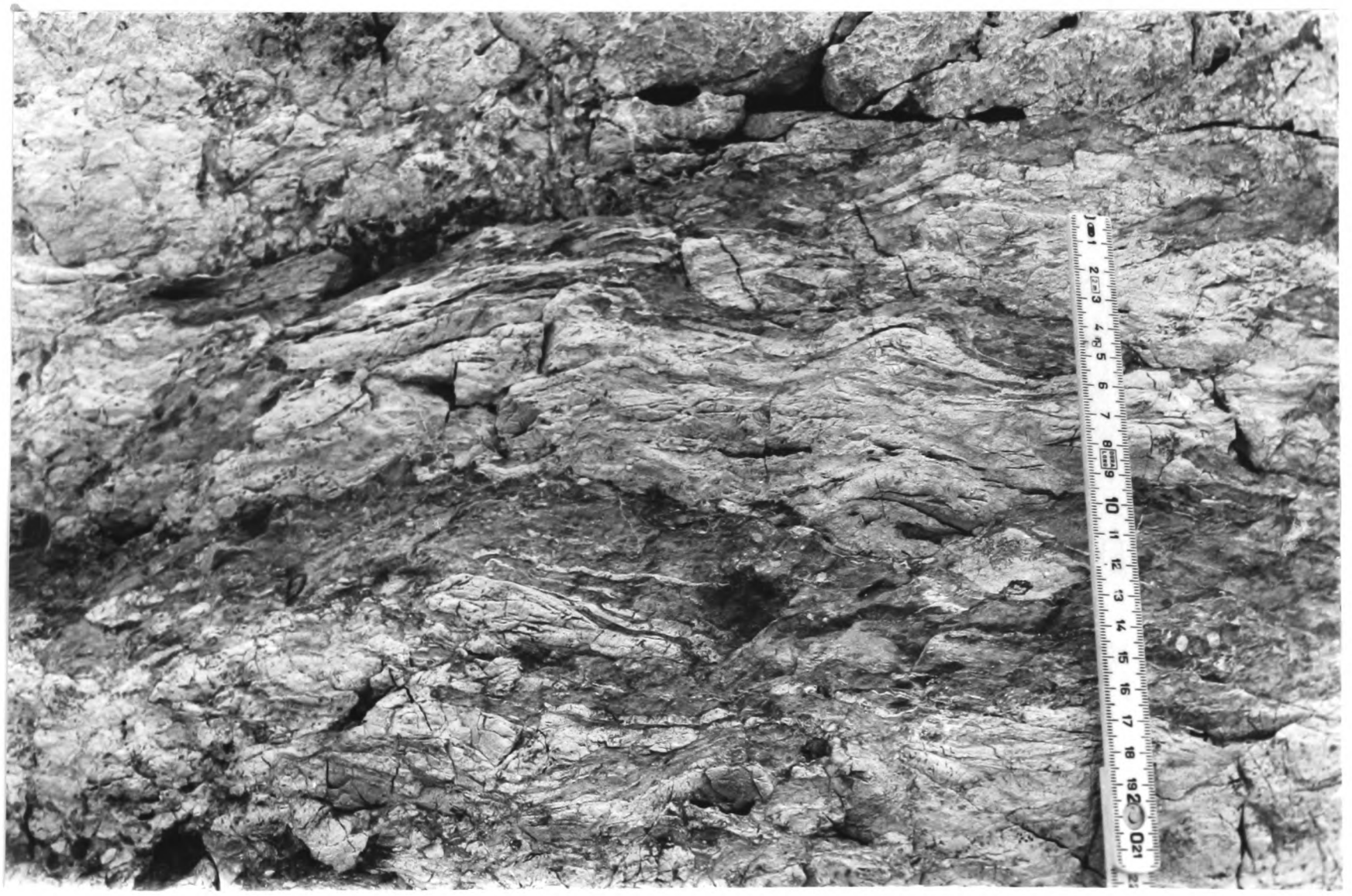

Fig.4.18. Close-up of muddy thrust zone from location 3 (fig.4.7 and 4.17). This shows thin wisps and pods of sandstone forming irregular patterns in a mud matrix. A generally horizontal fabric can be seen, but there are no distinct fault zones. This represents a broad zone of distributed soft-sediment deformation.

Fig.4.19. Mineralised fault brecia seen at location 3 (Figs. 4.7 and 4.17). This shows a contrast to the style of deformation in fig.4.18, with brittle fracturing forming angular clasts of sand and mud in a calcite vein matrix.

Fig.4.20. Sedimentary reworking of sandstones at location 4 (fig.4.7). The bottom part of the photograph is the upper surface of a sandstone bed that has been upthrusted at the contact with the mud sheet. Overlying this with an irregular erosive contact is an intraformational breccia, containing angular clasts of sandstone in a sandstone matrix. This demonstrates the reworking of lithified sandstone on the sea-floor, infilled by more sand. It is thought that this signifies a separation of the deformation of the Inner basin and the emplacement of the mud sheet.

a.

b.

Fig.4.21a. Location 5 (fig.4.7) showing the margin of a large sandstone block, with a 3m thick zone of injected sands into the mud sheet. The injections are dominantly sub-parallel to relict bedding in the block seen towards the top left of the photograph. b) is a close-up of the injected zone located just above the rucsac in a.

Fig.4.22. Ductile folding within the mud sheet with varying fold axes, truncated by the regional cleavage running vertically through the picture.

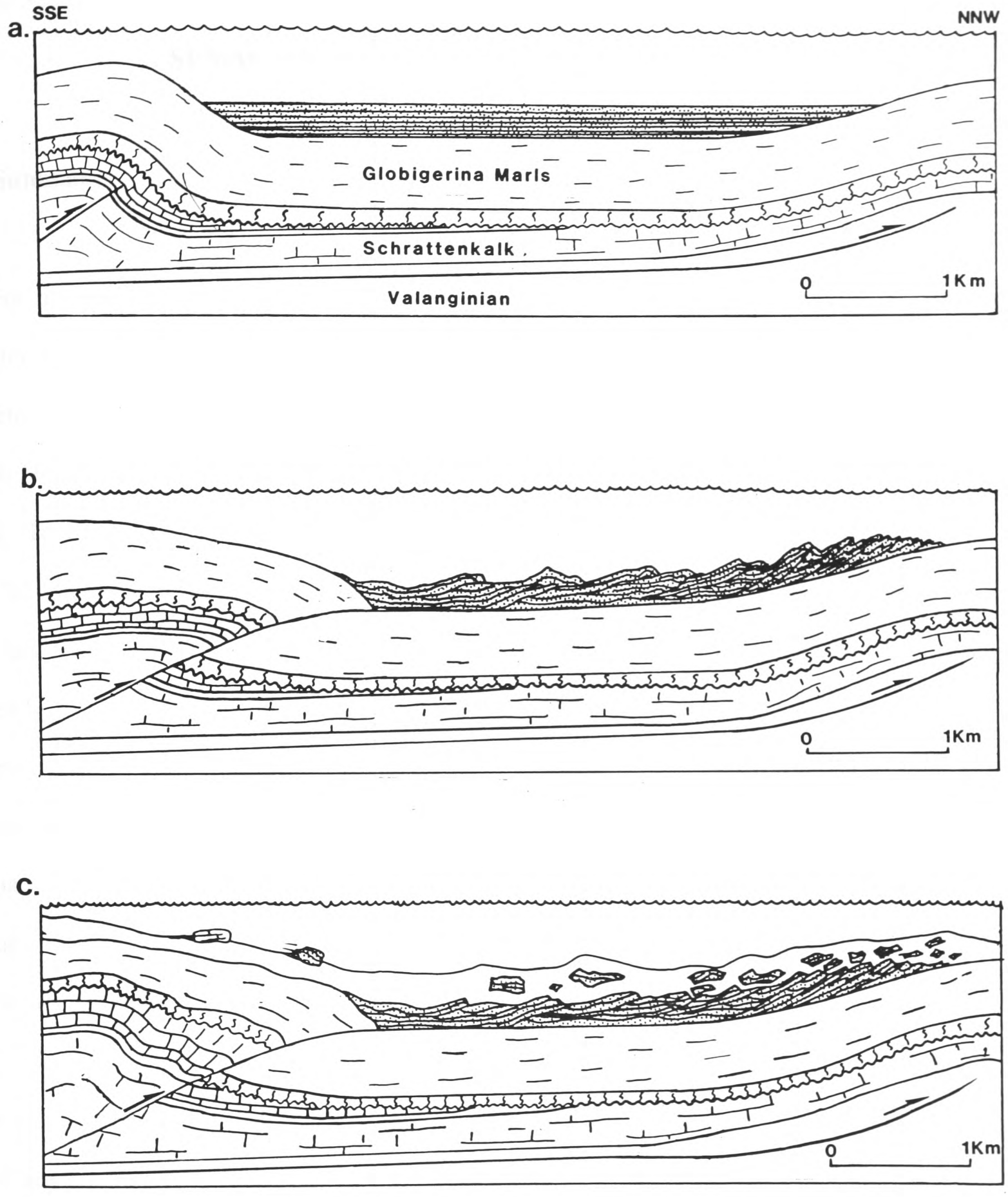

Fig.4.23. Interpreted evolution of shallow level deformation in the Inner basin of the Panixerpass section. a) Formation of thrust top basin causing confinement of Taveyannaz sandstones. b) Continued movement on the southern thrust leading to offscraping of the sandstones, detaching in the upper Globigerina marls. This deformation results in a hummocky topography on the sea-floor. c) Emplacement of mud sheet as a gravity glide sheet derived from more southerly part of the thrust wedge. The emplacement causes plucking of blocks of sandstone from thrust hanging wall topographic highs. Blocks of sandstone and limestone glide into the southern margin of the basin, off exposed thrust scarps.

CHAPTER 5

SUMMARY, DISCUSSION AND CONCLUSIONS

5.1 Summary

For the purpose of this thesis, it was considered necessary to firstly describe the present structural configuration of the area (chapter 2) prior to evaluating the sedimentological evidence (chapter 3). In this summary, the sedimentological and structural evolution of the North Helvetic realm will be reviewed in chronological order, focussing on the development of the Taveyannaz basins.

The Eocene marked a time of north-westward transgression over the southern margin of the European plate. The uppermost of the Helvetic nappes records an initial flooding during the early Eocene, reaching the North Helvetic domain by the lower part of the middle Eocene (Herb, 1988). This Tertiary transgression overstepped the underlying Mesozoic stratigraphy from the Upper Cretaceous to Jurassic as it onlapped the European margin. The resultant unconformity which underlies the Tertiary of the Helvetics was described by Trümpy (1973) as the "Palaeocene Restoration" and represents a major period of erosion followed by subsidence of the European plate.

The initial Tertiary sediments overlying the basal unconformity of the Helvetics are dominated by bioclastic limestones containing many large foraminifera, and sandstones which are commonly glauconitic. In the North Helvetic realm exposed in the tectonic window of the cantons of Glarus and Graubunden, the sediments are predominantly Nummulitic limestones and calcarenites with a thin Assilina-rich greensand at the base; they are dated as basal to middle Lutetian (Styger, 1961). This initial stratigraphic unit steadily onlapped the European margin (Herb, 1988) in a manner similar to transgressive systems

tracts formed at the onset of relative sea-level rise.

The shallow marine sediments described above, subsided rapidly and were covered by a thick succession of Globigerina marls, representing water depths of several hundred metres with NNW-SSE orientated bottom currents. This reflects subsidence outpacing sedimentation with the rate of relative sea-level rise at its maximum. The transition from the limestones into the marls is therefore considered to represent the level of maximum flooding of the transgressive sequence, with the marls representing highstand deposition.

The onset of Taveyannaz sandstone deposition at the beginning of the late Eocene represents a change in the depositional controls on the basin, with the onset of thrust wedge derived clastic sediments from the south. The Taveyannaz sandstones were deposited by turbidity currents running along the trench (WSW to ENE) at the frontal toe of the encroaching thrust wedge. The basin of deposition was divided into two sub-basins by the Jetzalp thrust-ramp palaeohigh also running WSW/ENE. The Inner basin developed as a thrust-top basin, with approximately 140m sedimentary thickness, dominated by very thick bedded turbidites caused by thrust-induced slope instability at the southern margin of the basin. The stratigraphy of the Inner basin pinches out towards the north onto the palaeohigh.

The Outer basin comprises at least 240m of medium to thin bedded turbidite sands and muds. The turbidites developed into sand packages, with roughly symmetrical vertical bed thickness variations, characterised by amalgamated sands in the centre of the larger packages. Separating sand packages are finely bedded muds and silts. The sand packages and intervening muds are interpreted as representing relative sea-level fluctuations caused by thrust activity on the shelf and upper slope. Sand deposition occurred during relative lowstands which resulted in erosion of the shelf, whereas relative highstands led to blanketing of the basin with muds.

The fundemental difference in the style of turbidite sedimentology between the Inner and Outer basins is considered to reflect differing mechanisms for the generation of the turbidite events. The Inner basin was perched on the surface of the sub-marine thrust wedge, and was mainly fed by major thrust induced seismic turbidite events which were confined by the thrusted topography on the wedge. The Outer basin represents the flexural trench in advance of the wedge. This is thought to have been fed by a point source such as an incised canyon, which transported material from the shelf, bypassing the slope and depositing in the frontal trench to the thrust wedge. The generating mechanism for the turbidite events would therefore be controlled by events on the shelf, dominated by relative sea-level fluctuations. It is possible that each very thick bedded turbidite within the Inner basin is a time equivalent to a sand package of the Outer basin; ie. thrust activity within the wedge resulted in large volume turbidites being trapped on the surface of the wedge, and also resulted in a relative lowering of sea-level on the shelf leading to the development of a sand package in the flexural trench via sediment transport through shelf canyon systems. However, the precision of relative timing is too poor to allow this possibility to be adequately tested. For the same reason, it is impossible to evaluate the precise frequency of these interpreted relative sea-level fluctuations. But, if we assume that deposition of the Taveyannaz sandstones continued throughout the Priabonian (upper Eocene), a period of approximately 4Myr, and that there are about 12 very thick bedded sands/sand package couplets, then the repeat interval for thrust-induced lowstand sedimentation would be of the order of 0.3Myr.

The Taveyannaz sandstones are comparable to a low-stand systems tract, underlain by a type 1 sequence boundary, based on the bypassing of sediment from the shelf to the trench. Unfortunately there is no correlatable shelf sequence due to subsequent structural deformation and therefore stratigraphic interpretation is limited. This situation differs

significantly from that of an eustatic fall in sea-level on a passive margin. A relative fall in sea-level as a consequence of thrust activity leads to erosion on the shelf and redeposition at the base of slope, which in this case is the outer flexural trench. But in contrast to the passive margin case, the base of slope is still undergoing a relative rise in sea-level due to flexural subsidence, whilst recording a relative sea-level fall on the shelf.

Gravitational instability during sedimentation is observed within the Taveyannaz sandstones. Rapid deposition of thick sand beds, alternating with thick sequences of muds led to overpressuring of trapped fluids and the development of extensive fluidisation and liquefaction structures, dominated by sandstone injections. Continued syn-depositional thrust movement led to the detachment of the Taveyannaz sandstones of the Inner basin at the basal contact with the Globigerina marls. As the sandstones were offscraped from the underlying sequence, they became imbricated whilst partially lithified on the sea-floor. The irregular topography at the sediment/water interface caused by this imbrication was soon smothered by the emplacement of a mud sheet which plucked and incorporated large blocks of the underlying sandstones. The sedimentology of the mud sheet comprises finely bedded turbiditic silts and muds, with minor bioturbation. The style of deformation within the mud sheet suggests that it was also partially lithified during emplacement.

Intense calcite veining within the Globigerina marls reflects a period of elevated pore-fluid pressures. Deformation associated with this mineralisation indicates southward directed relative motion of the overlying sandstones. The regional tectonic deformation is towards the north-north-west and overprints the earlier southward directed structures. The relative timing of the southward motion in the marls and the shallow level deformation in the overlying turbidites is not known, but probably represents a continuum of deformation into the regional tectonic development.

Tectonic deformation of the North Helvetic Tertiary sequence during the Oligocene and

early Miocene resulted in fold and thrust structures. Continued activity of the Jetzalp anticline divided the deformation of the Inner basin from that of the Outer basin. The Inner basin continued to detach in the Globigerina marls developing harmonic folds through the sandstone sequence with varying geometries. Thrust duplication within the Nummulitic limestones does not affect the overlying sandstones, indicating that the limestones and the sandstones acted as independent competent layers separated by the incompetent marls. If deformation had been greater in the limestones than in the immediately overlying sandstones, then the intervening marls would have accommodated southward relative movement as a passive roof backthrust; this would have been aided by relatively high pore-fluid pressures in the marls. This is considered an explanation for the southward relative motions described above.

The Taveyannaz sandstones of the Outer basin underwent severe shortening (approx. 300%) in the footwall to the Jetzalp anticline. Detachment in the upper Globigerina marls led to the formation of an antiformal stack containing three thrust sheets. The emergent sole thrust to the antiformal stack separates it from the relatively undeformed sequence to the north. The northerly continuation of the Outer basin is not known due to lack of suitable exposures. The last stages of deformation involve transport on the Glarus overthrust carrying the Helvetic nappes northwards.

5.2 Discussion

The sedimentological and structural characteristics of the Taveyannaz basins are highly analogous to modern accretionary wedges. It may seem that there is a fundamental difference in that the foreland basin is developed upon continental crust compared to oceanic crust in the accretionary wedge, but there is no evidence of any mechanical

variance between the two cases. The most comparable of accretionary wedges is that of the Middle America Trench off the west coast of Mexico. A sedimentological description of the Middle America Trench using DSDP data was carried out by Moore et al (1982). They observed that the bulk of sand deposition occurring in the trench was fed by canyons which bypass sediment through the slope. The slope is characterised by a ridged topography caused by emergent imbricate thrusts, forming small thrust-top basins. Sedimentation within these small basins is restricted, with muds deposited higher on the slope. This process of sediment bypassing is thought to control sediment deposition within the Taveyannaz basins, with the Inner basin representing a small thrust top basin at the base of slope, and the Outer basin representing trench sedimentation fed by a canyon along strike. This also provides a mechanism to explain mud deposition higher on the slope which becomes detached to form the mud Sheet and is emplaced into the Taveyannaz basins. Moore and Shipley (1988) illustrate seismic lines through the base of the Middle America Trench; an example of one of these lines is illustrated in figure 5.1. This illustrates a small (1.5km wide) thrust top basin overlying the frontal thrust, and a more internal, near horizontal thrust emerging to form a step in gradient at the base of slope; the bedding in the hanging wall to this internal thrust is truncated by slumping. Similar structures with small thrust top basins and slumping occurring at the internal edge of the basin are also illustrated by Stevens and Moore (1985) from the western Sunda arc, Indonesia. It is thought that in the case of the Taveyannaz basins, the reactivation of more internal thrusts carried the mud Sheet into the basins at the base of slope in a similar manner to that illustrated in the above examples.

Aside from furthering our understanding of the "flysch stage" of the North Alpine Foreland Basin via the use of modern analogues, this work also has implications for our understanding of the development of the Helvetic Alps as a whole. Primarily, it enables a

precise time bracket within which can be placed the arrival of the Alpine thrust front into the North Helvetic domain of Eastern Switzerland. The first structural event of this region has previously been ascribed to the emplacement of the Blattengrat and Sardona thrust sheets, which has been dated as post-early Oligocene as they structurally overlie the lower Oligocene Engi Slates (Trümpy, 1973; Milnes and Pfiffner, 1977). Chapters 3 and 4 of this work indicate that the thrust front reached the North Helvetic domain in the late Eocene. The fact that sedimentation of the Engi Slates occurred after the emplacement of the Mud sheet in the Taveyannaz basins indicates that the early emplacement of the South and Ultra-Helvetic thrust sheets was not a discrete event, but ranged from late Eocene to early Oligocene.

The bulk of the internal deformation within the overlying Helvetic nappes occurred within the Oligocene, but, they were then carried passively over the parautochthonous Infrahelvetic complex on the Glarus Overthrust (Frey et al, 1974; Groshong et al, 1984; Pfiffner, 1982, 1986; Hunziker et al, 1986). The last movements of the Helvetic nappes is approximately Aquitanian (early Miocene) based on their relationship with the Upper Marine Molasse (Trumpy, 1973). The presence of blocks of Mesozoic limestones within the mud sheet indicates that the initiation of thrusting of the Helvetic nappes occurred at the end of deposition of the Taveyannaz sandstones. This gives a lower time bracket for the initiation of the Helvetic nappes at approximately Priabonian (late Eocene).

This enables a sequential reconstruction of the events at the front of the Alpine thrust wedge during its early collision with the European margin (Fig.5.2):

1) A low angle accretionary wedge propagates onto the flexed European plate, with a thick sequence of turbidites (Taveyannaz sandstones) deposited in the trench and small perched basins.

2) Muds deposited on the upper parts of the slope (the mud sheet) are carried forewards

and dumped onto the perched basin and trench deposits.

3) Thrusting in the rear of the wedge carries material of Ultra and South Helvetic origin (Sardona and Blattengrat units) over the partially deformed Helvetic province, and emplaces them over the mud sheet.

4) Thrusting detaches thick Mesozoic limestone sequences of the Helvetic platform and transports them up to 40km northwards over the North Helvetic domain.

Stages 3 and 4 represent out-of-sequence thrust events within the external parts of the Alpine orogenic wedge during the late Eocene and early Oligocene.

On a broader analysis of the late Eocene/early Oligocene development of the external parts of the thrust wedge from around the Alpine arc, we find a similar sedimentological and structural history throughout Switzerland and SE. France. Lateltin (1988) describes the North Helvetic Flysch that lies stratigraphically upon the Helvetic Diablerets and Morcles nappes and on the autochthon of W.Switzerland and the Haute Savoie, France. These North Helvetic sediments were deposited as ponded turbidite sequences in two distinct basins running along the Alpine front during the early Oligocene; the palaeohigh separating the inner and outer basins is cautiously interpreted as being due to emergent thrusts during deposition. The inner of these basins contained the Taveyannaz sandstones, and the outer, the Val D'Illiez formation. These two basins have distinct petrographies, with the slightly older Taveyannaz containing andesitic debris (Vuagnat, 1952) and the Val D'Illiez containing a broader spectrum of clasts from the unroofing of more internal thrust sheets. The Taveyannaz basin is overlain by Wildflysch, which Lateltin (1988) interprets as an olistostrome containing exotic blocks. Mayoraz et al (1988) have also described olistostromes filling huge canyons into the Val D'Illiez formation underlying the Ultra-Helvetics at the base of the Pre-Alps.

Ravenne et al (1987) reconstructed the geometry of the Grès D'Annot basin in Haute

Provence, SE. France. They show the middle Eocene Nummulitic limestones overlying the base Tertiary unconformity to be controlled by normal faulting, with onlap of the Grès D'Annot onto the Globigerina marls. Apps (1987) contends that the Nummulitic limestones and the Grès D'Annot basins were controlled by emergent thrust surfaces. The Grès D'Annot are also overlain by an olistostrome (Schistes à Bloc) with clasts matching lithologies within the encroaching wedge (Kerckhove, 1969).

As can be seen, the late Eocene/early Oligocene sedimentological and structural development of the North Helvetic domain around the Alpine arc has a common underlying theme. This theme involves thrust-top turbidite basins overlain by gravity-driven olistostromes and/or glide sheets.

5.3 Conclusions

1) The earliest preserved thrust-derived clastic sediments of the North Alpine Foreland Basin are the Taveyannaz sandstones of the North Helvetic Flysch. These were deposited in two sub-basins which ran parallel to the thrust front during the Priabonian.

2) The Inner basin formed as a thrust-top basin separated from the Outer basin by a thrust-ramp palaeohigh running WSW/ENE.

3) Turbidite sedimentation in the basins was controlled by relative sea-level fluctuations which were probably related to episodes of thrusting.

4) The Inner basin underwent severe deformation at shallow levels whilst sediment was partially lithified.

5) A gravity glide mud sheet was emplaced into the Inner basin at or near the sediment/water interface.

6) Blocks of Mesozoic limestone incorporated into the mud sheet allow a timing of the

initiation of detachment of the Helvetic nappes during the late Eocene/early Oligocene.

7) Continued tectonic deformation during the Oligocene caused intense thrust duplication of the Outer basin to form an antiformal stack.

8) The Middle America Trench off the west coast of Mexico serves as a modern analogue for the sedimentation and shallow level deformation of the Taveyannaz basins.

5.4 Future research

The conclusions above are considered to be only a relatively minor contribution to the story of the early development of the North Alpine Foreland Basin. Research in progress is following on from this by studying the geometry and mechanism of formation of the underlying base Tertiary unconformity (Crampton in prep.). In modern accretionary wedges and foreland fold and thrust belts it is common for front runner thrusts to encounter normal faults in the underthrust plate. This leads to stress concentrations, resulting in the detachment surface ramping up to form a leading edge anticline (Moore and Shipley, 1988; Wiltschko and Eastman, 1983). It is hoped that through careful mapping of the base Tertiary unconformity, evidence of the structural controls and their relationship to the development of the Taveyannaz basins will be evaluated.

A post-doctorate research project intends to link the timing and development of the North Helvetic Flysch basins from around the Alpine arc, attempting to evaluate the relative influences of thrust wedge processes and eustatic variations on the stratigraphic development of these sediments. During this research certain lines of enquiry or techniques have not been followed simply because of constraints on time. Petrography of the

sandstones of the two Taveyannaz basins would undoubtedly further our understanding of the sedimentary system. In terms of foreland basins, the North Helvetic Flysch serves as an example of development of the underfilled stage of the basin. The transition between this and the filled or overfilled "Molasse stage" raises a number of questions which have been broached in the numerical experiments (chapter 6) and which are also the subject of future studies.

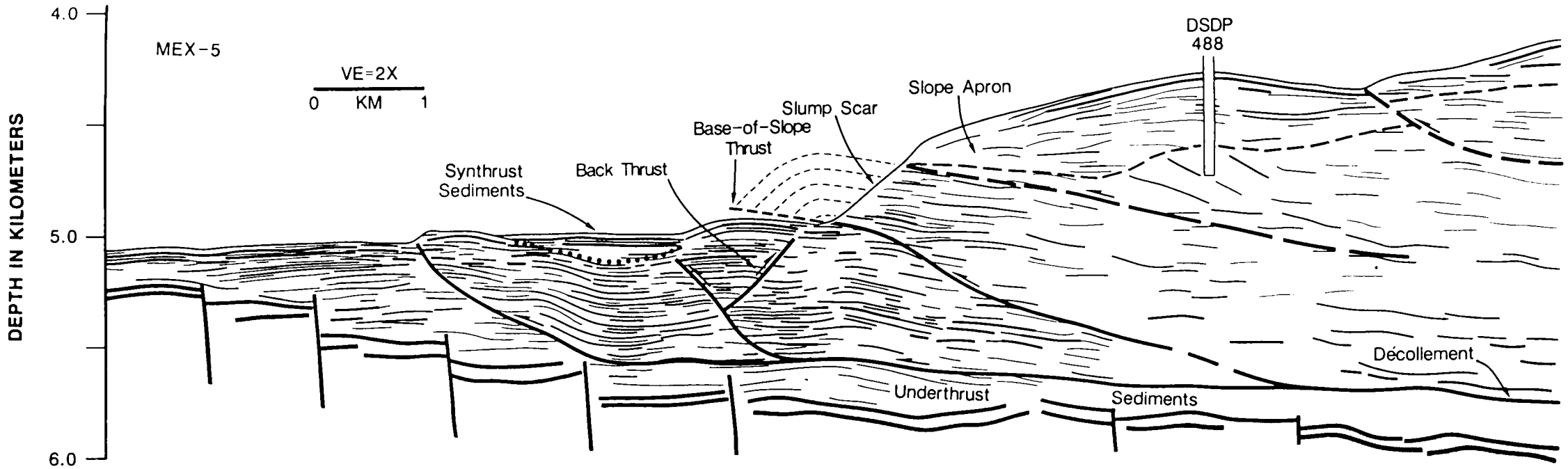

Fig.5.1. Line drawing of a seismic line through the base of the trench slope on the Middle America Trench off the west coast of Mexico. A basal decollement detaches the sandstones at the contact with the underlying hemipelagic sediments. The leading edge anticline forms a thrust-top basin behind it. A low angle base of slope thrust forms a slump scar. This is thought to be a modern analogue for the Taveyannaz basins.

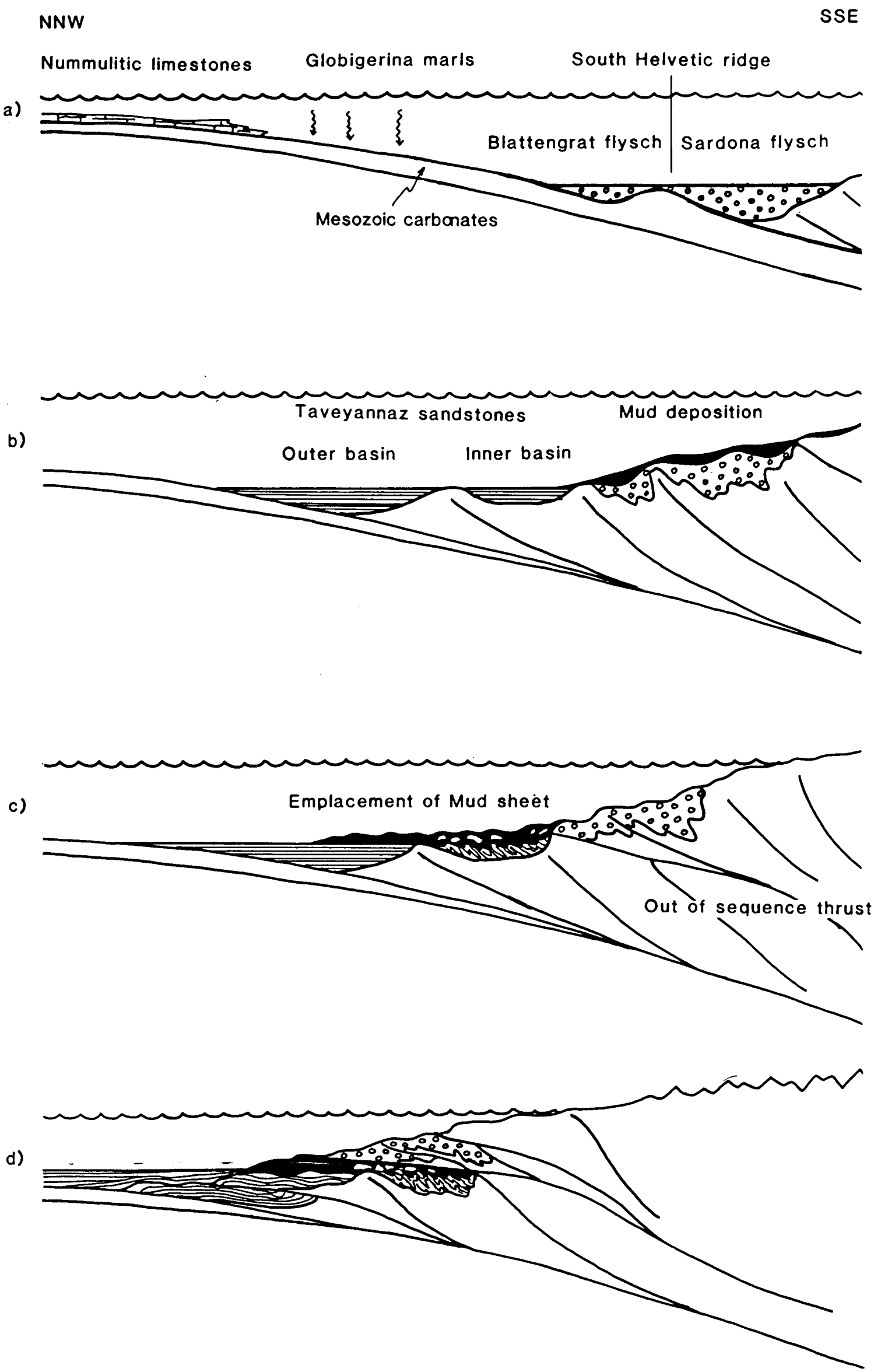

Fig.5.2. Schematic evolution of the Helvetic flysch of eastern Switzerland. **a)** Middle Eocene - Development of the Blattengrat and Sardona flysch basins separated by the South Helvetic ridge (Wegmann, 1961). Deposition of Globigerina marls and Nummulitic limestones over the North helvetic realm. **b)** Late Eocene - Deposition of the Taveyannaz sandstones as two sub-basins. **c)** Out-of-sequence thrusts transporting muds of the upper slope into the Taveyannaz sandstone basins aided by gravity gliding to form the mud sheet, incorporating blocks of the underlying sandstones. **d)** Continued movement on the out-of-sequence thrust places the Sardona and Blattengrat flysch units over the Taveyannaz sandstones and the mud sheet.

CHAPTER 6

SIMULATION OF FORELAND BASIN STRATIGRAPHY USING A DIFFUSION MODEL OF MOUNTAIN BELT UPLIFT AND EROSION: AN EXAMPLE FROM E.SWITZERLAND

(This chapter was written in collaboration with B.Coakley).

6.1 Introduction

Foreland basins are the flexural depressions that develop in front of migrating thrust loads in orogenic belts. The convergence of the orogenic thrust wedge and the foreland plate can be considered in simple mechanical terms as a vertical load migrating over a flexed plate. Erosion from the thrust wedge and sedimentation in the resultant flexural depression acts to redistribute the effective load, thereby modifying the geometry of the basin. The stratigraphy within the basin preserves a record of the development of the thrust wedge/foreland basin system through time. This study explores the possible controls on foreland basin stratigraphy by the dynamics of an eroding thrust wedge.

Qualitative understanding of the link between the thrust wedge and its associated foreland basin was first recognised by Price (1973) for the thin-skinned fold and thrust belt of the Southern Canadian Rockies. Price further suggested that through this link one might expect to read the history of the thrust wedge in the stratigraphy of the basin.

The concept of lithospheric flexure dates from gravimetric measurements in the oceans (Vening-Meinesz, 1941). Studies of the oceanic lithosphere at oceanic islands and sea-mounts (Watts and Cochran, 1974) and at the sites of plate subduction at deep-sea trenches

(Watts and Talwani,1974) indicate that the oceanic lithosphere can be treated as a linear elastic solid whose long-term (>10^6 yrs) strength is dependent on its thermal age (Watts,1978). Whether the continental lithosphere can be treated as a linear elastic solid, or whether it exhibits some form of stress relaxation on geological time-scales is a subject of controversy. For a linear elastic model to be valid, any relaxation of stress following loading must be on a short time scale (<10^5 -10^6 Myr). If the plate is initially elastic, but then shows significant stress relaxation on long time-scales (>20-30Myr), then the rheology can be considered as visco-elastic. Both models have been applied to foreland basins (Jordan, 1981; Quinlan and Beaumont, 1984).

If we consider a load on a linear elastic plate, the geometry of the deflection will remain constant through time. In contrast, a visco-elastic plate model predicts a narrowing of the deflection with time. Therefore, the stratigraphies of foreland basins should provide an ideal data-base for the testing of these rheologies. If we consider the simple case of a stationary load on an elastic plate, with successive stratigraphic units filling the basin to a horizontal datum level, each unit should overstep the previous unit, onlapping the flexural bulge. On a visco-elastic lithosphere, the narrowing of the basin causes each unit to be more confined than the previous unit. This results in stratigraphic offlap, with the depocentre migrating progressively closer to the thrust front. However, the testing of these two rheologies is complicated by three processes: 1) motion of the load relative to the plate, 2) changes in the shape and magnitude of the load, 3) erosion and sedimentation which has the effect of redistributing the load from the thrust wedge to the foreland basin, driving the forebulge towards the foreland. The steady advance of the load, and the redistribution of the load by erosion and sedimentation both result in the steady onlap of stratigraphy onto the foreland. Rejuvenation of the load in the internal parts of the thrust wedge by processes such as out-of-sequence thrusting, backthrusting and underplating, has

the opposite effect, dragging the forebulge towards the mountain belt and forming a regional unconformity in the outer portion of the basin.

The presence of unconformities in foreland basin stratigraphy, correlating, apparently with periods of tectonic quiescence and basin deepening close to the thrust front is the primary evidence for the documentation of visco-elastic relaxation of the lithosphere (Beaumont, 1978; Quinlan and Beaumont, 1984; Willets, Chapman and Neugebauer, 1985; Tankard, 1986; Beaumont et al, 1988). The aims of this paper are to demonstrate that unconformities within foreland basin stratigraphy can be developed on a purely elastic lithosphere by simply changing the spatial distribution of the load. The satisfactory resolution of the evolution of the load comprising the orogenic wedge requires sequential structural restoration of the thrust wedge.

We simulate the stratigraphy of a well documented foreland basin, the North Alpine Foreland Basin (NAFB) (Fig.6.1) by using a reconstructed load evolution and by incorporating the effects of erosion and sediment deposition. The stratigraphy of the NAFB is divided into two megasequences separated by a major unconformity (Fig.6.2). This unconformity is dated as base Burdigalian (early Miocene), and is correlated with the underplating of the crystalline basement of the foreland plate onto the base of the thrust wedge. This major event in the development of the Alpine thrust wedge changed the locus of loading, causing uplift of the external parts of the NAFB, so cutting the unconformity. This relationship between loading and peripheral uplift will be documented using radiometric, structural and stratigraphic data, and reproduced through computer modelling.

We cannot ignore that unconformities will result from eustatic fluctuations (Vail et al, 1977), but the aims of this work are to propose an alternative to either eustasy or stress relaxation in the lithosphere in the formation of unconformities in foreland basins. Consequently, we do not consider this to be an unique solution, but it is intended to lead

to a better physical insight into the possible controls on foreland basin stratigraphy.

6.2 The evolution of the load

Foreland basin stratigraphy results from the interaction of an applied force system (load) and the strength of the flexed plate, linked by erosion and sediment deposition. It is therefore essential to study the variation of these components through time. Ignoring in-plane forces and applied torques (bending moments), the load can be thought of as the distributed vertical forces imposed by the orogenic wedge plus the basin infill. The wedge is in a state of dynamic equilibrium. The plate deflection and the surface slope of the wedge control the redistribution of the load by erosion of material from the mountain belt and sedimentation in the basin. Erosion and redistribution into the basin can be approximated by a diffusional law whereby the transport rate is proportional to the gradient (Kenyon and Turcotte, 1985; Moretti and Turcotte, 1985; Flemings and Jordan, 1989).

The evolution of the thrust wedge has been constrained using published data from Pfiffner (1986), who constructed a series of sequentially restored cross-sections through the external Alps of eastern Switzerland from the middle Eocene to the present day (Fig.6.3). These sections utilise all available information on the maximum depths of burial at the base of the wedge, obtained from illite crystallinity on Liassic shales (Frey, 1978). He also used pebble and heavy mineral analyses (Mange-Rajetzky, 1985; Allen et al, 1985) to partly constrain the unroofing history of the wedge. Additional geophysical data (Hsu, 1969; Pfiffner et al, 1988) have enabled estimates of the depths to detachment for the external massifs to be made.

In our discussion of mountain belt evolution, we assume a thrust wedge in dynamic equilibrium (Chapple, 1978; Davis et al, 1983). The basic mechanical concept is of a non-cohesive Coulomb wedge whose taper angle is dictated by the balance between the compressive and gravitational forces against the basal resistance to sliding, which is a function of friction and slope. The foreland propagation of the wedge is achieved by frontal accretion, which, to maintain the critical taper angle must be compensated for by thickening within the wedge; this is accomplished by backthrusting, out of sequence thrusting and underplating of material onto the base of the wedge. The internal thickening will be counteracted by erosion of the upper surface.

Figure 6.3 illustrates the development of the Alpine thrust wedge between 40 and 17Ma, simplified from Pfiffner (1986). This illustrates an initial phase of rapid propagation of the thrust front between 40Ma and 30Ma, advancing northward onto the European margin at an approximate rate of 4mm/yr associated with a low angle of taper. The later evolution is characterised by a decrease in thrust front propagation rate and a transfer of the mass influx into the wedge from frontal accretion to internal thickening, dominated by the underplating of the external massifs. The evidence for the timing of underplating comes from isotope work by Hunziker et al (1986); the allochthonous cover to the Aar massif was incorporated at this stage into the Helvetic nappes, the deformation being dated as between 30 and 35Ma using K/Ar and Rb/Sr methods, whereas the underlying autochthon to the massif yields K/Ar dates between 25-15Ma for deformation. This reflects the accretion of the uppermost part of the foreland plate onto the base of the growing thrust wedge approximately 10Myr after the initial overthrusting of the area, and also correlates with a period of rapid uplift within the wedge between 22 and 18Ma (Werner, 1979). This period of thickening and rapid uplift in the wedge is also seen in the heavy mineral studies of the basin infill, where the appearance of blue amphiboles in the late Chattian and Burdigalian

marks the exposure of blueschists (Mange-Rajetzky, 1985; Allen et al, 1985).

6.3 The European foreland plate

6.3.1 Geological History

In considering the influence of the foreland plate on the basin stratigraphy, the primary factor is the mechanical strength of the lithosphere, which controls the horizontal distance of compensation of an applied load. The strength of the plate is described by the flexural rigidity, or the equivalent elastic thickness (see equation 7). The possible range of values and relevance of the flexural rigidity will be discussed more fully in the section on modelling. For the moment, we need only consider the flexural rigidity as a function of the thermal state of the plate.

Heating of the lithosphere is commonly associated with either stretching resulting in uplift of the geotherms (Burke and Dewey, 1973), or burial during underthrusting in collisional belts (Kominz and Bond, 1986). The European plate has a complex history of compressional and extensional tectonics. The Hercynian orogeny during the Permo-Carboniferous involved crustal thickening and the intrusion of granitoids with late stage uplift and erosion. Associated with these late Hercynian events was the formation of a system of SW-NE striking grabens with NW-SE connecting faults as part of a regional wrench system (Bachmann et al, 1987). The Entlebuch and Bodensee troughs of central and eastern Switzerland are part of this system (Fig.6.6b). The Triassic was a period of relative quiescence when evaporites were deposited which acted as an important decollement horizon during later Alpine compression. The Early to Middle Jurassic marked a period of

rifting during which thick carbonate sequences were deposited. By this time oceanic crust had started forming to the south as part of the Tethyan Ocean. From the Middle Jurassic until the Albian faulting decreased and limestones and shales blanketed the region. The trend of Jurassic faulting ran parallel to the present strike of the mountain belt in Switzerland. The Tertiary began with regional uplift of the European margin associated with the closure of Tethys, and the approach of the orogenic wedge from the south. This period is marked by the basal Tertiary unconformity, which Trümpy (1973) termed the "Palaeocene Restoration".

In summary, we are able to distinguish two features of the foreland plate that are considered to influence the development of the North Alpine Foreland Basin. Primarily, the relative youth of the basement resulting in the low strength of the plate,and secondarily, the presence of inherent fractures in the upper crust, such as the Permo-Carboniferous grabens and Jurassic normal faults.

6.3.2 Method for estimating the elastic thickness of the European plate

Gravity anomalies in mountain belts have been applied to the evaluation of the flexural rigidity of the foreland plate. Karner and Watts (1983) estimated the equivalent elastic thickness (see eqn. 7) of the European foreland to be between 25 and 50km. Lyon-Caen and Molnar (1989; in press) include a terrain correction into the reduction of the gravity data, and suggest that the gravity profiles of the Alpine belt, north of the Ivrea body, provide no compelling evidence of the lithospheric strength. This suggests that the dynamic processes which originally formed the NAFB have now ceased, precluding the use of gravity anomalies in evaluating the flexural rigidity of the European plate (Lyon-Caen and Molnar, 1989; in press).

It was therefore necessary to study the stratigraphy of the NAFB to calculate the curvature of the foreland plate and thereby to estimate the strength of the lithosphere during formation of the foreland basin. We used a simple model of end loading a broken plate of linear elastic properties. By using the reconstructed configuration of the mountain belt at a suitable point in time, we combined stratigraphic and structural data to give details of the basin geometry and load configuration respectively. The methodology of this simple model is illustrated in figure 6.4. The estimated load at 17Ma was placed onto the end of the plate causing an initial deflection and associated peripheral forebulge. The deflection caused by this downwarping was filled with water. The deflection was then filled to sea level with sediment, broadening the distributed load and so pushing the basin and forebulge towards the foreland.

The curvature of the European plate at 17Ma was ascertained by using eleven decompacted sediment columns taken from the restored cross-section running north from the Kusnacht borehole, located approximately 10km south of Zürich (Naef et al, 1985) (Fig.6.6a). To decompact the depth to basement we assumed a sandstone lithology throughout. The data points further to the south were estimated from the restored sections of Pfiffner (1986), and have been given broad error bars. The tight curvature of the plate suggests a very weak lithosphere with an equivalent elastic thickness of approximately 10+-5km (Fig.6.5). The maximum depth of the basin at this time was about 6km below the thrust front. Varying the size of the load alters the deflection of the plate, without significantly changing the width of the basin. A deflection of 6km at the thrust front was achieved in the model by assuming the frontal reconstruction of the load configuration to be correct and increasing its mass by placing the free end of the plate further beneath the mountain belt and so extending the hinterland termination of the load. The observed deflection of the plate from the borehole data was matched by using a load width of about

100km. It was noticeable that any further increase in the overthrust length of the load made negligible difference to the deflection since the underlying plate became near vertical under the mountain belt at large load magnitudes. The value of 10+-5km for Te at 17Ma can then be used as a fixed parameter in the diffusion modelling of the NAFB. The rationale behind keeping this value as a constant during the running of the model is based on the long time period (60Myr+) since rifting, allowing near complete thermal re-equilibration, and the lack of any evidence to the contrary.

6.4 Stratigraphy of the NAFB

The stratigraphy of the NAFB (Fig.6.2) exhibits a classical foreland basin sequence (sensu Covey 1986), starting at about 42Ma with an underfilled "flysch" stage. By 32Ma, the basin was occupied by shallow marine and fluvial deposits. This commences the "Molasse" stage, and similar terrestrial and shallow marine sediments continued to be deposited until approximately 11Ma when isostatic rebound caused general uplift of the basin.

Four main groups are traditionally distinguished within the NAFB stratigraphy (Matter et al 1980). The basin fill should, however, be extended to include the North Helvetic Flysch to make five groups. These are listed below in ascending stratigraphic order:

1) North Helvetic Flysch -(NHF), - A1

2) Lower Marine Molasse - (UMM), - A2

3) Lower Freshwater Molasse - (USM), - A3

4) Upper Marine Molasse - (OMM), - B2

5) Upper Freshwater Molasse - (OSM). - B3

The parenthetic abbreviations represent the Swiss/German names for the groups as used in previous European literature. For the purposes of this paper we have divided the entire basin into two shallowing upward megasequences, A and B. These two megasequences are then subdivided into environmental groups representing a simple three stage breakdown of a regressive sequence:

Stage 1 = Deep Marine,

Stage 2 = Shallow Marine,

Stage 3 = Continental.

Using this straightforward scheme, megasequence A contains all three stages from deep marine to continental. The base of the Upper Marine Molasse (B2) marks the lower boundary of megasequence B, and represents a return to shallow marine conditions. This is followed by continental sedimentation during the Upper Freshwater Molasse (B3).

6.4.1 Present Structural Setting

The present-day structure of the NAFB in eastern Switzerland can initially be divided into two zones: a more internal, topographically elevated and strongly deformed region to the south, and an external, relatively undeformed region to the north, termed the Plateau Molasse (Fig.6.6b). The former contains the sediments of most southerly palaeogeographic origin; these are the turbidites of the North Helvetic Flysch (A1), found wrapped around the uppermost Helvetic nappes (Pfiffner 1981), and in the underlying parautochthonous cover to the Aar massif. The parautochthonous examples are exposed in tectonic windows

to the south of the Helvetic nappes (Fig.6.6b) as seen in the Panixerpass region, Canton Glarus. Between the external Plateau Molasse and the highly deformed region to the south, the thickest deposits of the NAFB are steeply tilted within imbricate thrust blocks of the Sub-Alpine zone. North of the Plateau Molasse, the sediments thin and pinch-out into the Tafeljura.

6.4.2 The Palaeocene Restoration - a Forebulge Unconformity?

The first sign of the arrival of the thrust wedge onto the southern margin of Europe is seen at the present day as a break in sedimentation with a maximum chronostratigraphic gap of Malm to middle Eocene. This was described by Trümpy (1973) as the "Palaeocene Restoration". This unconformity underlies the whole basin, separating eroded Tethyan platform Helvetic carbonates from progressively younger Tertiary sediments as it is traced northwards into the foreland. Herb (1988) has constructed a series of palinspastic restorations of the unconformity, clearly illustrating that as it is traced from Panixerpass through the overlying Helvetic nappes, (i.e. heading south in terms of original palaeogeography), one observes a decrease in the amount of missing stratigraphy from the Cretaceous and Palaeogene (Trümpy 1980). Examination of the sequence within the Sardona nappe, which is considered to be of more southerly (Ultrahelvetic) origin than the Helvetic nappes (Ruefli 1959), shows a complete succession through the Cretaceous-Tertiary boundary (Wegmann 1961). The simplest explanation of this unconformity is to consider it as the cumulative effect over time of forebulge uplift, influenced by the original passive margin geometry of the foreland (Stockmal et al, 1986). Uplift of the bulge exposed the Tethyan platform sediments to erosion, similar to that recognised in the Appalachians (Jacobi, 1981) and in Alaska, N.America (Coakley and Watts, in press).

6.4.3 The North Helvetic Flysch - A1 (42-36Ma)

Although the North Helvetic Flysch has been the subject of this thesis, a brief summary in the context of this chapter is considered necessary.

After the initial uplift and during the Palaeocene, the first sign of flexural downwarping is the deposition during the early Lutetian of 10-50m of shallow marine nummulitic limestones overlying the unconformity (Styger 1961). These grade up into approximately 350m of Globigerina Marls representing water depths of several hundred metres (Herb, 1988). Above these marls are approximately 2km of turbidites (Siegenthaler 1974), representing the first southerly derived sediments. In both eastern and western Switzerland, the oldest of these turbidites (Taveyannaz Sandstones), display evidence of deposition in thrust-top (piggy-back) basins (Ori and Friend, 1984; Lateltin, 1988; Chapter 3, this thesis). The southern margin of the Tavayannaz basin is overlain by a 50-100m thick olistostrome deposit, indicating its proximity to the thrust wedge. The processes of deposition during this initial phase of development in the foreland basin are highly analogous to those in modern accretionary wedge environments (Moore and Shipley 1988).

6.4.4 Lower Marine Molasse- A2 (36-27Ma)

Marine conditions continued into the middle Oligocene, as a narrow branch off Tethys. The stratigraphy and sedimentology of A2 has recently been described by Diem (1986). It contains thick sequences of marine siliciclastics now exposed within the imbricate thrust slices of the Sub-alpine Zone. Lower A2 is represented by the Deutenhausen beds of early Rupelian age (P18-P19 foram zones). The Deutenhausen beds comprise about 1km of delta

front channel turbidites feeding progradational lobe systems shedding material northwards (Diem 1986). Ideally, this lower portion of A2 should be included into A1 due to its deep water environment, but this would cause confusion with reference to previous literature.

Middle A2 consists of the Horw Shales which comprise 700m of dominantly shallow marine mudstones rich in ostracods and forams yielding middle Rupelian ages (P20 foram zone). Towards the top of A2 these fine grained shelf deposits are overlain by a regressive series of coastal sands and fan delta conglomerates called the Horw Sandstones, dated at late Rupelian/Chattian (NP24 nannoplankton zone). Work by Diem (1985) on wave ripples from the Horw Sandstones indicates increasing palaeowave period and power towards the east, suggesting a funnel shaped basin during A2 deposition. Palaeogeographic reconstructions by Buchi and Schlanke (1977) indicate a basin width of 40-50km during A2, which is in agreement with Diem's data on the wave fetch. Consequently, during A2 we see the filling of a narrow basin from deeper water turbidites to shallow marine and coastal sediments, with the northern margin of the basin containing a thin continental deposit.

6.4.5 Lower Freshwater Molasse - A3 (29-22Ma)

At the onset of the Chattian sedimentation was dominated by seven large alluvial fans coming off the thrust front to the south (Buchi and Schlanke 1977). In eastern Switzerland the Rigi and Speer fans shed vast thicknesses (upto 4km) of conglomerates which are intercalated with silty marls at the lateral limits of the fans. The conglomerates contain material derived from the erosion of Cretaceous Penninic and Ultra-Penninic flysch.

Towards the end of the Chattian, large amounts of epidote entered the system; this arrival of epidote signifies the erosion of material involved in the Lepontine Greenschist

metamorphic event at about 38Ma, reflecting rapid uplift within the thrust wedge (Trümpy 1980). During the Aquitanian there is a gradual northward shift of the alluvial sediment supply, and the development of the Hornli fan. The Hornli fan is characterised by abundant dolomitic debris, as well as clasts of south and north Helvetic origin such as Nummulitic Limestones and Greensands from the erosion of A1.

A3 is the culmination of megasequence A. The underfilled basin containing turbidites and shales was succeeded by coastal and shallow marine sedimentation, and finally overfilling to give large thicknesses of fluvial deposits. During this period, there was a progressive northward stratigraphic onlap onto the foreland. Although the onlap pattern reveals an initial steady movement of the stratigraphic pinchout during A1 and A2, it is more erratic during A3. Pfiffner (1986) interpreted much of the rapid thickness changes in A3 as due to active normal faults during deposition.

6.4.6 Upper Marine Molasse - B2 (22-16Ma)

At the beginning of the Burdigalian, shallow seas flooded the Molasse basin. The southern margin of deposition was located within what is now the Sub-Alpine zone, the northern pinchout remaining in a similar position to that of A3, at present located near the R.Rhein. At this time the width of the basin of deposition was approximately 60-80km. The overall thickness of B2 in E.Switzerland varies between 200-800m. In the Kusnacht borehole B2 is approximately 450m thick.

In Switzerland, sedimentation was dominated by two large fans, located in positions controlled by earlier fans; in W.Switzerland this was the Napf fan, and in E.Switzerland the Hornli fan. These deltaic fans were fed by large fluvial systems coming off the thrust wedge and passing northwestward into wave- and tide-dominated marine conditions

(Homewood and Allen 1981). Petrological studies by Allen et al, (1985) reveal distinct heavy mineral provinces in the Burdigalian seaway, yielding information on the evolution of the thrust wedge. Material was also derived from Penninic blueschists exposed within the thrust wedge.

The basal unconformity to the B2 transgression indicates initial flooding from the Rhone sea to the west and Paratethys to the east. Berger (1985) dated the basal unconformity using a number of biostratigraphic indicators, including foraminifera and small mammal debris. He was able to show that the initial bi-directional flooding occurred during the late Aquitanian (NM2b micromammal zone), and that a marine link between the east and west occurred at the Aquitanian/Burdigalian boundary. This narrow seaway then started onlapping northwards over the deposits of A3 during the early Burdigalian (NM3).

In the cross section of this study B2 is divided into three sequences dated from the Kusnacht Tiefenbrunnen and Weiach boreholes (Fig.6a). Naef et al, (1985) produced a series of subsidence curves and recognised two internal unconformities. From 22-18Ma approximately 300m of shallow marine glauconitic sandstones, limestones and marls were deposited. This sequence is called the Muschelsandstein and is underlain by a transgressive conglomerate. The base of the Muschelsandstein represents a basinward shift in onlap, followed by renewed northward onlap over the base Burdigalian unconformity described above. At 18Ma there was a break in sedimentation followed by the deposition of 100m of sandy shales with a basal oyster-rich conglomerate in the south of the basin, while freshwater conglomerates were deposited in the more northern region of the Weiach borehole. Once again these beds show a basinward shift in onlap onto the underlying Muschelsandstein. At 17Ma net erosion occurred north of Tiefernbrunnen (Fig.6a), with simultaneous deposition occurring to the south. This bounding surface marks the transition into upper B2, and is marked by a basal conglomerate thinning out north of Kusnacht,

followed by 50m of sandstones.

6.4.7 Upper Freshwater Molasse -B3 (16-11Ma)

Towards the end of the Burdigalian the shallow seas of B2 were filled, with a return to continental sedimentation. The Napf and Hornli fans remained the main feeder sources in Switzerland, associated with an overall northward shift of the depocentre (Trümpy 1980). These huge alluvial fans drained northwards into longitudinal river systems. In places, thin coal seams and occasional freshwater limestones were deposited. A laterally extensive limestone band dated at 15Ma is seen within the section of this study (Fig.6a).

The maximum thickness of B3 is 1500m, occurring within the centres of the fans, with thicknesses decreasing rapidly northwards. The northern pinchout of the basin at this time is not clear due to erosion, but a glance at the taper of the stratigraphy suggests that it is only slightly north of the pinchout of B2, onlapping onto the Jura (Rigassi 1977).

6.5 Stratigraphic modelling

6.5.1 Previous work

Previous models of foreland basins have reproduced observed stratigraphy simply, by applying loads at instants in time on elastic (Jordan, 1981) or visco-elastic plates (Beaumont, 1981; Quinlan and Beaumont, 1984; Beaumont et al., 1988). The deflection is immediately enhanced and a new sedimentary layer occupies and expands the basin, filling

to a reference surface. However, thrust loading is not episodic, and should be considered as a continuous process (Davis et al, 1983; Platt, 1986; Boyer and Geiser, 1987). The partitioning of deformation within the thrust wedge is dictated by the mechanical requirements of the critical taper to the wedge. The processes by which taper is maintained are: frontal accretion, underplating, surficial erosion, back-thrusting and out-of-sequence thrusting. Modifications to the geometry of the wedge alters the configuration of the distributed load, and so influences the resultant deflection.

The interplay between the rate of thrusting which creates space for sediments, and the rate of sedimentation or basin filling which also expands the basin, is not represented in previous simple stratigraphic models. Jordan (1981) modelled the evolution of the Cretaceous Interior Seaway in terms of separate pulses of flexural subsidence as a response to discrete events of load emplacement. Later work (Beaumont, 1981; Quinlan and Beaumont, 1984; Beaumont et al, 1988) considered viscous delay of an initial elastic response, but loads were still emplaced as a series of large blocks over a number of time steps to simulate the development of the orogenic wedge. Thrust loading displaces the lithosphere, creating a sink, as well as providing a sedimentary source to fill the sink. Deposition and erosion redistribute some of the thrust load into the foreland basin. The flexural strength of the underlying lithosphere dictates how these different systems interact over time, with erosion driving uplift and basin filling, and thrust loading depressing the lithosphere. By imposing simple geometrical constraints on the development of the thrust load and using a transport relationship to describe sedimentation as a function of slope we have developed a simple, physically based model. This allows us to directly link the evolution of the thrust wedge and the adjacent foreland basin and to examine this relationship through variations of the model parameters.

Foreland basin stratigraphy has been used as evidence to support both visco-elastic

(Beaumont, 1981; Quinlan and Beaumont, 1984; Tankard, 1986; Beaumont et al, 1988) and elastic plate models (Jordan, 1981; Coakley and Watts, 1989; in press). Recent studies (Beaumont, 1981; Quinlan and Beaumont, 1984; Beaumont et al, 1988; Coakley and Watts, 1987; in press) have focussed on the timing, position and extent of unconformities over the flexural bulge. These unconformities have been cited as support for visco-elastic relaxation of the lithosphere; erosion occurs as the bulge migrates towards the load, uplifting the distal sediments above the reference level. It is possible to develop similar unconformities on an elastic lithosphere through a redistribution or increase of the load (Coakley and Watts, 1989; in press), thus presenting an alternative mechanism. Without conclusive documentation of visco-elasticity we assume a simple elastic lithosphere.

It is apparent that an approach which incorporates known sedimentary and tectonic processes is required. Flemings and Jordan (1989) have expanded on the method of Moretti and Turcotte (1985) to apply diffusion equation modelling of erosion and sedimentation to foreland basins. For these models, the diffusion equation describes how the topography of the thrust wedge decays, and how the basin fills. This change in sediment and thrust load is then used in the flexure equation to determine how the pre-existing basin is distorted by the redistribution of the load. Flemings and Jordan (1989) used a simplified version of a thrust wedge with a critical angle of taper, replenishing the load at every time step to maintain a constant, linear topographic profile in the source region. We adopt a similar approach here, seeking to reproduce the stratigraphy of the NAFB using a model which maintains the thrust wedge at a critical taper, as well as a diffusion model of sediment transport.

By maintaining a slope profile as a proxy for critical taper, we can describe the constructional topography of the thrust wedge. Utilising diffusion, we can examine how that topography is removed by erosion and redistributed by sedimentation. We model the

discontinuous foreland basin stratigraphy, reproducing the primary unconformity separating the two megasequences of the NAFB (figs.6.2 and 6.6a), by invoking close to continuous tectonic processes.

6.5.2 The Model

The diffusion equation is commonly used to describe transport, where the rate of transport is proportional to the gradient of potential. Both heat transport down a thermal gradient and the motion of chemical species down an activity gradient can be described by the diffusion equation. Here we use it to describe the transport of sediment down a topographic gradient (Hirano, 1976; Kirkby, 1971; Carson and Kirkby, 1972; Hanks and Andrews, 1989).

The relationship is based on two assumptions. First we assume that the amount of material transported through a vertical plane is proportional to the scaled slope at that point:

$$q(x) = -K\ dh/dx \qquad (1)$$

K is the transport coefficient, h is the topography, q is the amount of material transported and x is the spatial variable. Secondly we assume that the elevation change in an infinitesimal volume is equal to the difference between material brought in and material taken out. This is conservation of mass, expressed by:

$$dh(x)/dt = dq/dx \qquad (2)$$

Substituting 1 into 2 we obtain the diffusion equation:

$$dh(x)/dt = d/dx\ [-K\ .\ dh(x)/dx] \qquad (3)$$

We take K to be a constant, so $dK/dx = 0$, and the expression simplifies to:

$$dh(x)/dt = -K\ d^2h/dx^2 \qquad (4)$$

Given a topographic profile, we can use this relationship to specify erosion and deposition, and so calculate the change in the thrust and sediment load at every point on the x axis. Where topographic curvature is positive (highs) erosion occurs. Where curvature is negative (lows) deposition takes place. Using the change in load in the flexure equation (5) we can examine how the depositional basin profile changes over time, and develop a more complete understanding of foreland basin development.

The flexure equation describes the response of a linear elastic beam to loading. In the absence of horizontal in-plane forces and bending moments, this equation reduces to:

$$D\, d^4w/dx^4 + (\varrho m - \varrho i) g w(x) = p(x) \qquad (5)$$

Where D is the flexural rigidity in Nm, ϱi and ϱm are the densities of the infill and mantle respectively, g is average gravity, w(x) is the deflection, and p(x) is the load in N/m^2. The right hand side if the equation, p(x), is the net change in topography, weighted by gravity and the density of the material, ϱs. The change in the load is specified by diffusion plus the change in the thrust load for that time step, T(x):

$$p(x) = (dh(x)/dt + dT(x)/dt)\, g\varrho s \qquad (6)$$

To compute the flexure we set ϱi to zero, calculating each increment of deflection as air filled. All loads, due to thrusting, erosion and deposition are added above the initial basement surface and are accounted for in the modelling. The volume of material deposited at every time step is equal to the volume eroded. Conservation of mass, as assumed in diffusion, requires that the sediment density is equal to the load density. This density, ϱs, is taken to be 2650 kg/m^3, this being high for the sediments, but low for the load. Solving the flexure equation for this load gives the incremental subsidence and uplift for the interval dt. We assume a plate of linear elastic strength. The flexural rigidity D, defines the wavelength of regional compensation and is related to the effective elastic thickness, Te, by:

$$D = ETe^3/12(1-v^2) \qquad (7)$$

where D is in Nm, E is Young's modulus, and v is Poisson's ratio which is dimensionless.

The diffusion and flexure equations are solved numerically. Each is treated independently on the same finite difference grid. The diffusion equation is solved using an inherently stable alternating direction technique from Roache, (1982, p. 95-99). The solution is obtained by marching down the array, calculating every new value as a weighted sum of the previous spatial value for the current time step and the two previous spatial values from the previous time step. Two passes at diffusion, one forward (0 to n) and one backward (n to 0) provide the change in load for the flexure equation. Regional isostatic adjustment due to flexure distorts the topographic profile, modifying the next step in diffusion.

The flexure equation is solved by back substitution in a five band matrix. The solution provides values for uplift and subsidence at each point in the grid. The elevations of the stratigraphic horizons and topography are updated by these amounts. Each model layer is the sum of a series of numerical steps representing the previous evolution of the thrust wedge and basin. The quantity of steps is defined by the magnitude of K and the length of the time represented by the layer, more steps for larger K and longer time. This ensures the accuracy of the solutions obtained.

The model is sensitive to the boundary conditions which modify how transport and compensation are achieved. For diffusion we make $dh/dx\ (0) = 0$, indicating no transport through the plane at $x = 0$, equivalent to a drainage divide. At the opposite edge of the grid we set $d^2h/dx^2\ (n) = 0$, there is no change in elevation as sediment leaves the system. For flexure we assume a broken, linear elastic plate with the free end at $x = 0$. Physically this means that no moments are transmitted from the free end of the slab; $d^2w/dx^2\ (0) = 0$, and that shear force applied at $x = 0$ is equal to the load applied at $x = 0$, $d^3w/dx^3\ (0) = p(0)$. At the opposite end of the plate we take $w(n) = 0$ and $dw/dx = 0$, pinning the beam.

Mountain belts evolve continuously, advancing and rising in opposition to erosion. The evolution of this geometry is controlled by the strength of the overthrust material which rises until it has enough potential energy to advance over the foreland. For this model we adopt a simple dynamic wedge for the overthrust load, defined by two parameters; the topographic slope and the rate of advance of the wedge tip. The thrust wedge is maintained at constant slope; eroded material is replenished by material brought through the plane at x = 0.

6.5.3 The Parameters

For each model run, we specify four parameters, Te, K, slope angle and rate of thrust tip advance (Fig.6.7). The values define the length scale of flexural compensation, the rate of material flux into the thrust wedge, the rate at which sediments are delivered to the basin and how the depositional slope evolves through time. The trade off between how fast the basin is enlarged and how fast it is filled, defines the stratigraphy. No one parameter uniquely controls any one aspect of the final basin, each interferes with the others. This feedback complicates the model.

Figures 6.8 to 6.11 show how varying these parameters affects the model stratigraphy. Each parameter is assigned four different values, similar to those used in the final model of the NAFB. The models in these figures differ only by the parameter being considered in the figure, all other values being held constant. A reference model (K = 400.0 m^2/yr, rate of thrust tip advance = 0.0025 m/yr, Te = 20.0km, slope angle = 1.5 degrees) is plotted on each figure at the same scale to provide a reference for comparison.

Each model run is for 10Myr, which is divided into forty layers, each representing 250,000 years. The lines plotted in the stratigraphic diagram are isochronous and similar to

depositional interfaces, which are preserved beneath the advancing thrust wedge. The stratigraphy overlies a basement of passive marker layers, each of which was originally 100m thick, allowing an assessment of the extent and magnitude of basement erosion. Erosion of underlying passive margin sediments is commonly observed in foreland basins, and is recognised in the Alps (Trümpy, 1973; Herb, 1988), the Appalachians (Jacobi, 1981) and in the Colville trough of Northern Alaska (Coakley and Watts, in press). Chrono-stratigraphic (Wheeler) diagrams which plot the age versus the lateral extent of deposition for each layer in the model, provide a measure of the rate of basement onlap and erosion through time. The scale in the upper left hand corner indicates x and y scales as well as the vertical exaggeration and the slope of one, two and five degree lines. The x-scale is one-half of that for the stratigraphic diagrams.

Figure 6.8 shows the effect of varying the transport coefficient K, from 100.0 m^2/yr to 800.0 m^2/yr. When K is low, sediment transport is inhibited, and the basin remains underfilled. With a low K a steady state is achieved, sediments pond in the central basin, onlap tracks at a constant distance in advance of the thrust tip. Increasing K fills the basin and onlap exceeds the rate of thrust tip advance. The basin sediments aggrade as deposition climbs onto the flexural bulge. Since the topographic slope is held constant, increasing K also enhances the mass flux of material into the rear of the thrust wedge, and so increases the basin volume.

Diffusion models of slope development have been proposed by many workers (Kirkby, 1971; Hirano, 1976). The diffusion model can be derived from first principles for downslope transport in the case of a sheet wash (Kirkby, 1971). The diffusion model of slope evolution has been applied (Hanks and Andrews, 1989) in the case of a decaying fault scarp, providing estimates of the dates of seismic events.

The evaluation of suitable values for the transport coefficient is extremely difficult due

to the paucity of research on a suitably large scale. Flemings and Jordan (1989) compile a list of determinations of K from a variety of morphological settings. The values range over several orders of magnitude, larger values (10^4 m^2/yr) are derived from fluvial transport, smaller values (10^{-2} m^2/yr) from the decay of isolated slopes. Given that a number of erosional and sedimentary processes are operating synchronously and at different scales in a foreland basin, the precise meaning of the value of K is not clear. Here we use K to describe the sediment production and slope evolution of the system as a parameter that encompasses the effects of a number of processes into a single value. The value of transport coefficient compatible with the NAFB thrust wedge and stratigraphy is $800m^2/yr$, a figure that is intermediate between those listed by Flemings and Jordan (1989). This is considered appropriate as the processes involved on a mountain belt scale involve both fluvial transport and surface flow.

Figure 6.9 shows the effect of varying the topographic slope from one half a degree, to two degrees. The slope defines the rate at which material is brought into the thrust wedge, controlling how deep and how fast the basin develops. Increasing the slope increases the rate at which the load grows and due to the dependence of the sediment transport on the slope, increases the rate of sediment supply to the basin. The chronostratigraphic diagrams indicate that onlap is approximately the same for each case, illustrating that the sediment, and the space in which to put it, are generated in constant proportion to each other. The only difference in the time stratigraphic diagrams is the depth and extent of basement erosion, which is greater for the higher slope. This is due to the larger load which causes steeper slopes in the bulge region, leading to faster erosion of the basement.

Figure 6.10 shows the effect of varying Te, which controls the length scale of compensation. Te is set equal to 0.0 Km (Airy case), 10.0km, 20.0km and 40.0km. These values are low compared to most continents (McNutt and Kogan, 1988), but are similar to

those estimated from this paper for the Tertiary evolution of the NAFB. Lower values for Te cause the trapping of sediment closer to the source, leading to rapid aggradation in a narrow, deep basin. Lower Te also increases the thickness of the load, since more material is required to maintain a given slope than with a higher Te. The Airy example exposes a problem in the model. Onlap at each time step marks the dividing line between deposition and erosion. In the Airy case the loading is entirely local, no flexural bulge is created and no onlap occurs; the depositional slope is a simple decaying exponential from the thrust tip to the right edge of the model. To construct chronostratigraphic diagrams, we assume that sedimentation is continuous. Given the problem of sedimentary completeness, this is not accurate (Anders et al, 1987; Tipper, 1983). The model stratigraphies might best be viewed as a record of how space is made available in the basin, rather than as a simple geological cross-section.

Figure 6.11 shows how the rate of thrust tip advance affects the basin geometry. In every thrust belt there is a partitioning of deformation dictated by the energy balance of uplift and advance. This parameter defines the rate at which the entire thrust wedge slides stably over the foreland plate. The rate of thrust tip advance primarily controls the rate at which the load is increased by mass flux through the left hand side of the model. The parameter is varied from 0.0 m/yr to 0.0075 m/yr in 0.0025 m/yr steps. Rapid advance of the thrust tip creates an underfilled basin. Similar to the case of a low K, onlap tracks at a constant offset from the thrust tip. Lower values allow sedimentation to outpace the creation of space in the basin.

6.5.4 Simulated Model of the North Alpine Foreland Basin (NAFB)

We seek in our modelling to explain the broad stratigraphy of the NAFB with the

minimum number of parameters and by a minimum variation of those parameters. More complex models are certainly physically justifiable, but lacking independent constraints we chose a simpler route. Validation of the model is achieved by comparing the broad geometry of the basin, the position and timing of the major unconformity separating megasequences A and B, and the extent and rate of onlap onto the eroded basement. The reproduction of true stratigraphic thicknesses for individual sequences was not possible without varying parameters beyond our present understanding of the processes.

Any one of the four model parameters can be modified to obtain a fit to the stratigraphy. Lacking a physical rationale for varying Te and K, both were held constant throughout every model run. The fit was obtained entirely by modifying the parameters which describe the slope angle and the rate of thrust wedge advance. There are reasons for believing that Te and K might vary with time: for example, the Alps overthrusted the Tethyan margin (Trümpy, 1980), and stratigraphic models of passive margin development (Steckler and Watts, 1981; Steckler et al, 1988) have been reconstructed in which Te increases with time since rifting, similar to the oceanic lithosphere (Watts et al, 1980). The lithosphere cools and strengthens, each sedimentary load achieves compensation on a longer wavelength than that which preceded it, and so stratigraphy oversteps the previous depositional limit, onlapping the passive margin. Stockmal et al, (1986) modelled passive margin overthrusting and found that the resultant foreland basin was insensitive to the age, or equivalently the strength of the margin immediately beneath it, the compensation of the load being more dependent on the strength of the plate interior. While the underlying lithosphere may have strengthened over the course of the Alpine thrusting (although this is contested), it seems likely to have been a small effect, justifying a constant Te for the model.

The parameters that are used to simulate the stratigraphy of the NAFB are based on our

understanding of the geological processes involved. The value for Te is held constant throughout the model at 7.5km as approximated from the stratigraphy illustrated in figure 6.6a (Fig.6.5). The value for the transport coefficient (K) is currently the least understood. For the model we have chosen a fixed value of $800m^2/yr$.

The remaining two parameters characterise the thrust wedge. The rate of thrust front advance has been estimated from Pfiffner (1986) at approximately 4mm/yr during the early development of the NAFB. This value decreases after the main thickening event within the thrust wedge involving the underplating of the External Massifs. The slope of the wedge is indirectly obtained from typical topographic slopes for present day active wedges which range from 1°-6°(Davis et al, 1983), so defining acceptable limits for the model values. The sequence of parameters used to model the NAFB are summarised in cartoon form in Figure 6.14.

The model starts at 39Ma, with a thrust wedge advance rate of 4mm/yr and with a topographic slope of 1.5°. This parameter pair was run until 24Ma when the parameters were altered in an attempt to simulate the underplating of the External Massifs. This was done by halting the advance of the thrust wedge to zero, and increasing the topographic slope of the wedge from 1.5° to 4° over a period of 1.5Ma. After this thickening event, the advance rate was increased to 2mm/yr. These values were run for a further 4Ma depositing the lower part of megasequence B.

The results of this model are illustrated in Figures 6.12 and 6.13. During the initial parameter pair from 39-24Ma we see the development of megasequence A. The first deposits do not fill the deflection to a horizontal, indicating that they are marine sediments; the basin width at this stage is 40km. As the basin develops, forming the upper part of megasequence A, the onlap of stratigraphy onto the foreland outpaces the rate of thrust advance resulting in a broadening of the basin to a maximum of 100km. This rapid onlap

over the foreland is a consequence of filling of the deflection during the evolution from an underfilled "flysch" stage, to an overfilled "molasse" stage. The filling of the basin broadens the sediment load which pushes the forebulge out, and at the same time fills the deflection to sea level; both processes cause increased progradation of sediments over the foreland.

At 24Ma the underplating of the External Massifs onto the base of the thrust wedge causes internal rejuvenation of the thrust wedge and backtilting of the basin towards the thrust front due to uplift and orogenward migration of the forebulge (Fig.6.14). Sedimentation is then confined against the thrust front, and the underlying stratigraphy is eroded over the mobile forebulge (Fig.6.14b). The resultant stratigraphy illustrates a marked unconformity which becomes laterally conformable at about 35km into the basin (Fig.6.12b). The stratigraphy of megasequence B overlying the unconformity shows a basinward shift in onlap relative to the underlying stratigraphy. This simulates the base Burdigalian unconformity separating megasequences A and B.

Figure 6.13 illustrates the amount of erosion of the modelled foreland plate due to forebulge uplift prior to the progradation of the foreland basin sediments. The maximum erosion (120m) of the foreland plate occurred during the early underfilled stage. Later erosion of the forebulge was less severe due to rapid progradation of shallow marine and continental sediments. This basal unconformity simulates the geometry of the "Palaeocene Restoration" unconformity underlying the NAFB which shows rapid truncation through the Cretaceous sequence underlying A1 (Herb, 1988), but steady truncation down to the Jurassic Malm underneath the later overfilled sediments of the basin.

6.6 Discussion

There are two aspects of the simulated model which differ significantly from the observed stratigraphy of the NAFB: 1) The thickness of the simulated stratigraphy above and below the unconformity varies from that of the observed thicknesses of megasequences A and B. 2) The unconformities within B2 at 18Ma and 17.5Ma have not been simulated. These two problems can be addressed by considering firstly, the suitability of the diffusion law to describe the erosion, transport and deposition of sediments from mountain belts into their adjacent foreland basins. Secondly, we must consider the adequacy of surface slope angle as a parameter to describe the kinematics of the critical angle of taper of orogenic wedges. This discussion is not intended to doubt the credibility of this modelling technique, but is aimed at recognising that this is a first approximation in our understanding of an extremely complex system.

The diffusion law enables us to use a single parameter to describe the rate of mass transport as a function of regional gradient. Variations in the value of the transport coefficient will result dominantly from climatic fluctuations and varying source rock lithologies. Flemings and Jordan (1989) suggest that a reasonable range of values for transport coefficients within foreland basins would be from 100-5000m^2/yr. It is also recognised that if we are considering the evolution from a submarine to continental thrust wedge the values for the transport coefficient will differ significantly. Pinet and Souriau (1988) studied worldwide continental erosion on varying time scales and concluded that the dominant control on long term (10^2Myr) continental denudation is the relief; environmental factors such as climate are important on shorter time scales however (2Myr).

With the large number of possible influences on the value of transport coefficient mentioned above, we must assume that to keep a value of 800m^2/yr as a constant over a period of 20Ma in our modelling of the NAFB is simplistic. In realising the limits of our

understanding of values for transport coefficient it is considered imperative that it is held constant, enabling the influence of the evolution of the thrust wedge to be clearly assessed. With continued research presently being carried out, it is hoped that in the future we shall have sufficient confidence in our knowledge of the transport coefficient to apply it as a variable in the modelling of foreland basins.

The simulated model of the NAFB was stopped at 18Ma, just prior to the formation of the two unconformities seen within B2. Previous attempts had been made at simulating the upper unconformities within B2 by further increasing the slope angle of the thrust wedge; but these involved excessive increases in the mass influx into the rear of the wedge over short time intervals. These increases were considered geologically unreasonable. The base Burdigalian unconformity is attributed to changes in the spatial distribution of the load involving addition of material towards the rear of the wedge by underplating. The critical taper of an orogenic wedge is in dynamic equilibrium with three parameters: 1) The mechanical strength of the wedge; 2) the basal friction on the wedge; 3) the density of the wedge (Davis et al, 1983). If any of these are altered, the critical taper will adapt to compensate. It is likely that in the case of the Alpine thrust wedge, the underplating of the External Massifs occurred in response to increased friction on the base of the wedge, reflecting the buttress effect of the Tethyan passive margin. In this chapter, we have modelled the incorporation of the External Massifs into the Alpine thrust wedge by increasing the surface slope angle of the wedge, representing an increase in critical taper. The increase in surface slope angle causes an increase in sedimentation rates as governed by the diffusion law. But it is important to recognise that the relatively high density of the External Massifs compared to the bulk of the thrust wedge would counteract the need for increasing the surface slope and may even cause a decrease in slope. The lack of necessity to increase the slope is due to a greater degree of isostatic adjustment in the rear of the

wedge resulting in an increase in the dip of the basal decollement, which, because critical taper is preserved, may reduce the topographic slope correspondingly (Davis et al, 1983). Therefore, we have to recognise that the modelling of the thrust wedge in terms of a single density, with slope angle reflecting alterations in the kinematics of the orogenic wedge is again simplistic.

It is hoped that this discussion has placed the modelling into perspective in terms of the complex interaction of orogenic wedges and their associated foreland basins. We must recognise this as a preliminary investigation and not an unique solution.

CONCLUSIONS

1) The stratigraphy of the NAFB is divided into two shallowing- and coarsening-up megasequences, separated by a major unconformity (base Burdigalian, approx. 22Ma).

2) The Alpine thrust wedge of eastern Switzerland has been sequentially restored (Pfiffner, 1986). The restoration shows an initial period of rapid thrust wedge advance northward over the European plate from 40Ma to approximately 22Ma. At approx. 22Ma there was a slowing down and thickening of the thrust wedge during underplating of the External Massifs.

3) The effective elastic thickness of the continental lithosphere that best fits the observed basement configuration flanking the 17Ma load approximates 10+-5km. This value is within the range of determinations obtained by Royden (1987) for the Appenines, but is significantly less than estimates from the Appalachians and Ganges basins (e.g. Jordan, 1981; Karner and Watts, 1983).

4) We consider the development of foreland basins in terms of four parameters: 1) effective

elastic thickness of the foreland plate (Te); 2) The rate at which sediment is eroded from the thrust wedge and deposited in the basin, described using a transport coefficient (K) and governed by a diffusion law; 3) the rate of advance of the thrust wedge; 4) the surface slope angle of the thrust wedge.

5) The NAFB stratigraphy was simulated by varying the parameters that describe the evolution of the thrust wedge and by keeping the values of Te and K constant at 7.5km and 800m^2/yr respectively. Basin widths for megasequence A were simulated using the values of Te and K described above, with a time averaged thrust advance rate of 4mm/yr, and a slope angle of 1.5°

6) The geometry of the base Burdigalian unconformity is reproduced by a change in the parameters describing the thrust wedge in an attempt to simulate the underplating of the External Massifs. This is achieved by halting the thrust advance rate to zero, and increasing the surface slope angle from 1.5° to 4° over a period of 1.5Myr.

7) The renewed stratigraphic onlap of megasequence B is achieved by renewing the advance of the thrust wedge from zero to 2mm/yr, and by keeping all other parameters the same.

8) The base Burdigalian unconformity separating the two megasequences of the NAFB can be simulated by geologically acceptable modifications in the geometry of the thrust load moving over a linear elastic plate. This unconformity is reproduced without recourse to eustasy or anelastic behaviour of the continental lithosphere following loading.

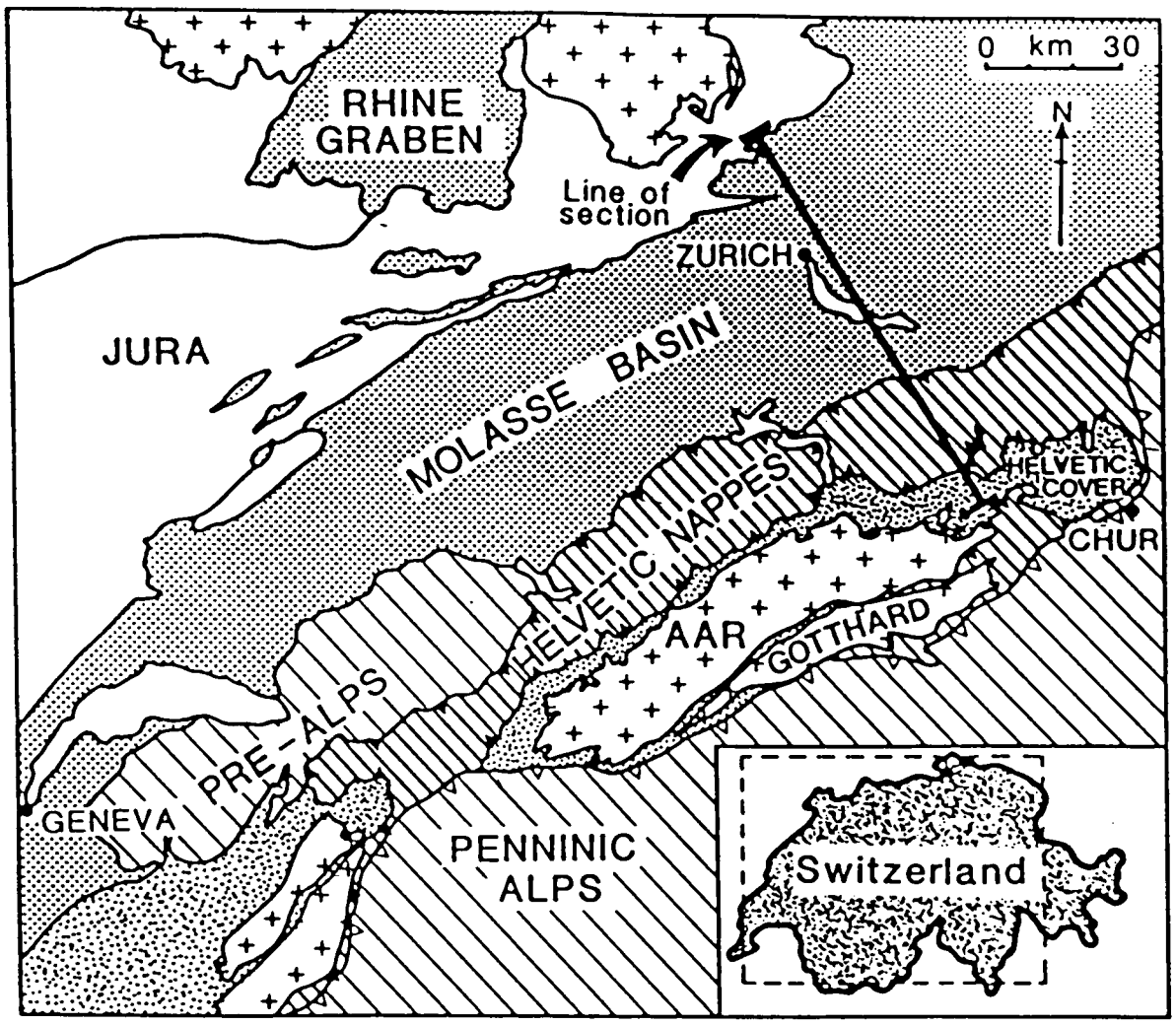

Fig.6.1. Simple tectonic map of northern Swiss Alps. Section of study through the North Alpine Foreland Basin (NAFB) is located.

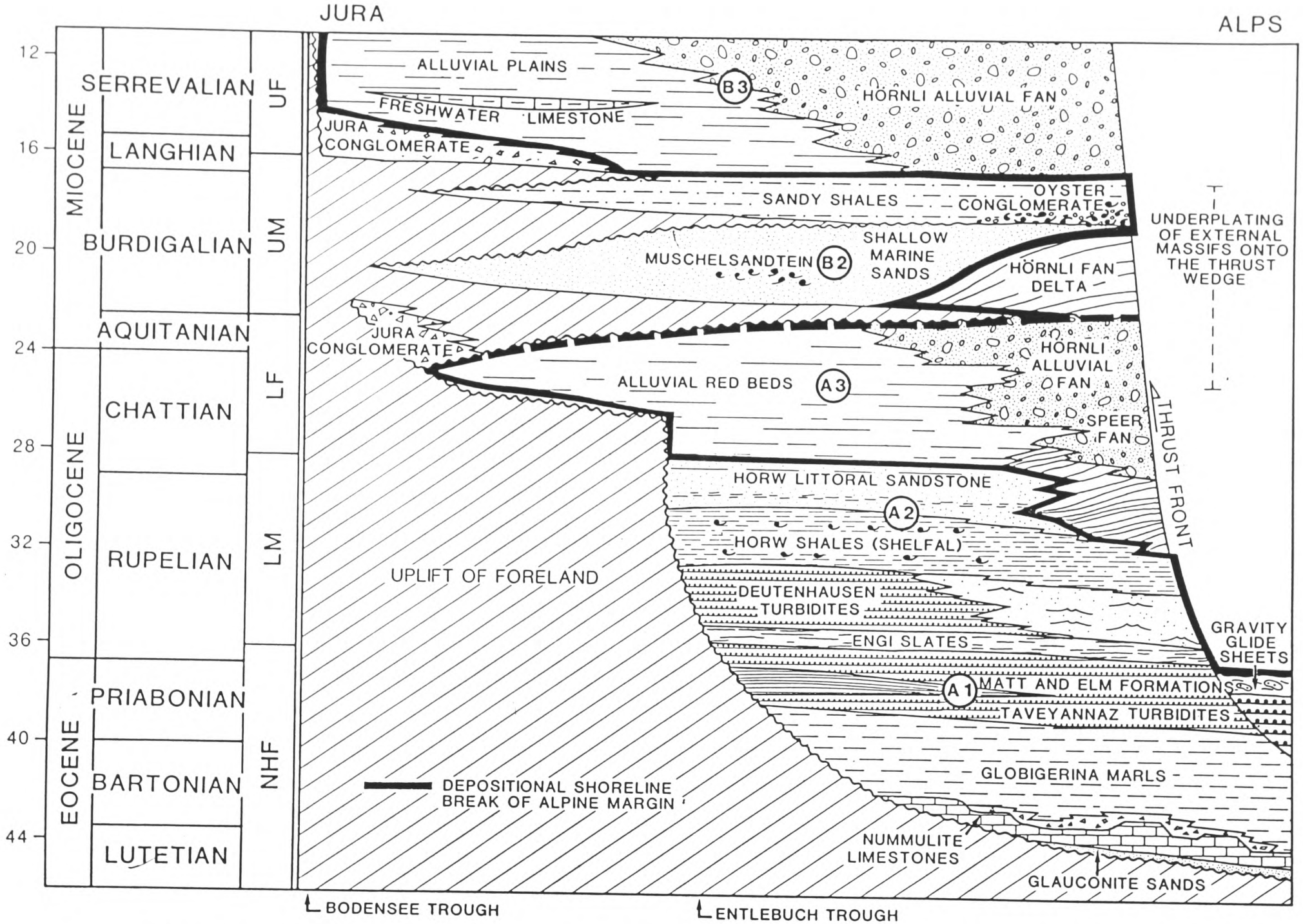

Fig.6.2. Chronostratigraphic (Wheeler) diagram of the NAFB. The stratigraphy is divided into two shallowing and coarsening upward megasequences (A and B) separated by the base Burdigalian (approx. 22Ma) unconformity. The approximate timing of the underplating of the External Massifs correlates to the megasequence boundary.

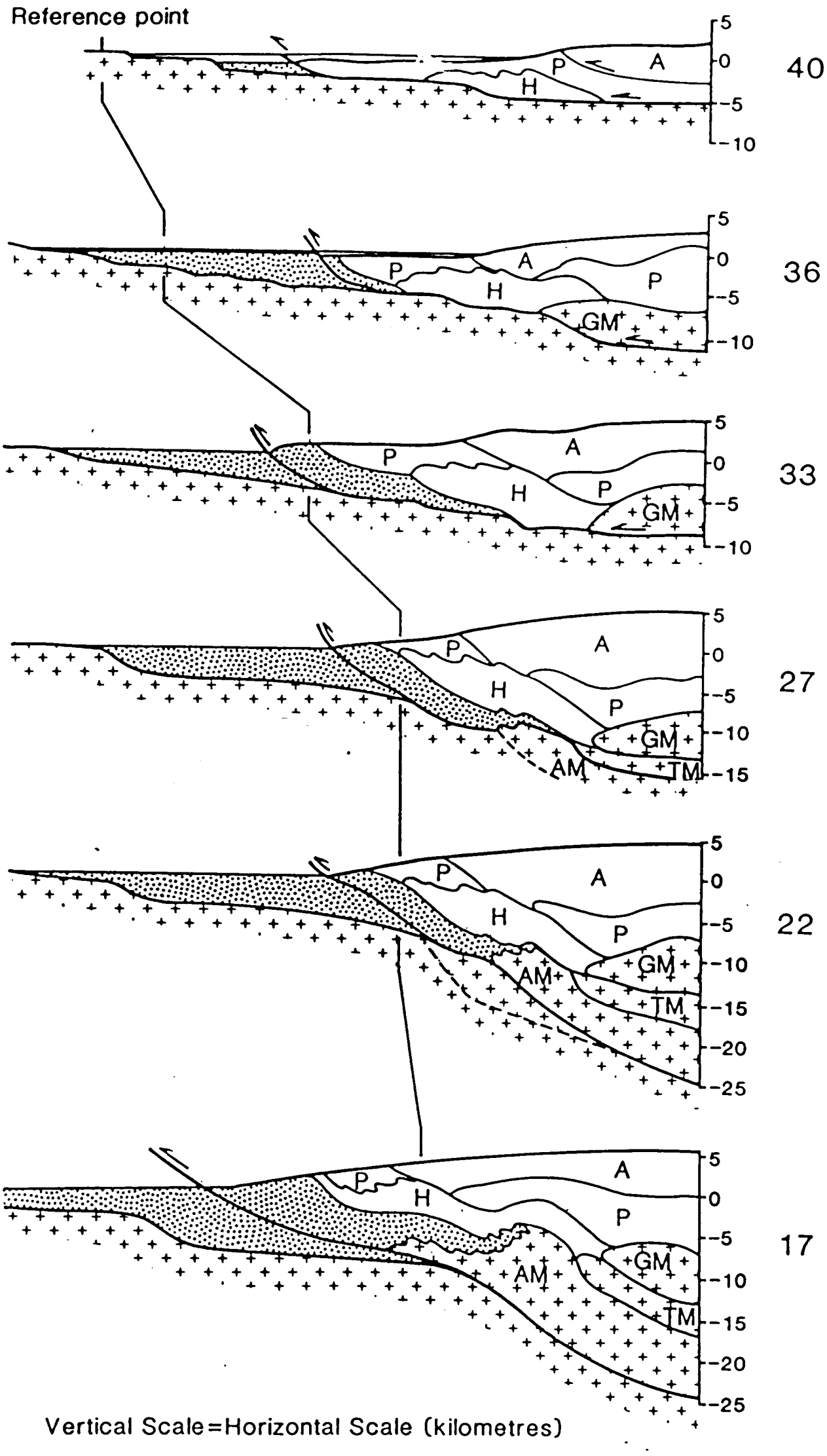

Fig.6.3. Sequential restoration of the Alpine thrust wedge of eastern Switzerland, based on Pfiffner (1986). This demonstrates an initial period of rapid wedge advance (4mm/yr), followed by thickening of the wedge by underplating of the External Massifs associated with a slowing of the thrust advance rate. H - Helvetic nappes, P - Penninic nappes, A - Austroalpine nappes, GM - Gotthard Massif, TM - Tavetsch Massif, AM - Aar Massif.

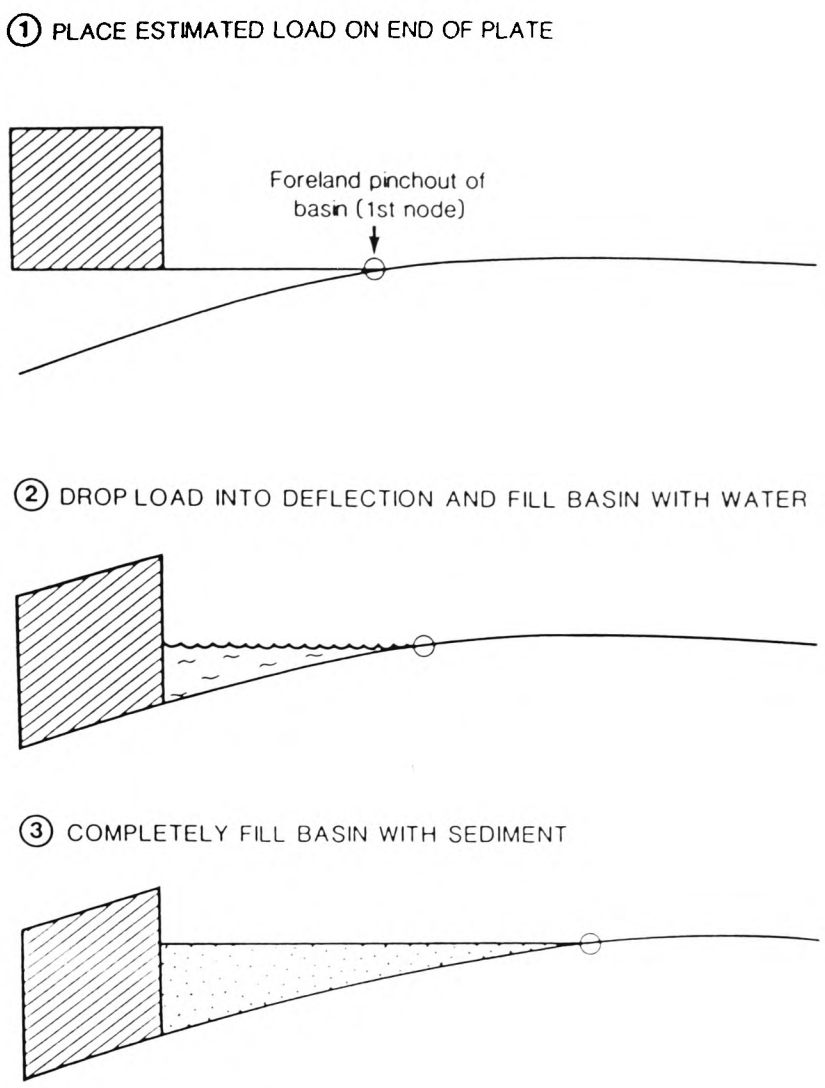

Fig.6.4. Methodology for simple model of end loading a plate to evaluate effective elastic thickness (fig.6.5).

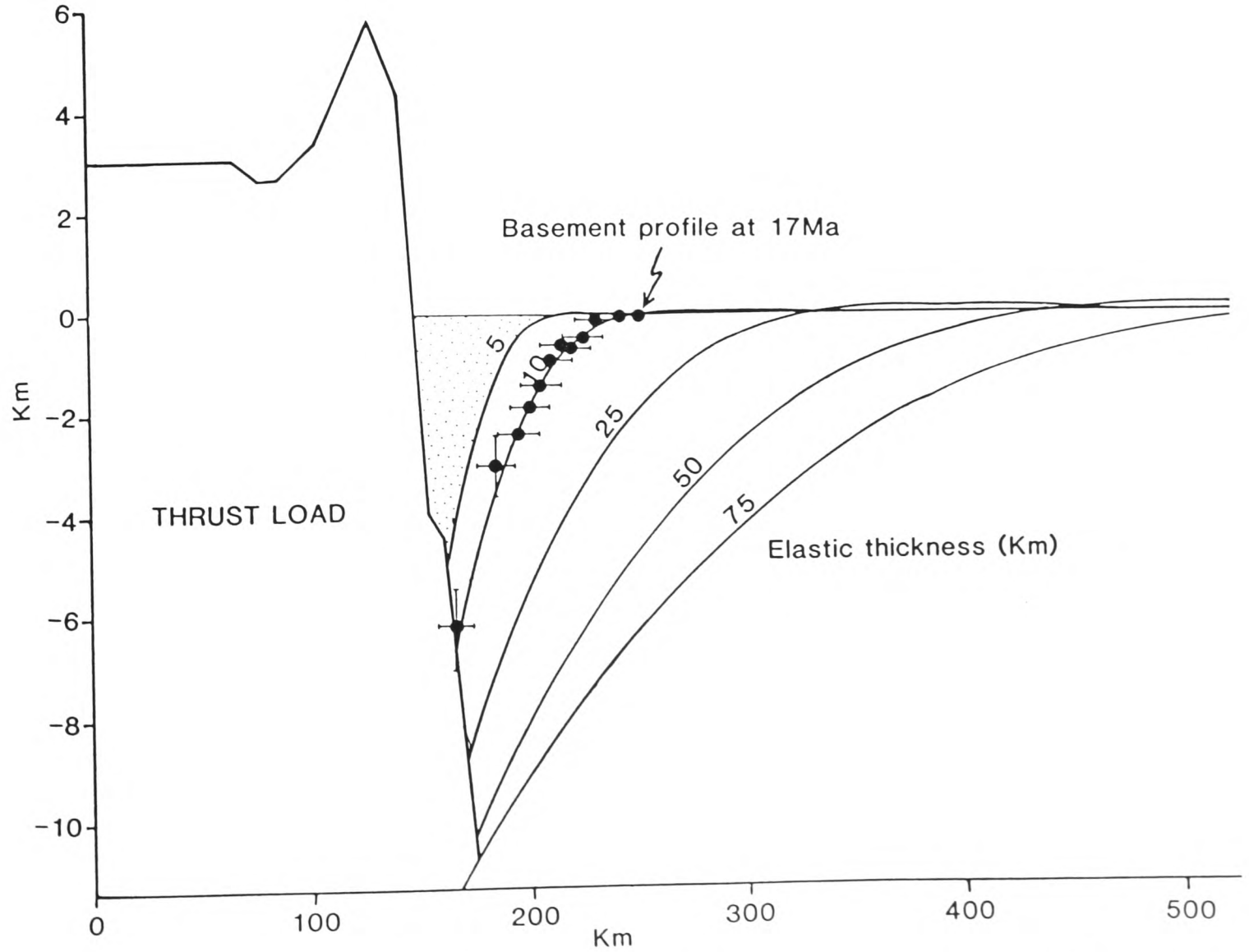

Fig.6.5. Estimation of the effective elastic thickness (Te) of the European foreland plate based on the basement configuration at 17Ma. The observed curvature approximates to a Te of 10+-5km.

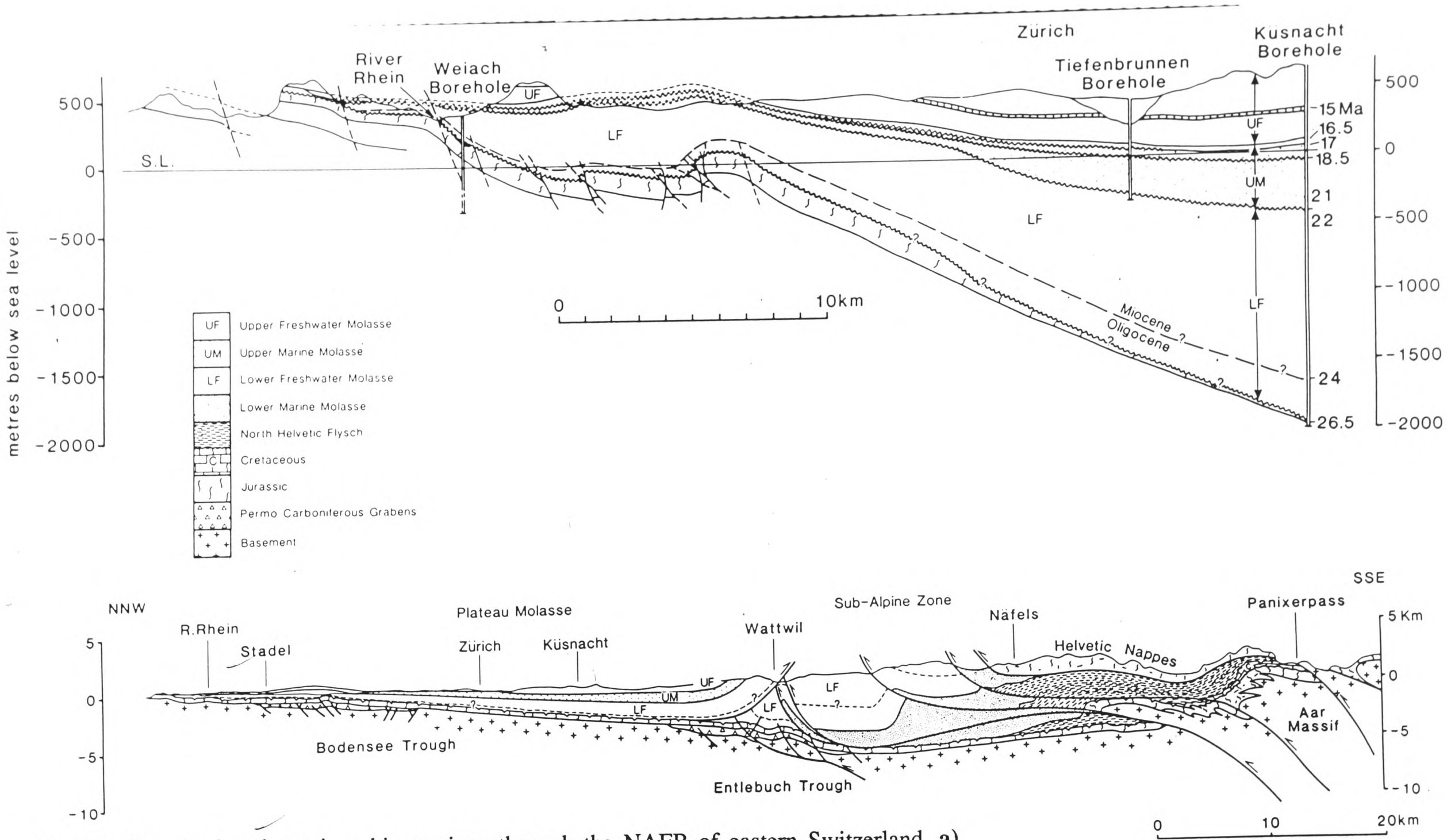

Fig.6.6. Structural and stratigraphic sections through the NAFB of eastern Switzerland. **a).** Detail of outer margin of NAFB,showing position of unconformities. **b).** General cross-section showing main structural features of NAFB. Note the locations of the Permo-Carboniferous grabens in the basement relative to the pinchouts in stratgraphy.

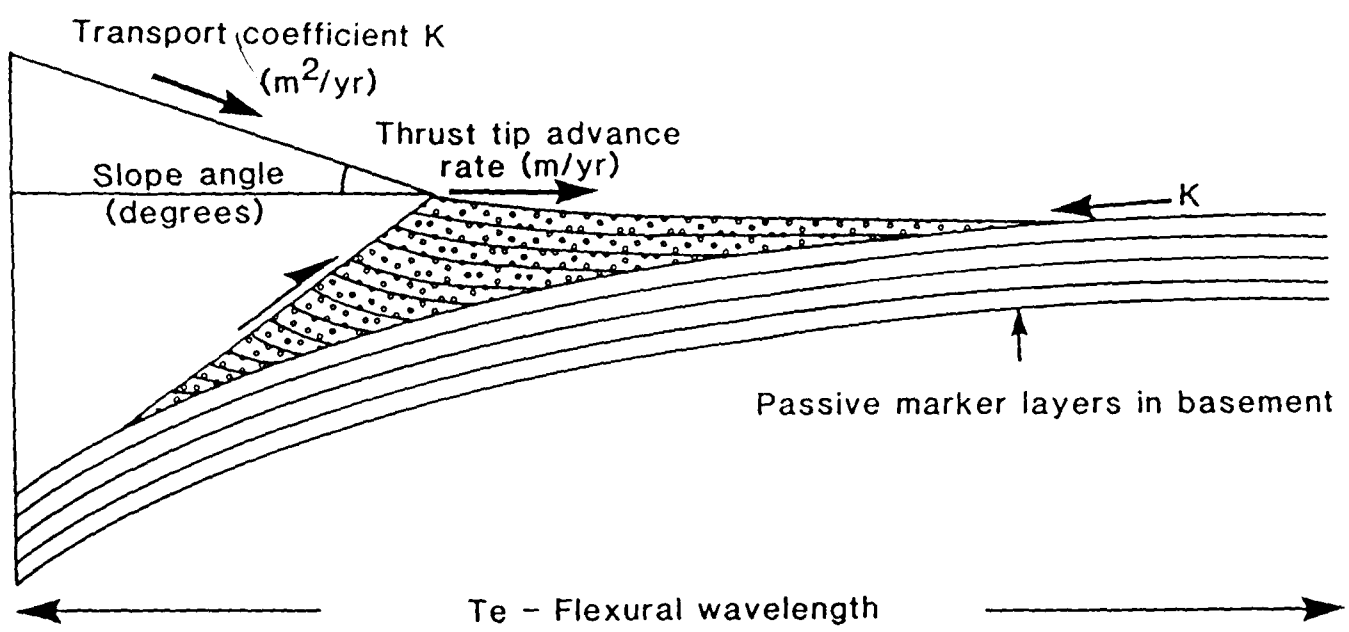

Fig.6.7. Representation of the four parameters used in the modelling to simulate the thrust wedge/foreland basin system.

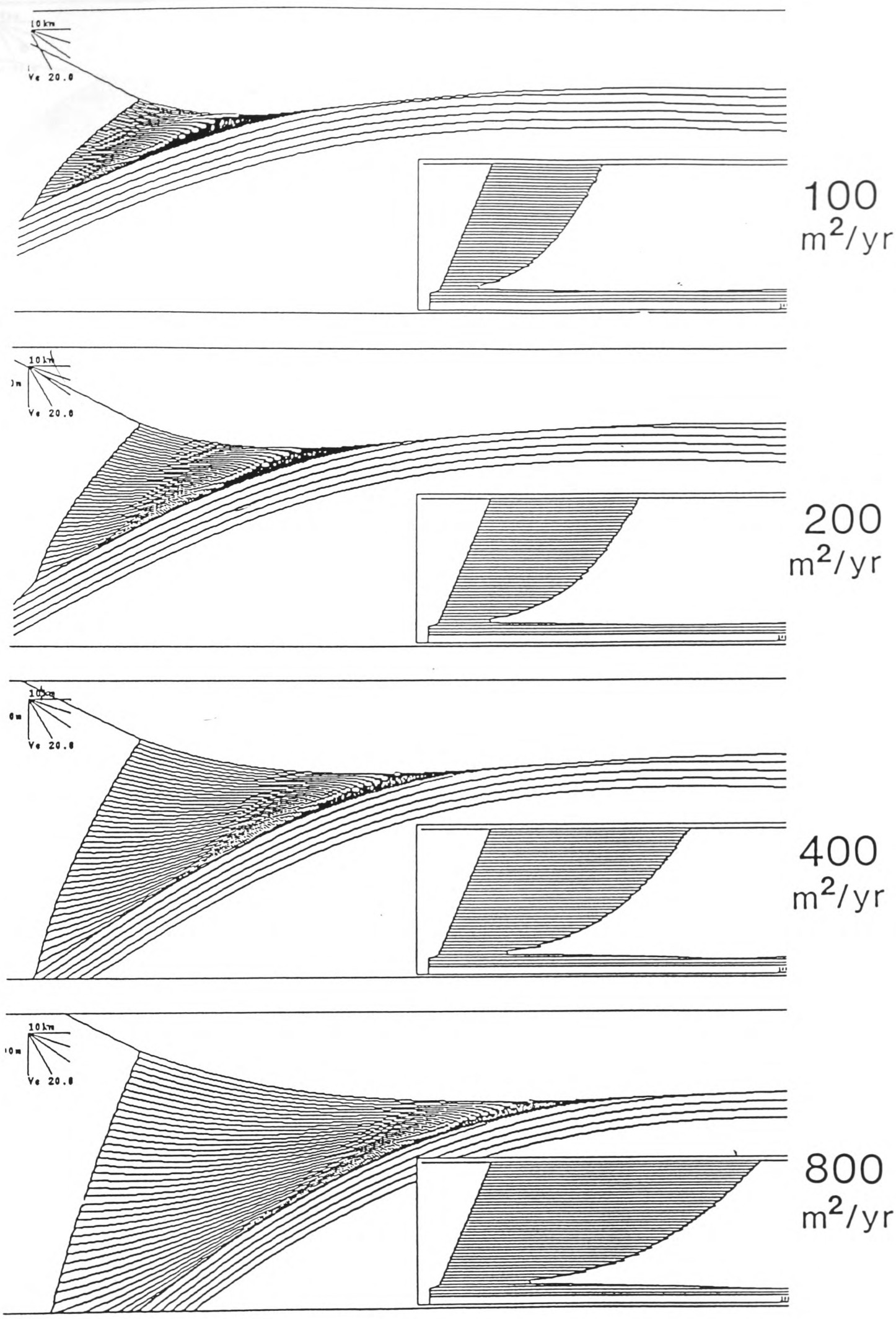

Fig.6.8. Influence of varying transport coefficient (K) while holding all other parameters constant. Increasing the value of K causes a broadening and deepening of the basin.

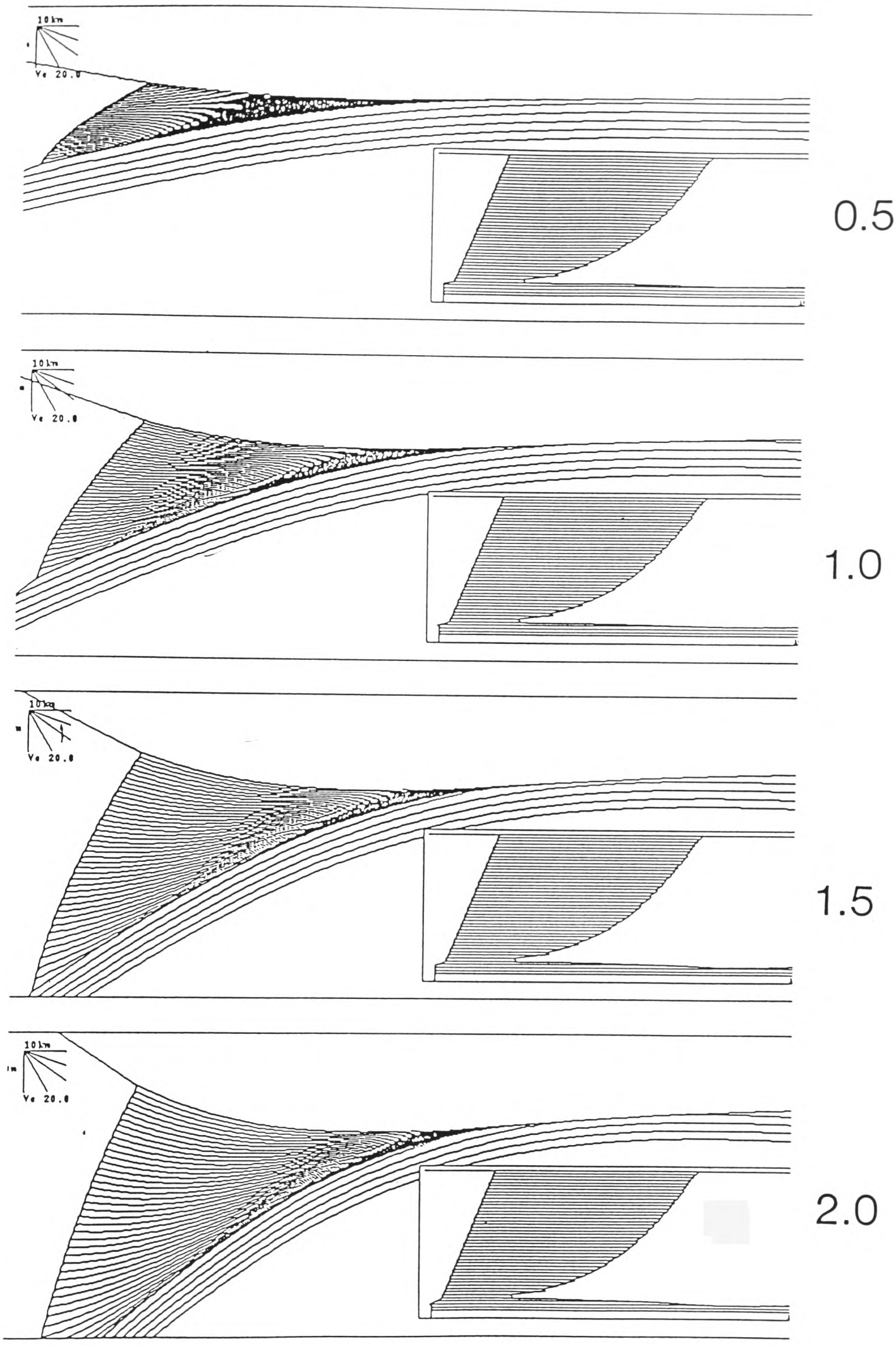

Fig.6.9. The influence of varying the surface slope angle of the wedge while keeping all other parameters constant. Increasing slope angle results in a deeper basin, but keeps a constant basin width.

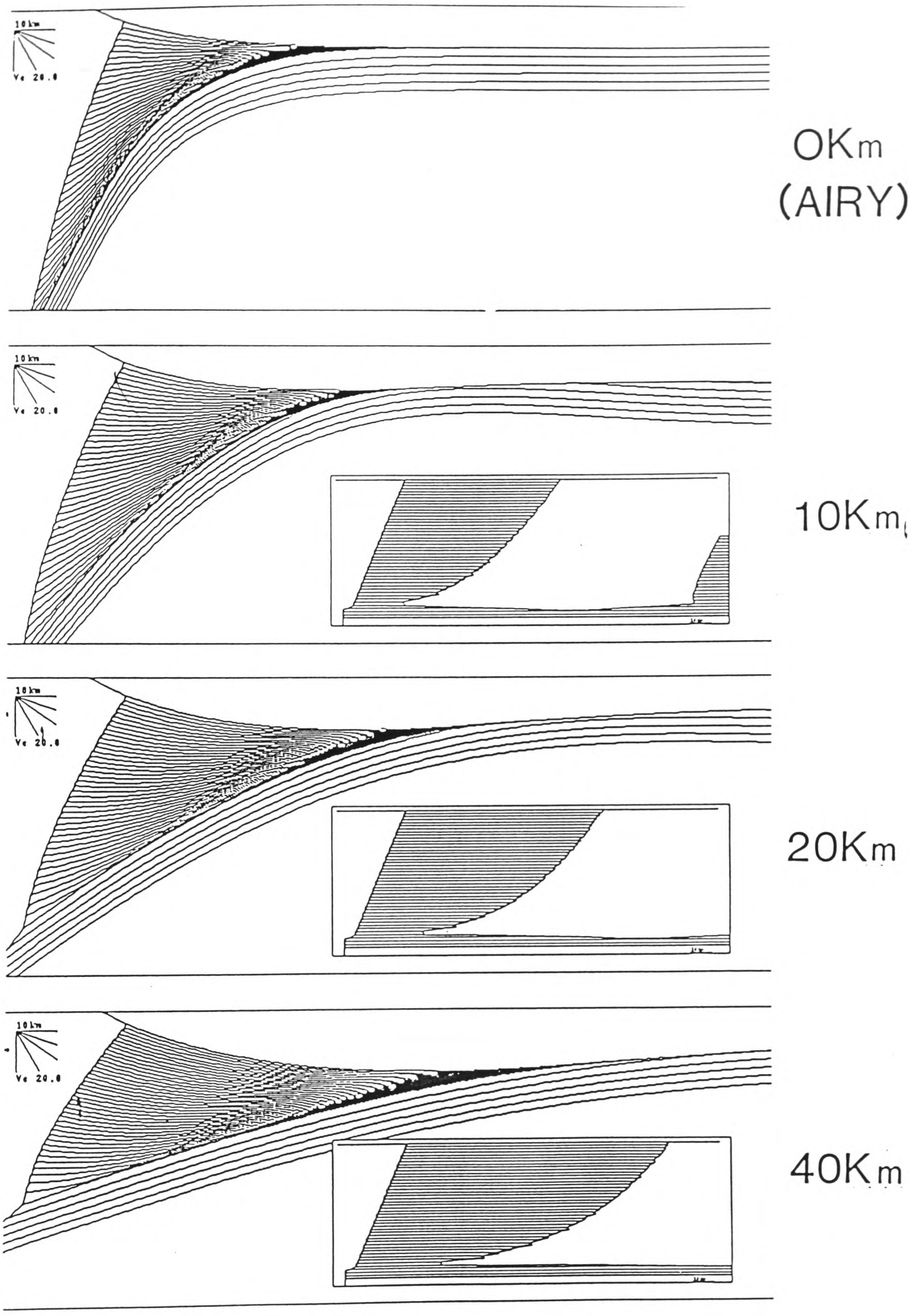

Fig.6.10. Influence of varying the effective elastic thickness (Te) while keeping all other parameters constant. This demonstrates a broadening and shallowing of the basin with increasing values of Te.

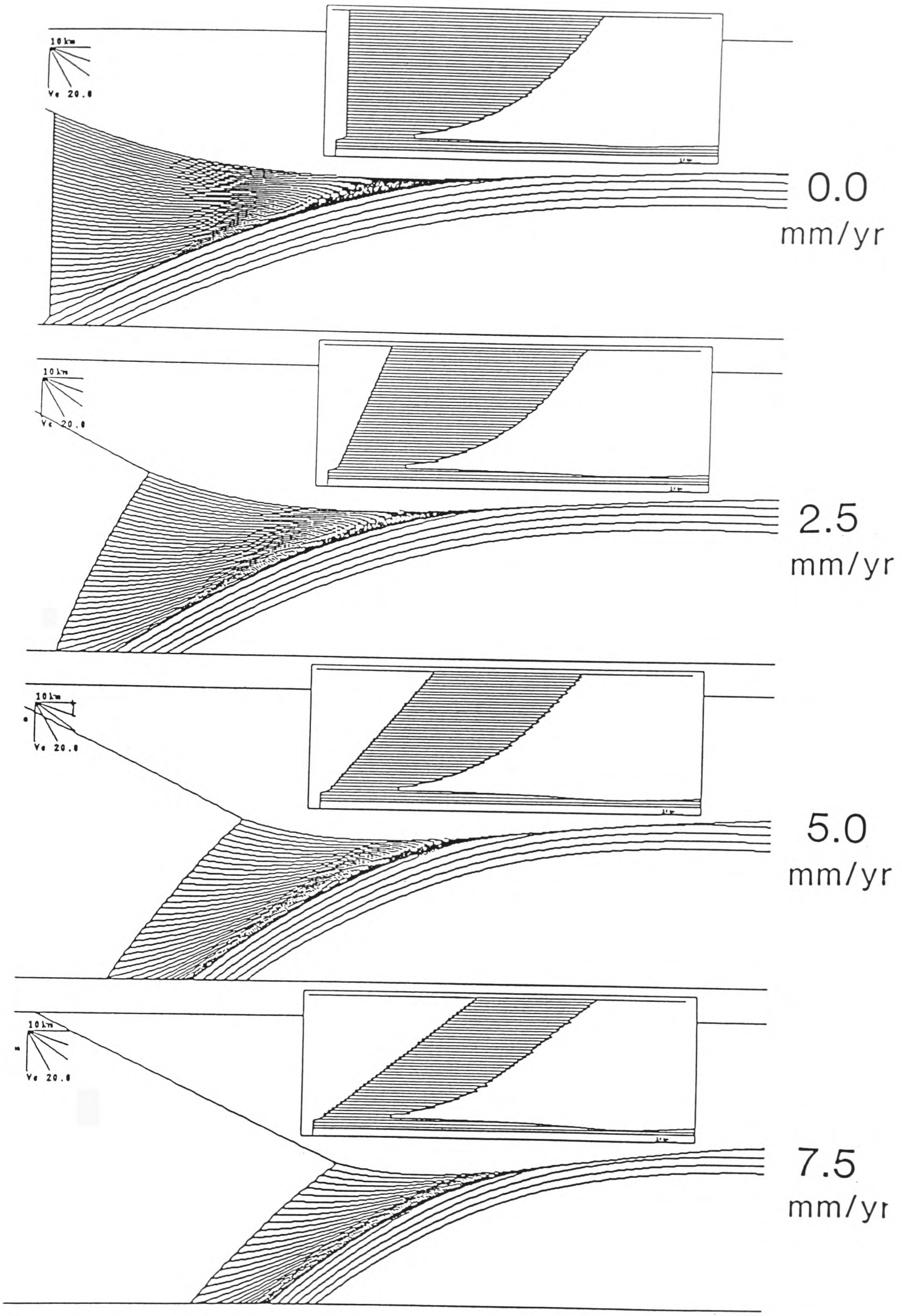

Fig.6.11. The influence of varying the thrust advance rate while holding all other parameters constant. Increasing the slope angle results in a nardrowing and underfilling of the basin.

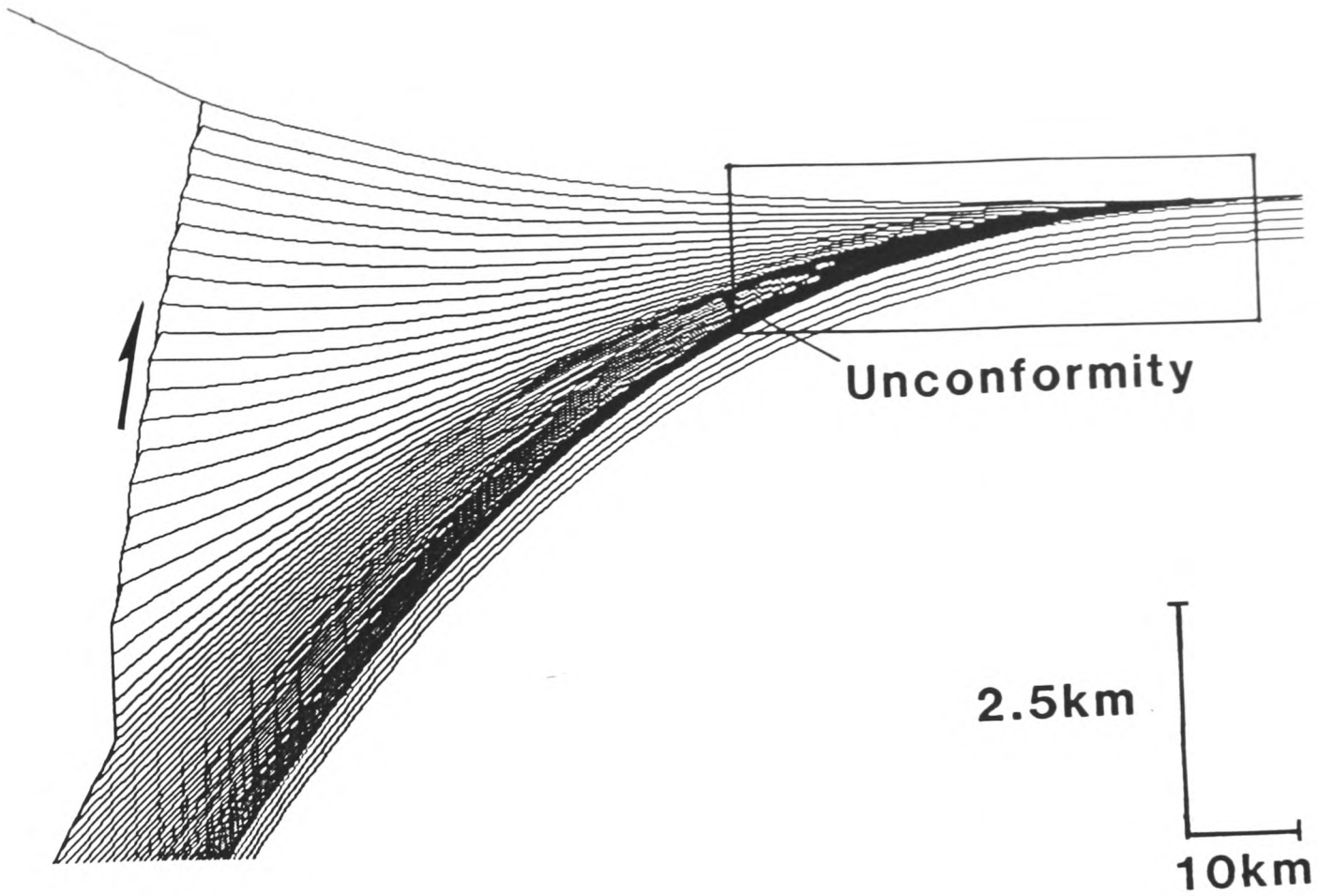

Fig.6.12a. Cross-section of the simulated model of the NAFB. Each stratigraphic unit represents 250,000yrs. The model was started with a thrust advance rate of 4mm/yr, and a surface slope angle of 1.5 degrees. After 15Ma, the thrust advance rate was halted to zero, and the slope angle was increased to 4 degrees over 1.5Ma. This simulated the underplating of the external massifs onto the base of the Alpine thrust wedge, and resulted in the formation of the base Burdigalian unconformity. The wedge was then allowed to continue at 2mm/yr, with all other constants held constant. Throughout the run, Te = 7.5km, and K = 800m^2/yr.

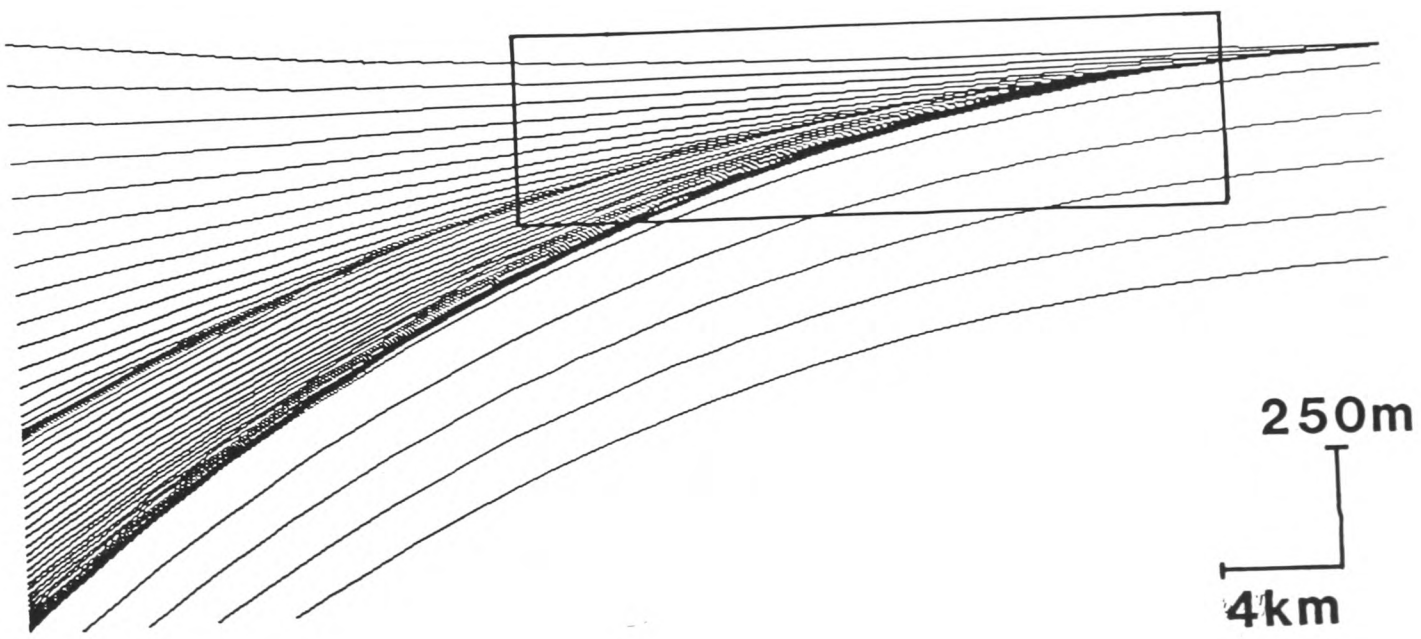

Fig.6.12b. Close-up of simulated unconformity from fig.6.12a. This shows truncation of the underlying stratigraphy, and a basinward shift in stratigraphic onlap in the overlying sequence.

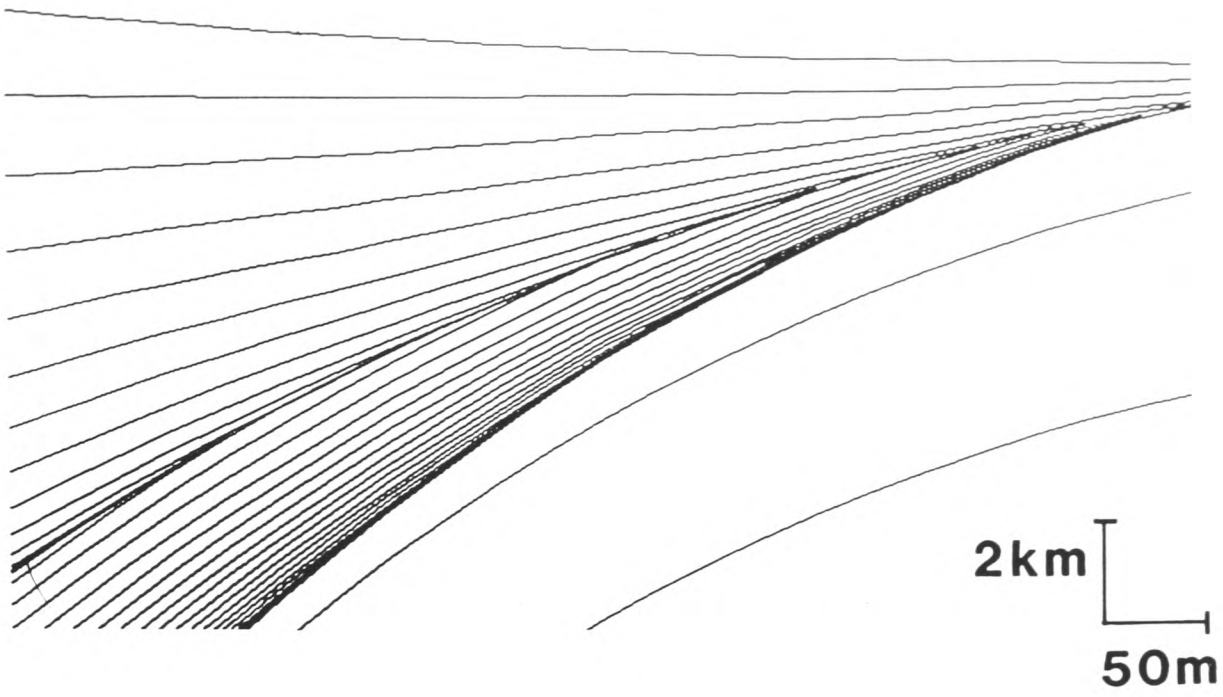

Fig.6.12c. Close-up of Fig.6.12b.

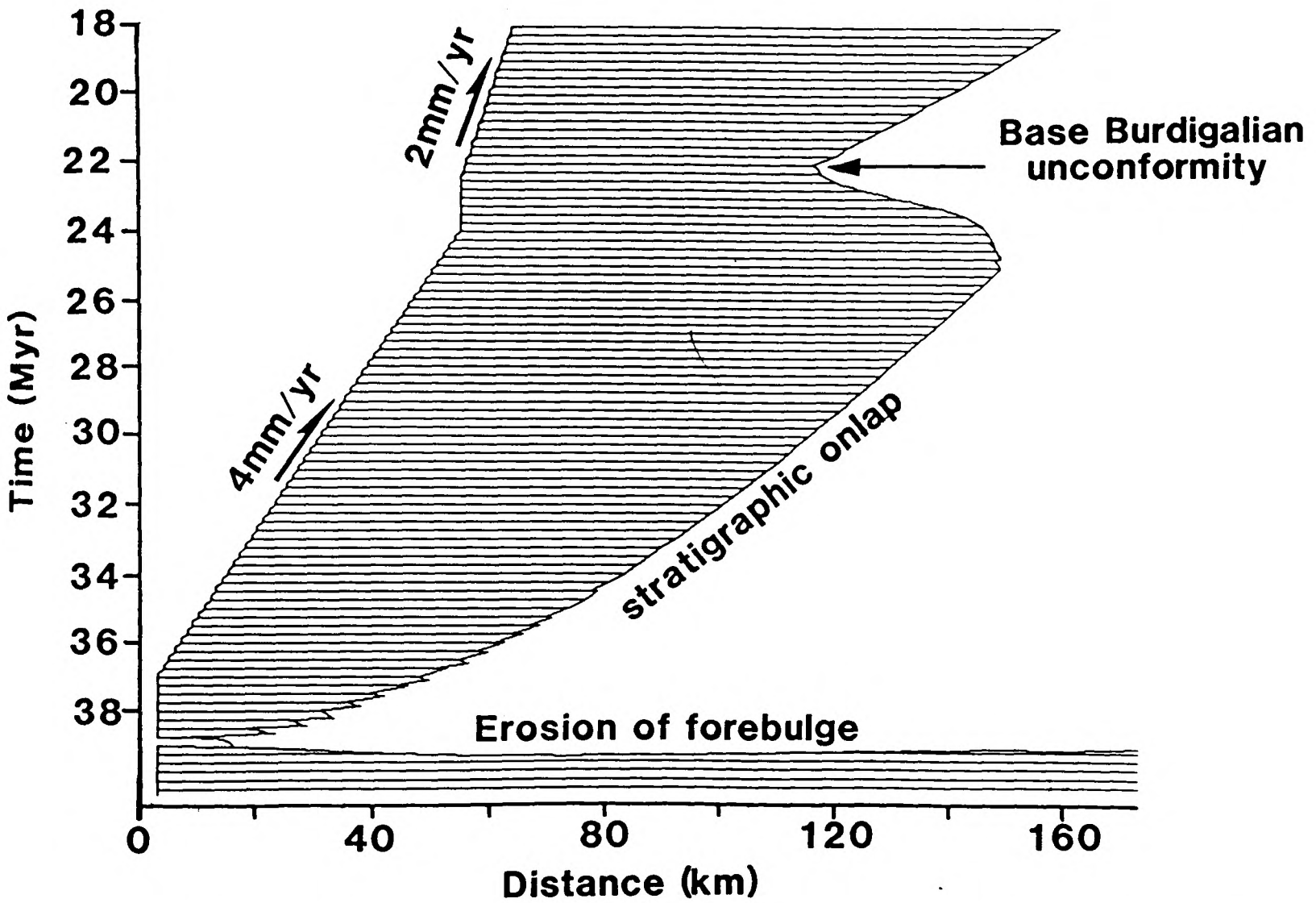

Fig.6.13. Chronostratigraphic (Wheeler) diagram of the simulation in fig.6.12a. This demonstrates initial steady onlap of the lower megasequence, with onlap outpacing thrust advance, resulting in a broadening of the basin. At 24Ma, the halting and thickening of the thrust wedge causes backtilting of the basin and truncation of the underlying stratigraphy simulating the base Burdigalian unconformity.

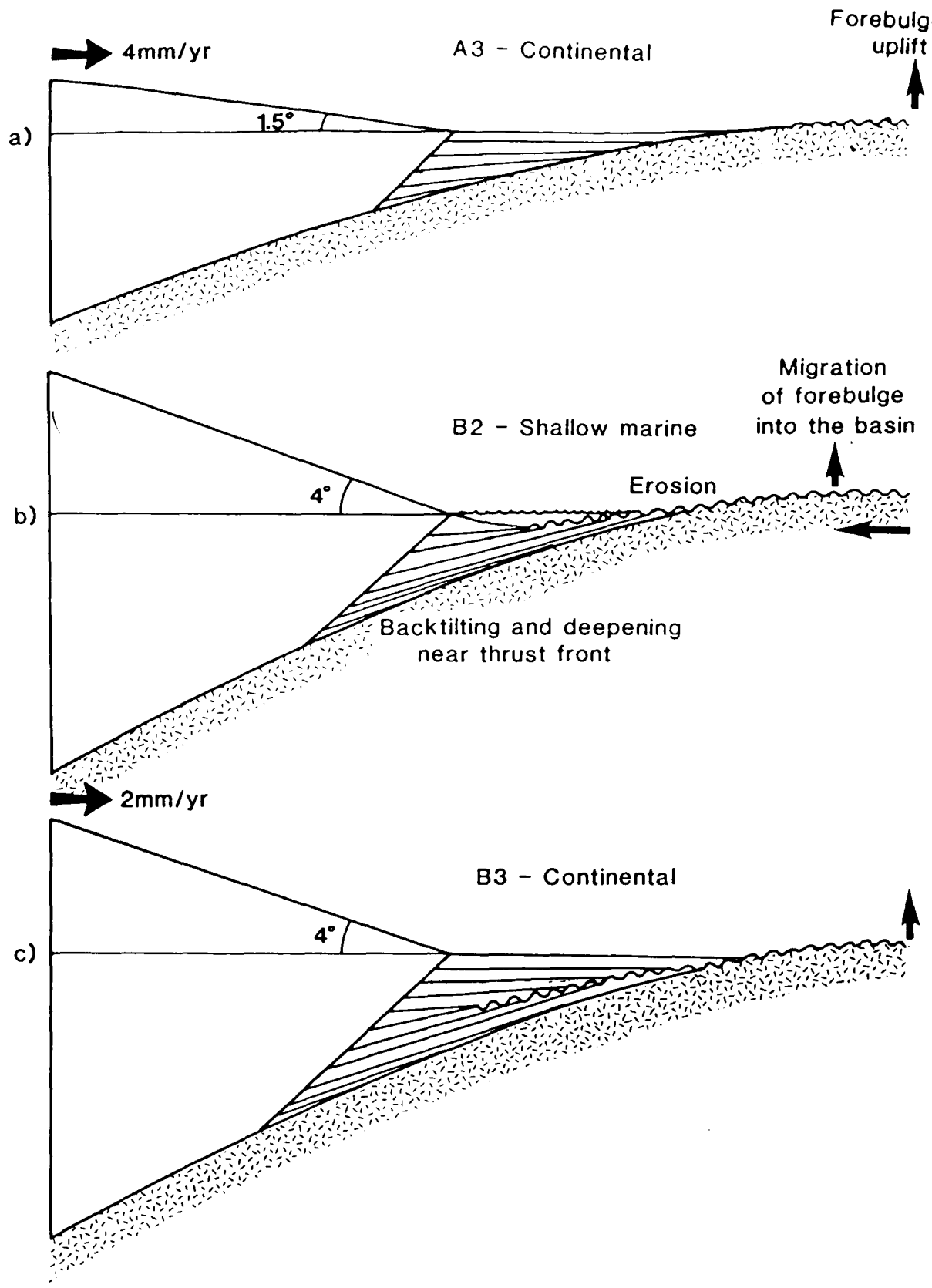

Fig.6.14. Schematic diagram to show the mechanism by which the simulated stratigraphy in Figures 6.12 and 6.13 was reproduced. **(a)** Rapid advance of a low angle thrust wedge, and the deposition of the lower megasequence. **(b)** Thickening and slowing down of the thrust wedge causes migration of the forebulge into the basin, with uplift and erosion of the underlying sequence. Sedimentation is confined near the thrust front, resulting in a basinward shift in stratigraphic onlap. Backtilting of the basin also causes increased subsidence near the thrust front, resulting in marine sedimentation. **(c)** Renewed advance of the wedge, keeping the slope angle constant results in filling of the basin, returning to continental deposition and steady stratigraphic onlap over the foreland.

REFERENCES

Allen, J.R.L., 1982, Sedimentary Structures: their character and physical basis.Developments in sedimentology, 30 B, Elsevier, Amsterdam.

Allen, P.A., Mange-Rajetzky, M., Matter, A., Homewood, P., 1985, Dynamic Palaeogeography of the Open Burdigalian Seaway, Swiss Molasse Basin. - Eclog. Geol. Helv. 78(2), 351-381.

Anders, M.H., Kruger, S.W., Sadler, P.M., 1987, A New Look at sedimentation rates and the completeness of the stratigraphic record. - J. Geol., 95, 1-14.

Apps, G., 1987, Evolution of the Grès D'Annot basin, SW Alps. Unpublished PhD thesis, University of Liverpool.

Bachmann, G.H., Muller, M., Weggen, K., 1987, Evolution of the Molasse Basin (Germany, Switzerland). - Tectonophysics, 137, 77-92.

Bagnold, R.A., 1962, Auto-suspension of transported sediment; turbidity currents. Proc. R. Soc. Lon., ser A., 265, 315-319.

Beaumont, C., 1978, The evolution of sedimentary basins on a visco-elastic lithosphere: theory and examples. Geophys. J. R.Astr. Soc. 55, 471-497.

Beaumont, C., 1981, Foreland Basins. - Geophys. J. R. Astr. Soc., 65, 291-329.

Beaumont, C., Quinlan, G., Hamilton, J., 1988, Orogeny and Stratigraphy: Numerical models of the Palaeozoic in the Eastern Interior of North America. -Tectonics, 7, 389-416.

Berger, J-P., 1985, La Transgression de la Molasse Marine Superièure (OMM) a Suisse Occidentale. - Munchner Geowissenschaftliche Abhandlungen: Riehe A, Geologie und Palaontologie; 5. Verlag Friedrich Pfeil, Munchen.

Bertrand, M., 1884, Rapports de structure des Alpes de Glaris et du bassin Houillier du Nord. Bull. Soc. Geol. France 12 p.318-330.

Bouma, A.H., 1962, Sedimentology of some flysch deposits: a graphic approach to Facies Interpretation. Elsevier, Amsterdam,168pp.

Boyer, S.E., Geiser, P.A., 1987, Sequential development of thrust belts: Implications for mechanics and cross-section balancing. - GSA abstracts with Programmes, p.597.

Büch, L.von, 1819, Uber die gebirgszuge der Alpes zwischen Glaris und Chiavenna. Leonards Taschenbuch 4.

Buchi, U.P., Schlanke, S., 1977, Zur Palaogeographie der Schweizerischen Molasse. - Erdol-Erdgas Z., 93 (Spec. Issue), 51-69.

Burke, E., Dewey, J.F., 1973, Plume generated triple junctions: Key indicators in applying plate tectonics to old rocks. J. Geol. Chicago, 81, 406-433.

Carson, M.A., Kirkby, M.J., 1972, Hillslope Form and Processes. - Cambridge University Press, 475p..

Chapple, W.M., 1978, Mechanics of thin-skinned fold and thrust belts. - Geol. Soc. Am. Bull., 89, 1189-1198.

Coakley, B.J., Watts, A.B., 1987, Flexural control of sedimentation in the vicinity of the Barrow Arch, Northern Alaska. - EOS, 68, 420.

Coakley, B.J., Watts, A.B., in press, Tectonic controls on the origin of unconformities, North Slope Alaska. - Tectonics.

Coleman, J.M., Prior, D.B., Lindsay, J.F., 1983, Deltaic influences on shelf-edge instability processes. SEPM Spec. publ. 33, 121-137.

Covey, M., 1986, The Evolution of Foreland Basins steady state: Evidence from the Western Taiwan Foreland Basin. - In: Foreland Basins. Spec. Publ. Int. Ass. Sediment., 8, 77-90. Eds. Allen, P.A., Homewood, P..

Cowan, D.S., 1982, Deformation of partly dewatered and consolidated Franciscan sediments near Piedras Blancas point, California. In: Leggett, J.K., (Ed), Trench-Forearc Geology:

Geol. Soc. Lon. Spec. Publ. 10, 439-457.

Cowan, D.S., 1985, Structural Styles in Mesozoic and Cenozoic Melanges in the Western Cordillera of North America. Geol. Soc. Am. Bull., 96, 451-462.

Davis, D., Suppe, J., Dahlen, F.A., 1983, Mechanics of fold and thrust belts and accretionary wedges. - J. Geophys. Res., 88, 1153-1172.

Diem, B., 1985, Analytical method for estimating palaeowave, climate and water depth from wave ripple marks. - Sedimentology, 32, 705-720.

Diem, B., 1986, Die Untere Meeresmolasse zwischen der Saane (Westschweiz) und der Ammer (Oberbayern). - Eclog. Geol. Helv. 79(2), 493-559.

Eckert, H.R., 1963, Die Obereozanen Gloigerinenschiefer (Stad und Schimbergschiefer) zwischen Pilatus und Schrattenfluh. Eclog. Geol. Helv. 56/2, 1001-1072.

Escher, (von der Linth), A., 1841, Geologische Karte des Cantons Glarus und Seiner Umgebungen, nebst profilen. Verh. Schweiz. natf. Ges. Zurich.

Escher, (von der Linth), A., 1846, Gebirgskunde. In: Heer, O., Blumer-Heer, J.J., (Eds.) Der Canton Glarus (Bd.7), Gemalde der Schweiz. - Huber, St Gallen, Bern.

Escher, H.C. 1809, Geognotische Beschriebung des Linthals. Leonhards Taschenbuch 3.

Flemings, P.B., Jordan, T.E., 1987, Synthetic Stratigraphy of Foreland Basins. - EOS, 68, 419.

Flemings, P.B., Jordan, T.E., 1989, A synthetic stratigraphic model of Foreland Basin development. - J. Geophys. Res., 94, 3851-3866.

Frey, M., Hunziker, J.C., Frank, W., Bocquet, J., Dal Piaz, G.V., Jager, E., Niggli, E., 1974, Alpine metamorphism of the Alps: a review. Schweiz Min. Pet. Mitt., 54, 247-290.

Frey, M., 1978, Progressive low grade metamorphism of a black shale formation, Central Swiss Alps, with special reference to pyrophyllite and margarite bearing assemblages. - J. Petrol., 19, 93-135.

Funk, H.P., 1985, Mesozoische subsidenzegeschichte im Helvetischen Schelf der Oostschweiz. Eclog. Geol. Helv. 78, 249-272.

Ghibaudo, G., 1980, Deep-sea fan deposits in the Macigno Formation (Middle/Upper Oligocene) of the Gordana valley, Northern Appennines, Italy. J. Sed. Pet. 50, 723-742.

Groshong, R., Pfiffner, O.A., Pringle, L.R., 1984, Strain partitioning in the Helvetic thrust belt of E. Switzerland from the leading edge to the internal zone. J.Struc.Geol. 6 p.5-18.

Heim, Alb., 1878, Untersuchungen uber den Mechanisms der Gebirgsbildung im Anschluss an die Geologische Monographie der Todi-Windgallen-Gruppe. Schwabe Basel.

Heim, Arn., 1908, Die Nummuliten und Flyschbildungen der Schweizeralpen-Versuch einer Revision der Alpinen Eocaen Stratigraphie. Abh. Schweiz. pal. Ges.,35.

Herb, R., 1988, Eocene palaogeographie und palaotektonik des Helveticums. - Eclog. Geol. Helv., 81(3), 611-657.

Hirano, M., 1976, Mathematical Model and the concept of equilibrium in connection with slope shear ratio, Quantitative Slope Models. (Ed. F. Ahnert), Z. Geomorphol., suppl., 25, 50-71.

Hiscott, R.N., 1981, Deep-sea fan deposits in the Macigno Formation (Middle/Upper Oligocene) of the Gordana Valley, Northern Appennines, Italy - Discussion. J.Sed.Pet. 51(3), 1015-1033.

Hiscott, R.N., Middleton, G.V., 1979, Depositional mechanics of thick bedded sandstones at the base of a sub-marine slope, Tourelle Formation, (Lower Ordovician). Quebec. Can. Soc. Econ. Palaeon. Min. Spec. Pub. 27, 307-326.

Hiscott, R., Pickering, K., Beeden, D., 1986, Progressive filling of a confined middle Ordovician Foreland Basin associated with the Taconic Orogeny, Quebec,Canada.

Homewood, P., Allen, P.A., Williams, G.D., 1986, Dynamics of the Molasse basin, W. Switzerland. Allen, P.A., Homewood, P.,(Eds.), Foreland Basins, I.A.S. Spec. publ. 8,

p.199-217.

Homewood, P., Allen, P.A., 1981, Wave-,tide- and current controlled sandbodies of Miocene molasse, western Switzerland. - Bull. Amer. Ass. Petr. Geol., 65, 2534-2545.

Hsu, K.J., 1969, Thin-skinned plate tectonics during Neo-alpine orogenesis. - Amer. J. Sci., 279, 353-366.

Hunziker, J.C., Frey, M., Clauer, N., Dallmeyer, R.D., Freidrichsen, H., Roggwiler, P., Schwander, H., 1986, The evolution of illite to muscovite: mineralogical and isotopic data from the Glarus Alps, Switzerland. - Contr. Miner. Petrol. 92, 157-180.

Ingram, R.L., 1954, Terminology for the thickness of stratification and parting units in sedimentary rocks. Bull. Geol. Soc. Am. 65, 937-938.

Jacobi, R.D., 1981, Peripheral bulge - a causal mechanism for the Lower/Middle Ordovician unconformity along the western margin of the northern Appalachians. - EPSL, 56, 245-251.

Jordan, T.E., 1981, Thrust loads and foreland basin evolution, Cretaceous, western United States. - AAPG Bull., 65, 2506- 2520.

Karner, G.D., Watts, A.B., 1983, Gravity anomalies and flexure of the lithosphere at mountain ranges. - J. Geophys. Res., 88, 10449-10477.

Kenyon, P.M., Turcotte, D.L., 1985, Morphology of a delta prograding by bulk sediment transport, Geol. Soc. Am. Bull., 96, 1457-1465.

Kerkhove, C., 1969, La zone du flysch dans les nappes de l'Embrunais-Ubaye (Alpes Occidentales). Geologie Alpine, 45, 5-204.

Komar, P.D., Neudeck, R.H., Kulm, L.D., 1972, Observation and significance of deep water oscillatory ripple marks on the Oregon continental shelf. In: Shelf Sediment Transport: Process and Pattern. D.J.P. Swift, D.B. Duane, O.H. Pilkey (Eds). pp.601-609. Dowden, Hutchinson and Ross. Stroudsburg.

Kominz, M.A., Bond, G.C., 1986, Geophysical modelling of the geothermal history of foreland basins. Nature 320, 252-256.

Krüsi, H.R., 1977, Geologische, inbesondre strukturelle untersuchungen am Panixerpass (Gl-Gr)., Unveroff Diplomarb. ETH. Zurich.

Lateltin, O., 1988, Les depots turbiditiques oligocenes d'avant pays entre Annecy (Haute Savoie) et la Sanetsch (Suisse). -Thesis No. 949, University of Fribourg. p.127.

Lateltin, O., Muller, D., 1987, Evolution Palaeogeographique du Bassin des gres de Taveyannaz dans les Aravis (Haute Savoie) a la fin du Palaeogene. Eclog. geol. Helv.80(1), p.127-140.

Leupold, M., 1937, Zur stratigraphie der Flyschbildungen zwischen Linth und Rhein. Eclog. Geol. Helv.,30, p.1-23.

Leupold, M., 1942, Neue Beobachtungen zur Gleiderung der Flyschbildungen der Alpen zwischen Reuss und Rhein. Eclog. Geol. Helv. 35, p.247-291.

Lowe, D.R., 1976, Grain flow and grain flow deposits. J. Sediment. Petrol. 46, 188-199.

Lowe, D.R., 1982, Sediment gravity flows, II. Depositional models with special reference to the deposits of high density turbidity currents. J. Sedim. Petrol. 52, 279-297.

Lugeon, M., 1902, Les Grandes Nappes des recouvrement des Alpes du Chablais et de la Suisse. Bull. Soc. Geol. France.(4)1, p.723-825.

Lugeon, M., 1923, Sur l'age du Gres de Taveyannaz. Eclog. Geol.Helv. 18/2.

Lyon-Caen, H., Molnar, P., 1989, Constraints on the deep structure and dynamic processes beneath the Alps and adjacent regions from an analysis of gravity anomalies. -Geophys. J. in press.

Mange-Rajetzky, M.A., 1985, Unroofing of orogenic belts as evidenced by heavy minerals in their foreland sediments: An example from the Peri-alpine molasse. - International Synopsium on Foreland Basins, Fribourg, Switzerland, Sept. 1985. Programme and Abstracts, p.88.

Mayoraz, R., Loup, B., Homewood, P., Lateltin, O., 1988, Un Paleocanyon oligocene dans le parautochthone du Haut Val D'Illiez (Valais, Suisse), Eclog. Geol. Helv., 81, 539-551.

Matter, A., Momewood, P., Caron, C., van Stuijvenberg,J., Weidmann, M., Winkler, W., 1980, Flysch and molasse of western and central Switzerland. In: Geology of Switzerland, a guide book (Ed. R. Trumpy), pp.261-293. Schweiz.Geol.Komm.

Maltman, A., 1984, On the term "soft sediment deformation". J.Str. Geol., 6(5), 589-592.

McManus, J., Duck, R.W., 1987, Landslides formed by Internal waves in Scottish freshwater lochs, BSRG, Aberdeen, Abstr.p.93.

McNutt, M.K., Diament, M., Kogan, M.G., Variations of elastic plate thickness at continental thrust belts. - J. Geophys. Res., 93, 8825-8838.

Moore, J.C., Watkins, J.S., Shipley, T.H., McMillen, K.J., Bachman, S.B., Lundberg, N., 1982, Geology and Tectonic evolution of a juvenile accretionary terrain along a truncated convergent margin: Synthesis of results from Leg 66 of the Deep Sea Drilling Project, southern Mexico. Geol. Soc. Am. Bull. 93, 847-861.

Moore, G.F., Shipley, T.H., 1988, Mechanisms of sediment accretion in the Middle America Trench off Mexico. J. Geophys. Res., 93(B8), 8911-8927.

Moretti,I., Turcotte, D.L., A model for erosion, sedimentation and flexure with respect to New Caledonia. - J. Geodynamics, 3, 155-168.

Murchison, R., 1849, On the Geological Structure of the Alps, Appenines and Carpathians. Quart. J. Geol. Soc. Lon. 5, p.157-312.

Milnes, A.G., Pfiffner, O.A., 1977, Structural Developement of the Infrahelvetic complex, E.Switzerland. Eclog. geol. Helv. 70, p.83-95.

Milnes, A.G., Pfiffner, O.A., 1980, Tectonic Evolution of the central Alps in the cross section St. Gallen-Como. Eclog. Geol. Helv. 73, p.619-633.

Mutti, E., 1985, Turbidite systems and their relations to depositional sequences, In: G.G. Zuffa

(Ed), Provenance of Arenites: NATO-ASI Series, Reidel publishing Co., Dordrecht, The Netherlands, p.65-93.

Mutti, E., Ricci Lucchi, F., 1972, Le torbidito dell' Appenino settentrionale: introduzione all'analisi di facies. Mem. Soc. Geol. Ital., 11: 161-199.

Mutti, E., Ghibaudo, G., 1972, Un esempio di torbidito di conoide sottomarina esterna- Le Arenarie di San Salvatore (formazione di Bobbio, Miocene) nell'Appennino di Piacenza, Memorie dell'Accademia della Scienze di \torino, Classe di Scienze Fisiche, Matematiche e Naturali, Serie 4, No16, 40p.

Mutti, E., Ricci Lucchi, F., 1975, Turbidite facies and facies associations. In: E. Mutti, et al (Eds), Examples of Turbidite Facies and associations from selected formations of the Northern Appennines. Field trip Guidebook A-11, 9th I.A.S. congress, Nice, pp.21-36.

Mutti, E., Nilsen, T.H., 1981, Significance of Intraformational rip-up clasts in deep-sea fan deposits, I.A.S. 2nd Eur.Mtg. Bologna,abstr. 117-119.

Mutti, E., Sonnino, M., 1981, Compensation Cycles: A diagnostic feature of turbidite sandstone lobes. I.A.S. 2nd Eur. Mtg.,Bologna, Abstr., 120-123.

Naef, H., Diebold, P., Schlanke, S., 1985, Sedimentation und Tektonik im Tertiar der Nordschweiz. - NAGRA techn. Ber., 85 - 14.

Oberholzer, J., 1933, Geologie der Glarneralpen. Beitr. Geol. Karte Schweiz. (N.F.)28.

Ori, G.G., Friend, P.F., 1984, Sedimentary basins, formed and carried piggy-back on active thrust sheets. - Geology, 12, 475-478.

Pantin, H.M., 1979, Interaction between velocity and effective density in turbidity flow: phase plane analysis, with criteria for autosuspension. Mar. Geol. 31, 59-99.

Pantin, H.M., Leeder, M.R., 1987, Reverse flow in turbidity currents: the role of internal solitons. Sedimentology, 34, 1143-1157.

Pickering, K.T., 1979, Possible retrogressive flow slide deposits from the Kongsfjord

Formation: a Precambrian sub-marine fan, Finmark, N.Norway. Sedimentology, 26, 295-305.

Pickering, K., Hiscott, R., 1985, Contained (reflected) turbidity currents from the M.Ordovician Cloridorme formations, Quebec, Canada. An alternative to the Anti-dune hypothesis. Sedimentology, 32,p.373-394.

Pickering, K., Stow, D., Watson, M., Hiscott, R.M., 1986, Deep water facies, processes and models:a Review and Classification Scheme for Modern and ancient Sediments. Earth. Sci.Rev. 23,p.71-174.

Piper, D.J.W., 1978, Turbidite muds and silts on deep sea fans and abyssal plains. In: D.J. Stanley and G. Kelling (Eds). Sedimentation in sub-marine canyons, fans and trenches. Dowden, Hutchinson and Ross, Stroudsburg, Penn. pp.163-176.

Pfiffner, O.A., 1977, Tectonische Untersuchungen im Infrahelveticum der Ostschweiz. Mitt. Geol. Inst. ETH. u. Univ. Zurich. (N.F.) 217, 432pp..

Pfiffner, O.A., 1978, Der Falten- und Kleindeckenbau im Infrahelveticum der Ostschweiz. Eclog. Geol. Helv. 71,p.61-84.

Pfiffner, O.A., 1980, Strain Analysis in folds (Infrahelvetic Complex, central Alps). Tectonophysics 61,p.337-362.

Pfiffner, O.A., 1981, Fold and thrust tectonics in the Helvetic nappes (eastern Switzerland). In: Thrust and Nappe Tectonics (Eds. K.R. McClay and N.J. Price), P.319-327. - Spec. Publ. Geol. Soc. Lon., 9. Blackwell Scientific Publications, Oxford.

Pfiffner, O.A., 1986, Evolution of the North Alpine Foreland Basin in the Central Alps. In: Foreland Basins (Eds. P.A. Allen and P. Homewood). - Spec. publ. Geol. Soc. Lon., 8, 219-228.

Pfiffner, O.A., Frei, W., Finckh, H., Valasek, P., 1988, Deep seismic reflection profiling in the Swiss Alps: Explosion seismology results for line NFP 20-EAST. - Geology 16, 987-

990.

Pinet, P., Souriau, M., 1988, Continental erosion and large scale relief, Tectonics,7(3), 563-582.

Platt, J.P., Dynamics of orogenic wedges and the uplift of high-pressure metamorphic rocks. - GSA Bull., 97, 1037-1054.

Price, R.A., 1973, Large scale gravitational flow of supracrustal rocks, Southern Canadian Rockies. In: Gravity and Tectonics. (Eds. K.A. De Jong, K. Scholten). New York, Wiley. 491-502.

Quervain, De F., 1928, Zur Petrographie und Und Geologie der Taveyannaz gesteine. Schweiz. Min. Petr. Mitt., 8/1 p.1-88.

Quinlan, G.M., Beaumont, C., 1984, Appalachian thrusting, lithospheric flexure, and the Palaeozoic stratigraphy of the eastern interior of North America. - Can. J. Earth Sci., 21, 973-996.

Ravenne, C., Vially, R., Riche, Ph., Tremolieres, P., 1987, Sedimentation et tectoniquedans le bassin marin eocene superieur-oligocene des Alpes du sud. Revue Institut Francais du Petrole. Vol. 42, No.5,sept-oct., p.529-553.

Ricci Lucchi, F., Valmori, E., 1980, Basin-wide turbidites in a Miocene over supplied deep-sea plain: a geometrical analysis. Sedimentology, 27, 241-270.

Rigassi, D., 1977a, Genese tectonique du Jura: une nouvelle hypothese. - Palaeolab. news 2, Terreaux du Temple, Geneva.

Rigassi, D., 1977b, Subdivision et datation de la Molasse d'eau douce Inferieure du Plateau Suisse. - Palaeolab. news 1, Terreaux du Temple, Geneva.

Roache, P.J., 1982, Computational Fluid Dynamics. - Hermosa publishers, Hermosa, New Mexico, U.S.A., 446p..

Royden, L., Patacca, E., Scandone, P., 1987, Segmentation and configuration of subducted

lithosphere in Italy: An important control on thrust-belt and foredeep basin evolution, Geology, 15, 714-717.

Ruefli, W.H., 1959, Stratigraphie und tectonik des eingeschlossenen Glarner Flysches im Weisstannental (St. Galler Oberland). Mitt. Geol. Inst. ETH., u. univ. Zurich, C/75, 194pp.

Schmid, S., 1975, The Glarus Overthrust: field evidence and mechanical model. Eclog. Geol. Helv.,68,p.247-280.

Siegenthaler, C., 1974, Die Nordhelvetischen flysch-gruppe im Sernftal (Kt. Glarus). - Ph.D. thesis, Univ. of Zurich, 83p..

Steckler, M.S., Watts, A.B., 1981, Subsidence history and tectonic evolution of Atlantic type continental margins. In: Dynamics of Passive margins (Ed. R.A. Scrutton), AGU/GSA Geodynamics ser. v. 6, 184-196.

Steckler, M.S., Watts, A.B., Thorne, J.A., 1988, Subsidence and basin modelling at the U.S. Atlantic Passive margin. In: The Atlantic continental margin: U.S., (Eds. R.A. Sheridan and J.A. Grow) GSA The Geology of North America v. 1-2, 399-416.

Stevens, S.H., Moore, G.F., 1985, Deformational and sedimentary processes in trench slope basins of the western Sunda Arc, Indonesia. Mar. Geol. 69, 93-112.

Stockmal, G.S., Beaumont, C., Boutilier, R., 1986, Geodynamic models of convergent margin tectonics: transition from rifted margin to overthrust belt and consequences for foreland basin development. - AAPG Bull., 70, 853-868.

Stow, D.A.V., Bowen, A.J., 1978, Origin of lamination in deep sea, fine grained sediments. Nature, 274, 324-328.

Stow, D.A.V., Shanmugan, G., 1980, Sequence of structures in fine grained turbidites, comparison of recent deep sea and ancient flysch sediments. Sediment. Geol. 25, 23-42.

Styger, G.A., 1961, Bau und stratigraphie der Nordhelvetischen Tertiarbildungen in der Hausstock- und westlichen Karpf-gruppe. -Mitt. Geol. Inst., ETH u. Univ., Zurich, C/77,

151p.

Tankard, A.J., 1986, On the depositional response to thrusting and lithospheric flexure: examples from the Appalachian and Rocky Mountain basins. - In: Foreland basins (Eds. Allen, P.A., and Homewood, P.). Spec. Publ. Int. Ass. Sediment., 8, 369-392.

Tipper, J.C., 1983, Rates of sedimentation, and stratigraphical completeness. -Nature, 302, 696-698.

Trümpy, R., 1969, Die Helvetischen Decken der Ostschweiz. Versuch einer palinspastischen Korrelation und Ansatze zu einer Kinematischen analyse. Eclog. Geol. Helv. 62, p.105-142.

Trümpy, R., 1973, The timing of orogenic events in the central Alps. - In: Gravity and Tectonics (Eds. DeJong, K.A., and Scholten, R.) pp.229-251. Wiley, London.

Trümpy, R., 1980, Geology of Switzerland, a guide book. Part A: an outline of the geology of Switzerland. Wepf and Co., 104pp..

Vail, P.R., Mitchum, Jr, R.M., Todd, R.G., Widmier, J.M., Thompson III, S., Sangree, J.B., Bubb, J.N., Hatelid, W.G., 1977, Seismic stratigraphy and global changes in sea-level, in: Payton, C.E., ed., Seismic stratigraphy - applications to hydrocarbon exploration: AAPG Memoir 26, p.49-212.

Vening Meinesz, F.A., 1941, Gravity over the Hawaiian Archipeligo and over the Maderia area. - Proc. Netherlands Acad., Wetensia, 44pp.

Vollmayr, v-T., Wendt, A., 1987, Die erdgasbohrung Entlebuch 1, ein teifenaufschluss am Alpennordrand. - Bull. Ver. Schweiz. Petrol. Geol. u. -Ing., 53(125), 67-79.

Vuagnat, M., 1952, Petrographie, Repartition et origine des microbreches du flysch Nordhelvetique. Mat. Carte geol. Suisse, NS.97.

Watts, A.B., 1978, An analysis of isostasy in the worlds' oceans,1, Hawaiian-Emperor sea-mount chain, J. Geophys. Res., 83, 5989-6004.

Watts, A.B., Cochran, J.R., 1974, Gravity anomalies and flexure of the lithosphere along the Hawaiian-Emporer seamount chain. Geophys. J. R. Astr. Soc. 38, 119-141.

Watts, A.B., Talwani, M., 1974, Gravity anomalies seaward of deep sea trenches and their tectonic implications, Geophys. J. R. Astr. Soc., 36, 57-90.

Watts, A.B., Bodine, J.H., Ribe. N.M., 1980, Observations of flexure and the geological evolution of the Pacific Ocean basin. - Nature 283, 532-537.

Wegmann, R., 1961, Zur geologie der flyschgebeite Sudlich Elm. Mitt. Geol. Inst. ETH u. Univ. Zurich, C/76, 256p..

Werner, D., 1979, Fig. 4 in: Rybach, L., 1979, Geothermic and radiometric investigations. - Schweiz. Min. Pet. Mitt., 59, 141-148.

Willett, S.D., Chapman, D.S., Neugebauer, H.J., 1985, A thermo-mechanical model of continental lithosphere. Nature, 314, 520-523.

Wiltschko, D.V., Eastman, D.J., 1983, Role of Basement warps and faults in localising thrust fault ramps. Mem. Geol. Soc. Am., 158, 177-190.

Zwahlen, P., 1986, Die Kandertal Stoerung. Eine Transversale Diskontinuitaet im Bau der Helvetischen decken. Ph.D. thesis. Univ. Bern.

ACKNOWLEDGEMENTS

This research took a new lease of life on being introduced to the wonders of geophysics by Bernie Coakley who collaborated in writing chapter 6. Tony Watts is thanked for many flexural discussions.

John Platt as joint supervisor has helped greatly in the structural aspects of the work, both in the field, and at Oxford. Bill Fitches, enthusiastically as ever, encouraged work on the dilemmas of soft sediment deformation.

During fieldwork I was assisted by Karyna Rodriguez, Michelle Norris, Jon Booler and Karen Owen, all of whom enabled me to retain some form of sanity, and made fieldwork all the more fun.

Many thanks to all the postgraduates in the department who have contributed to such an enjoyable work environment, especially Sriyanee for tolerating various degrees of chaos in the office.

Finally, I thank Phil Allen for enabling me to do the project in the first place, and providing patient and excellent supervision for which I am sincerely indebted.

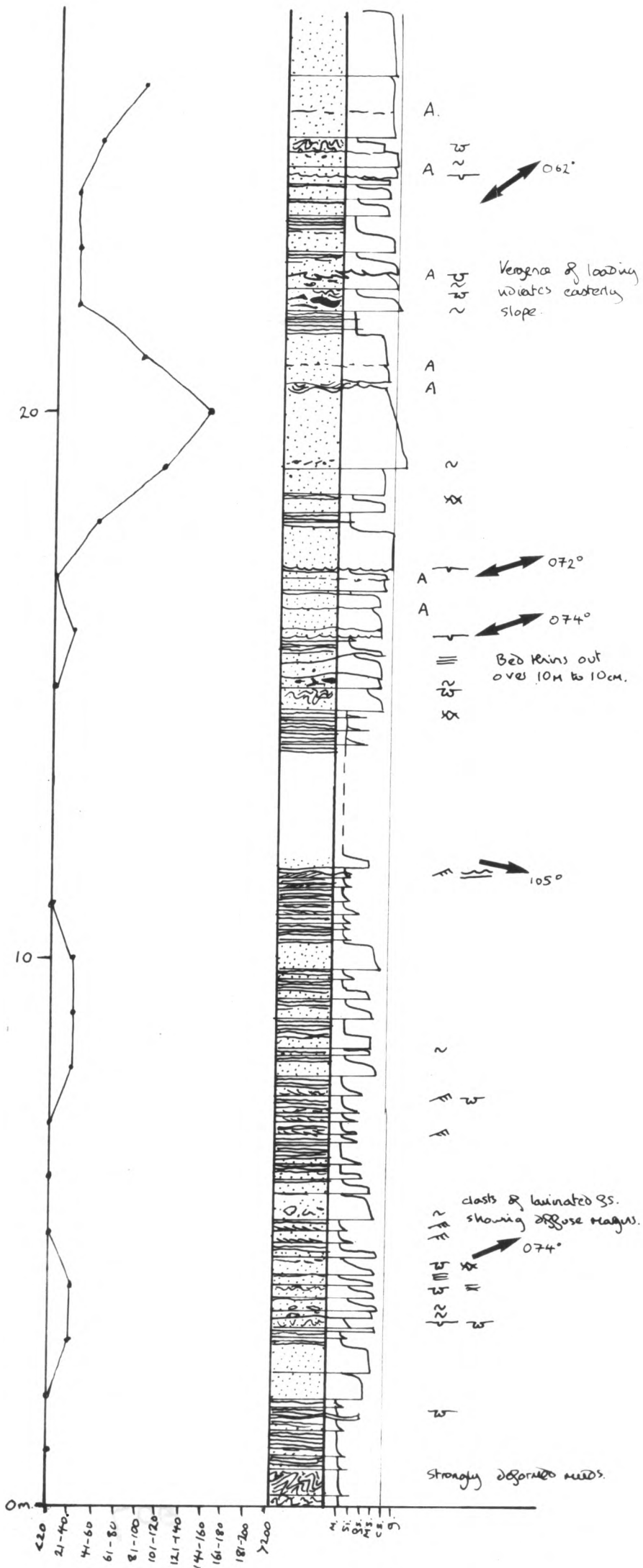

LOG WOLFISBACH, GRID REF. (72237, 19610).